MARTIN MARIETTA ENERGY SYSTEMS LIBRARIES
3 4456 0134136 5

CENTRAL RESEARCH LIBRARY
DOCUMENT COLLECTION

4

ORNL-3425
UC-34 – Physics
TID-4500 (20th ed.)

PHYSICS DIVISION
ANNUAL PROGRESS REPORT
FOR PERIOD ENDING JANUARY 31, 1963

OAK RIDGE NATIONAL LABORATORY
CENTRAL RESEARCH LIBRARY
CIRCULATION SECTION
4500N ROOM 175
LIBRARY LOAN COPY
DO NOT TRANSFER TO ANOTHER PERSON.
if you wish someone else to see this report, send in name with report and the library will arrange a loan.
ORNL-118 (6-97)

OAK RIDGE NATIONAL LABORATORY
operated by
UNION CARBIDE CORPORATION
for the
U.S. ATOMIC ENERGY COMMISSION
OAK RIDGE, TN

CENTRAL
RESEARCH LIBRARY
DOCUMENT COLLECTION
ORNL-4500

Errata: ORNL-3429

PHYSICS DIVISION ANNUAL PROGRESS REPORT

for Period Ending January 31, 1963

Note: These errata are printed on gummed paper so that they can be cut apart and glued directly into the report.

Printed in USA. Price: $2.75 Available from the
Office of Technical Services
U. S. Department of Commerce
Washington 25, D. C.

LEGAL NOTICE

as an account of Government sponsored work. Neither the United States, any person acting on behalf of the Commission:

or representation, expressed or implied, with respect to the accuracy, efulness of the information contained in this report, or that the use of paratus, method, or process disclosed in this report may not infringe s; or

ies with respect to the use of, or for damages resulting from the use of ratus, method, or process disclosed in this report.

'person acting on behalf of the Commission" includes any employee or ssion, or employee of such contractor, to the extent that such employee mmission, or employee of such contractor prepares, disseminates, or information pursuant to his employment or contract with the Commission, uch contractor.

ORNL-3425
UC-34 – Physics
TID-4500 (20th ed.)

Contract No. W-7405-eng-26

PHYSICS DIVISION
ANNUAL PROGRESS REPORT
for Period Ending January 31, 1963

J. L. Fowler, Director
E. O. Wollan, Associate Director

DATE ISSUED

MAY 21 1963

MARTIN MARIETTA ENERGY SYSTEMS LIBRARIES

3 4456 0134136 5

OAK RIDGE NATIONAL LABORATORY
Oak Ridge, Tennessee
operated by
UNION CARBIDE CORPORATION
for the
U. S. ATOMIC ENERGY COMMISSION

FOREWORD

This is the fifth Physics Division progress report made on an annual basis. As in previous years, the report contains the abstracts for papers which have been published or which have been prepared for publication. In such cases, reprints or preprints of the articles will be available. Preliminary results of work in progress are reported, as previously, in some detail. Since this work is of a preliminary nature, the authors should be contacted with regard to the inclusion of any of these results in other publications.

TABLE OF CONTENTS AND SUMMARY

NUCLEAR STRUCTURE AND THE INELASTIC SCATTERING OF HIGH-ENERGY NUCLEONS

T. Terasawa, R. Haybron, and G. R. Satchler 1

A program has been initiated for the theoretical analysis of the inelastic scattering of high-energy nucleons by the use of the impulse approximation and by taking into account distortion effects as exactly as possible.

ANALYSIS OF ANGULAR CORRELATION FOR INELASTIC PROTON SCATTERING ON Fe^{56} AND Ni^{58}

G. R. Satchler and E. Sheldon 2

Abstract of paper to be published in *Proceedings of International Symposium on Direct Interactions and Nuclear Reaction Mechanisms*, Padua, Italy, 1962.

COLLECTIVE EFFECTS AND ELASTIC SCATTERING FROM ODD NUCLEI

G. R. Satchler 3

Abstract of paper to be published in *Nuclear Physics*.

SCATTERING FROM ORIENTED DEFORMED NUCLEI

K. T. R. Davies, G. R. Satchler, R. M. Drisko, and R. H. Bassel 3

Abstract of paper to be published in *Nuclear Physics*.

DISTORTED-WAVES THEORY OF DOUBLE EXCITATION BY INELASTIC SCATTERING

N. Austern, R. M. Drisko, E. Rost, and G. R. Satchler 3

Abstract of published paper: *Phys. Rev.* **128,** 733 (1962).

ANALYSIS OF THE INELASTIC SCATTERING OF ALPHA PARTICLES. I

R. H. Bassel, G. R. Satchler, R. M. Drisko, and E. Rost 4

Abstract of published paper: *Phys. Rev.* **128,** 2693 (1962).

ANALYSIS OF INELASTIC SCATTERING OF ALPHA PARTICLES. II

E. Rost 4

Abstract of published paper: *Phys. Rev.* **128,** 2708 (1962).

DISTORTED-WAVES ANALYSIS OF QUASI-ELASTIC (p,n) AND (He^3,t) REACTIONS

R. M. Drisko, R. H. Bassel, and G. R. Satchler 5

Abstract of published paper: *Phys. Letters* **2,** 318 (1962).

DISTORTED-WAVE THEORY OF DIRECT NUCLEAR REACTIONS

G. R. Satchler 5

Abstract of paper to be published in *Proceedings of International Symposium on Direct Interactions and Nuclear Reaction Mechanisms*, Padua, Italy, 1962.

VALIDITY OF THE DISTORTED-WAVES THEORY OF STRIPPING REACTIONS

G. R. Satchler, R. H. Bassel, and R. M. Drisko 5

The validity of the distorted-waves theory of stripping reactions is being studied by comparison with experiment, using optical potentials which give good fits to elastic-scattering data. Finite range, spin orbit, and other effects are included.

NUCLEAR SHELL-MODEL CALCULATIONS

J. N. Ginocchio, J. E. Rayburn, and G. R. Satchler 8

One- and two-particle fractional parentage coefficients are being computed for mixed neutron and proton configurations of the type j^n. The calculations for $n \leq 6$, $j \leq 7/2$ are complete; those for larger values are in progress.

ANALYSIS OF PICKUP REACTIONS IN THE $A = 90$ REGION

R. H. Bassel, R. M. Drisko, and G. R. Satchler 9

Abstract of paper to be published in *Proceedings of International Symposium on Direct Interactions and Nuclear Reaction Mechanisms*, Padua, Italy, 1962.

THE REACTION $V^{51}(n,d)Ti^{50}$ AT 14.4 Mev

K. Ilakovac, L. G. Kuo, M. Petravic, I. Slaus, P. Tomas, and G. R. Satchler 9

Abstract of published paper: *Phys. Rev.* **128**, 2739 (1962).

ALPHA-GAMMA ANGULAR CORRELATIONS AND THE DISTORTED-WAVES THEORY

D. K. McDaniels, D. L. Hendrie, R. H. Bassel, and G. R. Satchler 9

Abstract of published paper: *Phys. Letters* **1**, 295 (1962).

FLUCTUATIONS AND THE STATISTICAL MODEL OF NUCLEAR REACTIONS

D. M. Brink and G. R. Satchler 10

Expressions are given for the mean square deviations of nuclear cross sections when the transition amplitude contains a slowly varying, "direct," part and a fluctuating, "compound nucleus," part.

LYAPUNOV'S STABILITY CRITERIA FOR PLASMAS

T. K. Fowler 11

Abstract of a paper to appear in the April 1963 issue of the *Journal of Mathematical Physics*.

ON INTEGRATING THE VLASOV EQUATION

T. K. Fowler 11

Abstract of a paper accepted for publication by the *Journal of Nuclear Energy: Part C*.

CORRECTION OF ELECTRON LENSES

T. A. Welton and J. Kronsbein 11

A discussion is given of the limitations on resolving power of electron and proton microscopes. A novel method, called annular optics, is proposed for obtaining improved resolution.

CHARGED-PARTICLE NUCLEAR CROSS-SECTION COMPILATION

F. K. McGowan, W. T. Milner, and H. J. Kim 15

A literature search of charged-particle-induced reactions has been completed for 1948–1962. Tabular data of results for the elements manganese through zinc are being collected.

THE LIFETIME OF THE Λ^0 HYPERON

M. M. Block, R. Gessaroli, S. Ratti, L. Grimellini, T. Kikuchi, L. Lendinara, L. Monari, E. Harth, W. Becker, W. M. Bugg, and H. Cohn 15

Abstract of a paper submitted for publication to the *Physical Review*.

ELASTIC SCATTERING OF ALPHA PARTICLES BY O^{18}

R. D. Powers, J. K. Bair, J. L. C. Ford, Jr., and H. B. Willard 16

Differential elastic-scattering cross sections for alphas on O^{18} were obtained at center-of-mass angles of 90, 125.3, 140.7, and 164.37° for alpha energies from 2.4 to 3.5 Mev.

ELASTIC SCATTERING OF ALPHA PARTICLES FROM Si^{28}

J. K. Bair and H. B. Willard 17

The $Si^{28}(\alpha,\alpha)Si^{28}$ scattering has been rerun with improved resolution.

THE $O^{18}(\alpha,p)F^{21}$ REACTION AND THE BETA DECAY OF F^{21}

H. B. Willard, J. K. Bair, J. L. C. Ford, Jr., and C. M. Jones 18

The relative cross section for the reaction $O^{18}(\alpha,p)F^{21}$ has been measured from 8 to 10 Mev. A value of 4.3 ± 0.2 sec has been determined for the half-life of F^{21}.

TOTAL (p,n) CROSS SECTIONS FOR LIGHT-ELEMENT TARGETS IN THE BOMBARDING ENERGY RANGE 5 TO 15 Mev

J. K. Bair, C. M. Jones, and H. B. Willard 20

Preliminary total (p,n) cross-section measurements for light elements in the bombarding energy range 5 to 15 Mev are described.

NUCLEAR RESONANCE EFFECTS IN COULOMB EXCITATION

J. K. Bair, J. L. C. Ford, Jr., R. L. Robinson, and H. B. Willard 21

An investigation of the interference between Coulomb excitation and compound nuclear inelastic scattering is described.

COULOMB EXCITATION WITH Ne^{20} IONS

R. C. Ritter, P. H. Stelson, F. K. McGowan, and R. L. Robinson 21

Abstract of published paper: *Phys. Rev.* **128**, 2320 (1962).

LOW-LYING LEVELS OF Cu^{63} AND Cu^{65}

R. L. Robinson, F. K. McGowan, and P. H. Stelson 22

Properties of the 668-, 961-, 1323-, and 1412-kev levels in Cu^{63} and the 771-, 1115-, and 1474-kev levels in Cu^{65} are investigated by means of the Coulomb-excitation process.

COULOMB EXCITATION OF NUCLEAR STATES IN THE ISOTOPES OF OSMIUM

F. K. McGowan, R. L. Robinson, P. H. Stelson, and J. L. C. Ford 26

A discussion is given of the results obtained from Coulomb excitation of nuclear states in the isotopes of osmium.

GAMMA-GAMMA ANGULAR CORRELATION IN V^{51}

R. L. Robinson, N. R. Johnson, and G. D. O'Kelley 30

The angular correlation of the 613-319-kev gamma-ray cascade in V^{51} has been measured. It was fitted by the function $W(\theta) = 1 + (0.013 \pm 0.030)P_2(\cos\theta) - (0.04 \pm 0.05)P_4(\cos\theta)$.

DECAY OF Cs^{132}

R. L. Robinson, N. R. Johnson, and E. Eichler 31

Abstract of published paper: *Phys. Rev.* **128**, 252 (1962).

TOTAL NEUTRON CROSS SECTIONS IN ISOTOPES OF Zr, Fe, Cr, AND Ca

H. J. Kim, J. A. Biggerstaff, and W. M. Good 32

Neutron transmission measurements have been made on separated isotopes of $Zr^{90,91,92,94,96}$, Ca^{43}, Cr^{53}, and Fe^{57}. A list of the principal resonances in each isotope is given. Analysis and interpretation have only begun.

PARAMETERS OF NEUTRON RESONANCES IN W^{184}

F. A. Khan and J. A. Harvey 32

Abstract of a paper to be submitted for publication in *Nuclear Science and Engineering*.

NEUTRON CROSS-SECTION MEASUREMENTS FROM 1 TO 30,000 ev ON ENRICHED SAMPLES OF THE ZIRCONIUM ISOTOPES

R. C. Block 32

The neutron total cross sections of highly enriched samples of Zr^{90}, Zr^{91}, Zr^{92}, Zr^{94}, and Zr^{96} have been measured from 1 to 30,000 ev. Over 25 resonances were observed and assigned to individual isotopes. These resonances were analyzed for resonance parameters, and these parameters were combined to give information about the *s*-wave and *p*-wave strength functions.

LEVEL SPACINGS AND *s*-WAVE NEUTRON STRENGTH FUNCTIONS OF THE ISOTOPES OF TIN

T. Fuketa, F. A. Khan, and J. A. Harvey 36

Neutron transmission measurements from 0.2 to 10,000 ev have been made on highly enriched samples of the ten tin isotopes from Sn^{112} to Sn^{124}. Nearly 100 resonances were analyzed to obtain their parameters. Average level spacings and *s*-wave strength functions obtained from the data are compared with theoretical predictions.

NEUTRON CROSS-SECTION MEASUREMENTS ON FISSION PRODUCT SAMARIUM AND IODINE

N. J. Pattenden 45

Abstract of a paper submitted for publication in *Nuclear Science and Engineering*.

MODIFICATIONS TO PROGRAMS FOR NUMERICAL ANALYSIS OF NEUTRON RESONANCES

S. E. Atta and J. A. Harvey 46

An addendum to ORNL-3205 has been prepared.

EXCITATION OF COLLECTIVE STATES BY INELASTIC SCATTERING OF 14-Mev NEUTRONS

P. H. Stelson and R. L. Robinson 46

Neutrons of 14 Mev energy have been used to excite collective states in lead, bismuth, tin, and sulfur. Absolute differential cross sections for these excitations were determined and compared with the direct interaction theory.

DIFFERENTIAL CROSS SECTION OF NEUTRON SCATTERING FROM Pb^{208}

J. L. Fowler 49

Apparatus for the measurement of neutron cross sections with a few kilovolts energy spread is described, and results of such measurements on Pb^{208} are presented for the energy range 0.715 to 1.342 Mev.

AVERAGE RADIATIVE CAPTURE CROSS SECTIONS FOR 30- AND 65-kev NEUTRONS

R. L. Macklin, J. H. Gibbons, and T. Inada 56

Abstract of paper to be published in the *Physical Review*.

NEUTRON CAPTURE IN TIN ISOTOPES AT STELLAR TEMPERATURES

R. L. Macklin, T. Inada, and J. H. Gibbons 56

Abstract of published paper: *Nature* **194**, 1272 (1962).

THE 30-kev NEUTRON CAPTURE IN THE SAMARIUM ISOTOPES

R. L. Macklin, J. H. Gibbons, and T. Inada 56

Abstract of paper to be published in *Nature*.

NEUTRON CAPTURE CROSS SECTIONS NEAR 30 kev USING A MOXON-RAE DETECTOR

R. L. Macklin, J. H. Gibbons, and T. Inada 57

Abstract of paper to be published in *Nuclear Physics*.

RESONANT NEUTRON CAPTURE GAMMA-RAY SPECTRA

J. H. Gibbons, W. M. Good, J. R. Bird, and J. A. Biggerstaff 57

Capture gamma-ray spectra measurements have continued. Improvements in time resolution and two-dimensional data acquisition have permitted E_n vs E_γ observations. Gamma-ray spectra are observed in some cases to change drastically with energy; new resonances have been detected in Ca^{40}, Pb^{206}, and Pb^{207}. A resonating character for capture to the 3^- state in Pb^{208} is indicated.

GAMMA-RAY SPECTRA FROM NEUTRON CAPTURE

G. G. Slaughter, J. A. Harvey, G. T. Chapman, and J. R. Bird 60

A 9-in.-diam by 12-in.-long NaI crystal has been installed at the fast-chopper neutron time-of-flight spectrometer. Gamma-ray spectra obtained with this crystal from neutron capture in Sn, Cu, Ca, and Ti are discussed.

ORNL-RPI CAPTURE EXPERIMENT

R. C. Block, J. E. Russell, and R. W. Hockenbury 64

Neutron radiative capture measurements have been made on samples of W, Fe, Fe^{56}, Hf^{177}, Hf^{178}, Hf^{179}, and Hf^{180} by use of a new 1.25-m-diam liquid scintillator at the Rensselaer Polytechnic Institute's (RPI) linear accelerator laboratory.

CHANNEL ANALYSIS OF FAST-NEUTRON-INDUCED FISSION NEAR THRESHOLD

R. W. Lamphere 72

Evidence is presented which favors the existence of a K-band sequence of $\frac{1}{2}^+$, $\frac{3}{2}^-$, $\frac{1}{2}^-$ in the heavy nuclei Th^{231}, Th^{233}, and U^{235} near the saddle-point deformation.

Several foils of Np^{237} have been prepared as standards for cross-section work.

MASS DISTRIBUTION AND KINETICS OF U^{235} THERMAL-NEUTRON-INDUCED BINARY AND TERNARY FISSION

H. W. Schmitt, J. H. Neiler, F. J. Walter, A. Chetham-Strode, and M. J. Mader 76

The mass distributions and kinetics of U^{235} thermal-neutron-induced binary and ternary fission are obtained from multiparameter fragment energy correlation experiments. Strong influence of the closed-shell nuclei is indicated.

FRAGMENT MASS DISTRIBUTION FOR THERMAL- AND RESONANCE-NEUTRON-INDUCED FISSION OF Pu^{239}

F. J. Walter, J. H. Neiler, H. W. Schmitt, and C. W. Williams 79

The fragment mass distributions for thermal- and resonance-neutron-induced fission of Pu^{239} have been determined from correlated energy measurements of fragment pairs.

RESONANCE-NEUTRON-INDUCED FISSION OF ORIENTED U^{235} NUCLEI

J. W. T. Dabbs, F. J. Walter, and G. W. Parker 82

The observed fragment anisotropy varies markedly with energy.

INTERNAL BREMSSTRAHLUNG IN THE BETA DECAY OF He^6

J. K. Bienlein and Frances Pleasonton 89

Measurements were made to determine the yield of internal bremsstrahlung (IB) relative to beta emission and also the shape of the internal bremsstrahlung spectrum in the beta decay of He^6. Preliminary analysis of the data gives a value of 0.024 ± 0.006 for the IB yield and a spectral shape that is in good agreement with theory.

ANALYSIS OF THE RECOIL ENERGY SPECTRUM FROM THE BETA DECAY OF He^6

C. H. Johnson, Frances Pleasonton, and T. A. Carlson 92

The analysis gives an electron-neutrino angular correlation coefficient of -0.3343 ± 0.0029. This is interpreted in terms of a limit for the tensor interaction in beta decay.

HALF-LIFE OF He^6

J. K. Bienlein and Frances Pleasonton 94

Abstract of published paper: *Nucl. Phys.* **37,** 529 (1962).

ELECTRON SHAKE-OFF FOLLOWING THE β^- DECAY OF He^6

T. A. Carlson, Frances Pleasonton, and C. H. Johnson 94

Abstract of paper to be published in the *Physical Review.*

ELECTRON SHAKE-OFF FOLLOWING THE BETA DECAY OF Ne^{23}

T. A. Carlson 94

Abstract of paper submitted to the *Physical Review.*

FORMATION OF FRAGMENT IONS FROM CH_3Te^{125} AND $C_2H_5Te^{125}$ FOLLOWING THE NUCLEAR DECAYS OF CH_3I^{125} AND $C_2H_5I^{125}$

T. A. Carlson and R. M. White 95

Abstract of paper submitted to the *Journal of Chemical Physics.*

MASS SPECTROMETRIC ANALYSES OF THE IONS RESULTING FROM THE NUCLEAR DECAY OF CH_3I^{130} AND $C_2H_5I^{131}$: STUDY OF XENON-HYDROCARBON IONS

T. A. Carlson and R. M. White 95

Abstract of paper to be published in the *Journal of Chemical Physics.*

FRAGMENT IONS RESULTING FROM β^- DECAY OF CH_3Br^{82} AND β^+ DECAY OF CH_3F^{18}

T. A. Carlson and R. M. White 96

A mass spectrometer has been used to measure the relative abundances of fragment ions resulting from the nuclear decay of CH_3Br^{82} and CH_3F^{18}. The data have been discussed principally in terms of the consequence of excitation that arises from the sudden nonadiabatic change in nuclear charge.

ELECTRON SHAKE-OFF FOLLOWING THE β^- DECAY OF Ar^{41}

T. A. Carlson 98

Abstract of paper submitted to the *Physical Review.*

MEASUREMENTS OF THE HYPERFINE SPLITTING IN Fe-Rh AND Fe_2O_3 USING THE MÖSSBAUER EFFECT

F. E. Obenshain, L. D. Roberts, H. H. F. Wegener, J. O. Thomson, and D. W. Forester 99

Under certain conditions Fe-Rh may be either ferromagnetic or antiferromagnetic, and Fe_2O_3 is antiferromagnetic below $T_N = 975°K$. The temperature dependence of the internal magnetic fields have been measured for both of these materials by use of the Mössbauer effect.

CORRELATION OF THE MÖSSBAUER ISOMER SHIFT WITH THE RESIDUAL ELECTRICAL RESISTANCE FOR GOLD ALLOYS

L. D. Roberts, R. L. Becker, F. E. Obenshain, and J. O. Thomson 103

Measurements have been made of the isomer shift of gold for a number of gold alloys. The experimental results are compared with a simple theory which gives information about the filling of the *s* band in the alloy.

SOLID STATE AND NUCLEAR RESULTS FROM A MÖSSBAUER-TYPE STUDY OF Au^{197}
L. D. Roberts and J. O. Thomson 112

Abstract of published paper: *Phys. Rev.* **129**, 664 (1963).

TOTAL REFLECTION OF RECOIL-FREE NUCLEAR RESONANCE RADIATION FROM Fe^{57}
E. C. Campbell and S. Bernstein 112

Coherent resonant recoil-free scattering of gamma rays by Fe^{57} nuclei, studied by the method of total reflection, exhibits characteristic nuclear anomalous dispersion.

SOME MAGNETIC STRUCTURE PROPERTIES OF TERBIUM AND TERBIUM-YTTRIUM ALLOYS
W. C. Koehler, H. R. Child, E. O. Wollan, and J. W. Cable 117

Abstract of paper to be published in the *Journal of Applied Physics, Supplement.*

MAGNETIC STUDY OF DYSPROSIUM-YTTRIUM ALLOYS
H. R. Child, W. C. Koehler, E. O. Wollan, and J. W. Cable 118

Effects of dilution on magnetic properties of dysprosium are investigated in the system dysprosium-yttrium.

ANTIFERROMAGNETISM OF THE ANTIPHASE DOMAIN STRUCTURE OF Pd_3Mn
J. W. Cable, E. O. Wollan, W. C. Koehler, and H. R. Child 120

Abstract of published paper: *Phys. Rev.* **128**, 2118 (1962).

ATOMIC MAGNETIC MOMENTS IN DILUTE IRON-PALLADIUM ALLOYS
J. W. Cable, E. O. Wollan, and W. C. Koehler 120

Abstract of paper to be published in the *Journal of Applied Physics, Supplement.*

MAGNETIC PROPERTIES OF THE Pd_3Mn-Pt_3Mn SYSTEM
J. W. Cable, E. O. Wollan, W. C. Koehler, and H. R. Child 120

Neutron diffraction and magnetization measurements were made on ordered alloys of composition $Pd_3Mn \cdot Pt_3Mn$ and $3Pd_3Mn \cdot Pt_3Mn$. $Pd_3Mn \cdot Pt_3Mn$ was found to be ferromagnetic below 210°K with an average moment of 1.02 μ_B/atom. For $3Pd_3Mn \cdot Pt_3Mn$, the data indicate ferromagnetic clusters of about 17 A diam which couple antiparallel at low temperatures.

HYDROGEN ATOM POSITIONS IN FACE-CENTERED CUBIC NICKEL HYDRIDE
E. O. Wollan, J. W. Cable, and W. C. Koehler 123

Abstract of paper to be submitted to the *Physical Review.*

NEUTRON DIFFRACTION INVESTIGATION OF THE MAGNETIC PROPERTIES OF COMPOUNDS OF RARE-EARTH METALS WITH GROUP V ANIONS
H. R. Child, M. K. Wilkinson, J. W. Cable, W. C. Koehler, and E. O. Wollan 124

Abstract of paper to be submitted to the *Physical Review.*

MAGNETIC MOMENT DISTRIBUTION IN Cu_2MnAl
G. P. Felcher, J. W. Cable, and M. K. Wilkinson 124

Abstract of paper to be submitted to the *Physical Review.*

MAGNETIC STRUCTURE OF RARE-EARTH IRIDIUM COMPOUNDS RIr_2
Gian Felcher and W. C. Koehler 124

Neutron diffraction measurements on $TbIr_2$ and $HoIr_2$ confirm the low molecular moments deduced from magnetic measurements. Partial quenching of the orbital angular momentum of the rare-earth atoms is indicated. The coherent scattering amplitude of iridium was determined to be $(1.00 \pm 0.02) \times 10^{-12}$ cm.

ON THE CRYSTAL STRUCTURE OF THE MANGANESE(III) TRIOXIDES OF THE HEAVY LANTHANIDES AND YTTRIUM

H. L. Yakel, W. C. Koehler, E. F. Bertaut, and E. F. Forrat 127

Abstract of paper to be published in *Acta Crystallographica*.

LECTURES ON NEUTRON DIFFRACTION

W. C. Koehler 128

Abstracts of papers published in *Proceedings of Advanced Course on Neutron Crystal Spectrometer*, Netherlands-Norwegian Reactor School, 1962.

OPTICAL PHYSICS

G. W. Charles, P. M. Griffin, H. W. Morgan, O. B. Rudolph, P. A. Staats, K. L. Vander Sluis, T. A. Welton, and G. K. Werner 128

A detailed study has been made of an electrically excited krypton-mercury mixture as a possible amplifying medium for an optical maser. Although optical pumping remains a possibly feasible approach, collisional pumping has been ruled out.

RESPONSE OF SILICON SOLID-STATE DETECTORS TO HEAVY IONS AND FISSION FRAGMENTS

H. W. Schmitt, F. J. Walter, J. H. Neiler, C. D. Moak, W. M. Gibson, and T. D. Thomas 130

The pulse-height vs energy relation has been measured for high-energy bromine and iodine ions (artificial fission fragments) incident on solid-state detectors. The Oak Ridge Tandem Van de Graaff accelerator was used to accelerate the ions; energies up to 120 Mev were obtained.

STUDY OF THE TRANSITION OF SMALL NIOBIUM-ZIRCONIUM SUPERCONDUCTING SOLENOIDS TO THE NORMAL STATE

R. W. Boom and L. D. Roberts 133

Abstract of a paper submitted for publication in the *Journal of Applied Physics*.

PUBLICATIONS 135

PAPERS PRESENTED AT SCIENTIFIC AND TECHNICAL MEETINGS 138

ANNOUNCEMENTS 141

ADVISORY COMMITTEE 143

ACTIVITIES RELATED TO EDUCATIONAL INSTITUTIONS 143

ORNL PHYSICS SEMINARS 152

NUCLEAR STRUCTURE AND THE INELASTIC SCATTERING OF HIGH-ENERGY NUCLEONS

T. Terasawa[1] R. Haybron[2] G. R. Satchler

For incident energies of about 100 Mev and above, nucleon wavelengths become comparable with the distance between nucleons in the nucleus, and multiple scattering effects become much less important. Further, one may use the impulse approximation and treat the scattering from each target nucleon as though it were free; in this way it is claimed we know the effective interaction between nucleon and target nucleus in terms of the results of nucleon-nucleon experiments.[3] The scattering then becomes a very useful probe of nuclear structure.

Even at these energies, however, distortion of the incident and emitted waves by elastic scattering is still important; this is illustrated by Fig. 1, where it is seen that distortion effects (mainly absorption) reduce the cross section by a factor of 3 from the predictions using plane waves (a reduction of 20% is still observed at 800 Mev energy). This introduces complications because the effective interaction depends upon the local momentum transfer at the nucleon-nucleon collision and distortion introduces a spread of momenta for each observed scattering angle. One way, called "approximate," is to use the asymptotic momentum transfer, which one might expect to be a good approximation since the nucleon-nucleus elastic scattering is mostly forward. More accurately, one takes the Fourier transform of the wave functions and folds in the momentum dependence; this is called "exact," but the calculations illustrated in Fig. 2 still ignore some nonlocality that this introduces. The "exact" and "approximate" calculations, in this case, differ by about 20% at forward angles; there are some indications that the "approximate" form is poorer for calculating quantities like the polarization and p-γ correlation. These calculations were carried out "by hand" using amplitudes from current distorted-wave codes available at ORNL, but currently they are being coded for the IBM 7090.

Other effects being studied include the use of realistic wave functions (generated from a Saxon well) for the target nucleons and the effects of spin-orbit coupling in the distorted waves. Preliminary results with the latter indicate that it alone can produce polarization in the inelastic scattering comparable to that observed, even without the spin dependence of the nucleon-nucleon interaction.

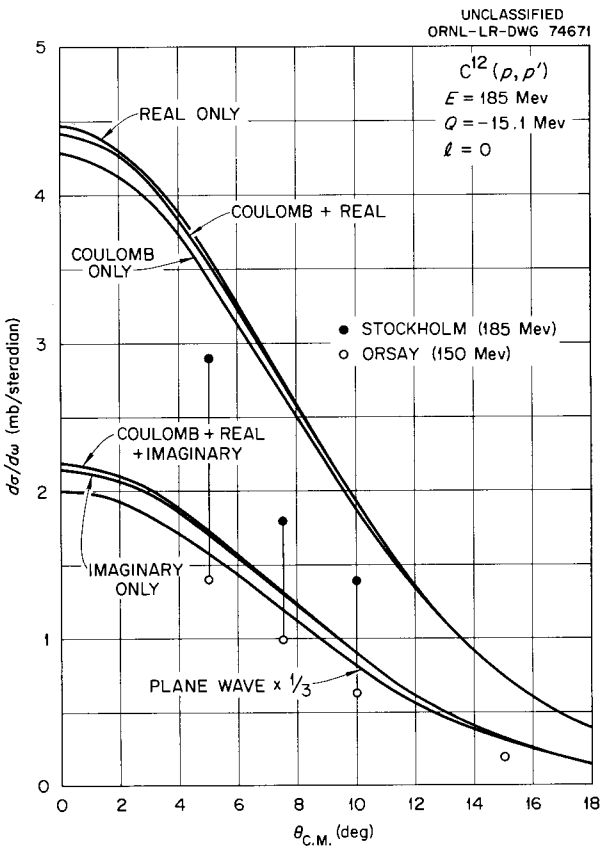

Fig. 1. Distortion Effects in the Excitation of the 15.1-Mev Level in C^{12}. The various curves illustrate the effect of the Coulomb repulsion and the real and imaginary parts of the optical potential (which was chosen to fit the observed elastic scattering at this energy). The inelastic interaction is taken, in impulse approximation, from nucleon-nucleon scattering data.[3] The agreement with experiment is gratifying since the only adjustable parameter in the theory is the harmonic oscillator parameter determining the size of the $1p$ nucleon orbit in C^{12}; the value used is one favored by shell-model calculations.

[1]Summer visitor from Western Reserve University, Cleveland (on leave from Tokyo University).

[2]Visitor from Michigan State University, East Lansing.

[3]A. Kerman, H. McManus, and R. M. Thaler, *Ann. Phys.* (*N.Y.*) **8**, 551 (1959).

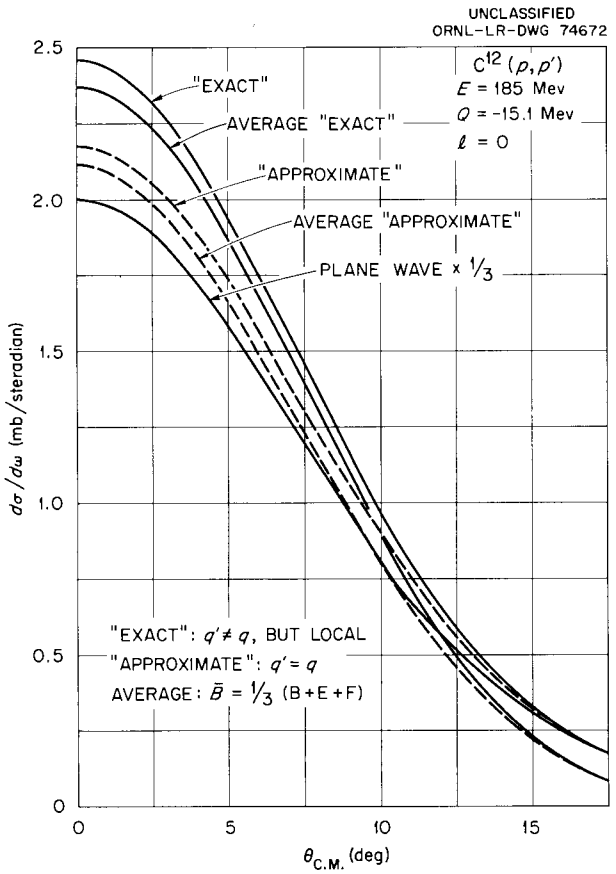

Fig. 2. Comparison of the "Exact" and "Approximate" Treatment of the Effects of the Momentum Dependence of the Nucleon-Nucleon Interaction When Distorted Waves Are Used. The "average" curves ignore the tensor-like part of the interaction.

ANALYSIS OF ANGULAR CORRELATION FOR INELASTIC PROTON SCATTERING ON Fe^{56} AND Ni^{58} [1]

G. R. Satchler E. Sheldon [2]

The $(p,p'\text{-}\gamma)$ angular correlation measurements for proton inelastic scattering on Fe^{56} and Ni^{58} at 4.22 and 5.73 Mev, respectively, have been analyzed theoretically in the light of statistical compound-nucleus and distorted-wave direct interaction theory.

[1] Abstract of paper to be published in *Proceedings of International Symposium on Direct Interactions and Nuclear Reaction Mechanisms*, Padua, Italy, 1962.

[2] Laboratorium fur Kernphysik, Zurich, Switzerland.

COLLECTIVE EFFECTS AND ELASTIC SCATTERING FROM ODD NUCLEI[1]

G. R. Satchler

It is suggested that a difference could be observed between the elastic scattering from even and odd nuclei whenever the nuclei are nonspherical. To second order in the "deformation" the difference is shown to be due mainly to an additional diagonal matrix element which occurs for odd nuclei with spin $> \frac{1}{2}$. Numerical evaluation of this matrix element by the use of the distorted-waves Born approximation is used to give an estimate of the size and qualitative behavior of this effect in a number of typical cases. It is found that, while not large, the effect need not be negligible, and it may be important for understanding the variations in optical potential parameters from nucleus to nucleus.

[1]Abstract of paper to be published in *Nuclear Physics*.

SCATTERING FROM ORIENTED DEFORMED NUCLEI[1]

K. T. R. Davies
G. R. Satchler
R. M. Drisko[2]
R. H. Bassel[3]

The elastic scattering of particles from oriented, deformed, odd nuclei is studied using the collective model of the nucleus. Numerical results, obtained by the use of the distorted-waves Born approximation, are presented for some typical cases, namely, neutrons of 2, 5, and 14 Mev, protons of 5 and 14 Mev, and alphas of 43 Mev incident on Mn^{55} and Ho^{165} target nuclei. It is found that the differential cross section shows large azimuthal asymmetries when the target is oriented perpendicular to the incident beam. The experimental observation of this effect would be valuable; for rotational nuclei it could measure the sign and magnitude of the deformation, while for vibrational nuclei it could yield important information about the coupling of the odd nucleon to the core.

[1]Abstract of paper to be published in *Nuclear Physics*.

[2]Presently at ORNL, Electronuclear Division. Permanent address: University of Pittsburgh, Pittsburgh, Pa.

[3]Electronuclear Division.

DISTORTED-WAVES THEORY OF DOUBLE EXCITATION BY INELASTIC SCATTERING[1]

N. Austern[2]
R. M. Drisko[3]
E. Rost[4]
G. R. Satchler

It is shown how the distorted-waves theory of inelastic scattering can give rise to angular distributions with "anomalous phase," such as observed in recent experiments with alpha particles. These occur when the scattering takes place through second-order effects; excitation of a two-phonon vibrational state is studied explicitly.

[1]Abstract of published paper: *Phys. Rev.* **128**, 733 (1962).

[2]University of Pittsburgh, Pittsburgh, Pa.

[3]Presently at ORNL, Electronuclear Division. Permanent address: University of Pittsburgh, Pittsburgh, Pa.

[4]Palmer Physical Laboratory, Princeton University, Princeton, N.J.

There is an important cancellation between the amplitude for simultaneous excitation and part of that for successive excitation, without which the anomalous phase would not be observed. These conclusions are contrasted with the predictions of a theory using plane-wave Born approximation. Further study of the cancellation is suggested as a sensitive test of the optical model.

ANALYSIS OF THE INELASTIC SCATTERING OF ALPHA PARTICLES. I[1]

R. H. Bassel[2] R. M. Drisko[3]
G. R. Satchler E. Rost[4]

The inelastic scattering of medium-energy alpha particles is interpreted as a direct interaction by use of the distorted-waves theory. A deformed potential-well interaction based on the collective model of the nucleus is found to give results in good agreement with experiment. The parameters of the potential well are determined by fitting the elastic scattering, and the multipole deformations obtained from the magnitudes of the inelastic cross sections agree reasonably well with those obtained by other techniques. The effects on the theoretical predictions of variations in the parameters are described. A preliminary study of the effects of including Coulomb excitation is also included.

[1]Abstract of published paper: *Phys. Rev.* **128**, 2693 (1962).

[2]Electronuclear Division.

[3]Presently at ORNL, Electronuclear Division. Permanent address: University of Pittsburgh, Pittsburgh, Pa.

[4]Palmer Physical Laboratory, Princeton University, Princeton, N.J.

ANALYSIS OF INELASTIC SCATTERING OF ALPHA PARTICLES. II[1]

E. Rost[2]

The analysis of the inelastic scattering of medium-energy alpha particles is continued using the distorted-waves theory. Attention is given to the qualitative features of these reactions, in particular the characteristic oscillations in the angular distributions and the associated phase rule. The weak-coupling approximation is studied and is shown to be valid for most medium-energy (α,α') reactions. The distorted-waves theory is compared with alternative theories of inelastic scattering and also with a preliminary sample of experimental data.

[1]Abstract of published paper: *Phys. Rev.* **128**, 2708 (1962).

[2]Princeton University, Princeton, N.J. (work performed at ORNL).

DISTORTED-WAVES ANALYSIS OF QUASI-ELASTIC (p,n) AND (He^3,t) REACTIONS[1]

R. M. Drisko[2] R. H. Bassel[3] G. R. Satchler

The "quasi-elastic" charge-exchange scattering of protons and He^3 nuclei, in which a state is excited in the residual nucleus which is the analog of the target nucleus ground state, was studied with the distorted-waves method. Some preliminary results were also given for "quasi-inelastic" scattering.

[1]Abstract of published paper: *Phys. Letters* **2**, 318 (1962).

[2]Presently at ORNL, Electronuclear Division. Permanent address: University of Pittsburgh, Pittsburgh, Pa.

[3]Electronuclear Division.

DISTORTED-WAVE THEORY OF DIRECT NUCLEAR REACTIONS[1]

G. R. Satchler

Recent applications of the distorted-wave theory of direct nuclear reactions were reviewed. The analysis of strong transitions in the inelastic scattering of neutrons, protons, and alpha particles was discussed. The analysis provides strong evidence for the generalization of the optical model suggested by the collective model, namely, the use of nonspherical potential wells. Recent work with stripping and pickup reactions was also described and particular stress laid on the problems and uncertainties which remain before a realistic, detailed distorted-wave analysis of these reactions can be carried out.

[1]Abstract of paper to be published in *Proceedings of International Symposium on Direct Interactions and Nuclear Reaction Mechanisms*, Padua, Italy, 1962.

VALIDITY OF THE DISTORTED-WAVES THEORY OF STRIPPING REACTIONS

G. R. Satchler R. H. Bassel[1] R. M. Drisko[2]

The distorted-waves (DW) theory, in conjunction with the collective model of the nucleus, has had considerable success in the interpretation of inelastic-scattering experiments. The work reported here is intended to study the extent to which this theory can be applied to rearrangement collisions, in particular to deuteron stripping reactions. Several DW calculations of (d,p) reactions have been published recently, but most of these have involved some parameter varying in order to fit the data. This is unfortunate because parameter-juggling is not in the spirit of the DW approach, and its use obscures the advantages of the method. One should use optical-model potentials which fit the observed elastic scattering until all other effects have been studied. This has been greatly facilitated by recent optical-model analyses at ORNL of elastic-scattering data for both nucleons and deuterons, so that a realistic and consistent

[1]Electronuclear Division.

[2]Presently at ORNL, Electronuclear Division. Permanent address: University of Pittsburgh, Pittsburgh, Pa.

study of the validity of the DW theory of deuteron stripping is now possible. The overall results are very encouraging; angular distributions are reproduced, at least qualitatively, over the whole angular range, and absolute magnitudes are predicted correctly to within at most a factor of 2. Previous plane-wave theories only "fitted" the main peak of an angular distribution (by means of varying a radius parameter) and were usually wrong in magnitude by factors of 10 to 100. Uncertainties still remain, however; for example, several optical potentials are found to give equally good fits to the elastic deuteron scattering (see Fig. 1), and these lead to different predictions for the (d,p) reaction (Fig. 2). These differences arise because the deuteron wave function inside the nucleus (Fig. 3) differs for the two potentials. If the interior contribution is eliminated by using a radial cutoff, the potentials give identical predictions. They also agree with experiment, but this may not be significant; other cases have shown a worse agreement with experiment when a cutoff is employed (see Fig. 4). The reason for this may be that, while we may doubt the physical significance of the optical-model wave for deuterons inside the nucleus, crudely eliminating it may be equally invalid. We hope an answer to this may be obtained by studying the systematics of DW analyses of stripping reactions.

Closed-shell nuclei are particularly useful for testing the absolute-magnitude predictions, since we believe we populate single-particle states

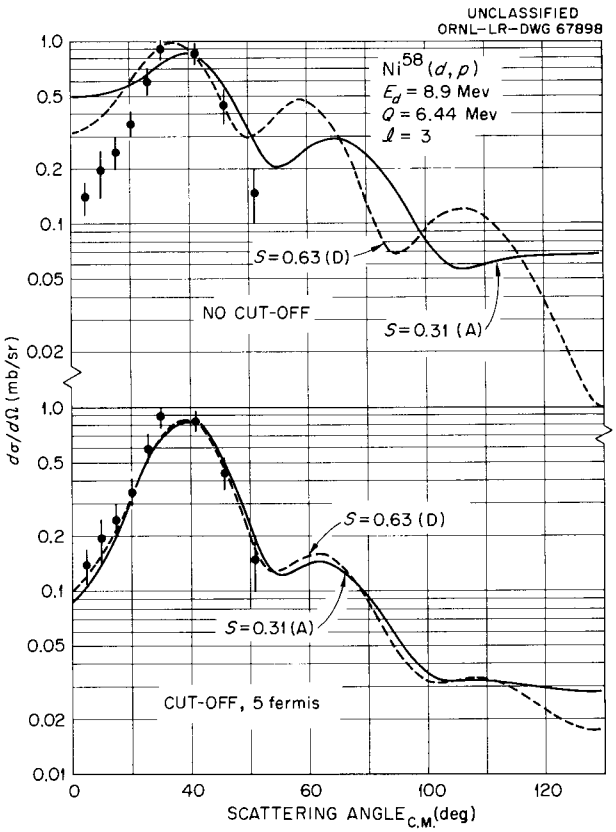

Fig. 2. Distorted-Waves Predictions with the Elastic Fits Shown in Fig. 1. The two potentials predict identical scattering at 8.9 Mev also.

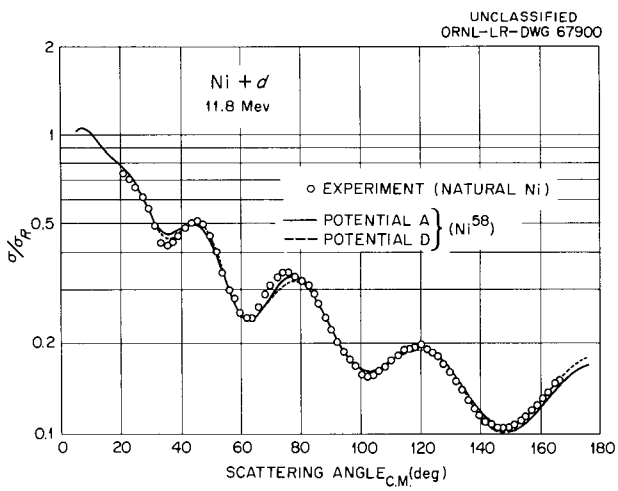

Fig. 1. Two Optical-Model Fits to Data on the Elastic Scattering of Deuterons from Nickel.

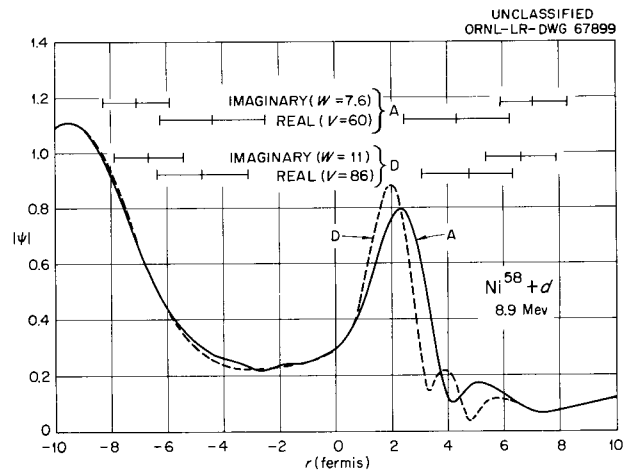

Fig. 3. Total Deuteron Wave Function Along the Incident-Beam Axis for the Potentials in Fig. 1. The center of the nucleus is at $r = 0$; negative r corresponds to the illuminated side of the nucleus.

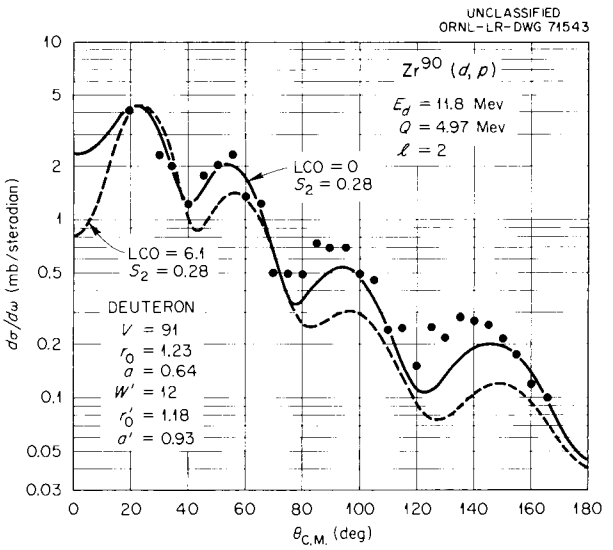

Fig. 4. Distorted-Waves Predictions for Zr(d,p) with a Potential Which Fits the Elastic Scattering of Deuterons at the Same Energy. LCO is the lower radial cutoff.

whose strength is known. For example, a preliminary analysis has been made of (d,d) and (d,p) data on Ca^{40} at 7 to 12 Mev and 21 Mev obtained recently at Argonne. In this case a radial cutoff is preferred, and good fits to the angular distributions are obtained; the average transition strength for $l = 3$ capture to the ground state of Ca^{41} was found to be 0.99 ± 0.25, which is in satisfactory agreement with the expected value of unity. Without a cutoff, this figure becomes 0.70 ± 0.23.

Distorted-waves calculations of stripping have so far used a "zero-range" approximation: the product of the n-p interaction and the internal deuteron wave function is replaced by a delta function. A DW code has now been written which dispenses with this approximation, albeit at an increase in computing time. Preliminary results indicate that "finite range" effects, while often not negligible, do not significantly change any of the results obtained in zero range. In particular, these effects seem to be quite small when a radial cutoff is employed and also, as expected, for low-Q reactions.

Similarly, it has been found that including spin-orbit coupling in the distorted waves produces quite small effects on the differential cross section. Of course, polarization predictions are sensitive to the spin-orbit coupling (Fig. 5) (and also to the use of a radial cutoff, see Fig. 6), but comparison with experiment is not too fruitful in the absence of information on the spin-orbit coupling for deuterons.

While there are still uncertainties in the detailed application of DW analysis, ratios of peak cross sections appear to be predicted with considerable accuracy, and different angular momentum transfers are readily identified (Fig. 7). For this reason several hundred calculations of stripping cross sections have been made in the past year for use by experimental groups, both in universities and at other national laboratories, in the analysis of their data.

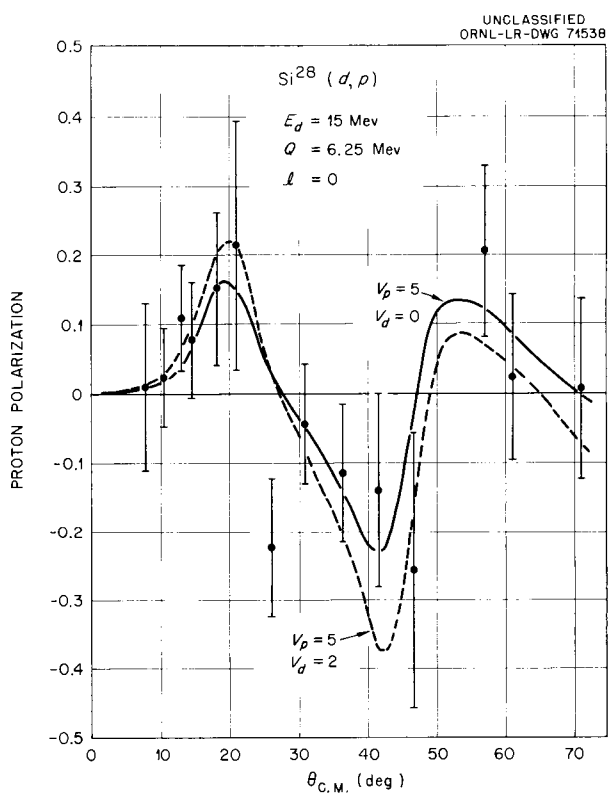

Fig. 5. Distorted-Waves Predictions for the Proton Polarization from Si^{28}(d,p). Results are shown for spin-orbit potentials of 2 and 5 and 0 and 5 Mev, for deuteron and proton respectively. No radial cutoff is employed.

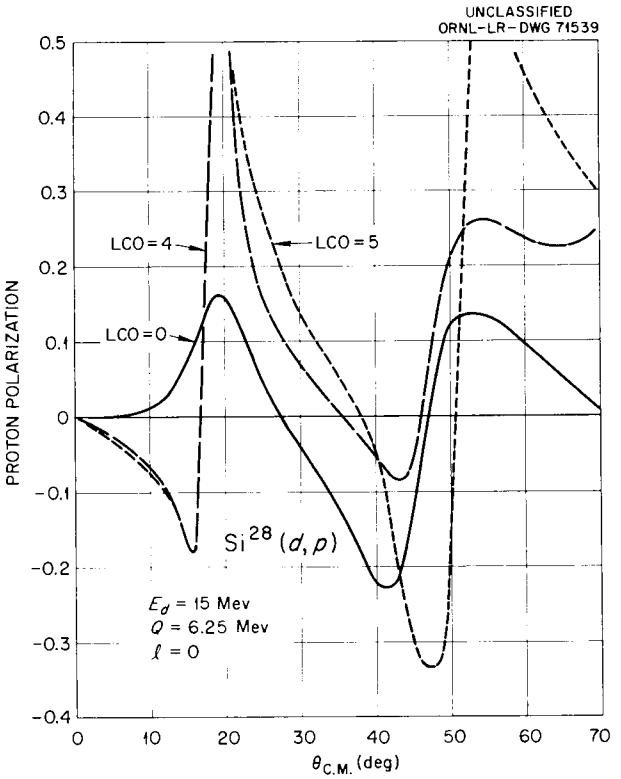

Fig. 6. Effect of Radial Cutoff (LCO) on the Polarization Predictions Shown in Fig. 5.

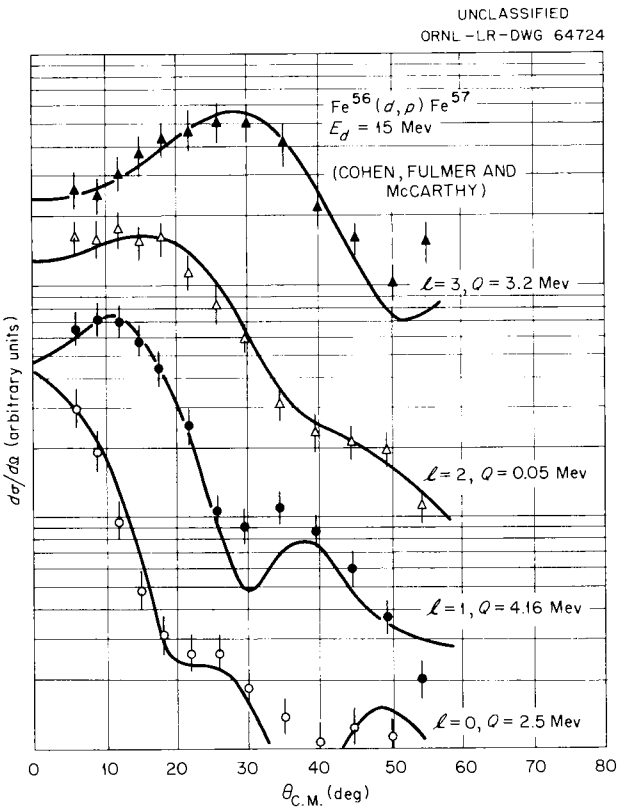

Fig. 7. Illustration of the Use of DW Curves to Identify l Values in (d,p) Reactions.

NUCLEAR SHELL-MODEL CALCULATIONS

J. N. Ginocchio[1] J. E. Rayburn[2] G. R. Satchler

A ladder process, devised by J. N. Ginocchio, for computing fractional parentage coefficients has been coded for the IBM 7090. One- and two-particle coefficients for n equivalent nucleons in an orbit j have been calculated for $n \leq 6$, $j \leq 7/2$, and those for $n = 7$ and 8 will be available shortly. The calculations are being extended to $j \leq 13/2$, at least for states of maximum isotopic spin and maximum-minus-one.

[1]Consultant, University of Rochester, Rochester, N.Y.

[2]Mathematics Division.

ANALYSIS OF PICKUP REACTIONS IN THE $A = 90$ REGION[1]

R. H. Bassel[2] R. M. Drisko[3] G. R. Satchler

The pickup of a $d_{5/2}$ neutron from Zr^{91}, Zr^{92}, Zr^{94}, Zr^{96}, and Nb^{93} was analyzed by distorted-wave approximation. Deuteron wave functions consistent with deuteron elastic scattering from zirconium were found to yield good agreement with neutron pickup from Zr^{90}, but the remaining analyses required slight modification of the deuteron optical potential. Spectroscopic factors for Zr^{92}, Zr^{94}, and Zr^{96} are in the ratio 1:2:3, as expected from the shell model.

[1]Abstract of paper to be published in *Proceedings of International Symposium on Direct Interactions and Nuclear Reaction Mechanisms*, Padua, Italy, 1962.

[2]Electronuclear Division.

[3]Presently at ORNL, Electronuclear Division. Permanent address: University of Pittsburgh, Pittsburgh, Pa.

THE REACTION $V^{51}(n,d)Ti^{50}$ AT 14.4 Mev[1]

K. Ilakovac[2] M. Petravic[2,3] P. Tomas[2]
L. G. Kuo[2,3] I. Slaus[2] G. R. Satchler

Measurements have been made of the differential cross sections for the $V^{51}(n,d)$ reaction at 14.4 Mev, which excites the 0^+, 2^+, 4^+, and 6^+ states in Ti^{50}. A distorted-waves Born approximation (DWBA) analysis of the results shows them to be consistent with the predictions of the simple shell model, that is, pure $(f_{7/2})^3$ configuration for V^{51} ground state, with seniority a good quantum number, within the uncertainties of both the experiment and the analysis. In particular, the data are consistent with pure $l = 3$ transitions, although small amounts of $l = 1$ pickup to the 2^+ and 4^+ states cannot be excluded. The uncertainties in the DWBA analysis, and their effects on quantitative determination of the spectroscopic factors, are fully discussed.

[1]Abstract of published paper: *Phys. Rev.* **128**, 2739 (1962).

[2]Institut "Ruder Boskovic," Zagreb, Yugoslavia.

[3]Present address: Physics Department, University of Birmingham, England.

ALPHA-GAMMA ANGULAR CORRELATIONS AND THE DISTORTED-WAVES THEORY[1]

D. K. McDaniels[2] D. L. Hendrie[2] R. H. Bassel[3] G. R. Satchler

The angular correlation between the inelastically scattered alphas and the 4.43-Mev gamma ray when C^{12} is bombarded with 42-Mev alphas was measured and analyzed in terms of the distorted-waves theory of direct interaction. The results depart strongly from the predictions of the plane-wave or adiabatic theories but are in good agreement with the distorted-waves theory.

[1]Abstract of published paper: *Phys. Letters* **1**, 295 (1962).

[2]University of Washington, Seattle.

[3]Electronuclear Division.

FLUCTUATIONS AND THE STATISTICAL MODEL OF NUCLEAR REACTIONS

D. M. Brink[1] G. R. Satchler

It has been emphasized by many authors that the use of any statistical theory of nuclear reactions also implies the existence of fluctuations in nuclear cross sections.[2] A qualitative discussion of these fluctuations for strongly overlapping resonances has been given by Ericson,[3] who emphasized that their observation gives a measure of the average compound-nucleus "lifetime." To study these effects in more detail, we take for the collision matrix the form

$$U = \overline{U} + \hat{U} ,$$

where $\overline{U}$ is the value of U averaged over an energy region $\delta \gg \Gamma$, the mean width of the compound states (we assume $\Gamma \gg D$, the mean spacing between compound levels), so that the average value of $\hat{U}$ is zero. We may then identify $\overline{U}$ with direct interactions (though this interpretation is not unique) and $\hat{U}$ with the fluctuating, or compound-nucleus, transitions. The term $\hat{U}$ can be written as a sum of contributions from different compound states; for transitions from channel α to channel β ("channel" includes angular momentum quantum numbers),

$$\hat{U}_{\alpha\beta} = i \sum_{\lambda} \frac{g_\alpha^\lambda g_\beta^\lambda - \overline{(g_\alpha^\lambda g_\beta^\lambda)}}{E - W_\lambda} , \qquad W_\lambda = E_\lambda + \frac{i}{2}\Gamma_\lambda .$$

The random sign (or statistical) assumption for the reduced widths which form part of the g_α^λ ensures that $\hat{U} = 0$ if averaged over $\delta \gg \Gamma$. For the same reason the interference terms between $\overline{U}$ and $\hat{U}$ vanish on average. The average cross section then can be written as the sum of a direct and compound part, $\overline{\sigma} = \sigma_D + \sigma_c$.

With this form for U it is straightforward to obtain expressions for the mean square deviation of the differential or integrated cross sections

$$\overline{(\sigma - \overline{\sigma})^2} \leqq \overline{\sigma}^2 - \sigma_D^2 .$$

If the particles are all spinless, the equality sign holds when σ is the differential cross section. The integrated cross section, however, shows less strong fluctuations; if N partial waves contributed equally, the left side would be $1/N$ times the right side. If the particles have spin, the transitions between different polarization states add incoherently, and the mean square deviations of both integrated and differential cross sections are reduced by, roughly,

$$\frac{2}{(2i_1 + 1)(2I_1 + 1)(2i_2 + 1)(2I_2 + 1)} .$$

Observation of the polarization of all the particles involved would restore the fluctuations to full strength.

The correlation between cross sections at different energies is of particular interest. The mean square deviation becomes

$$\overline{\sigma(E)\,\sigma(E + \Delta)} - \overline{\sigma(E)}^2 \leqq [\Gamma^2/(\Gamma^2 + \Delta^2)]\,[\overline{\sigma(E)}^2 - \sigma_D(E)^2] ,$$

where it is assumed that $\overline{\sigma(E + \Delta)} \approx \overline{\sigma(E)}$. This correlation immediately gives a measure of the mean lifetime $\hbar/\Gamma$ associated with the compound states. Another quantity of interest is the fluctuation in the back-forward asymmetry of the differential cross section. If there is no direct interaction contribution, this becomes, simply,

$$\overline{[\sigma(\theta) - \sigma(\pi - \theta)]^2} \leqq \overline{2\sigma(\theta)}^2 ,$$

where $\sigma(\theta) = \sigma(\pi - \theta)$. The equality sign holds approximately at $\theta = 0$ when all particles have zero spin, and, of course, the left side is zero at $\theta = \frac{1}{2}\pi$.

---

[1]Clarendon Laboratory, Oxford University, England.

[2]H. Feshbach, *Proceedings of Conference on Statistical Aspects of the Nucleus, Brookhaven,* 1955, BNL-331; C. E. Porter, *Proceedings of Conference on Neutron Interactions with the Nucleus, Columbia, 1957,* TID-7547; G. R. Satchler, *Proceedings of Conference on Reactions Between Complex Nuclei, Gatlinburg, 1958,* ORNL-2606.

[3]T. Ericson, *Advan. Phys.* **9**, 425 (1960).

LYAPUNOV'S STABILITY CRITERIA FOR PLASMAS[1]

T. K. Fowler

The orbit stability theory of Lyapunov has been adapted to the Vlasov-Boltzmann equation governing plasmas. Both linear and nonlinear stability are considered. The theory is characterized by a search for Lyapunov functions, whose existence implies stability in analogy with particles trapped in a potential well, as in the energy principle. The most important result is an existence theorem for Lyapunov functions quadratic in perturbations in all linearly stable cases in which perturbations damp asymptotically (sufficiently fast). As a corollary, without damping, the existence of a quadratic Lyapunov function is necessary and sufficient to prevent exponential growth of perturbations. A prescription is given for finding Lyapunov functions which are constants of motion. An example is treated. The implication of nonlinear stability from linear stability with damping is discussed, and C. S. Gardner's direct proof of nonlinear stability of a Maxwellian plasma by Lyapunov's method is reported.

[1]Abstract of a paper to appear in the April 1963 issue of the *Journal of Mathematical Physics.*

ON INTEGRATING THE VLASOV EQUATION[1]

T. K. Fowler

A first step in analyzing the stability of solutions of the Vlasov equation governing hot plasmas of low density is to solve the linearized equation for the perturbed space and velocity distribution function in terms of the perturbed electric and magnetic fields. This paper presents an explicit Green's function solution for the distribution, together with two samples of its use. The Green's function is found by first transforming to equilibrium constants of motion as variables.

[1]Abstract of a paper accepted for publication by the *Journal of Nuclear Energy: Part C.*

CORRECTION OF ELECTRON LENSES

T. A. Welton J. Kronsbein[1]

Many of the most important questions in modern biology could be answered much more easily if there were available a simple method for resolving the structure of complicated molecules. Where crystals are available, x-ray and electron diffraction, coupled with sophisticated interpretation methods, can yield a picture of the molecule with many of the atoms effectively resolved, hydrogen atom locations usually being obtained by inference because of the low scattering power of such light atoms. These methods, in combination with the existing arsenal of biochemical analytical techniques, have sufficed to elucidate the structure of several simple proteins, as well as the complicated and important DNA molecule.

It is then reasonable to inquire whether a supermicroscope can be built which is capable of di-

[1]Summer visitor, University of Florida.

rectly registering on a photographic emulsion an actual picture of a single organic molecule. It is known that (and understood why) no existing microscope or one using presently perfected principles can do this, but it is not at all clear that the problem is an impossible one.

One most ingenious approach to the problem has been made by Müller[2] with his field ion microscope. This very simple device allows single atoms to be resolved, providing they are atoms of a hard metal (platinum, tungsten, rhodium, etc.) which has been formed into a sharp point. Although this device produces extremely fine pictures at very low cost, it is, unfortunately, not at all applicable to organic molecules. We have accordingly chosen to study the potentialities of the transmission electron microscope and the transmission proton microscope, each of which offers the desired potentiality.

The electron microscope in its present state of development is routinely able to resolve structures with a separation of between 8 and 10 A. It has long been known that this resolution limit is set by the irreducible spherical aberration of an electron objective lens, in combination with the diffraction blurring of the image. In the conventional electron objective, the magnetic (or electric, if desired) field is invariant under rotation about the axis of the instrument. The object is located very close to this axis, and only rays which make small angles with the symmetry axis are accepted by the focusing system. If the angular half-aperture (at the object) is α radians, and if all rays within this angular range emanating from a point object were to be precisely focused at an image point on the axis, assuming geometrical optics to hold, then the apparent diameter of the diffraction disk at the object position is approximately

$$d_D = \frac{0.30}{\alpha V^{1/2}} \text{ A} . \tag{1}$$

Here V is the energy of the incident electron beam in kilovolts, and the angle α is assumed to be small compared with unity, as is always the case in practice.

If this were the only limit on the resolving power, reasonable choices for V and α could reduce d_D to 1–2 A, and individual atoms could be resolved. Unfortunately, it has been shown by Scherzer[3] that *any* electron lens of this axially symmetric, paraxial type is necessarily subject to an aberration which is analogous to the spherical aberration of conventional optics but which differs from it in several essential respects. The spherical shape of the surfaces of an ordinary lens causes rays emanating from an axial object point, at a varying angle with the axis, to focus at a varying image distance. In the optical microscope this aperture defect (as it more generally can be called) causes no limitation on resolution, since the usual process of correction compounds positive and negative lenses with different focal lengths and aberrations to achieve a focusing element with an arbitrarily small aperture defect.

As Scherzer showed theoretically and as much subsequent work has verified, the aperture defect of the conventional electron objective (arising from the requirement that the lens magnetic field must satisfy the static Maxwell equations for free space) cannot be eliminated. The apparent diameter, in the object plane, of the circle of confusion due to the aperture defect is

$$d_A = Cf\alpha^3 \times 10^8 \text{ A} , \tag{2}$$

where C is a dimensionless coefficient (necessarily positive) which depends on the shape (but not the strength) of the lens field, and f is the focal length of the objective in centimeters.

A simple approximation for the diameter of the composite circle of confusion is

$$d = d_A + d_D . \tag{3}$$

This is minimized with respect to the aperture α by taking

$$d_A = \frac{1}{3} d_D \tag{4}$$

and

$$\alpha^4 = 10^{-9}(Cf)^{-1} V^{-1/2} , \tag{5}$$

which yield

$$d = 71(Cf)^{1/4} V^{-3/8} . \tag{6}$$

For a magnetic lens (the electrostatic lens being not normally competitive), the minimum feasible

[2]E. Müller, *Z. Physik* **131**, 136 (1951).

[3]O. Scherzer, *Z. Physik* **101**, 593 (1936).

focal length is proportional to V, being approximately given by

$$f = \frac{V}{200} \tag{7}$$

for a lens with iron pole pieces and nonrelativistic V. By combination of Eqs. (5), (6), and (7), there result

$$d = 19C^{1/4}V^{-1/8} \tag{8}$$

and

$$\alpha = 2.1 \times 10^{-2}\, C^{-1/4}V^{-3/8} . \tag{9}$$

Estimates by Rebsch[4] give approximately 0.2 for the minimum value of C, while V should not be increased beyond 50 kv, if reasonable contrast is to be achieved for very small structures. These values yield

$$d = 7.7 \text{ A} \tag{10}$$

and

$$\alpha = 0.72 \times 10^{-2} \text{ radian} . \tag{11}$$

It is important to note that none of the essential factors involved in these estimates enter in a sensitive fashion, and it is therefore not easy to imagine reducing d by the factor of 3 or 4 required to resolve individual atoms in molecules. If, for example, a superconducting magnet can be used, it is reasonable to assume that the maximum magnetic field can be increased by a factor of 4. The coefficient of V in Eq. (7) could then (in principle at least, although the tolerances then become very close) be reduced by a factor of 16. The effect on Eq. (8) is to reduce the coefficient 19 by a factor of 2, so that the final result, Eq. (10), becomes not yet small enough to resolve adjacent atoms.

Another improvement which is possible in principle is to substitute protons for electrons. The coefficient in Eq. (1) should be decreased by a factor of 43 ($= \sqrt{1840}$), and the coefficient in Eq. (7) should be increased by 1840. The net result is a decrease in the coefficient of Eq. (8) by a factor of $1840^{1/8}$ or 2.56. This is not enough in itself to yield the desired resolution, but the superconducting magnet can now be used without going to forbiddingly small dimensions and close tolerances. The final result (for $C = 0.2$) is

$$d = 2.5V^{-1/8} , \tag{12}$$

from which it is found that $d = 2$ A for $V = 6$ kv. At this energy a proton has a velocity of only about one-half the mean electronic velocity in a normal hydrogen atom and is thus unlikely to remove or excite electrons in the molecule under study. In the electron case the incident particles will always be easily capable of removing or exciting electrons, so that molecular dissociation may take place before image formation.

The work reported here has proceeded on the assumption that either the proton or the electron microscope would gain importantly in resolution if the aberration law in Eq. (2) could be altered in form. Note that a simple reduction in the value of C is unlikely to be strongly beneficial, because of the low power of C in the final result. Rather, a technique for true correction of a magnetic lens (analogous to the correction of optical lenses) is sought, in order that Eq. (2) may be replaced by a higher-order law such as

$$d_A = Cf\alpha^4 \times 10^8 \text{ A} , \tag{13}$$

or

$$d_A = Cf\alpha^5 \times 10^8 \text{ A} , \tag{14}$$

for example.

A technique which appears very promising, although conclusive results have not yet been obtained, has been devised for this purpose and briefly reported.[5] Briefly, the paraxial assumption (all rays making a small angle with the symmetry axis), combined with the assumption of the current-free static Maxwell equations, allows the deduction of Eq. (2), with a necessarily positive value of C, in a very few lines.[3] If it is now assumed that only those rays emanating from an axial object point are retained which make initial angles with the axis between $\beta - \alpha$ and $\beta + \alpha$, then it becomes a very complex matter to prove any assertion as to the form of the aberration. Our failure to produce any such proof (after diligent effort) has led us to surmise that the coefficient C in Eq. (2) can actually be reduced to zero by the

[4] R. Rebsch, *Ann. Physik* **31**, 551 (1938).

[5] T. A. Welton and J. Kronsbein, *Am. Phys. Soc. Bull.* **6**, 29 (1961).

use of *annular optics*, as this configuration is conveniently termed.

In annular optics, either an axially symmetric magnetic or electric field may be used, just as in paraxial optics. A new and possibly useful alternative now exists for the arrangement of the focusing fields. Because only an annulus of the lens is needed for trajectories, field-shaping structures (electrodes, dielectric material, or ferromagnetic material) can now be placed within the annulus of focused rays. This alternative (with electric focusing) has been chosen recently by Wilska[6] for an annular instrument which is presently under development.

It is our belief that this alternative is relatively less promising than another, which will be explained. The reason is that axial symmetry is very difficult to maintain when a structure must be supported within the annular ray region. This is particularly true with electric fields, since no structural material exists which will not strongly perturb an electric field and the supports cannot be axially symmetric and still leave an open annulus for the rays. Such inner field shaping is probably possible in the magnetic case because of the availability of structural materials which are magnetically equivalent to vacuum. One qualification is, however, necessary. The inner field shaping should be done with permeable or remanent materials, rather than with currents, since the current leads would tend to destroy the axial symmetry.

If a single lens element, without inner field shaping, is used to focus an annular bundle of rays, it is easily shown that the radius of the circle of confusion has the form

$$d_A = Cf\alpha^2 \times 10^8 \text{ A} , \qquad (15)$$

where C is apparently necessarily positive. The purpose of inner field shaping is to cancel this aberration completely and replace it by an expression identical with Eq. (2).

We have shown that a reduction to the cubic form, Eq. (2), can be made equally well in principle (and probably preferably in practice) by combining two annular, *externally* shaped lenses in sequence. These must be separated axially by a sufficient distance to allow an intermediate focus *between* them. This intermediate focus must be annular in character; that is, if $R(z)$ is the radius of the central ray of the annular bundle and $r(z)$ is the radius of a deviated ray of the bundle, then $r(z) = R(z)$, but $R(z) \neq 0$. It is easily seen that for a system without magnification, the two lenses must be equal and symmetrically located with respect to the object and image points.

It is not at all clear that the coefficient of the resulting cubic aberration must be nonzero, and we have undertaken a computational program to explore this question. An IBM 7090 program has been written and thoroughly tested for tracing rays through a series of as many as six annular lenses. Each lens has an arbitrary strength, an axial location, and a singularity-free radius. The flux density along the axis has the form

$$B(z) = \sum_{i=1}^{6} \frac{b_i}{\{[(z - z_i)/a_i]^2 + 1\}^2} , \qquad (16)$$

and simple, exact algebraic expressions for the off-axis field components are used, which satisfy the current-free, static Maxwell equations except on certain singular surfaces. For the ith lens this singular surface is a sheet of current in the θ direction, located in the plane $z = z_i$ and extending from $r = a_i$ to $r = \infty$. It is anticipated that this degree of flexibility will allow the cubic aberration to be canceled exactly, if this is possible in principle.

The program has been checked by numerical verification of the analytically calculable properties (focal length and cubic aberration) of a single, paraxial lens. Extensive tables have been prepared of the properties of nonparaxial rays in the field of a single lens of the type used in Eq. (16) for all reasonable values of the parameters a and b. Practically, the properties of rays passing through several successive lenses can often be estimated to useful accuracy from such single-lens tables, and the difficulty of the numerical search problem can be thereby much reduced. Further calculations are in progress on the generalized two-lens problem, with no definitive results yet available.

[6] A. P. Wilska, *Norelco Reptr.* **8**, 115 (1961).

CHARGED-PARTICLE NUCLEAR CROSS-SECTION COMPILATION

F. K. McGowan W. T. Milner H. J. Kim

A literature search of nuclear cross sections for charged-particle-induced reactions has been completed for 1948–1962. The bibliography contains abstracts of all the papers from this literature search. Most of the materials from requests for either reprints, tabular data, larger graphs of results, or Xerox copies of the papers have been received for the very light elements and for the elements manganese through tin.

Data for manganese, iron, cobalt, nickel, copper, and zinc are being compiled in tabular form. In many cases data read from small figures in the published papers with the X-Y point plotter are in analog form. Computer programs have been written and are running to process the analog information and to make transformations from the laboratory frame of reference to the center-of-mass system. The program will also generate a magnetic tape for the Calcomp 570 digital plotter, which plots the data in the desired form for the compilation. To this end, special semilog graph paper, which permits angular distributions to be plotted on an 8½- by 11-in. format size, has been procured.

A bibliography of charged-particle cross-section information relating to Apollo vehicle materials was supplied to Atomics International. In addition, copies of 125 papers not accessible to Atomics International were supplied.

THE LIFETIME OF THE Λ^0 HYPERON[1]

M. M. Block R. Gessaroli[2] S. Ratti[3]
Northwestern University

L. Grimellini T. Kikuchi[4] L. Lendinara L. Monari
University of Bologna

E. Harth W. Becker
Syracuse University

W. M. Bugg H. Cohn
Oak Ridge National Laboratory

The mean lifetime of the Λ^0 particle is not yet well known. The latest summary on the subject[5] shows essentially two groups of experiments in considerable disagreement, the first leading to $\tau = (2.29 \pm 0.15) \times 10^{-10}$ sec and the other to $\tau = (2.72 \pm 0.16) \times 10^{-10}$ sec. This indicated the necessity of a careful measurement of the Λ^0 lifetime with increased statistical accuracy and with particular attention paid to possible sources ot bias and background contamination.

A beam of stopping K^- mesons in the helium bubble chamber ($10 \times 12.5 \times 20$ cm operated in a 14,000-gauss magnetic field) provided a copious source of low-momentum Λ^0 hyperons with a mean momentum of about 250 Mev/c. Because of the low average momentum, the mean potential time is about five times the lifetime, and the corresponding corrections are small.

A carefully selected sample of 2239 Λ^0 decays yielded a mean lifetime $\tau = (2.36 \pm 0.06) \times 10^{-10}$ sec.

---

[1]Abstract of a paper submitted to the *Physical Review* for publication.

[2]Now at the University of Bologna, Italy.

[3]On leave of absence from the University of Milan, Italy. NATO Science Fellowship.

[4]Now at Northwestern University, Department of Physics.

[5]*Proceedings of the 10th International Conference on High Energy Physics, University of Rochester, 1960*, p 879, Interscience, New York; also *1958 Proceedings*, p 279.

ELASTIC SCATTERING OF ALPHA PARTICLES BY O^{18}

R. D. Powers[1]
J. K. Bair
J. L. C. Ford, Jr.
H. B. Willard

The differential elastic scattering cross section of alpha particles by O^{18} has been measured for alpha-particle energies between 2.4 and 3.5 Mev and for $\theta_{c.m.}$ = 90, 125.3, 140.7, and 164.37° in order to determine the level parameters of excited states in Ne^{22}. Thin targets (<2 kev for 2.4-Mev alphas) of O^{18} were prepared by oxidizing tung-

[1]Summer research participant from Baylor University, Waco, Tex.

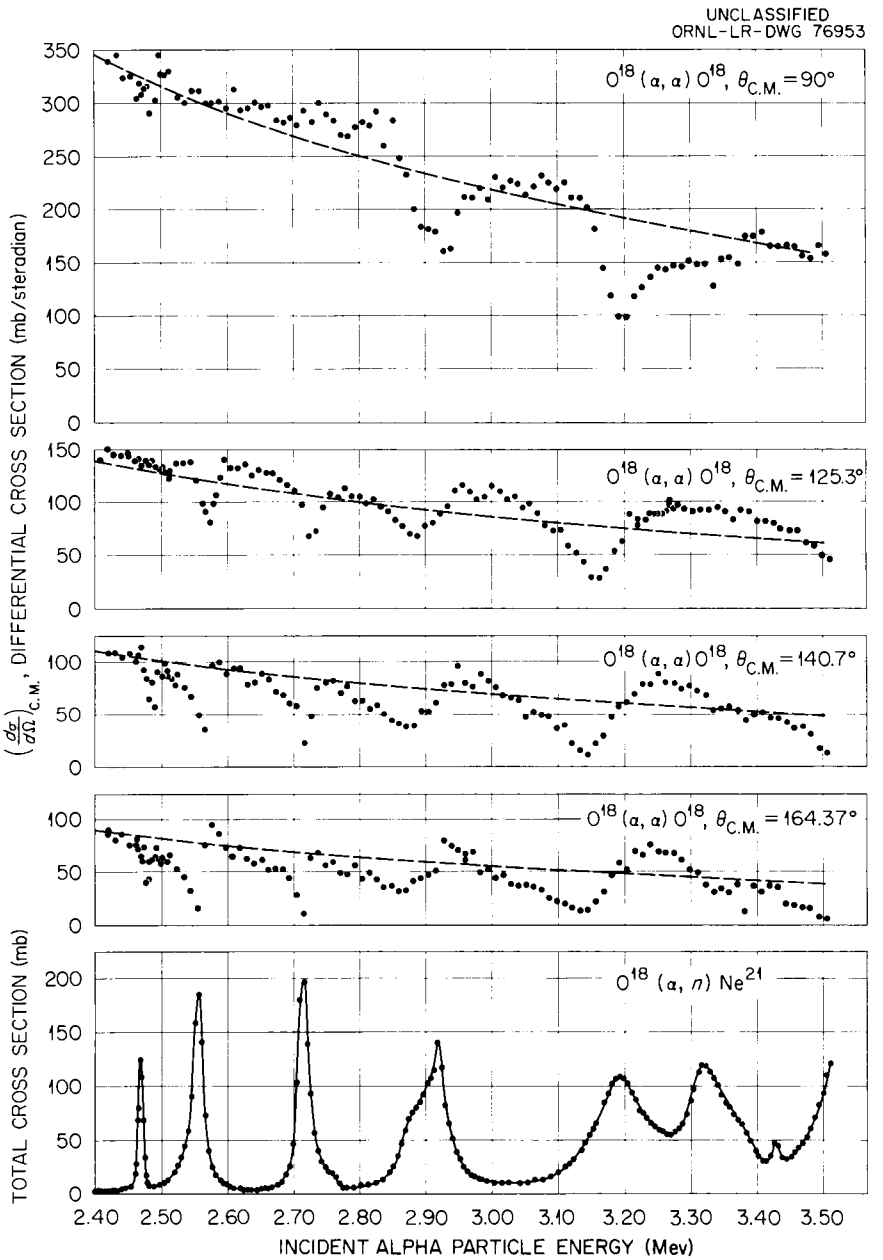

Fig. 1. Yield of the $O^{18}(\alpha,\alpha)O^{18}$ and $O^{18}(\alpha,n)Ne^{21}$ Reactions.

sten in an H_2O^{18} atmosphere and then by evaporating the tungsten oxide onto thin carbon backings. The scattered alpha particles were measured at 90 and 125.3° with a double-focusing uniform-field reaction-product magnet. The data at the backward angles were measured with a movable solid-state counter mounted in the scattering chamber. Previous work[2] on the $O^{18}(\alpha,n)Ne^{21}$ reaction indicates eight resonances in the above energy range corresponding to excitation energies in Ne^{22} between 11.686 and 12.38 Mev. Six of these eight resonances have been observed in the scattering data (see Fig. 1); preliminary results give $J^{\pi} = 2^+, 1^-, 1^-, 0^+, 0^+$, and 2^+, corresponding to the resonances at $E_{\alpha}^{lab} = 2.47, 2.57, 2.72, 2.90, 3.19$, and 3.32 Mev respectively. Qualitative fits to the data using dispersion theory have been obtained for three of the six levels.

[2]J. K. Bair and H. B. Willard, *Phys. Rev.* **128**, 299 (1962).

ELASTIC SCATTERING OF ALPHA PARTICLES FROM Si^{28}

J. K. Bair H. B. Willard

Previous data on the scattering of alpha particles by Si^{28} have been reported[1] using targets about 12 kev thick for 3-Mev alpha particles. These preliminary data have been rerun with improved resolution using targets about 3 kev thick for 3-Mev alpha particles, as shown in Fig. 1. Whereas the original data indicated only four prominent resonances in the energy region covered, the higher resolution data show a far more complex structure, as might be expected from the $P^{31}(p,\alpha)Si^{28}$ data of Clarke *et al.*[2] The general trend of the $\phi_{c.m.} = 90°$ data agrees with the theoretical variation of the Coulomb scattering cross section with energy, and the numbers appearing on the curve as "relative cross section" can be interpreted as millibarns per steradians on this basis. It should be pointed out that with this normalization the experimental cross section at 2 Mev appears to be about twice the calculated Coulomb value.

[1]H. B. Willard and J. K. Bair, *Bull. Am. Phys. Soc.* **7**, 73 (1962).

[2]R. L. Clarke, E. Almqvist, and E. B. Paul, *Nucl. Phys.* **14**, 472 (1960).

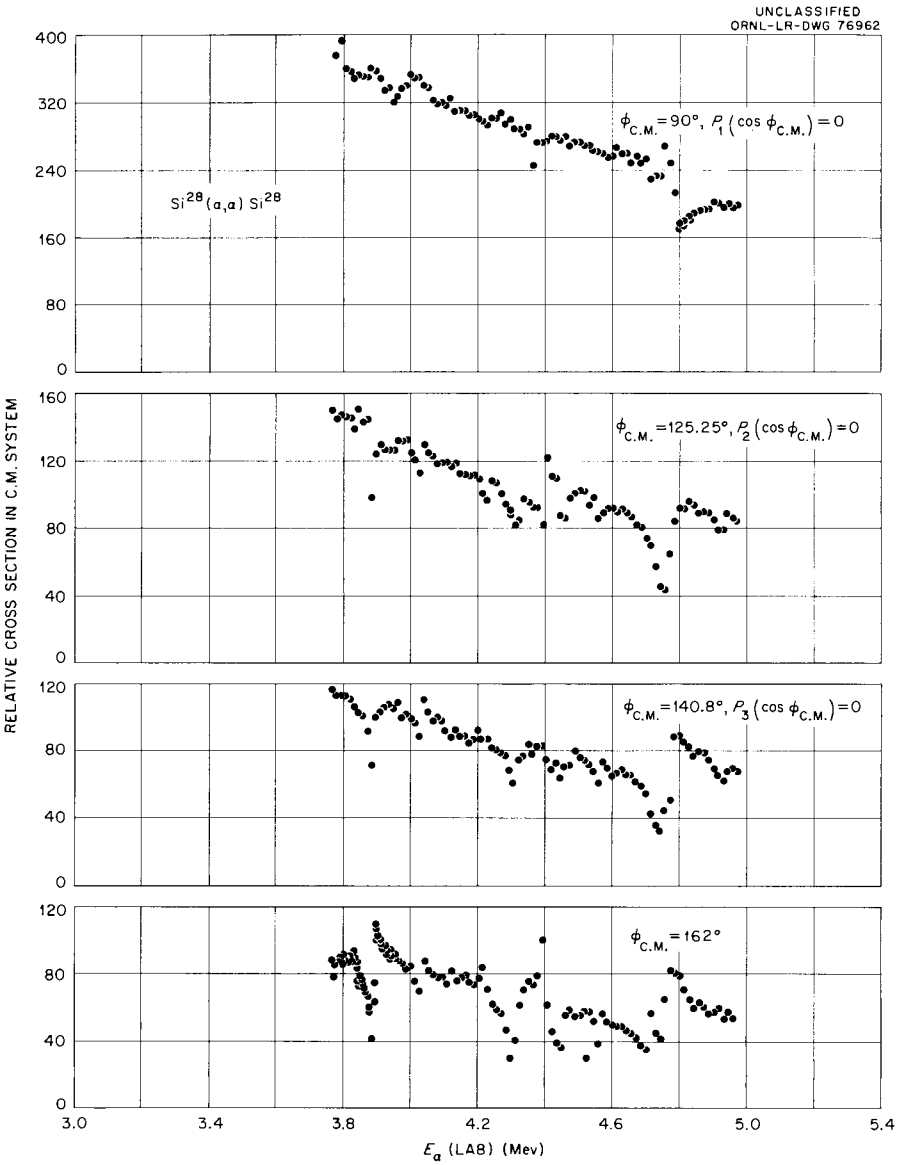

Fig. 1. Yield Curve of the $Si^{28}(\alpha,\alpha)Si^{28}$ Reaction.

THE $O^{18}(\alpha,p)F^{21}$ REACTION AND THE BETA DECAY OF F^{21}

H. B. Willard
J. K. Bair
J. L. C. Ford, Jr.
C. M. Jones

The reaction $O^{18}(\alpha,p)F^{21}$ has been studied for alpha bombarding energies from 8 to 10 Mev by observing the betas following F^{21} decay. Doubly ionized helium ions were produced in the 5.5-Mv Van de Graaff, and the betas were detected in approximately 2π geometry by a 1.25-in.-diam

1-in.-long anthracene crystal in conjunction with an electrostatic beam deflector and an electronic timer.[1] Targets were prepared by anodizing tantalum blanks with water enriched to 97% in O^{18}.[2] The energy loss of 8-Mev alphas in the anodized layer of these targets was about 75 kev.

An early study[3] of the F^{21} produced by the $F^{19}(t,p)F^{21}$ reaction inside a reactor indicated a half-life of 5 ± 1 sec. According to mass tables,[4] the maximum energy available for beta decay is 5.683 ± 0.008 Mev. The beta spectrum observed with the anthracene crystal employed in this experiment is shown in Fig. 1, where the data were taken at an alpha energy of 9.7 Mev and a cycle period of 5 sec (2.5 sec beam on, 2.5 sec beam off and count gate open).

Measurements of the F^{21} half-life were carried out for pulse-height biases greater than 0.6, 1.2, and 1.8 Mev. A typical run is shown in Fig. 2. The average value of the half-life for F^{21} beta decay as determined from several runs at the three biases is 4.3 ± 0.2 sec.

The relative cross section for the $O^{18}(\alpha,p)F^{21}$ reaction was obtained by measuring the yield of betas with energy greater than 1 Mev and a cycling period of 5 sec. The results are shown in Fig. 3 for alpha energies between 8 and 10 Mev. This

[1] P. H. Stelson and E. C. Campbell, *Phys. Rev.* **106**, 1252 (1957).

[2] J. K. Bair and H. B. Willard, *Phys. Rev.* **128**, 299 (1962)

[3] E. C. Campbell and J. E. Strain, *Phys. Div. Quart. Progr. Rept. Dec. 20, 1952*, ORNL-1496, pp 9–10.

[4] T. Lauritsen and F. Ajzenberg-Selove, *Energy Levels of Light Nuclei*, National Bureau of Standards, Washington, D.C., 1962.

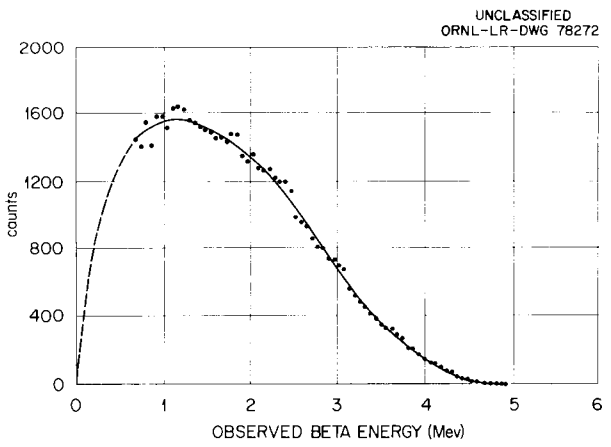

Fig. 1. The $F^{21}(\beta^-)Ne^{21}$ Beta-Ray Spectrum as Observed with a 1.25 × 1.0 in. Anthracene Crystal.

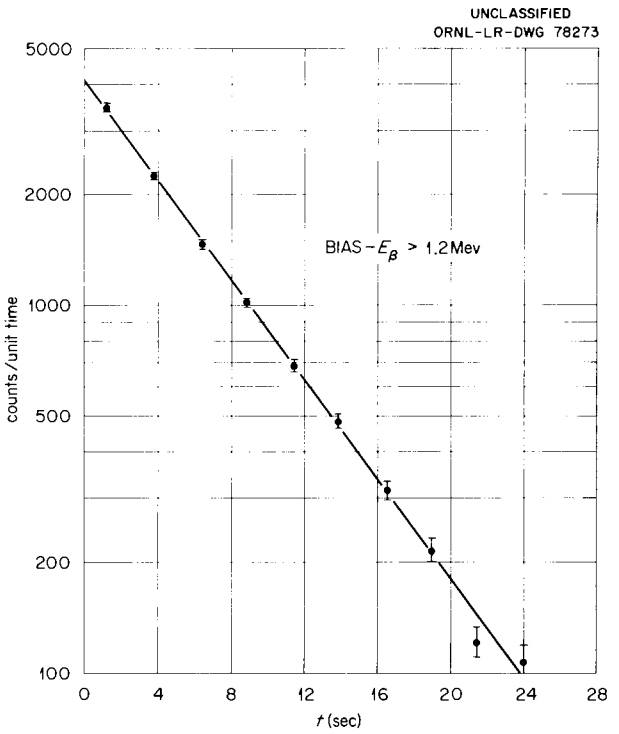

Fig. 2. Typical Measurement of the $F^{21}(\beta^-)Ne^{21}$ Decay.

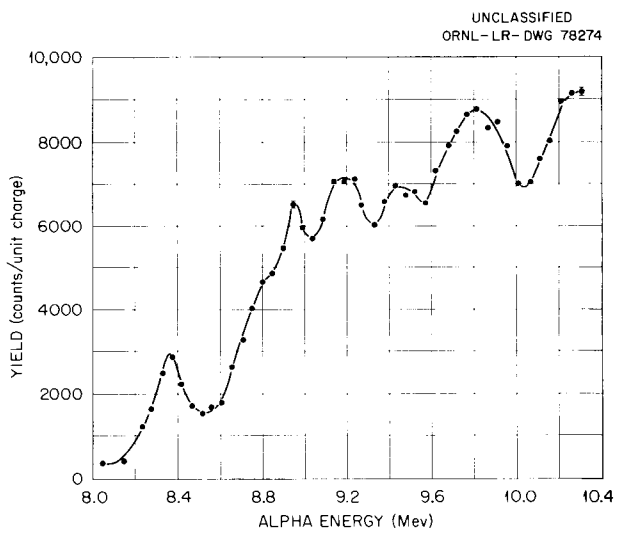

Fig. 3. Relative Cross Section for the $O^{18}(\alpha,p)F^{21}$ Reaction As Obtained by Measuring the Yield of Betas with Energy Greater than 1 Mev and a Cycling Period of 5 sec.

reaction should have a threshold of about 6.85 Mev, as determined from the mass tables.[4] However, the Coulomb barrier for the outgoing proton inhibits the cross section near threshold. The resonance structure observed is, in general, wider than the experimental resolution.

TOTAL (p,n) CROSS SECTIONS FOR LIGHT-ELEMENT TARGETS IN THE BOMBARDING ENERGY RANGE 5 TO 15 Mev

J. K. Bair C. M. Jones H. B. Willard

A study has been made of experimental problems associated with using the graphite-sphere neutron detector[1] in conjunction with the ORNL Tandem Van de Graaff to measure total (p,n) cross sections for light-element targets in the bombarding energy range 5 to 15 Mev. The principal problem is the high neutron background associated with the high-energy proton beam. The following techniques were used to minimize this background.

The graphite sphere was located in a room which was well shielded from the accelerator, the analyzing magnet, and the second 90° "deflecting" magnet. After emerging from this second magnet, the beam was passed through a concrete wall and focused by a magnetic quadrupole lens onto a thin target at the center of the graphite sphere. After emerging from the target, the beam was collected in a cup located approximately 9 ft from the center of the sphere. The rear of this cup was lined with Ni^{58}, and the cup was surrounded by a cylinder of lithiated paraffin of length and diameter about 3 ft. Careful control was exercised over the position and focal properties of the beam to ensure that it did not strike the walls of the vacuum system or the target frame. This was done primarily by viewing the beam size and position on pneumatic quartzes with closed-circuit television. The graphite sphere was covered with a thin sheet of cadmium.

Preliminary yield curves have been measured in the energy range 4.5 to 12.5 Mev with targets of Li^6, Li^7, Be^9, B^{11}, and natural carbon. These measurements indicate that for targets whose thickness is less than 50 $\mu g/cm^2$, the background problem will not be severe. The principal sources of neutron background appear to be (1) neutrons produced by the $C^{13}(p,n)$ reaction in the C^{13} present in the natural carbon target backings, (2) neutrons produced in the walls of the vacuum system due to angular dispersion of the beam after passing through the target, and (3) neutrons produced in the beam collecting cup. The relative contributions of these sources have not yet been determined.

To facilitate this determination and to provide a means of easily measuring background while taking data, a new target chamber is now being constructed. This chamber will have four movable target holders whose position will be adjustable from outside the vacuum system. In addition, the chamber is being equipped with a small surface-barrier detector located at an angle of approximately 165° with respect to the beam. By observing elastically scattered protons, this detector will provide spectroscopic information about the targets under study.

---

[1] R. L. Macklin, *Nucl. Instr.* 1, 335 (1957).

NUCLEAR RESONANCE EFFECTS IN COULOMB EXCITATION

J. K. Bair
J. L. C. Ford, Jr.
R. L. Robinson
H. B. Willard

The modification of the Coulomb-excitation process due to nuclear forces has been studied by several authors.[1,2] Excitation of a state in a target nucleus, by means of inelastic scattering proceeding through the formation of a compound nucleus, may interfere with the Coulomb excitation of this state, modifying the form of the angular distributions of the inelastically scattered particles and gamma rays emitted as well as the shape of the resonance observed in the total inelastic cross section. As the well-resolved resonances in the $Na^{23}(p,p')$ reaction at 0.871 Mev and in the $F^{19}(p,p')$ reaction at 0.780 Mev are situated upon continua which have been fitted with an $E2$ Coulomb-excitation curve,[3,4] these reactions would appear to be favorable cases for the observation of such an interference effect.

The total cross section for the $Na^{23}(p,p')$ reaction has been measured between proton energies of 0.840 and 1.100 Mev by detecting the 0.439-Mev gamma radiation emitted from the first excited state of Na^{23} in a 3- by 3-in. NaI crystal mounted in essentially 2π geometry. The yield of the 0.198-Mev gamma ray emitted from the second excited state of F^{19} was measured in the $F^{19}(p,p')$ reaction. The NaCl and CaF_2 targets evaporated onto thick tantalum backings were approximately 4 kev thick, whereas the natural widths of the resonances are between 7.5 and 10 kev.

Primarily because of the low counting rate, the present $Na^{23}(p,p')$ data are not sufficiently accurate to measure the estimated asymmetry of 10% introduced in the total cross section by the interference term. The measurement of the resonance shape for the $F^{19}(p,p')$ reaction is facilitated by a greatly increased counting rate. However, in this case the effect of the nearby resonance at 0.831 Mev makes an unambiguous interpretation of the shape difficult.

[1]T. A. Griffy and L. C. Biedenharn, *Nucl. Phys.* **32**, 273 (1962).

[2]M. Micu, Abstract 134, *Proceedings of International Symposium on Direct Interactions and Nuclear Reaction Mechanisms*, Padua, Italy, 1962; private communication, 1962.

[3]G. M. Temmer and N. P. Heydenburg, *Phys. Rev.* **104**, 989 (1956).

[4]C. A. Barnes, *Phys. Rev.* **97**, 1226 (1955).

COULOMB EXCITATION WITH Ne^{20} IONS[1]

R. C. Ritter[2]
P. H. Stelson[3]
F. K. McGowan
R. L. Robinson

Neon ions with energies ranging from 8 to 15 Mev have been obtained by the acceleration of doubly and triply charged ions in a 5.5-Mv Van de Graaff. These projectiles have been used to study Coulomb excitation in 18 nuclei ranging from Li^7 to Th^{232}. In particular, the levels of Ti^{47}, V^{51}, Fe^{57}, Ni^{61}, Zn^{67}, Ge^{73}, and As^{75} were investigated. The spin of the 320-kev state of V^{51} is uniquely assigned as $\frac{5}{2}$ and the mixing ratio $\delta = (E2/M1)^{1/2}$ is 0.52 ± 0.07. Strong evidence is found against previous assignments of $\frac{5}{2}$ for the spin of the 184-kev state in Zn^{67}. The yields and angular distributions of the gamma rays require spin assignments of $\frac{3}{2}$ and $\frac{1}{2}$ for the 184- and 93-kev states, respectively, in Zn^{67}.

[1]This work is based upon a thesis submitted by R. C. Ritter to the Graduate School of the University of Tennessee in partial fulfillment of the requirements for the Ph.D. degree; abstract of published paper: *Phys. Rev.* **128**, 2320 (1962).

[2]Oak Ridge Institute of Nuclear Studies Predoctoral Fellow. Present address: Department of Physics, University of Virginia, Charlottesville.

[3]Presently on leave at the William Marsh Rice University, Houston, Tex.

LOW-LYING LEVELS OF Cu^{63} AND Cu^{65}

R. L. Robinson F. K. McGowan P. H. Stelson[1]

The single-particle–core coupling model would be expected to be most applicable to nuclei which have one odd particle beyond a closed shell. We have investigated the low-lying level properties of two such nuclei, Cu^{63} and Cu^{65}, by means of the Coulomb-excitation process and compared the results with this model.[2–4]

Coulomb excitation was effected with 4- to 8-Mev alpha particles that were obtained from the 5.5-Mv Van de Graaff generator. Thick targets of Cu^{63} and Cu^{65} which were each isotopically enriched to more than 97% were used. The resulting gamma rays were detected with a 3 × 3 in. NaI scintillation spectrometer. Examples of the gamma-ray spectra are shown in Figs. 1 and 2. In each spectrum the yields of the gamma rays were determined and compared with the excitation functions predicted for Coulomb excitation. It was found from these comparisons that only the transitions in the Cu^{63} spectra at 668, 961, 1323, and 1412 kev and in the Cu^{65} spectra at 771, 1115, and 1474 kev could be attributed to Coulomb excitation of these nuclei. The relative yields of these transitions are shown in Figs. 3 and 4 as a function of the energy of the bombarding particles. The solid curves give the energy dependence predicted for the yields of gamma rays from electric quadrupole ($E2$) Coulomb-excited states with energies ΔE above the ground state.

Spectra in coincidence with the 668- and 961-kev gamma rays of Cu^{63} and the 771- and 1115-kev gamma rays of Cu^{65} were investigated for an alpha-particle energy of 5.58 Mev. A 364-kev transition was found in coincidence with the 961-kev transition. Its energy indicates it de-excites the level at 1323 kev. From its intensity the ratio of cascade-to-crossover gamma rays from this level

[1]Presently on leave at William Marsh Rice University, Houston, Tex.

[2]R. D. Lawson and J. L. Uretsky, *Phys. Rev.* **108**, 1300 (1957).

[3]A. de Shalit, *Phys. Rev.* **122**, 1530 (1961).

[4]M. Bouten and P. Van Leuven, *Nucl. Phys.* **32**, 499 (1962).

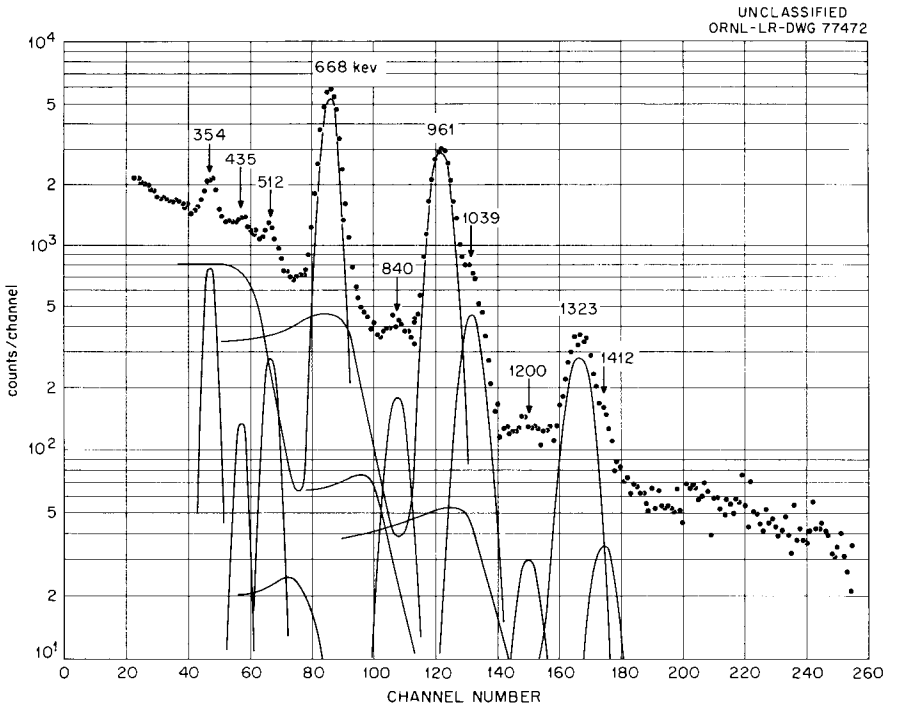

Fig. 1. Gamma-Ray Spectrum for 6.56-Mev Alpha Particles on Cu^{63}.

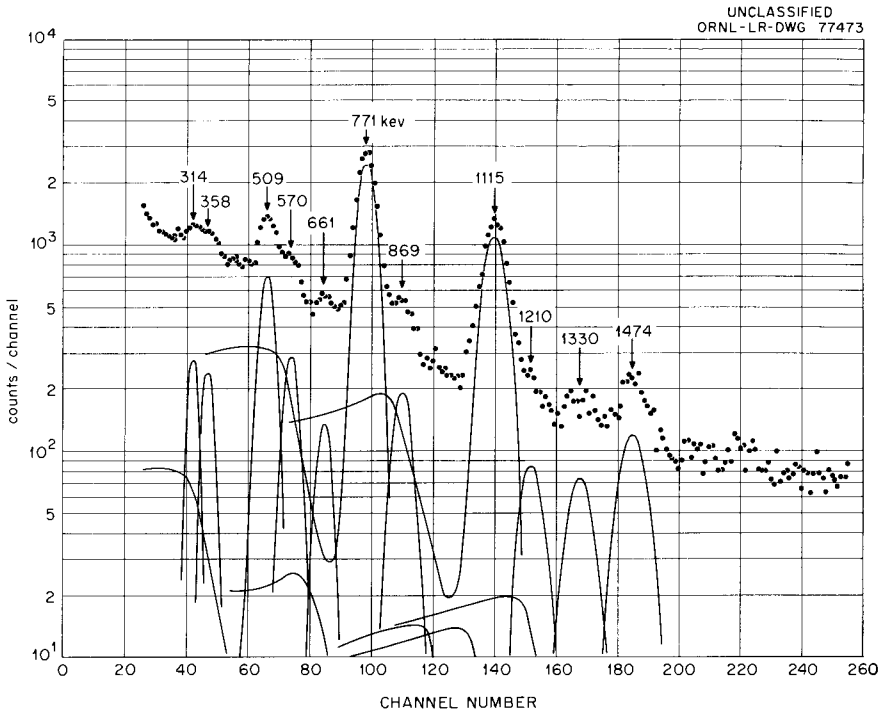

Fig. 2. Gamma-Ray Spectrum for 6.56-Mev Alpha Particles on Cu^{65}.

was estimated to be 0.17 ± 0.04. In Cu^{65} an analogous transition was observed with an energy of 355 kev in coincidence with the 1115-kev gamma ray. Its intensity gives a value of 0.16 ± 0.09 for the cascade-to-crossover branching ratio of gamma rays from the 1474-kev level. No other transitions of copper were seen in the coincidence spectra.

Angular correlations of several gamma rays have been measured relative to the direction of the incident beam. The results are listed in Table 1. In two cases where data were only taken at the two angles 0 and 90°, the ratio $R = W(0°)/W(90°)$ is given. In the other cases, data were taken at ten angles and fitted to the equation $W(\theta) = 1 + a_2 g_2 A_2 P_2(\cos\theta) + a_4 g_4 A_4 P_4(\cos\theta)$, where a_ν and g_ν are the thick target particle parameters[5,6] and the corrections for the finite angular resolution of the detector[7] respectively.

The isotropic distributions observed for the 668- and 771-kev transitions are compatible with previous spin assignments of ½ for levels of these energies.[8] The angular correlation coefficients uniquely establish the spins of the 961-kev level in Cu^{63} and 1115-kev level in Cu^{65} as ⅝. Of the two values of δ, where $\delta^2 = E2/M1$, for the 961-kev transition consistent with these measurements, only one is in agreement with the half-life of the 961-kev level.[9] This value of δ and the more probable value for the 1115-kev transition are listed in Table 2. The angular correlation results indicate that the level at 1323 kev in Cu^{63} has a spin of ⅞.

From the gamma-ray yields the reduced transition probabilities for excitation, $B(E2)_{ex}$, have been extracted by a procedure discussed previously.[10] These are given in column 3 of Table 2. In column 7 of this table the $B(E2)$'s for decay, as obtained for the spins of the excited states

[5] K. Alder *et al.*, *Rev. Mod. Phys.* **28**, 432 (1956).

[6] F. K. McGowan and P. H. Stelson, *Phys. Rev.* **106**, 522 (1957).

[7] M. E. Rose, *Phys. Rev.* **91**, 610 (1953).

[8] J. B. Cumming, A. Schwarzschild, A. W. Sunyar, and N. T. Porile, *Phys. Rev.* **120**, 2128 (1960).

[9] *Nuclear Data Sheets*, National Academy of Sciences, National Research Council, U.S. Government Printing Office, Washington, D.C.

[10] F. K. McGowan and P. H. Stelson, *Phys. Rev.* **116**, 154 (1959).

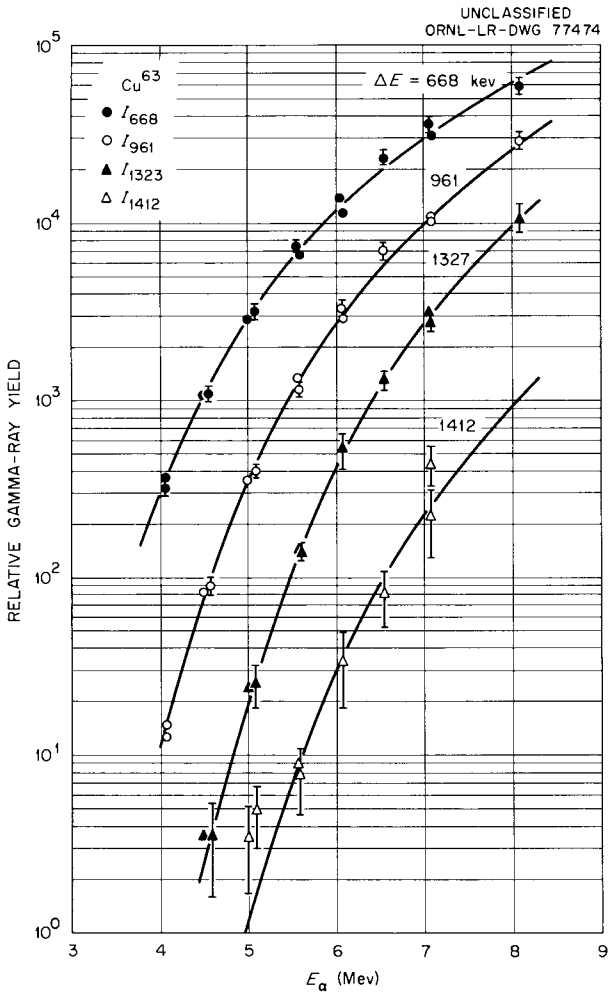

Fig. 3. Relative Yields of the Cu^{63} Gamma Rays as a Function of Alpha-Particle Energy.

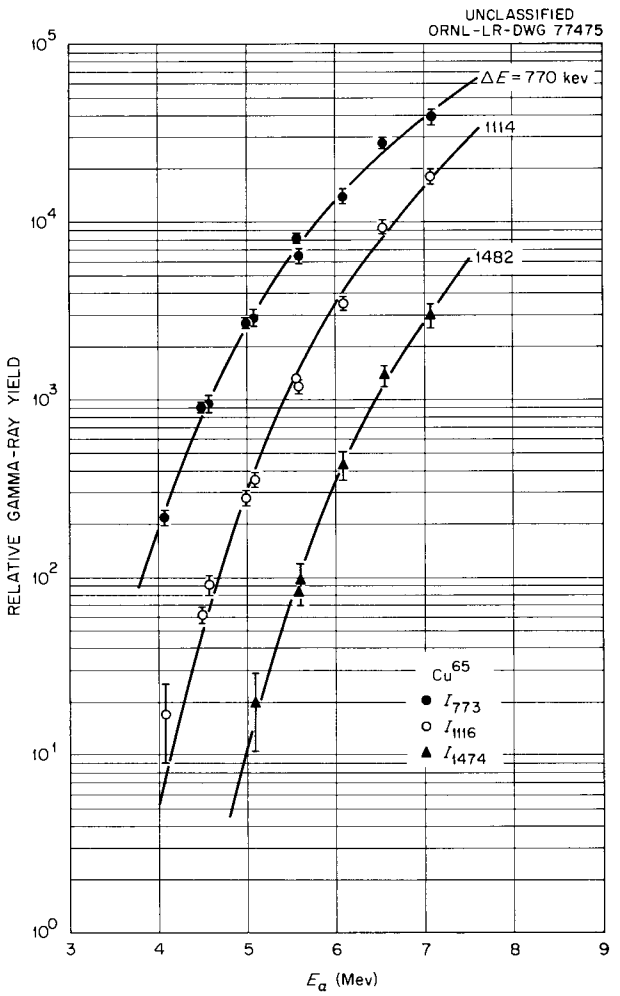

Fig. 4. Relative Yields of the Cu^{65} Gamma Rays as a Function of Alpha-Particle Energy.

Table 1. Angular Correlation Results

E_α(Mev)	E_γ(kev)	R	$a_2 g_2 A_2$	A_2
Cu^{63}				
5.04	668		+0.004 ± 0.012	+0.005 ± 0.014
5.54			+0.016 ± 0.020	+0.019 ± 0.024
5.04	961		−0.187 ± 0.018	−0.186 ± 0.018
5.54			−0.171 ± 0.020	−0.180 ± 0.021
5.54	1323		+0.252 ± 0.050	+0.24 ± 0.05
6.08		1.216 ± 0.139		+0.14 ± 0.09[a]
7.08		1.297 ± 0.061		+0.20 ± 0.04[a]
Cu^{65}				
5.54	771		+0.004 ± 0.016	+0.005 ± 0.018
	1115		−0.141 ± 0.016	−0.142 ± 0.016

[a]In obtaining this value, $a_4 g_4 A_4 = -0.01$.

Table 2. Summary of Level and Gamma-Ray Properties

E(kev) Present	E(kev) Mazari *et al.*[a]	$B(E2)_{ex}/e^2$ (cm^4)	Relative Error (%)	Absolute Error (%)	I_f	$B(E2)_d/e^2$ (cm^4)	$B(E2)_d/B(E2)_{sp}$	δ	$B(M1)_d/(e\hbar/2Mc)^2$	$T_{1/2}$(sec)
		$\times 10^{-50}$				$\times 10^{-50}$				
Cu^{63}										
364 ± 8									0.21 ± 0.06	
668 ± 4	668 ± 5	1.16		± 10	$\frac{1}{2}$	2.32	16		0.6	
961 ± 6	961 ± 5	3.49	± 6	± 10	$\frac{5}{2}$	2.33	16	$-0.41^{+0.07}_{-0.11}$	$0.09^{+0.04}_{-0.03}$	$\left(4.3^{+2.1}_{-1.6}\right)\times 10^{-13}$
1323 ± 16	1327 ± 5	4.15	± 8	± 12	$\frac{7}{2}$	2.08	14			$(5.7 \pm 0.8)\times 10^{-13}$
1412 ± 25	1412 ± 5	0.91	± 15	± 22	$\frac{3}{2}$	0.91	6			$<1.2\times 10^{-12}$
Cu^{65}										
355 ± 8									0.35 ± 0.20	
771 ± 7	770 ± 4	1.02		± 11	$\frac{1}{2}$	2.04	13		0.5	
1115 ± 11	1114 ± 4	3.47	± 6	± 11	$\frac{5}{2}$	2.31	15	-0.22 ± 0.06	$0.4^{+0.4}_{-0.2}$	$\left(6.5^{+0.4}_{-0.2}\right)\times 10^{-14}$
1474 ± 19	1482 ± 4	3.99	± 12	± 17	$\frac{7}{2}$	2.00	13			$(3.5 \pm 0.7)\times 10^{-13}$

[a]M. Mazari, W. W. Buechner, and R. P. de Figueiredo, *Phys. Rev.* **108**, 373 (1957). Because of the smaller errors, their energy values were used in the determination of the thick target integrals.

shown in column 6, are listed. Since Cu^{63} and Cu^{65} appear to have similar low-lying level structures, the spin for the 1474-kev level has been taken as $\frac{7}{2}$. A spin of $\frac{3}{2}$ has been tentatively assigned to the 1412-kev level of Cu^{63}. For this value the four low-lying levels would have the spins suggested by the single-particle–core coupling model.[2,3] In column 8, the $B(E2)_d$'s are compared with the single-particle estimate as given by the equation $B(E2)_{sp} = (e^2/4\pi)|\frac{3}{5} R_0^2|^2$. The value of R_0 was taken as $1.2 \times 10^{-13} A^{1/3}$ cm. The $B(M1)_d$'s given in column 10 are approximately in single-particle units. For the 961- and 1115-kev transitions they were deduced from the δ's in column 9 and from the $B(E2)_d$'s. Those shown for the 668- and 771-kev transitions were obtained from the $B(E2)_d$'s and reported half-lives[9,11] for the corresponding levels. The $B(M1)_d$'s for the 364- and 355-kev transitions were determined from the $B(E2)_d$'s of the 1323- and 1474-kev transitions and from the ratio of cascade-to-crossover gamma rays from levels of these energies. It was assumed that the $B(E2)_d$'s of the 364- and 355-kev transitions were less than $100B(E2)_{sp}$. The final column of Table 2 contains the half-lives of the levels as found from the present measurements.

The similarity of the $B(E2)_d$'s for three transitions in Cu^{63} and for three transitions in Cu^{65} is in agreement with the predictions of the single-particle–core coupling model discussed by de Shalit.[9] This model also predicts that the $B(E2)_d$'s should be equal to the $B(E2)_d$'s of the $2^+ \longrightarrow 0^+$ transitions in neighboring even-even nuclei. For one such nucleus, Ni^{62}, the $B(E2)_d$ of this transition is $1.7 \times 10^{-50}\ e^2\ cm^4$.[12] The smaller value obtained for the $B(E2)_d$ of the 1412-kev state in Cu^{63} can result from the admixture of this state with the ground state.[13] Admixtures of states may also account for the relatively large values found for the $B(M1)_d$'s of the ground-state transitions. This was considered by Bouten and Van Leuven,[4] who extended the single-particle–core coupling model. Using this model they determined values of 0.3 and 0.09 $(eh/2Mc)^2$ for the $B(M1)_d$'s of the 668- and 961-kev transitions of Cu^{63} respectively.

[11] E. C. Booth, *Bull. Am. Phys. Soc.* **5**, 239 (1960).

[12] P. H. Stelson and F. K. McGowan, *Nucl. Phys.* **32**, 652 (1962).

[13] A. Braunstein and A. de Shalit, *Phys. Letters* **1**, 264 (1962).

COULOMB EXCITATION OF NUCLEAR STATES IN THE ISOTOPES OF OSMIUM

F. K. McGowan
P. H. Stelson[1]
R. L. Robinson
J. L. C. Ford

In the transition between a region of rotational spectra and a region of near-harmonic spectra, the asymmetric rotor model of Davydov and Filippov[2] (D-F) fits energy-level spectra with rather striking success. However, the deviations are still several times larger than the experimental errors.[3] A comparison of the experimental and the theoretical values for relative transition probabilities usually requires the asymmetry parameter gamma to be 2 to 4° less than the one required to fit the energy levels in this transition region. This shift in the value of gamma is in the direction expected when

[1] Presently on leave at the William Marsh Rice University, Houston, Tex.

[2] A. S. Davydov and C. F. Filippov, *Nucl. Phys.* **8**, 237 (1958).

[3] G. T. Emery *et al.*, *Proceedings of Conference on Electromagnetic Lifetimes and Properties of Nuclear States*, p 246, Nuclear Science Series Report No. 37, NAS-NRC Publication No. 974, Washington, D.C., 1962; BNL-6507; to be published in *Physical Review*.

the coupling between rotational and beta-vibrational motion is included.[4]

The validity of the asymmetric rotor model has been questioned by many people who point out that many of the predictions of the D-F model near $\gamma = 0$ and $30°$ are also in quantitative agreement with the symmetric rotor and the vibrational models, respectively, with appropriate refinements. In this transition region, the asymmetric rotor explains, however, more experimental data with fewer adjustable parameters.

The osmium nuclei offer a good test of the D-F model because the asymmetry parameter gamma is large and the equilibrium shape may still be well defined (small rotation-vibration interaction). Coulomb-excitation measurements have been made by proton and alpha-particle bombardment of metallic targets enriched in the different isotopes of osmium. The $B(E2)$'s for excitation of the first and second 2^+ states in the even-A nuclei have been obtained from the gamma-ray yields. The $B(E2, 0 \rightarrow 2)$ values for Os^{188}, Os^{190}, and Os^{192} are larger than the single-particle estimate by factors ranging from 70 to 100. The $B(E2, 0 \rightarrow 2')$ for the second 2^+ is about 0.1 of the $B(E2, 0 \rightarrow 2)$. The sign of $\delta = (E2/M1)^{1/2}$ in the $2' \rightarrow 2$ transition deduced from an analysis of the three-stage correlation $p\gamma\gamma(\theta)$ $[0(E2)2'(E2 + M1)2(E2)0]$ is negative for $Os^{188,190,192}$. The $B(M1)$ values obtained are exceedingly small, being about 10^{-3} times the single-particle estimate.

Figure 1 is an up-to-date plot of the ratio $B(E2,2' \rightarrow 2)/B(E2,2 \rightarrow 0)$ vs the parameter gamma in the asymmetric rotor model of D-F. Values of gamma are assigned from the ratio of the energies of the second $2'^+$ and the first 2^+ states. In those cases where a 0^+ excited state is known,

[4] A. S. Davydov and A. A. Chaban, *Nucl. Phys.* **20**, 499 (1960).

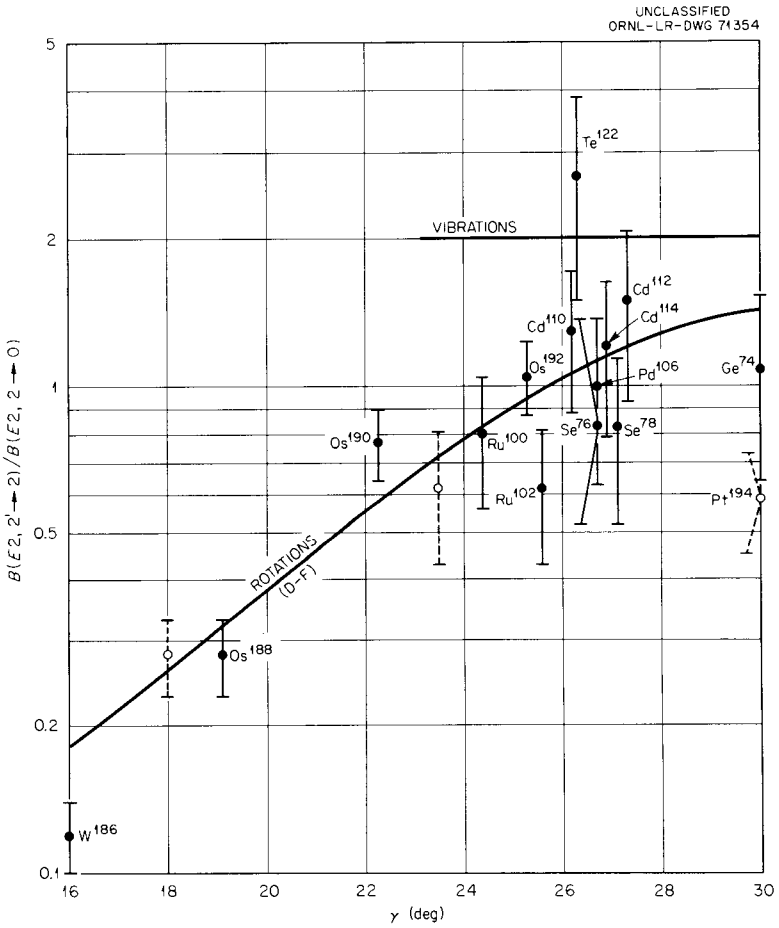

Fig. 1. Plot of the Ratio $B(E2, 2' \rightarrow 2)/B(E2, 2 \rightarrow 0)$ as a Function of the Parameter Gamma. The Davydov-Filippov model predicts the curve labeled rotations.

the influence of the rotation-vibration interaction is included. These cases are indicated by dash points. The overall agreement of the predictions by the D-F model with the results from $Os^{188,190,192}$ is good.

The results from Coulomb excitation of states in Os^{187} are shown in Fig. 2. Very extensive results on the properties of nuclear energy levels in Os^{187} and Os^{189} have been deduced from radioactive decay studies by Harmatz *et al.*[5] We have relied heavily on their relative intensities for the transitions from the decay of these states to deduce the total $B(E2)$'s for excitation. The $B(E2, \frac{1}{2}^{L} \rightarrow \frac{5}{2}^{L})$ and $B(E2, \frac{1}{2}^{L} \rightarrow \frac{3}{2}^{H})$, where L and H refer to lower and higher bands, are not uniquely determined. For instance, if we assume only direct excitation of the $\frac{5}{2}^{L}$ state at 75.05 kev the resulting $B(E2)$ is $9.0 \times 10^{-48}\, e^2\, cm^4$ which is about 3 times the total quadrupole strength expected for Os^{187}. On the other hand, if we assume only direct excitation of the $\frac{3}{2}^{H}$ state at 74.35 kev the resulting $B(E2)$ is $0.75 \times 10^{-48}\, e^2\, cm^4$. We have with some arbitrariness assigned 10% of the observed gamma radiation to direct excitation of the $\frac{5}{2}^{L}$ state. The resulting total quadrupole strength for Os^{187} is in agreement with the strength for the neighboring even-even nuclei.

Figure 3 summarizes the $B(E2)$'s for the transitions in the decay of the states which are Coulomb-excited in Os^{187}. The spin assignments for the states are those proposed by Harmatz *et al.* Those assignments are based on a comparison of their results on the properties of the levels with the predictions of the Nilsson model.[6] It is well known[7] that it is possible to interpret the spectra of odd-*A* deformed nuclei in quite great detail in terms of rotational bands associated with the different states of binding of the last odd nucleon.

The moment of inertia of the ground-state band $K = \frac{1}{2}^{-}$ is at least a factor of 2 too large and the $B(E2)$'s for decay from states in the $K = \frac{3}{2}^{-}$ band to states in the $K = \frac{1}{2}^{-}$ band are about 100 times too large. These discrepancies are, however, something one would like to understand if the spectra are to be interpreted in terms of a symmetric rotor model. A rotation-particle coupling (RPC) calculation has been carried out for several

[5] B. Harmatz, T. H. Handley, and J. W. Mihelich, *Phys. Rev.* **128**, 1186 (1962).

[6] S. G. Nilsson, *Kgl. Danske Videnskab. Selskab, Mat.-Fys. Medd.* **29**(16), 1–68 (1955).

[7] B. R. Mottelson and S. G. Nilsson, *Kgl. Danske Videnskab. Selskab, Mat.-Fys. Skrifter* **1**(8), 1–105 (1959).

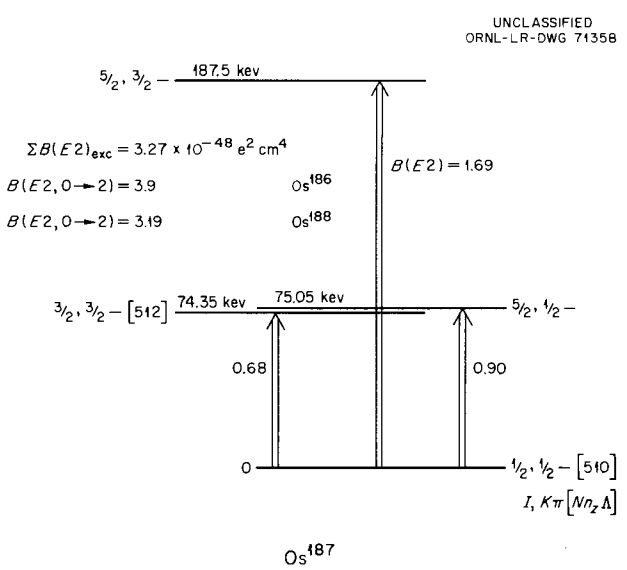

Fig. 2. Nuclear States Excited in Os^{187} by Coulomb Excitation.

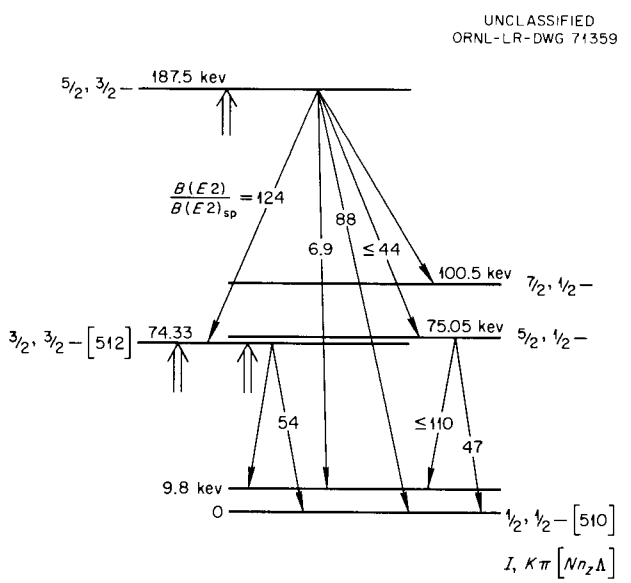

Fig. 3. Summary of the $B(E2)$ Values Expressed in Units of $B(E2)_{sp}$ for the Transitions in the Decay of States Which Are Coulomb-Excited in Os^{187}.

amplitudes of mixing resulting from the effect of the Coriolis force.[8] The relative $B(E2)$'s for transitions from the $\frac{5}{2}^{H}$ state to various members of the $K = \frac{1}{2}^{-}$ band are reproduced fairly well for the square of mixing amplitudes taken to be ~10%. But the magnitudes of the $B(E2)$'s from the RPC calculation are a factor of 6 too small. We have examined the extreme case where the interacting particle states are almost degenerate and the mixing is fifty-fifty. With complete mixing the $B(E2, \frac{5}{2}^{H} \rightarrow \frac{1}{2}^{L})$ is still 60% too small. In addition the positions of the $\frac{7}{2}^{L}$ and $\frac{7}{2}^{H}$ states are missed by 50 kev and the moment of inertia is about 30% too large.

The situation in Os^{189} (see Figs. 4 and 5) is very much like that in Os^{187} (i.e., large cross-over $E2$ transition probabilities to the ground state). Since this is the most characteristic feature of the spectrum, it must be concluded that the symmetric rotor model with RPC included does not fit the low-lying levels of Os^{187} and Os^{189}.

[8] A. K. Kerman, *Kgl. Danske Videnskab. Selskab, Mat.-Fys. Medd.* **30**(15), 1–25 (1956).

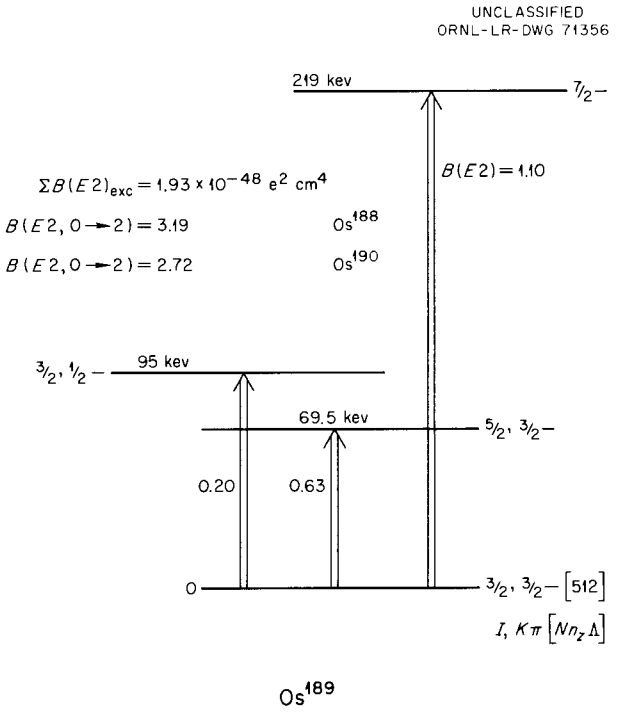

Fig. 4. Nuclear States Excited in Os^{189} by Coulomb Excitation.

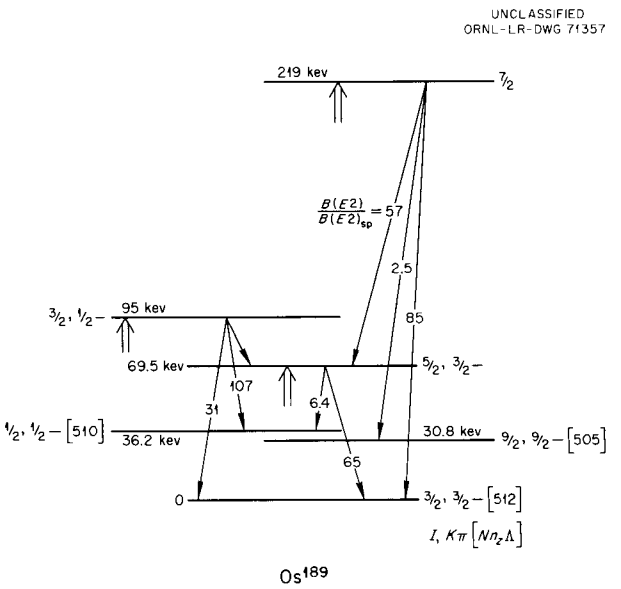

Fig. 5. Summary of the $B(E2)$ Values Expressed in Units of $B(E2)_{sp}$ for the Transitions in the Decay of States Which Are Coulomb-Excited in Os^{189}.

GAMMA-GAMMA ANGULAR CORRELATION IN V^{51}

R. L. Robinson N. R. Johnson[1] G. D. O'Kelley[1]

The nucleus V^{51} has the relatively simple structure of three $f_{7/2}$ particles beyond a doubly magic core configuration. According to the *jj* coupling shell model, the three $f_{7/2}$ particles can couple to give levels with spins of $\frac{3}{2}$, $\frac{5}{2}$, $\frac{7}{2}$, $\frac{9}{2}$, $\frac{11}{2}$, and $\frac{15}{2}$. For a nucleus like V^{51}, which has a ground-state spin of $\frac{7}{2}$ (ref 2), this model predicts that the first and second levels will have spins of $\frac{5}{2}$ and $\frac{3}{2}$ respectively.[3,4] Ritter *et al.*[5] have verified this prediction for the spin of the first level in V^{51} at 319 kev by means of Coulomb-excitation studies.

It has been suggested that the second level of the $(f_{7/2})^3$ configuration is the one observed[6] at 933 kev. In an effort to ascertain the nature of this level, we investigated the angular correlation of the 613-319-kev gamma-ray cascade which de-excites it. This study was made with the 5.8-min isotope Ti^{51}. It was produced by irradiation of normal titanium in the Oak Ridge Graphite Reactor. The gamma rays were detected with two 3 × 3 in. NaI crystals which were each placed 10 cm from the source. One detector with its associated electronics was adjusted to accept gamma rays

[1]Chemistry Division.

[2]B. Bleaney, D. J. E. Ingram, and H. E. Scovil, *Proc. Phys. Soc.* **64A**, 601 (1951).

[3]Dieter Kurath, *Phys. Rev.* **80**, 98 (1950).

[4]A. R. Edmonds and B. H. Flowers, *Proc. Royal Soc. (London)* **A215**, 120 (1952).

[5]R. C. Ritter *et al.*, *Phys. Rev.* **128**, 2320 (1962).

[6]J. E. Schwäger, *Phys. Rev.* **121**, 569 (1961).

Table 1. Angular Correlation of the 613-319-kev Gamma-Ray Cascade

For the theoretical coefficients, δ_{319} was taken as +0.52

	δ_{613}	A_2	A_4
Experimental			
Solid source		+0.025 ± 0.038	−0.05 ± 0.07
Liquid source		+0.002 ± 0.038	−0.02 ± 0.06
Average		+0.013 ± 0.030	−0.03 ± 0.05
Theoretical			
$\frac{1}{2}(Q)\frac{5}{2}(D+Q)\frac{7}{2}$		−0.394	−0.02
$\frac{3}{2}(D+Q)\frac{5}{2}(D+Q)\frac{7}{2}$	+0.18	+0.013	0.00
	−9.3	+0.013	+0.02
$\frac{5}{2}(D+Q)\frac{5}{2}(D+Q)\frac{7}{2}$	−0.41	+0.013	0.00
	+6.3	+0.013	−0.01
$\frac{7}{2}(D+Q)\frac{5}{2}(D+Q)\frac{7}{2}$	−0.085	+0.013	0.00
	−4.5	+0.013	0.00

with energies between 302 and 336 kev. Spectra in coincidence with these gamma rays were taken at 10° intervals for angles from 90 to 180° between the two detectors. A least-squares fit of the data was made to the equation $W(\theta) = 1 + A_2P_2(\cos\theta) + A_4P_4(\cos\theta)$ on an IBM 7090 computer.

The experimental angular correlation coefficients which have been corrected for the finite angular resolution of the detectors are listed in Table 1. Those obtained with the solid and liquid sources are in good agreement. In order to deduce information about the 613-kev transition from these coefficients, it is first necessary to know the character of the 319-kev transition. Ritter *et al.*[5] reported a value of $+0.52 \pm 0.07$ for the mixing ratio of the 319-kev gamma ray, δ_{319}, where $\delta = (Q/D)^{1/2}$. With this admixture a comparison has been made between the theoretical and experimental coefficients for spins of the 933-kev level which are consistent with an $E2$-$M1$ character for the 613-kev transition. The theoretical coefficients are included in Table 1. Values listed for δ_{613} give theoretical A_2's that are identical to the measured A_2. It can be seen that the correlation results are in agreement with a spin assignment of $\frac{3}{2}$, $\frac{5}{2}$, or $\frac{7}{2}$ for the 933-kev level. Spin $\frac{7}{2}$, however, has been ruled out by beta decay studies.[7,8]

If the level has spin $\frac{3}{2}$, as expected for the second excited state of the $(f_{7/2})^3$ configuration, the correlation coefficients are compatible with a δ_{613} of $+0.18$ or -9.3. For these values and a half-life for the 933-kev level of 4×10^{-12} sec, which was determined from Coulomb-excitation results,[9] the 613-kev $E2$ transition probability is, respectively, 1 and 32 times that given by the single-particle model. For these two δ_{613}'s the $M1$ transition probability is smaller than the single-particle estimate by factors of 170 and 14,000. For pure jj coupling, the $M1$ transition probability would vanish for transitions between two states with the same configuration of identical nucleons.

[7] W. C. Jordon, S. B. Burson, and J. M. LeBlanc, *Phys. Rev.* **96**, 1582 (1954).

[8] M. E. Bunker and J. W. Starner, *Phys. Rev.* **97**, 1272 (1955).

[9] *Nuclear Data Sheets*, National Academy of Sciences, National Research Council, U.S. Government Printing Office, Washington, D.C. An average value for $B(E2)$ of $0.8 \times 10^{-50}\ e^2\text{cm}^4$ was used.

DECAY OF Cs^{132}[1]

R. L. Robinson N. R. Johnson[2] E. Eichler[2]

The singles and coincidence gamma-ray spectra of Cs^{132} have been investigated with scintillation spectrometers. Energies in kiloelectron volts (and relative intensities) of the gamma rays which were observed are 464(21 ± 5), 509(5.1 ± 1.5), 511(12 ± 4), 569(2.7 ± 0.8), 631(8.5 ± 1.8), 669(1000 ± 30), 1035(1.6 ± 0.3), 1139(5.2 ± 0.5), 1304(0.9 ± 0.5), 1319(6.2 ± 0.6), and 2000(0.53 ± 0.06). From the results of these spectral studies and from gamma-gamma angular correlation measurements, it is proposed that Cs^{132} decays to levels with energies in kiloelectron volts (and spins) of 669 ± 4(2^+), 1300 ± 10(2^+), 1808 ± 13(2 or 3), and 1988 ± 12(2) in Xe^{132}, and 464 ± 5(2^+) and 1034 ± 9(2^+) in Ba^{132}. The ratios of the intensities of quadrupole to dipole radiation for the 631- and 1319-kev transitions in Xe^{132} and for the 569-kev transition in Ba^{132} were found to be 10, 0.006, and $\gtrsim 200$ respectively. The predominately quadrupole character of the transitions between the second and first spin-2 levels is attributed to the collective behavior of the nuclei. From the ratio of decay by electron capture and by positron emission to the 669-kev level, the energy separation between Cs^{132} and Xe^{132} was estimated to be 2.15 Mev.

[1] Abstract of published paper: *Phys. Rev.* **128**, 252 (1962).

[2] Chemistry Division.

TOTAL NEUTRON CROSS SECTIONS IN ISOTOPES OF Zr, Fe, Cr, AND Ca

H. J. Kim J. A. Biggerstaff W. M. Good

Total cross-section measurements continue to be made with the pulsed Van de Graaff at ORNL on separated isotopes for which the amount of material is small ($\approx \frac{1}{20}$ mole) and the level spacing of the order of 100 v or more. Measurements have been made with 1 to 2% energy resolution in the region of 2 to 30 kev on the following nuclides: Zr^{90}, Zr^{91}, Zr^{92}, Zr^{94}, Zr^{96}, Cr^{53}, Ca^{43}, and Fe^{57}. Following are the principal resonances observed in kev units of energy:

Zr^{90}: 3.8, 7.4, 13.5, 17.4, 18.0, 26.5, 41.3;
Zr^{91}: 6.7;
Ca^{43}: 4.3, 5.2, 8.8, 13.8, 19.2, 22.5, 26.6, 31.4, 37.0;
Zr^{92}: 6.7, 15.4, 17.1, 22.7;
Zr^{94}: 5.7, 6.8, 10.7, 12.8, 15.8, 17.8, 19.5;
Zr^{96}: 2.62, 2.82, 3.7, 4.2, 5.25, 6.7, 29.3;
Cr^{53}: 19.3, 26.3, 34.7, 39.0, 28.8, 37.0.

No levels other than those already known at 3.90 and 6.42 could be detected with the Fe^{57} sample employed up to 30 kev. Other levels, either small or overlapping so as to make energy assignment uncertain, were observed but not listed. Interpretation of the data is as yet incomplete but is under way.

PARAMETERS OF NEUTRON RESONANCES IN W^{184}[1]

F. A. Khan[2] J. A. Harvey

Transmission measurements on samples of normal tungsten and samples enriched in W^{184} have been made with the ORNL fast-chopper neutron time-of-flight spectrometer. Measurements were taken at the 180-m flight station with a resolution of 10 nanoseconds/m between 40 and 10,000 ev and at the 45-m station with an energy resolution of $1\frac{1}{2}$% below 50 ev. The transmission data have been analyzed to give the parameters for 16 resonances in W^{184} up to 2100 ev. From these parameters the following data for W^{184} have been determined: an average level spacing of 130 ± 30 ev, an *s*-wave strength function of $(2.8 \pm 1.2) \times 10^{-4}$, and a resonance capture integral of 12 ± 2 barns.

[1]Abstract of a paper to be submitted for publication in *Nuclear Science and Engineering*.

[2]Visiting scientist from the Pakistan Atomic Energy Commission.

NEUTRON CROSS-SECTION MEASUREMENTS FROM 1 TO 30,000 ev ON ENRICHED SAMPLES OF THE ZIRCONIUM ISOTOPES

R. C. Block

Introduction

The study of low-energy-neutron total cross sections of the isotopes of zirconium (Zr^{90}, Zr^{91}, Zr^{92}, Zr^{94}, and Zr^{96}) is interesting both from the standpoint of nuclear physics and the requirements of reactor designers. These isotopes are in the mass-number region where the *p*-wave strength function is a maximum and where the *s*-wave strength function is a minimum. Information can be extracted from these measurements about the relative strengths of these interactions, and parameters for the individual resonances can be obtained. Also, zirconium is a metal which is

now frequently used in reactor construction. Hence, the determination of the resonance parameters is invaluable to reactor designers in their calculations of the neutron absorption of zirconium in the resonance energy region.

Accordingly, neutron transmission measurements were made on highly enriched zirconium isotopes with the ORNL fast-chopper facility. These measurements extended from about 1 to 30,000 ev, and both the high-intensity and high-resolution choppers were utilized. Over 25 resonances were observed and assigned to individual isotopes. These resonances were analyzed for resonance parameters, and these parameters were combined to give information about the *s*-wave and *p*-wave strength functions.

Experimental Technique

The enriched zirconium isotope samples are part of the AEC Neutron Cross-Section Sample Pool and were obtained from the ORNL Isotopes Division in the form of ZrO_2. With the exception of Zr^{96} the oxides were each packed into a thin-walled aluminum container with inside dimensions approximately 10 × 2.8 × 2.0 cm. The chopper beam was passed through either the 2.0-cm or the 10-cm dimension to achieve a factor of 5 difference in the sample thickness. In order to make fullest use of the small amount of the Zr^{96} sample, this material was packed into ten separate plastic and aluminum containers, each 2.7 × 2.5 × 0.08 cm inside dimensions. The sample properties are listed in Table 1.

The transmission measurements were carried out with the ORNL fast-chopper equipment; this equipment and general technique have been described previously by Block *et al.*[1] The thinner samples were measured with the high-resolution chopper and with BF_3 detectors at 180 m. An overall resolution of about 10 nanoseconds/m was achieved, and these measurements extended over a neutron energy range from 170 ev to about 30,000 ev. The thicker samples were measured with the high-intensity chopper and with BF_3 detectors at 45 m. These transmission measurements extended down to 1 ev, and the resolution varied from about 45 to 360 nanoseconds/m. In all cases the "open" spectrum of neutron counts was obtained with aluminum plates placed in the beam to compensate for the aluminum windows in the sample cells.

The raw counting data were reduced to transmission data with the aid of the Oracle computer. The transmission data were inspected for resonances, and these resonances were then analyzed for parameters by the IBM 7090 computer using the area code of Atta and Harvey.[2] Recent transmission measurements from Saclay[3] indicate that the radiation width Γ_γ for the zirconium resonances is equal to 0.3 ± 0.1 ev. This value of Γ_γ was assumed in the area analysis of the resonance parameters. Results from the different experimental runs and samples were combined to produce the "best" set of parameters for each resonance; these results are summarized in Tables 2 through 6.

[1]R. C. Block, G. G. Slaughter, and J. A. Harvey, *Nucl. Sci. Eng.* **8**, 112 (1960).

[2]S. E. Atta and J. A. Harvey, *Numerical Analysis of Resonances*, ORNL-3205 (1961).

[3]J. Morgenstern *et al.*, *Bull. Am. Phys. Soc.* **7**(4), 288 (1962).

Table 1. Specifications of the Zirconium Samples

Nuclide	Enrichment	Oxide (g)	N (atoms/barn) thin	N (atoms/barn) thick
Zr^{90}	97.8	54	0.00910	0.0472
Zr^{91}	90.9	37	0.00614	0.0318
Zr^{92}	95.7	56	0.00915	0.0474
Zr^{94}	96.5	53	0.00860	0.0446
Zr^{96}	57.4	4.4	0.00982	

Table 2. Parameters of Resonances of Zr^{90}

E_0 (ev)	Γ_n (ev)	Γ_n^0 (ev)
		$\times 10^{-4}$
3,880	8.2 ± 1.3	1,310
(13,500)[a]	(37 ± 19)	(3,190)
17,800 (doublet)[b]	240 ± 44	18,000

[a]Doubtful resonance.
[b]See ref 6.

Table 3. Parameters of Resonances of Zr^{91}

E_0 (ev)	$2g\Gamma_n$ (ev)	$2g\Gamma_n^0$ (ev)	$2g\Gamma_n^1$ (ev)
		$\times 10^{-4}$	$\times 10^{-1}$
182.2	$(11 \pm 2) \times 10^{-3}$	8.2	21,800
240	$(3.8 \pm 0.4) \times 10^{-3}$	2.4	5,000
293	0.68 ± 0.05	400	
445	$(3.4 \pm 1.0) \times 10^{-3}$	1.7	1,860
683	0.88 ± 0.09	340	
890	$(28 \pm 10) \times 10^{-3}$	9.4	5,170
1540	8.4 ± 0.8	2200	
2490	7.2 ± 1.1	1400	
2740	11.0 ± 1.5	2010	
(5600)[a]	(7 ± 4)	(940)	

[a]Doubtful resonance.

Table 4. Parameters of Resonances of Zr^{92}

E_0 (ev)	Γ_n (ev)	Γ_n^0 (ev)
		$\times 10^{-4}$
2700	23 ± 2	4800
4140	4.1 ± 1.5	640
4670	12.5 ± 3.5	1800
6890	72 ± 9	8700

Table 5. Parameters of Resonances of Zr^{94}

E_0 (ev)	Γ_n (ev)	Γ_n^0 (ev)
		$\times 10^{-4}$
2,250	2.0 ± 0.6	420
5,840	22 ± 5	2,900
7,100	22 ± 7	2,600
(12,600)[a]	(23 ± 18)	(2,000)
20,000	220 ± 50	15,500
(24,000)[a]	(90 ± 50)	(5,800)

[a]Doubtful resonance.

Table 6. Parameters of Resonances of Zr^{96}

E_0 (ev)	Γ_n (ev)	Γ_n^0 (ev)
		$\times 10^{-4}$
301	0.22 ± 0.03	130
2,690	8 ± 3	1540
(3,830)[a]	(2 ± 1)	(320)
4,110	11 ± 4	1900
5,430	25 ± 4	3400
5,940	9 ± 5	1300
15,400	120 ± 40	9700

[a]Doubtful resonance.

Discussion

It is convenient for the purpose of discussion to divide these data into two groups: the Zr^{91} data and the even-even isotope data. The Zr^{91} data are listed in Table 3 in four columns: the observed resonance energy E_0; the neutron width $2g\Gamma_n$; the *s*-wave reduced neutron width $2g\Gamma_n^0 \equiv 2g\Gamma_n\sqrt{1\ \text{ev}/E_0}$; and the *p*-wave reduced neutron width $2g\Gamma_n^1$, which according to the notation of Saplakoglu *et al.*[4] is equal to

$$\Gamma_n\sqrt{\frac{1\ \text{ev}}{E_0}}\left(\frac{x_0^2+1}{x_0^2}\right),$$

where the term in parentheses is the $l = 1$ penetration factor at the resonance energy. Seven resonances were observed up to 1600 ev, but only three levels were seen in the next 4000 ev. Apparently many weak resonances are being missed above 1600 ev. Up to 1600 ev, the neutron widths of the resonances reported here are in excellent agreement with the neutron widths reported from Saclay,[3] although the resonance at 445 ev was not observed at Saclay. The Saclay resonance energies, however, are systematically lower by 1 to 2% than the energies in Table 3; since energy determinations by the ORNL fast

[4]A. Saplakoglu, L. M. Bollinger, and R. E. Coté, *Phys. Rev.* **109**, 1258 (1958).

chopper consistently agree with independent energy determinations at Brookhaven, Columbia, and Rensselaer, the energies listed in Tables 2 through 6 are presumed to be correct to within 0.5 to 1.0% up to 4000 ev.

The ten resonances listed in Table 3 for Zr^{91} fall into two categories: four resonances with $2g\Gamma_n^0 < 10 \times 10^{-4}$, and six resonances with $2g\Gamma_n^0 < 300 \times 10^{-4}$. It is, of course, possible that a group of only ten *s*-wave resonances can have such an unusual distribution, but it is probable that some, if not all, of the four small resonances are actually *p*-wave resonances. It is then possible to get an estimate of the upper limit of the *p*-wave strength function by assigning these four weak resonances to $l = 1$ neutron. The *p*-wave strength function $\overline{\Gamma_n^1}/D$ is, in the notation of Saplakoglu, equal to $1/[2(2l + 1)(E_2 - E_1)] \times \Sigma 2g\Gamma_n^1$, where $l = 1$ and $(E_2 - E_1)$ is the energy range of summation. Up to 900 ev, where few small resonances are being missed, $\overline{\Gamma_n^1}/D \gtrsim 6 \times 10^{-4}$ to an accuracy of about 60% for only four resonances. Although these results are severely limited by the statistical accuracy obtainable with only four resonances, this high value of the *p*-wave strength function is consistent with the high values expected in the region of the maximum of the *p*-wave strength function near $A = 100$. (It should be noted that the value of 6×10^{-4} depends primarily upon the relatively strong 182-ev resonance. However, recent measurements at Saclay[5] on very thick zirconium samples confirm that this resonance is not excited by *s*-wave neutrons.)

An *s*-wave strength function can be assigned to the remaining resonances in Zr^{91}. However, since the *s*-wave strength function is expected to vary only slowly with mass number in this region, it is perhaps more significant to combine the even-even isotope data, where many more large resonances are observed, the level spacing is much greater, and analysis is permitted to higher neutron energies.

The resonance parameters for the even-even zirconium isotopes are listed in Tables 2, 4, 5, and 6. Earlier transmission measurements at Duke University[6] on separated Zr^{90}, Zr^{92}, and Zr^{94} are essentially in agreement with the resonance energy and isotopic assignments reported here. However, the Duke measurements do indicate that the 17,800-ev resonance in Zr^{90} is probably a doublet. For the seven Zr^{96} resonances listed in Table 6, it is interesting to note that in four cases a resonance in Zr^{96} occurs at approximately the same energy as a resonance in one of the other even-even isotopes. However, since the strengths of the observed resonances in the Zr^{96} sample cannot be explained by the presence of the other isotopes (9% of Zr^{90}, 27% of Zr^{92}, and 4% of Zr^{94}), these resonances were assigned to Zr^{96}. (As an additional check the Zr^{96} sample has been reanalyzed on a mass spectrometer, and the original isotopic content was confirmed.)

There is a total of 20 resonances in the even-even isotopes from 1 to 30,000 ev; four of these resonances are so weak as to be considered doubtful, and at least one (Zr^{90} at 17,800 ev) may be a doublet. If all these resonances are combined, an average *s*-wave strength function of $(0.7 \pm 0.2) \times 10^{-4}$ is obtained. The error is based on the statistical uncertainty resulting from 16 definite resonances. This average value of the *s*-wave strength function is somewhat higher than many of the strength functions reported in this mass region, but within the stated error of $\pm 0.2 \times 10^{-4}$ the result reported here is consistent with the general trend of results.

[5] J. Julien, private communication.

[6] H. W. Newson *et al.*, *Ann. Phys.* (N.Y.) **8**, 211 (1959).

LEVEL SPACINGS AND *s*-WAVE NEUTRON STRENGTH FUNCTIONS OF THE ISOTOPES OF TIN

T. Fuketa[1] F. A. Khan[2] J. A. Harvey

Neutron transmission measurements have been made on highly enriched samples of the ten tin isotopes from Sn^{112} to Sn^{124} by use of the fast-chopper time-of-flight neutron spectrometer at the ORR. The measurements were made from ~30 to 10,000 ev with a resolution of 11 to 18 nanoseconds/m by use of the 180-m flight path, and from 0.2 to 100 ev with an energy resolution of 1.5% with the 45-m flight path.

The enriched tin isotopes were all used in the metallic form except Sn^{115}, which was an oxide. Each metal sample was rolled into a strip ~1 in. wide and 0.030 in. thick. For the seven abundant isotopes Sn^{116} to Sn^{124}, nine to twelve pieces measuring 1.00 × 1.030 in. were obtained for each sample. For Sn^{112} and Sn^{114}, only five pieces of each sample were obtained, measuring 0.20 × 1.030 in. and 0.15 × 1.030 in. respectively. For Sn^{115} the oxide powder was packed into five plastic sample holders, with inside dimensions 0.030 × 1.030 × ~0.2 in. The samples were held with brass spacers to align the samples with the slits in the collimator and rotor. The specifications of the samples are listed in Table 1.

The transmission data at the 180-m flight path were taken with nine to twelve slits for the seven isotopes Sn^{116} to Sn^{124} and with five slits for the three isotopes Sn^{112} to Sn^{115}. The open beam counting rate was 0.6 count per 1-μsec channel per min with ten slits, and the room background was about 10%. The time-of-flight neutron spectra for sample-out and sample-in were stored in separate halves of a 2048-channel time analyzer. The backgrounds were determined by the technique of "blacked-out" resonances, such as the 132-ev cobalt resonance, and were stored in a 256-channel time analyzer. The sample was alternated with the background in about a 1-hr cycle, and a run was continued for several days until ~1500 counts/channel with the sample in the beam were collected. Each run was repeated to confirm the existence of small transmission dips. The data were processed with the Oracle or IBM 7090 computer to obtain the transmissions for the samples. Typical transmission data are shown in Fig. 1 (200 to 30 ev) and Fig. 2 (10,000 to 160 ev). The data in Fig. 1 were taken with 2-μsec channels and a resolution of 18 nanoseconds/m;

[1]Visiting scientist from the Japan Atomic Energy Research Institute, Tokai.

[2]Visiting scientist from the Pakistan Atomic Energy Commission.

Table 1. Specifications of the Enriched Samples of the Tin Isotopes

Isotope	Enrichment (%)	Form	Amount Used (g)	Transmission Thickness (atoms/barn)
Sn^{112}	70.05	Metal	3.31	0.0178
Sn^{114}	56.85	Metal	2.45	0.0135
Sn^{115}	29.11	SnO_2 powder	1.33	0.00513
Sn^{116}	95.74	Metal	34.68	0.0912
Sn^{117}	89.2	Metal	35.38	0.0922
Sn^{118}	97.15	Metal	42.88	0.0932
Sn^{119}	89.8	Metal	35.59	0.0929
Sn^{120}	97.9	Metal	30.15	0.0864
Sn^{122}	90.8	Metal	36.79	0.0928
Sn^{124}	92.8	Metal	37.47	0.0924

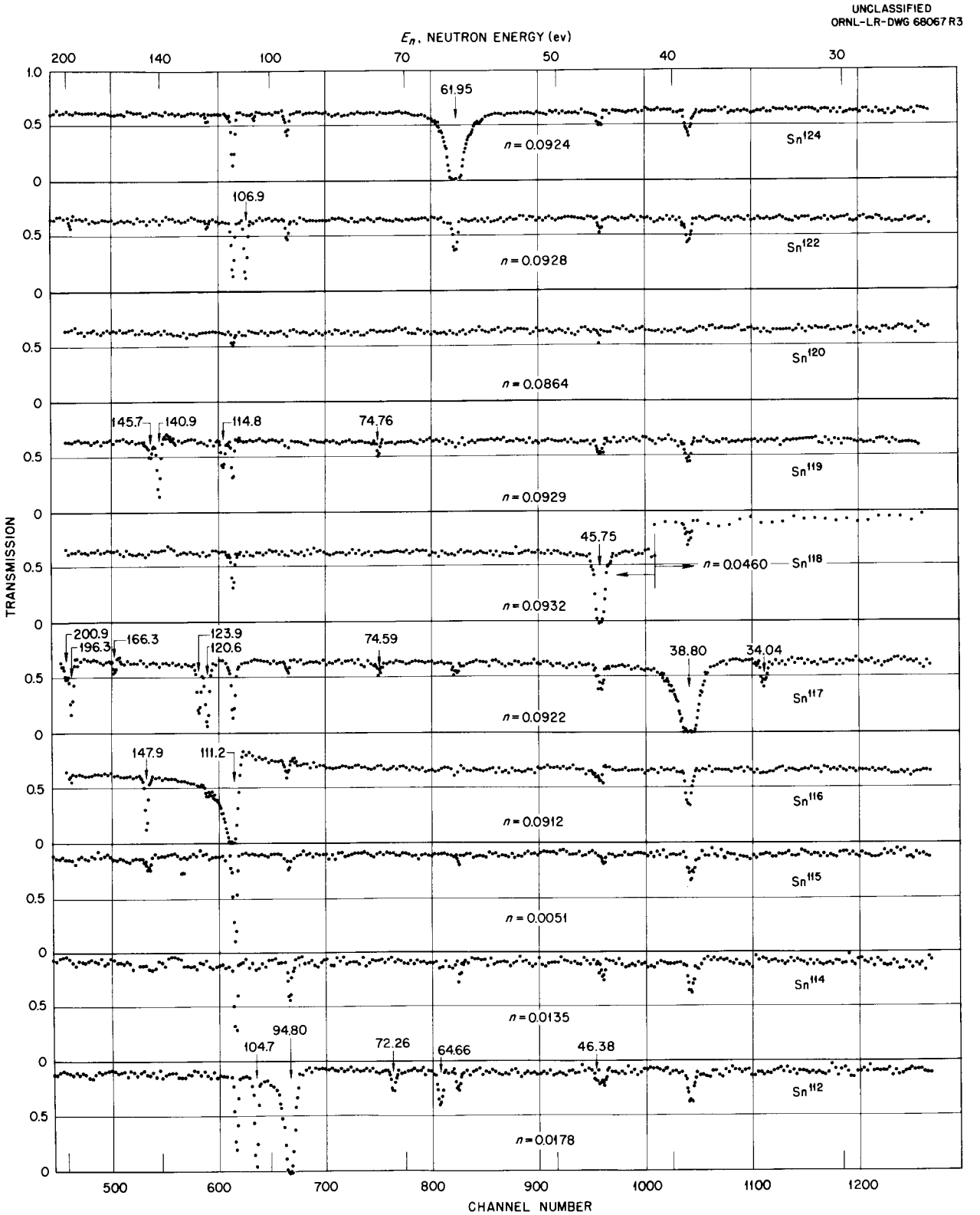

Fig. 1. Transmission of Samples of Enriched Tin Isotopes from 200 to 30 ev with a Resolution of 18 nanoseconds/m.

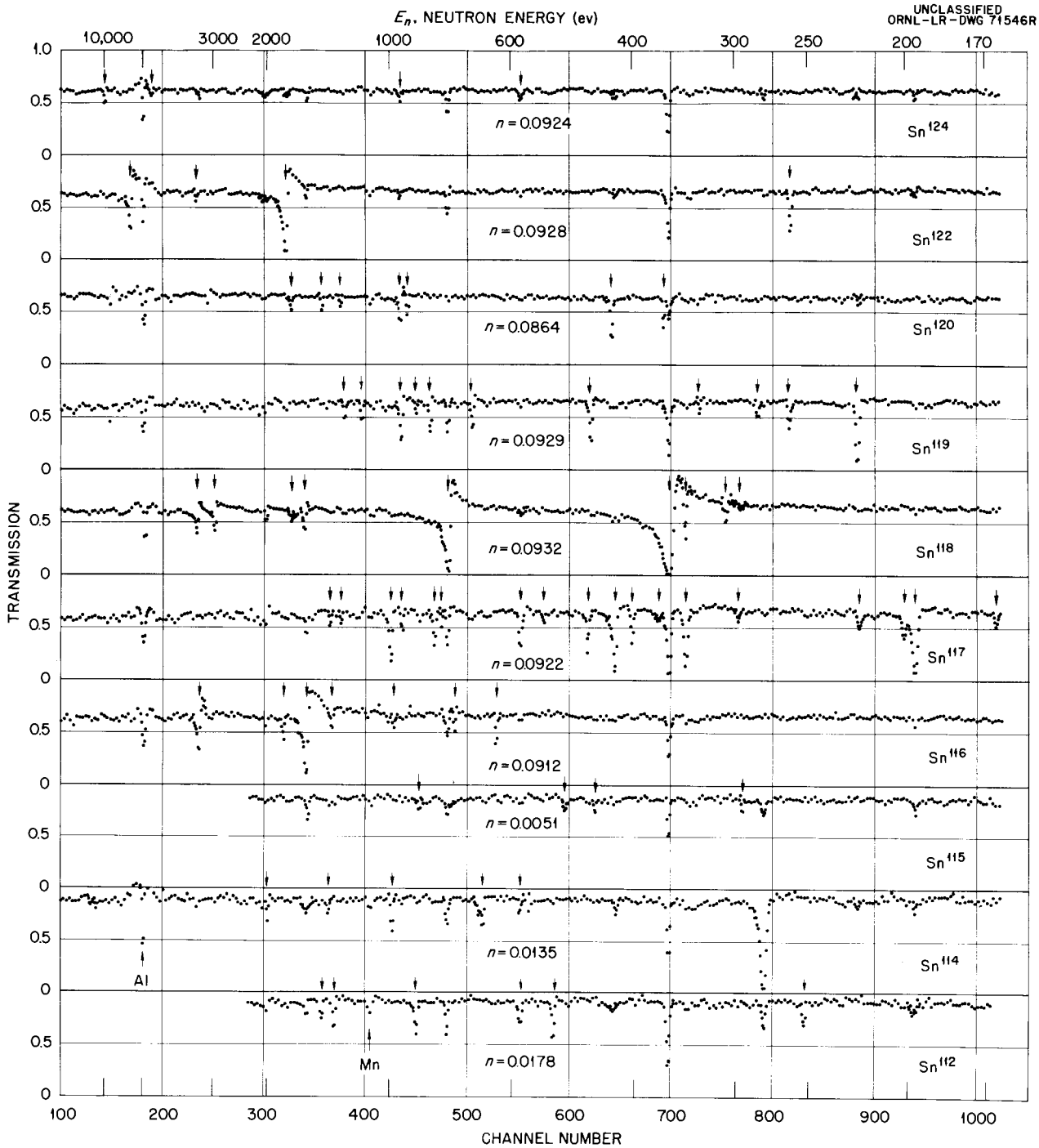

Fig. 2. Transmission of Samples of Enriched Tin Isotopes from 10,000 to 160 ev with a Resolution of 11 nanoseconds/m.

and those in Fig. 2 were taken with 1-μsec channels and a resolution of 11 nanoseconds/m. The transmission dips indicated by arrows are due to resonances in the sample isotope. The other transmission dips are due to small amounts of other tin isotopes in the sample. For example, the dip at 38.8 ev in the Sn^{116} sample, which contains about 1% Sn^{117}, is due to the large resonance in Sn^{117}.

The data obtained at the 45-m flight path were taken with high statistical accuracy in search of small previously unobserved resonances below 35 ev. For the Sn^{116} to Sn^{124} samples, more than 20,000 counts/channel were accumulated, and for the Sn^{112} to Sn^{115} samples, about 5000 counts/channel. In addition to several resonances which could be attributed to small impurities, three new resonances were found at 1.32 ev in Sn^{117}, 6.22 ev in Sn^{119}, and 21.0 ev in Sn^{112}.

Nearly 100 resonances have been assigned to the ten isotopes of tin. The transmission data have been analyzed using the area analysis method,[3] and neutron widths have been obtained for the resonances assuming $\Gamma_\gamma = 0.110$ ev and $g = \frac{1}{2}$ for the odd-A target nuclides. The results are given in Table 2. The values listed for the reduced

[3]S. E. Atta and J. A. Harvey, *Numerical Analysis of Neutron Resonances*, ORNL-3205 (1961).

Table 2. Parameters of the Neutron Resonances in the Tin Isotopes

Target Isotope	Resonance Energy, E_0 (ev)	Neutron Width, Γ_n (mv)	Error (%)	Reduced Neutron Width, Γ_n^0 (mv)
Sn^{112}	21.02	0.0039	30	0.0009
	46.38	0.028	100	0.004
	64.66	0.44	10	0.055
	72.26	0.34	15	0.040
	94.80	86	4	8.8
	104.7	9.2	11	0.90
	251.1	2.6	15	0.16
	514	51	20	2.2
	577	24	25	1.0
	877	200	25	6.8
	1321	700	30	19
	1416	120	50	3.2
Sn^{114}	277.5	370	5	22.2
	578	20	40	0.83
	666	250	25	9.7
	984	460	30	15
	1367	210	50	6
	1980	900	80	20
Sn^{115}	292.8	33	25	1.9
	448.0	90	30	4.3
	493.7	120	30	5.4
	866	280	60	10
Sn^{116}	111.2	66	5	6.3
	147.9	3.0	12	0.25
	632	30	20	1.2
	750	4.3	20	0.16
	981	16	35	0.51
	1340	300	25	8

Table 2. (continued)

Target Isotope	Resonance Energy, E_0 (ev)	Neutron Width, Γ_n (mv)	Error (%)	Reduced Neutron Width, Γ_n^0 (mv)
Sn^{116}	1545	2000	10	51
	1800	270	40	6
	3400	3200	15	55
Sn^{117}	1.32	0.00020	10	0.00018
	34.04	0.034	6	0.0058
	38.80	6.0	5	0.96
	74.59	0.075	13	0.0087
	120.6	8.5	5	0.77
	123.9	3.9	10	0.35
	166.3	5.0	20	0.39
	196.3	30	10	2.1
	200.9	0.95	15	0.067
	222.0	0.90	10	0.060
	297.7	0.67	30	0.039
	342.3	50	20	2.7
	371.3	1.0	30	0.052
	400.5	9.2	11	0.46
	422.0	146	10	7.1
	459.4	22	20	1.0
	532	4.8	30	0.21
	570	90	15	3.7
	790	7	35	0.25
	815	140	20	4.9
	940	120	25	3.9
	995	700	10	22
	1282	28	50	0.8
	1363	70	70	1.9
Sn^{118}	45.75	0.72	5	0.106
	289	0.50	30	0.029
	307.5	0.80	10	0.046
	343.9	2.3	10	0.124
	359.1	330	5	17.4
	770	700	10	25
	1580	310	15	7.8
	1710	33	40	0.8
	2960	1600	15	29
	3450	1800	15	31
Sn^{119}	6.22	0.0037	5	0.00146
	74.76	0.062	14	0.0072
	114.8	0.55	9	0.051
	140.9	4.5	12	0.38
	145.7	0.58	15	0.048
	222.6	11.5	6	0.77
	261.6	2.1	10	0.130
	283.1	0.88	15	0.052

Table 2. (continued)

Target Isotope	Resonance Energy, E_0 (ev)	Neutron Width, Γ_n (mv)	Error (%)	Reduced Neutron Width, Γ_n^0 (mv)
Sn^{119}	330.0	0.38	30	0.021
	455.8	38	13	1.8
	697	50	20	1.9
	830	110	20	3.8
	885	11	40	0.37
	948	350	14	11.4
	1150	35	40	1.0
	1258	80	50	2.3
Sn^{120}	364.8	2.2	12	0.115
	426.9	26	15	1.3
	922	23	50	0.8
	953	90	30	2.9
	1289	39	80	1.1
	1428	140	70	4
	1714	300	100	7
Sn^{122}	106.9	0.77	10	0.075
	259.9	1.75	7	0.108
	1750	3200	10	76
	3450	120	80	2
	6850	16,000	20	190
Sn^{124}	61.95	11.0	5	1.40
	579	1.5	30	0.062
	950	6	50	0.2
	5360	700	100	10
	9680	6000	60	60

neutron widths Γ_n^0 were computed on the assumption that the resonances were *s*-wave resonances. It is possible that a few of the smallest resonances might be *p*-wave resonances. (For the resonances where the errors are large, they should be interpreted as the errors on the logarithms of the values, that is, $10 \pm 100\% \equiv 10^{+10}_{-5}$.) Except for the three resonances below 30 ev the table is based entirely on the 180-m data.

From Figs. 1 and 2 it is obvious that many more resonances were found in Sn^{117} and Sn^{119} than in the even-*A* target nuclides. In Figs. 3 and 4 the number of resonances is plotted vs neutron energy for the odd-*A* target nuclides and the even-*A* target nuclides respectively. The average level spacing D_{obs} for each isotope is given by the slope of the straight line which includes a correction for the "missed resonances." This correction varies from ~10% to about a factor of 5 for Sn^{115}. A summary of the average level spacings is given in Table 3. The gradual increase in the average level spacing in the compound nuclei from Sn^{115} to Sn^{125} is expected, due to the decrease in the neutron binding energy. However, the low value for the compound nucleus Sn^{113} is anomalous. The small average level spacings for the even-*A* compound nuclides are expected, since the neutron binding energies of these nuclides are larger by ~2 Mev than those of the odd-*A* compound nuclides.

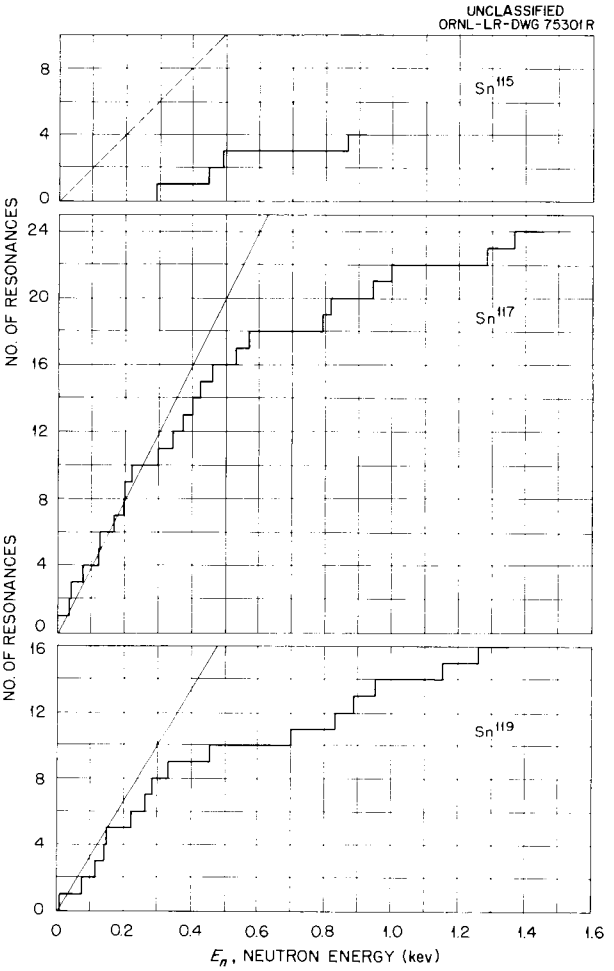

Fig. 3. Plot of the Number of Resonances vs Neutron Energy for the Odd-*A* Target Nuclides.

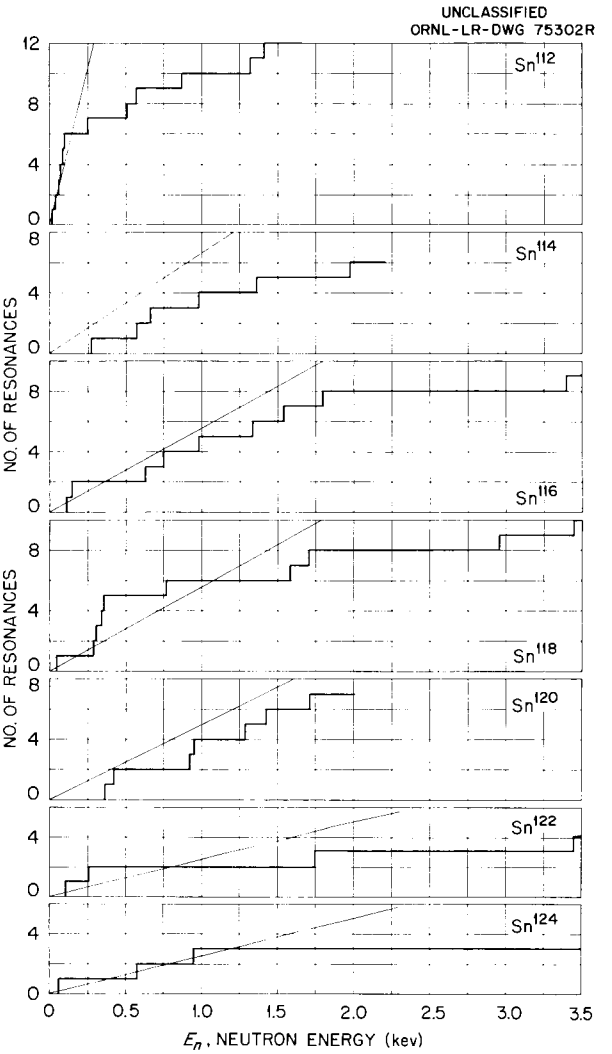

Fig. 4. Plot of the Number of Resonances vs Neutron Energy for the Even-*A* Target Nuclides.

Table 3. Average Level Spacing D_{obs} and s-Wave Strength Function $\overline{\Gamma_n^0}/D$ of the Tin Nuclides

Compound Nuclide	Average Level Spacing, D_{obs} (ev)	s-Wave Strength Function $\overline{\Gamma_n^0}/D \times 10^4$	
		Experiment	Theory ($\Delta = 3$ Mev)
Sn^{113}	25 ± 7	0.5 ± 0.2	0.51
Sn^{115}	150 ± 60	0.7 ± 0.3	0.48
Sn^{117}	180 ± 50	0.37 ± 0.14	0.41
Sn^{119}	180 ± 50	0.32 ± 0.12	0.38
Sn^{121}	200 ± 70	0.09 ± 0.04	0.095
Sn^{123}	400 ± 200	0.20 ± 0.10	0.081
Sn^{125}	400 ± 200	0.04 ± 0.02	0.086
Sn^{116}	50 ± 30	0.3 ± 0.2	
Sn^{118}	25 ± 5	0.19 ± 0.05	
Sn^{120}	30 ± 8	0.08 ± 0.03	

In Figs. 5 and 6 the sums of Γ_n^0 are plotted vs neutron energy for the odd-A target nuclides and even-A target nuclides respectively. The s-wave strength function $\overline{\Gamma_n^0}/D$ for each isotope is given by the slope of the straight line which includes a correction for "missed resonances." The s-wave strength function is generally insensitive to "missed resonances" for all isotopes except Sn^{115}, where the correction is nearly a factor of 3. A summary of the s-wave strength functions is given in Table 3.

The s-wave strength function is much lower in this region of mass number than was at first predicted from theory. Several attempts have been made to obtain this low value from an optical nuclear model with a high absorption at the nuclear surface or by including nuclear shell effects. Recently, Shakin[4] computed the s-wave strength functions for the even-A target isotopes of tin based on the shell and optical models of the nucleus. He computed the excitations and strengths of the three-quasi-particle states (two particles and one hole) based on the unified theory of nuclear reactions by Feshbach.[5] The summation of these model states is taken over an energy region Δ centered at the neutron binding. The parameter Δ is a measure of the energy range over which the strength of a quasi-particle state is spread when the residual interaction between the particles is taken into account. Values of the s-wave strength function were calculated for rectangular distributions with $\Delta = 1$, 2, and 3 Mev by Shakin,[4] and the results for $\Delta = 3$ Mev are shown in Fig. 7. The agreement between the experimental data and the theoretical calculation is good. The decrease in $\overline{\Gamma_n^0}/D$ with increasing mass number from Sn^{113} to Sn^{125} has not been obtained from other nuclear models.

[4]Carl Shakin, "On Model Calculations of Neutron Widths and Strength Functions," to be submitted to *Annals of Physics*.

[5]H. Feshbach, *Ann. Phys.* **5**, 357 (1958); *Ann. Phys.* **19**, 287 (1962).

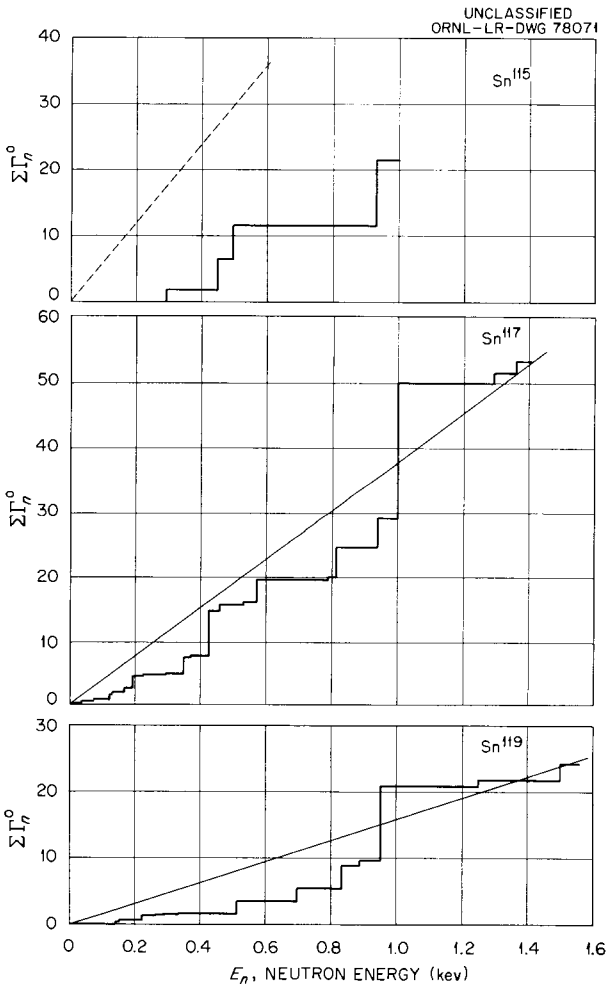

Fig. 5. Plot of the Sum of Γ_n^0 vs Neutron Energy for the Odd-A Target Nuclides.

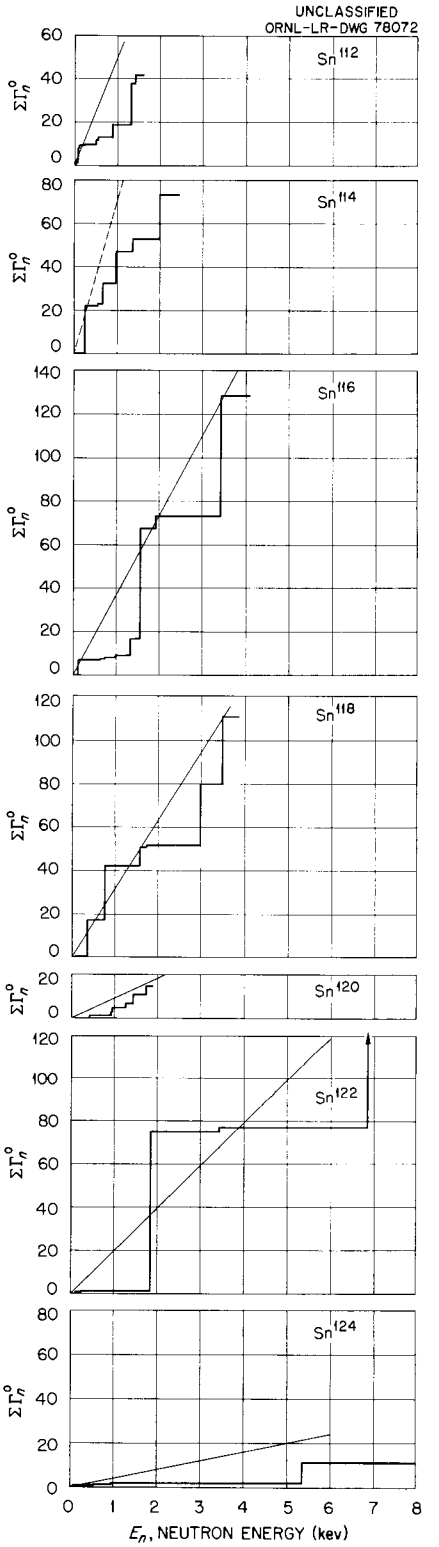

Fig. 6. Plot of the Sum of Γ_n^0 vs Neutron Energy for the Even-A Target Nuclides.

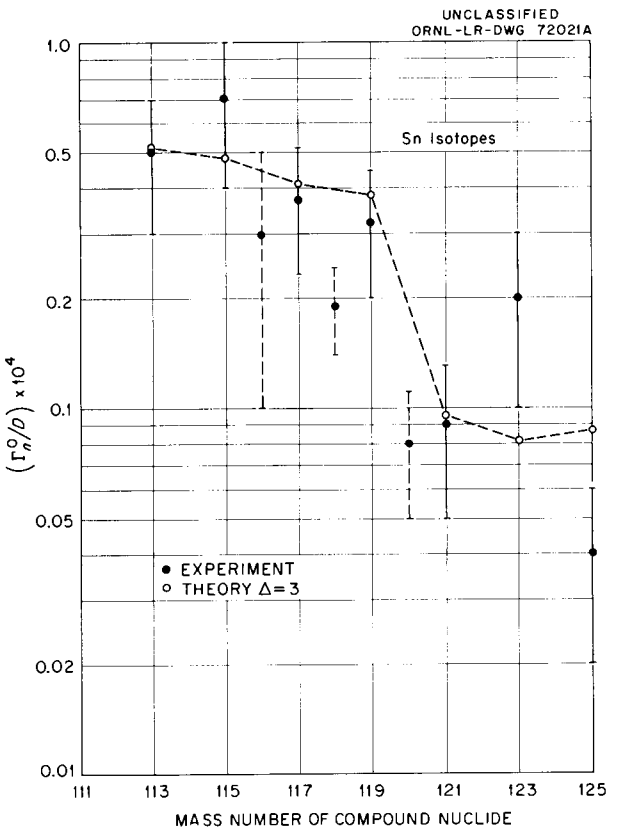

Fig. 7. Comparison of the Experimental Data and Theoretical Prediction of *s*-Wave Strength Functions for the Odd-*A* Compound Nuclides of Tin.

NEUTRON CROSS-SECTION MEASUREMENTS ON FISSION PRODUCT SAMARIUM AND IODINE[1]

N. J. Pattenden[2]

The ORNL chopper has been used to measure the neutron total cross sections of samples of fission product samarium and iodine in the thermal and resonance energy regions. At 2200 m/sec, the total cross section of Sm^{151} was found to be 15,000 ± 1,800 barns, and the absorption cross section of I^{129}, 28.0 ± 2 barns. The variation of cross section with energy in the thermal region of Sm^{151} was found to be strongly affected by a bound level, but in the case of I^{129} the absorption cross section could be described by a "$1/v$" dependence. For both nuclides, resonance parameters were obtained by area analysis of the observed transmissions in the higher energy region. The resonance absorption integrals, level spacings, and strength functions for Sm^{151} and I^{129} were 3000 barns, 3.5 ev, and 3.6×10^{-4} (per spin state), and 27 barns, 64 ev, and 0.3×10^{-4} respectively.

[1]Abstract of a paper submitted for publication in *Nuclear Science and Engineering*.

[2]Visiting ORNL from Atomic Energy Research Establishment, Harwell, Berkshire, England (now at AERE).

MODIFICATIONS TO PROGRAMS FOR NUMERICAL ANALYSIS OF NEUTRON RESONANCES

S. E. Atta[1] J. A. Harvey

After using the area and shape programs for resonance analysis,[2] it was recognized that several additions and changes to the programs would make them more useful and valuable. An addendum to ORNL-3205 has been prepared which outlines these additions and changes.

[1]Mathematics Division.

[2]Susie E. Atta and J. A. Harvey, *Phys. Div. Ann. Progr. Rept. Feb. 10, 1961*, ORNL-3085, p 44; *Numerical Analysis of Neutron Resonances*, ORNL-3205 (1961).

EXCITATION OF COLLECTIVE STATES BY INELASTIC SCATTERING OF 14-Mev NEUTRONS

P. H. Stelson[1] R. L. Robinson

Recent developments in the distorted-wave theory by Bassel *et al.*[2] and in the strong-coupling theory by Buck[3] for direct interactions have led to the prediction that cross sections for excitation of collective states are much larger than given by the statistical theory for compound nucleus interactions. According to these theories, the nuclear deformation parameters and therefore transition probabilities of the transitions from the collective states to the ground state can be determined from the measured cross sections. In view of these predictions we have undertaken an investigation of the excitation of collective states by inelastic scattering of 14-Mev neutrons and have compared our results with these theories.

The 14-Mev neutrons were produced by the *d-t* reaction. The inelastically scattered neutrons were separated from the elastically scattered neutrons by the time-of-flight method. A combination of beam-chopping and subsequent klystron bunching was used to generate a deuteron beam pulse of less than 2-nanosecond width with a current intensity greater than 3 ma at the tritium target. Figure 1 illustrates the experimental arrangement. The scatterer was a ring with a 14 in. ID and with a 1 × 3 in. cross section. To diminish the direct beam, which was several thousand times stronger than the intensity of the inelastically scattered neutrons, an iron shadow cone was placed as shown in Fig. 1 between the target and detector. The scattering angle was varied by moving the ring scatterer along an axis concentric with the beam direction. An essential feature of the experiment was a shield of paraffin and lead which surrounded the neutron detector to reduce the background caused by room-scattered neutrons.

Figure 2 shows a typical spectrum from the time-to-pulse-height converter for a lead scatterer. In addition to the elastic peak centered at channel 184, there are peaks at channel numbers 144 and 110 which establish that states are excited in lead at 2.5 ± 0.15 and 4.1 ± 0.2 Mev. The 2.5-Mev state corresponds in energy to the known 3^- level in Pb^{208}; the level at 4.1 Mev has been

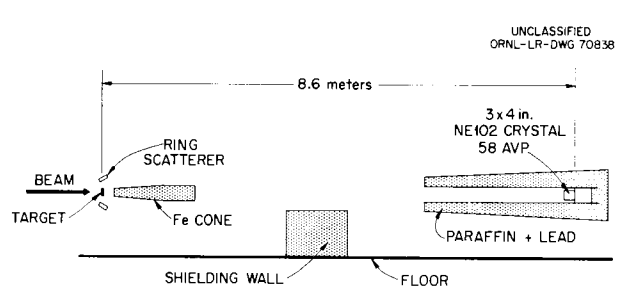

Fig. 1. Diagram of the Experimental Setup.

[1]Presently on leave at William Marsh Rice University, Houston, Tex.

[2]R. H. Bassel *et al.*, *Phys. Rev.* **128**, 2693 (1962).

[3]B. Buck, to be published in the *Physical Review*.

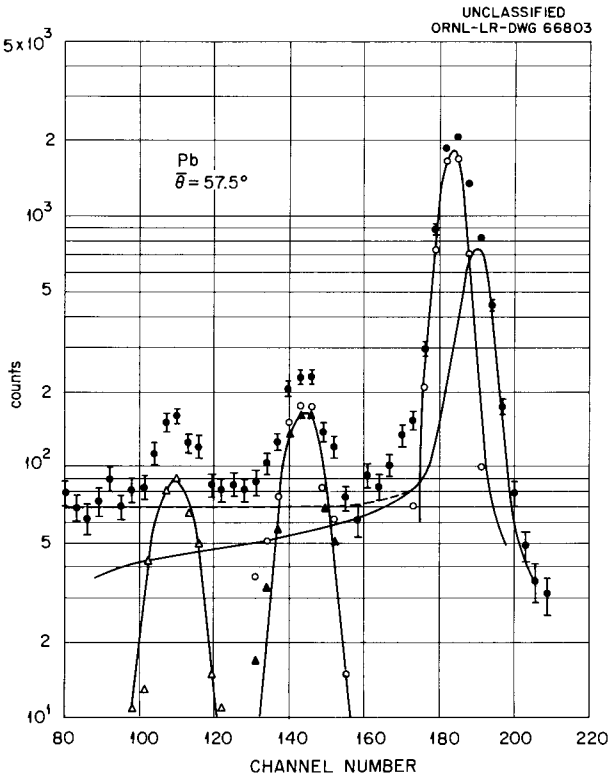

Fig. 2. Neutron Time-of-Flight Spectrum for 14-Mev Neutrons Scattered from Lead Through an Angle of 57.5°. A background spectrum taken with the lead ring removed is also shown.

assigned spin and parity of 4^+ by Crannell *et al.*[4] from their electron scattering studies. The differential cross sections for elastic scattering and for inelastic scattering leading to the 2.5-Mev state are given in Fig. 3. No corrections have been applied for multiple scattering. As can be seen in this figure, the elastic scattering cross sections agree reasonably well with those obtained by Coon.[5] The differential cross sections for excitation of the 2.5- and 4.1-Mev levels are compared with the distorted-wave theory[2] in Figs. 4 and 5. From this comparison the transition probabilities of the 2.5-Mev $E3$ and 4.1-Mev $E4$ transitions were found to be approximately 35 times that predicted by the single-particle model. These values are consistent with the enhancements of 31 ± 11 and 37 ± 12 reported for these two transitions, respectively, by Crannell *et al.*[4]

The behavior of the bismuth scatterer is essentially identical to that of lead. States are observed at 2.6 and 4.2 Mev (see Fig. 6) with cross sections like those for lead. However, there is no evidence for excitation of the known single-particle levels at 0.9 and 1.6 Mev. The cross section for possible excitation of the 1.6-Mev level is less than 10% of the cross section for excitation of the 2.6-Mev level.

For a tin scatterer, neutron groups were present which corresponded to excitation of states at 1.15 and 2.32 Mev. The former is ascribed to excitation of the first 2^+ levels in the even-even tin isotopes. The energy of the latter suggests it is from excitation of the octupole levels. A comparison of the

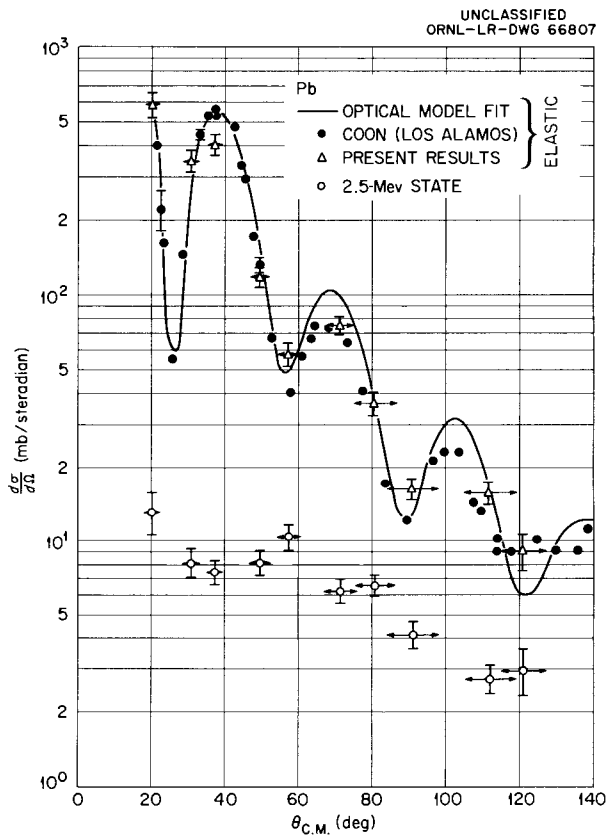

Fig. 3. Differential Cross Sections for Elastic and Inelastic (2.5-Mev State) Scattering of 14-Mev Neutrons from Lead.

[4]H. Crannell *et al.*, *Phys. Rev.* **123**, 923 (1961).

[5]J. H. Coon, *Tabulated Differential Neutron Cross Sections*, pt III, vol 1, UCRL-5573 (1961).

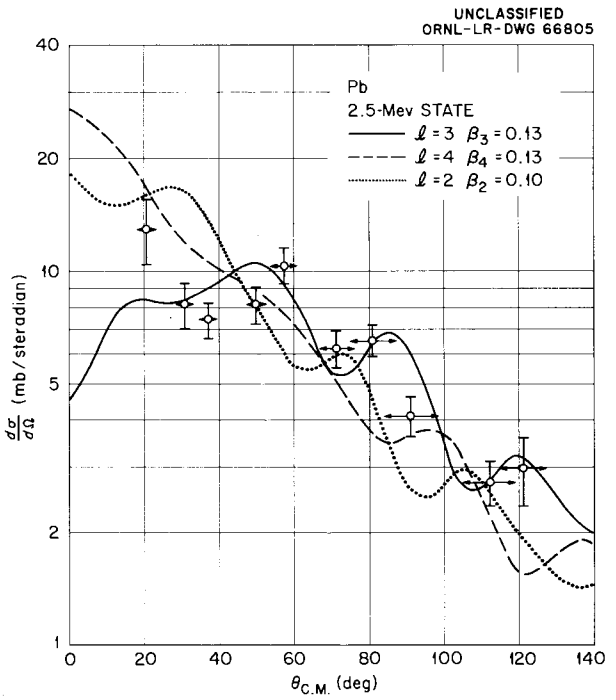

Fig. 4. Differential Cross Sections for Excitation of a Level in Lead at 2.5 Mev by Inelastically Scattered 14-Mev neutrons. The theoretical curves are for excitation of quadrupole (l = 2), octupole (l = 3), and hexadecapole (l = 4) states.

experimental results with theory yields values of 0.12 and 0.17 for the quadrupole and octupole deformation parameters β_2 and β_3 respectively. This quadrupole deformation parameter is in good quantitative agreement with the β_2 obtained from Coulomb-excitation measurements (β_2 = 0.11).[6] The octupole deformation parameter establishes that the $E3$ transition probability is 30 times the single-particle estimate.

The differential cross sections which were measured for neutron scattering from sulfur are illustrated in Fig. 7. The cross sections for elastic scattering agree with those reported by St. Pierre *et al.*[7] and by Elliot.[8] Cross sections for excitation of the 2.24-Mev quadrupole state have previously been measured by Clarke and Cross.[9] Our values are quite different from their results (see Fig. 7) for angles between 80 and 120°, but do agree with theory. Since the deformation parameter for sulfur is large, the distorted-wave theory of Bassel *et al.*[10] is inadequate. The calculations of Buck,[11] who accounts for the strong coupling between the 2^+ level and ground state, have been used to obtain the theoretical curve illustrated in Fig. 7. This theoretical fit gives an enhancement of 16 for the 2.24-Mev transition over the single-particle value. This is consistent with an enhancement of 15 as determined from the electron scattering studies of Helm.[12]

[6]P. H. Stelson and F. K. McGowan, *Phys. Rev.* **110**, 489 (1958).

[7]C. St. Pierre, M. K. Machwe, and P. Lorrain, *Phys. Rev.* **115**, 999 (1959).

[8]J. O. Elliot, *Phys. Rev.* **101**, 684 (1956).

[9]R. L. Clarke and W. G. Cross, *Elastic and Inelastic Scattering of 14-Mev Neutrons from Carbon, Magnesium, and Sulfur*, TNCC (Can.) 32, 1961.

[10]R. H. Bassel *et al.*, *Phys. Rev.* **128**, 2693 (1962).

[11]B. Buck, to be published in the *Physical Review*.

[12]R. H. Helm, *Phys. Rev.* **104**, 1466 (1956).

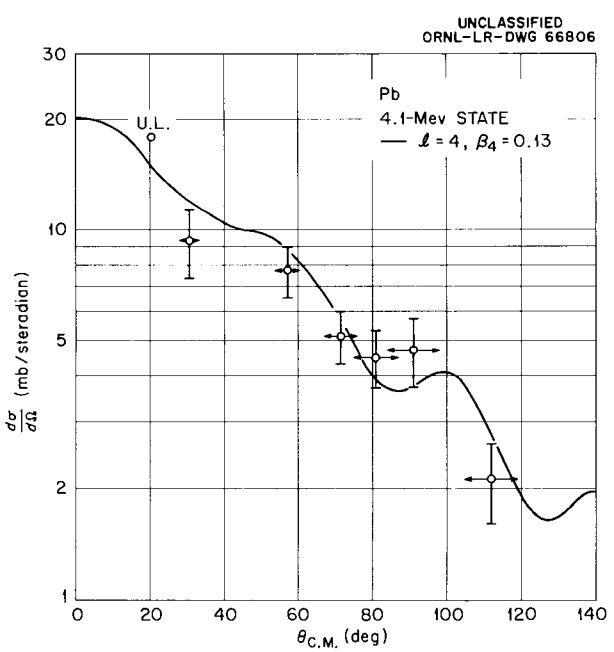

Fig. 5. Differential Cross Sections for Excitation of a Level in Lead at 4.1 Mev by Inelastically Scattered 14-Mev Neutrons. The theoretical curve is for excitation of a hexadecapole state.

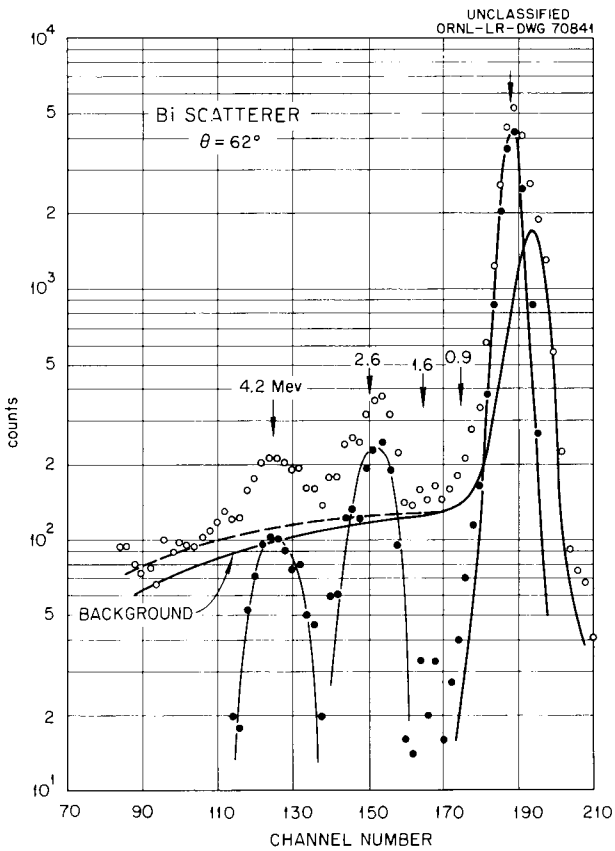

Fig. 6. Neutron Time-of-Flight Spectrum for 14-Mev Neutrons Scattered from Bismuth Through an Angle of 62°.

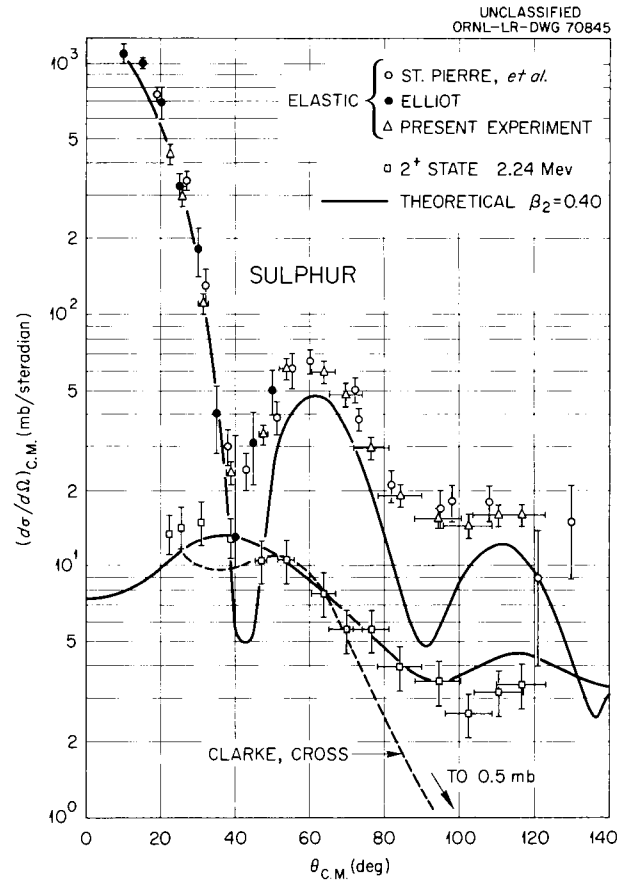

Fig. 7. Differential Cross Sections for Elastic and Inelastic (2.24-Mev State) Scattering of 14-Mev Neutrons from Sulfur.

DIFFERENTIAL CROSS SECTION OF NEUTRON SCATTERING FROM Pb^{208}

J. L. Fowler

Recent total neutron cross-section measurements[1] on Pb^{208} have revealed many more resonances than had been generally anticipated. Indeed, as shown in Fig. 1, there appear to be at least 85 resonances between 0.7 and 1.9 Mev. About one-third of these have widths greater than 3 kev, but of the order of 50 times narrower than single-particle widths. Since there is promise that theoretical methods[2] may enable one to interpret these rather short-lived compound nuclear states, it is important to identify the quantum parameters of the resonances. Although the J-value assignments of the resonances can be made from the total cross section, in general for the parity assignments one needs angular distributions of scattered neutrons.

In order to measure differential cross sections with ~3 kev energy spread, about 5 to 10 times smaller than is customary in this type of work,

[1] J. L. Fowler and E. C. Campbell, *Phys. Rev.* **127**, 2192 (1962).

[2] Carl Shakin, to be submitted to *Annals of Physics*.

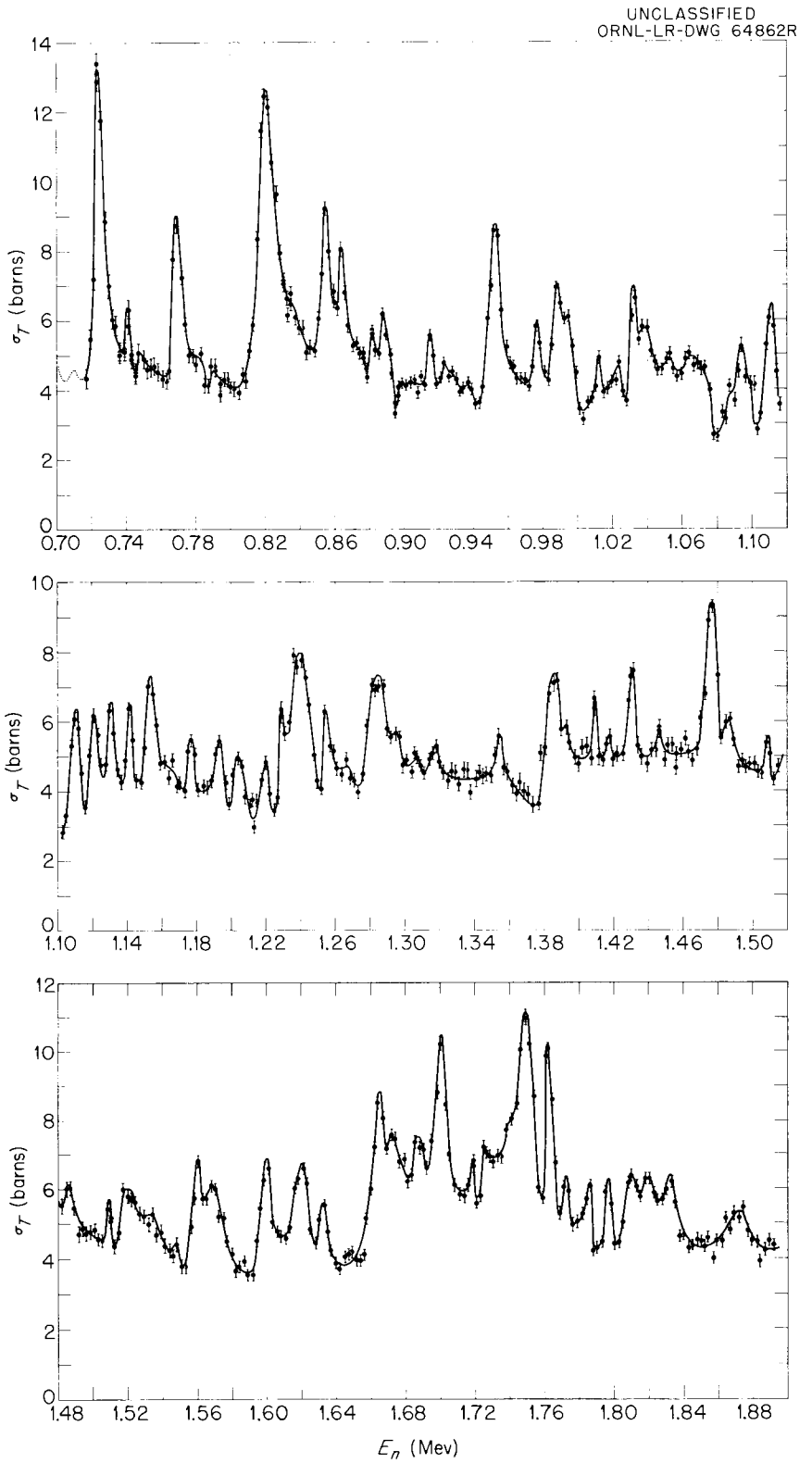

Fig. 1. Total Neutron Cross Section of Pb^{208}.

special apparatus had to be designed. Furthermore, the quantity of the Pb^{208} separated isotope available ($\sim\frac{1}{2}$ mole) was at least a factor of 2 less than that used in such previous experiments with light elements at resonant energies.[3-5]

Figure 2 is a drawing of the apparatus built to do this job.[6] Neutrons from the $Li^7(p,n)Be^7$ reaction are collimated by a doubly tapered 1.2 × 4.6 cm slot through a 50-cm lithium-loaded paraffin shield. They are incident upon the scattering sample supported in the center of a space ~1 m square and 60 cm deep, shielded by tanks of water. In order to reduce neutron capture in hydrogen, B_2O_3 was dissolved in the water to form a saturated solution. The collimated neutron beam leaves the shielded space through a slot in the backwater shield. The sample can be rotated out of the beam by remote control for background measurement.

Neutrons are detected with a stilbene crystal from which pulses due to gamma rays are depressed by Brooks-Owen pulse shape discrimination. The crystal and photomultiplier are mounted

[3]H. B. Willard, J. K. Bair, and J. D. Kington, *Phys. Rev.* **98**, 669 (1955).

[4]J. L. Fowler and C. H. Johnson, *Phys. Rev.* **98**, 728 (1955).

[5]J. L. Fowler and H. O. Cohn, *Phys. Rev.* **109**, 89 (1958).

[6]J. L. Fowler, *Bull. Am. Phys. Soc.* **7**, 576 (1962).

UNCLASSIFIED
ORNL-LR-DWG 67369

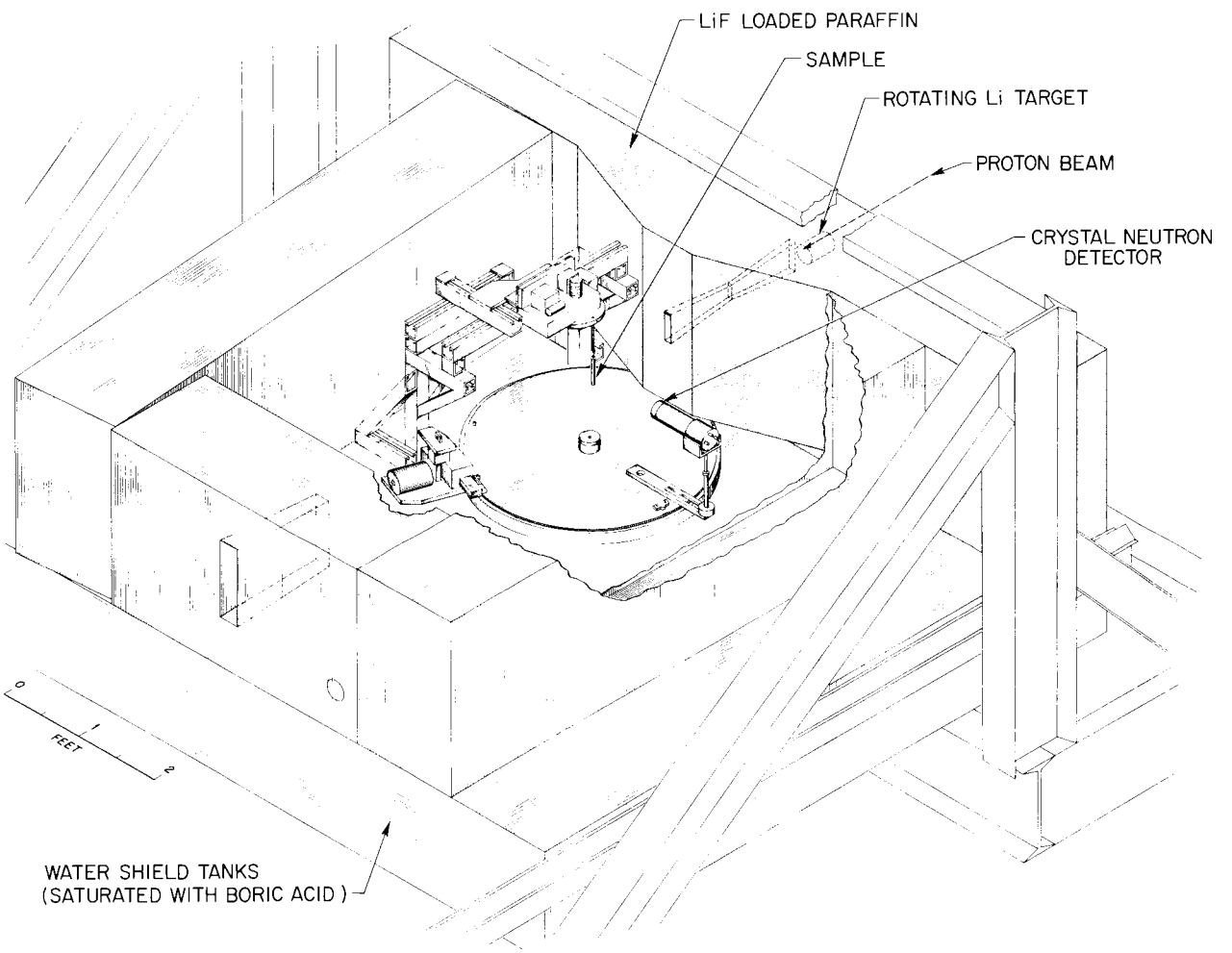

Fig. 2. Apparatus for Differential Scattering Measurements.

on a disk which is rotated by a remotely controlled worm gear which drives the disk at its edge. A system of selsyns allows one to read the angular position of the counter to at least 5 min of arc from the control room. The experimental equipment is on a gun mount, so that the entire apparatus can be rotated about the target position. This makes neutron polarization measurements possible with the apparatus.

In a typical differential cross-section measurement the sample is rotated out of the beam, the crystal is rotated to 0°, and the counts from the crystal for a fixed monitor count are determined. Neutron monitoring is done with a long counter at back angles from the target. The crystal is then rotated to the desired angle, the sample is rotated in place, and the scattered neutrons are detected for 10 times the monitor count of the 0° measurement. Background is found by rotating a blank sample support into place. Then the procedure is repeated for another angle. Since the stilbene crystal is of the order of 10% efficient, data with adequate statistics are acquired in a reasonable time in spite of the thin target and the small sample.

Figure 3 shows the differential cross sections at a number of resonant and nonresonant energies. This gives the cross section in the center-of-mass system plotted against the cosine of the center-of-mass angle. The approximate neutron energy spread is noted beside each curve. The arrows indicate the energy position of the differential measurements as they are related to the total cross section, taken from the data of Fig. 1. The resonant energies were relocated prior to the differential measurements by neutron transmission determinations made with a 72% Pb^{208} sample. The differential cross-section data have been corrected for multiple scattering by use of a procedure described in the literature.[5] At forward angles this correction amounted to, in some cases, the order of 20%. The errors shown here include an error for the multiple scattering correction which is assumed to be one-third the correction. For energies at which the cross section is not changing rapidly with energy, the absolute differential cross section integrated over all solid angle agrees with the measured total cross section within about 5%.

A partial phase-shift analysis, considering phase shifts up to *d* waves, has been made for the low-energy differential cross sections. The *s*-wave phase shifts have been extrapolated from lower energy measurements.[7] This analysis indicates the 0.723-Mev peak is a $J = 5/2$, $l = 2$ resonance. Similarly, the 0.769-Mev peak is identified as a $J = 3/2$, $l = 1$ resonance. From its similarity to the 0.723-Mev resonance, one deduces that the 0.821-Mev peak is also due to $J = 5/2$, $l = 2$ resonance.

Figure 4 shows an extension of the measurements to 1.111 Mev. The 0.855-Mev peak is a $J = 3/2$, $l = 2$ resonance. As one proceeds up the energy scale the potential scattering phase shifts for other than *s* waves become so important that one has to be more analytical in deducing the l values. This phase-shift analysis, including phase shifts up through *g* waves, has been coded for computation on the IBM 7090.

Figure 5 shows the measurements up to 1.342 Mev. For these higher energy differential cross sections there is a slight correction for the second group of neutrons from the Li(*p*,*n*) reaction. Because the neutron-detecting crystal has a lower efficiency for low-energy neutrons, this correction is small – of the order of 3% for the 1.342-Mev curve shown here. This correction has not been made for these curves. This sequence of differential cross-section measurements has been extended to 1.761 Mev.

Table 1 summarizes the information on the quantum parameters of the first few resonances above 0.7 Mev as obtained from the differential cross-section data and from the total cross-section measurements.[8]

[7] Mary Jo Mader and J. L. Fowler, *Tenn. Acad. Sci.* **37**, 70 (abstract) (1962).

[8] J. L. Fowler and E. C. Campbell, *Phys. Rev.* **127**, 2192 (1962).

Table 1. Quantum Parameters of First Few Resonances

Resonant Energy (Mev)	J	Parity	Reduced Width in Units $3\hbar^2/2ma^2$
0.723	$5/2$	+	0.02
0.769	$3/2$	–	0.01
0.821	$5/2$	+	0.04
0.855	$3/2$	+	0.02

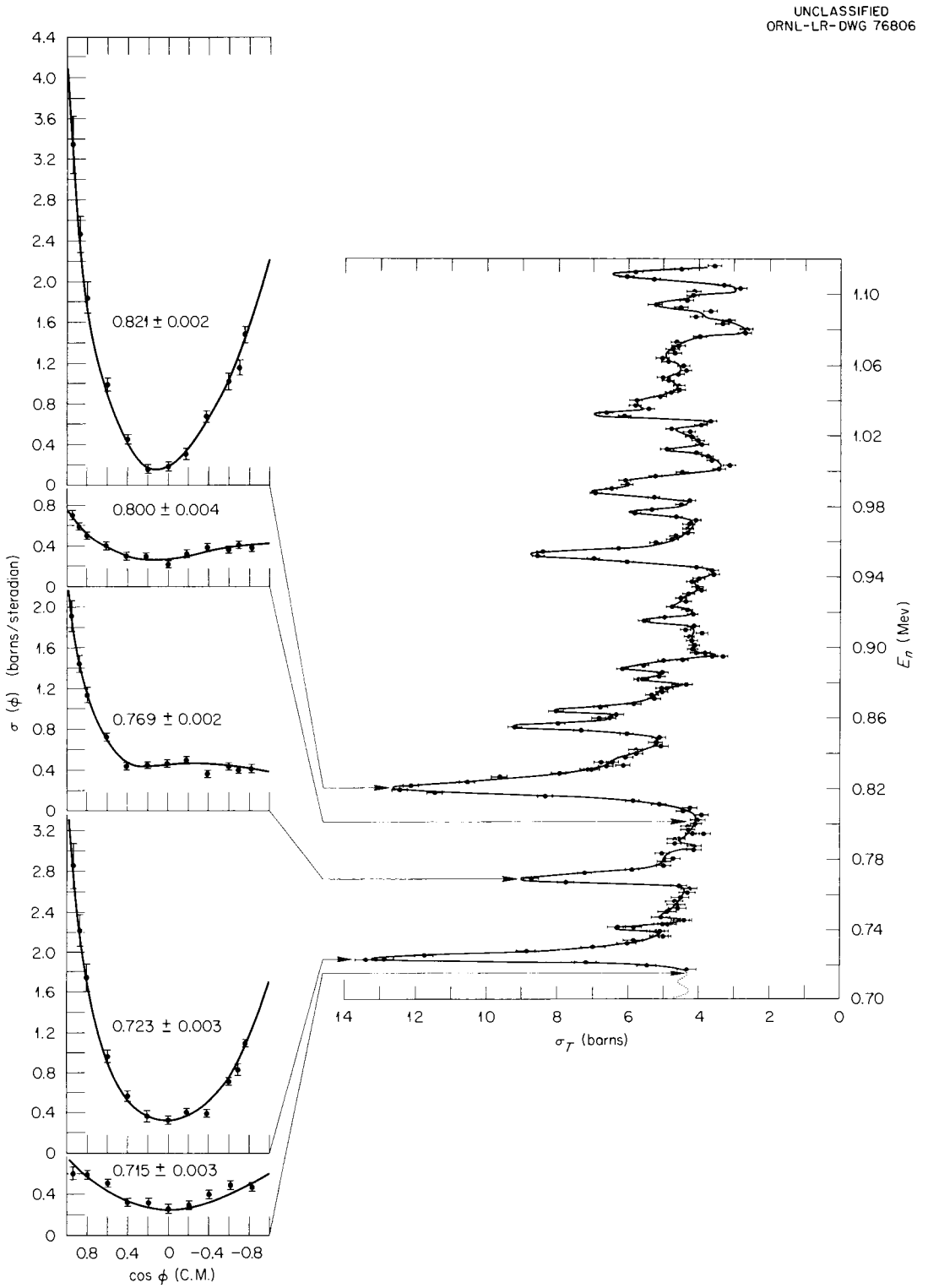

Fig. 3. Differential Cross Sections of Pb^{208} as a Function of Neutron Energies Between 0.715 and 0.821 Mev.

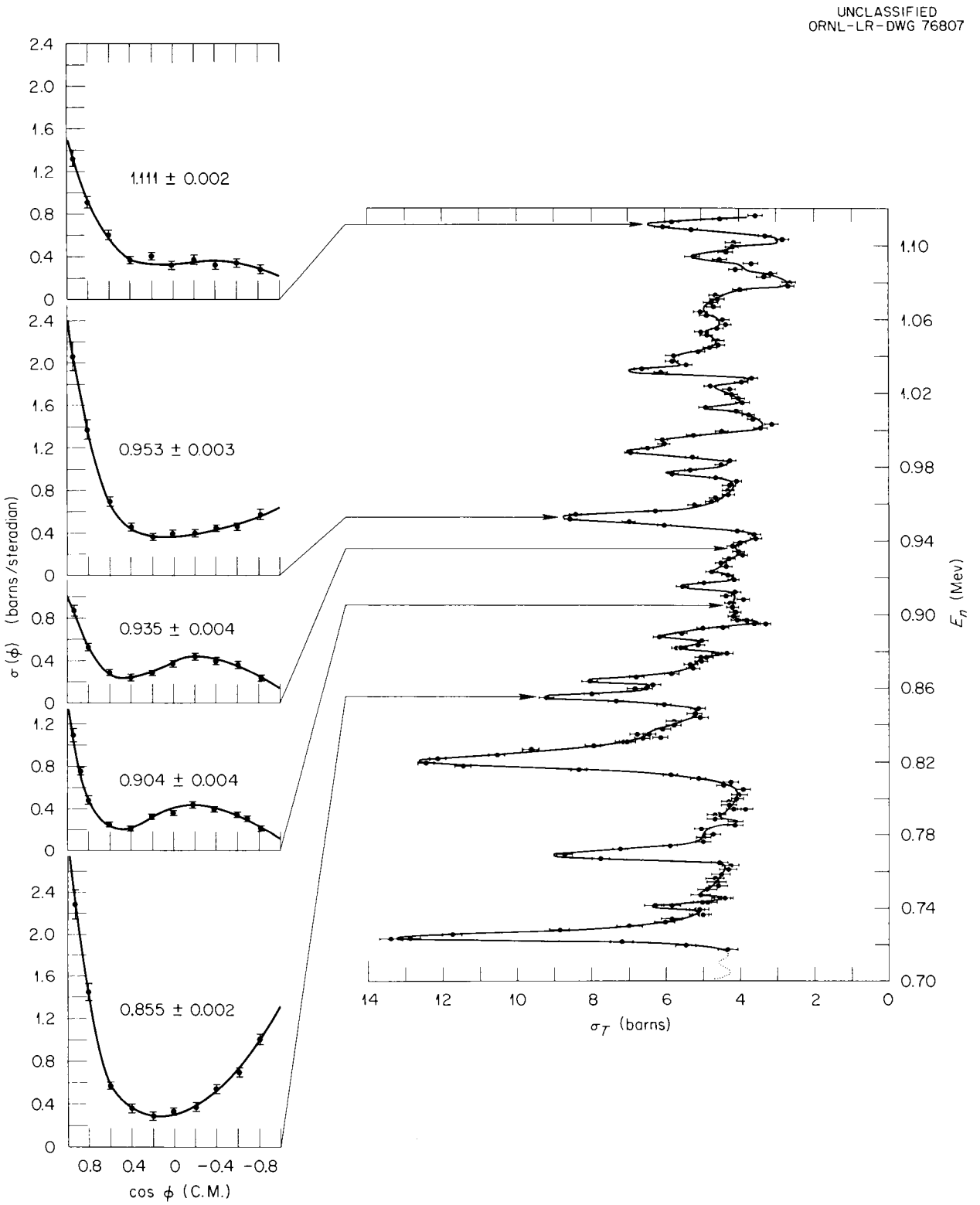

Fig. 4. Differential Cross Section Between 0.855 and 1.111 Mev.

UNCLASSIFIED
ORNL-LR-DWG 76829

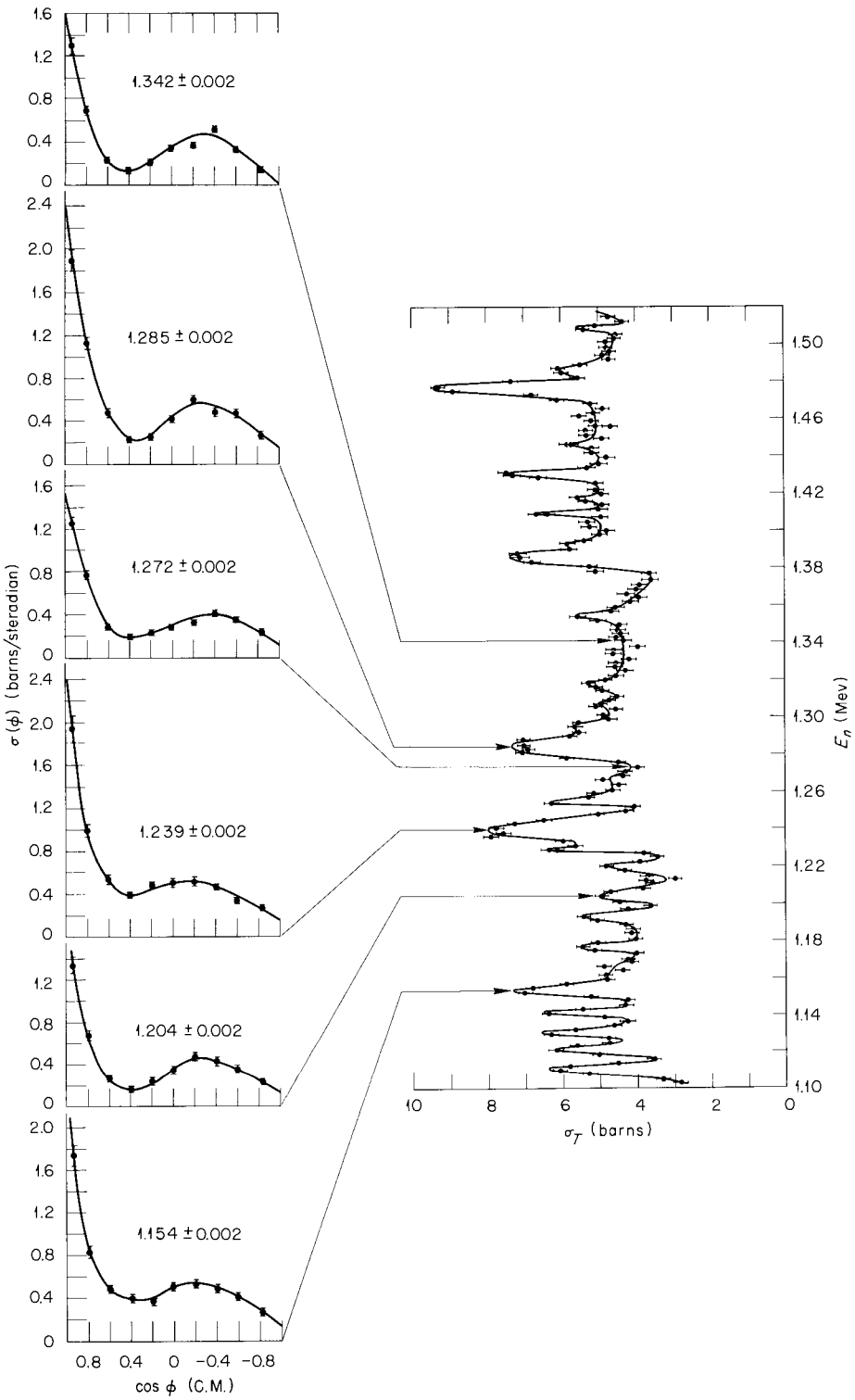

Fig. 5. Differential Cross Sections Between 1.154 and 1.342 Mev.

AVERAGE RADIATIVE CAPTURE CROSS SECTIONS FOR 30- AND 65-kev NEUTRONS[1]

R. L. Macklin J. H. Gibbons T. Inada[2]

Neutron radiative capture cross sections near 30 and 65 kev have been measured for a large number of elements by means of a large liquid scintillator and a pulsed neutron source. The results show definitive even- vs odd-A effects as well as systematic variations due primarily to effects of nuclear shells. Calculations of the scintillator efficiency for various capture gamma-ray cascade modes are in good agreement with experimental results.

[1]Abstract of paper to be published in *Physical Review*.

[2]Visiting scientist from NIRS, Japan.

NEUTRON CAPTURE IN TIN ISOTOPES AT STELLAR TEMPERATURES[1]

R. L. Macklin T. Inada[2] J. H. Gibbons

The 30-kev neutron capture cross sections of seven tin isotopes ($Sn^{116,117,118,119,120,122,124}$) were measured with the ORNL pulsed 3-Mv Van de Graaff and a fast Moxon-Rae detector. The results are in reasonable agreement with the theory of element formation in red giant stars and provide information which helps determine further parameters of related theories.

[1]Abstract of published paper: *Nature* **194**, 1272 (1962).

[2]Visiting scientist from NIRS, Japan.

THE 30-kev NEUTRON CAPTURE IN THE SAMARIUM ISOTOPES[1]

R. L. Macklin J. H. Gibbons T. Inada[2]

Recent theories concerning the formation of the elements are based on neutron capture in red giant stars and supernovae. The isotopic capture cross sections of the samarium isotopes are particularly significant because two of them, Sm^{148} and Sm^{150}, cannot be formed by neutron capture in supernovae. The red giant process predicts the cross-section ratio (from the observed isotopic abundance N) for these two cases. Measurements near 30 kev (comparable with thermal energies in a star) confirm the predicted cross-section ratio very closely. For the ratio $N\sigma_c(Sm^{150})/N\sigma_c(Sm^{149})$ we find a value 1.02 (±6%), where the theory predicts a value close to 0.98. From the measured cross sections of the other isotopes, some information on the supernova process can be derived. The high capture cross section of Sm^{149} below a few electron volts neutron energy does not seem to have resulted in any appreciable shift in the expected values. This places some restriction on theories accounting for deuterium formation by neutron capture in solid or liquid planetesimal bodies.

[1]Abstract of paper to be published in *Nature*.

[2]Visiting scientist from NIRS, Japan.

NEUTRON CAPTURE CROSS SECTIONS NEAR 30 kev USING A MOXON-RAE DETECTOR[1]

R. L. Macklin J. H. Gibbons T. Inada[2]

Neutron radiative capture cross sections for neutrons near 30 kev have been measured using a Moxon-Rae detector. A time-of-flight system with a resolution of less than 3 nanoseconds and a 7-cm flight path has been shown applicable to small sample measurements. The 30-kev results for molybdenum, cadmium, tin, tantalum, tungsten, platinum, and gold and cross section vs energy curves for fluorine, sulfur, and yttrium are presented.

[1]Abstract of paper to be published in *Nuclear Physics*.

[2]Visiting scientist from NIRS, Japan.

RESONANT NEUTRON CAPTURE GAMMA-RAY SPECTRA

J. H. Gibbons J. R. Bird[1]
W. M. Good J. A. Biggerstaff

The facilities for the study of neutron capture gamma-ray spectra at electron kilovolt neutron energies have been refined to permit studying the energy dependence of the spectra. The refinements, which have been made, consist of (1) converting the 2040-channel analyzer to a 16 × 128 channel to permit two-dimensional (E_n vs E_γ) data acquisition, (2) increasing peak neutron intensities by means of bunching of the pulsed ion beam, and (3) attention to detector shielding. The earlier studies[2] have therefore been extended to obtain information on the dependence of gamma-ray spectral distributions on neutron energy. One other extension of the earlier data has been to study separated isotopes in certain instances where this has been feasible.

The neutron capture spectra from Al, F, Fe, Ca, Ni, and Pb have been reported.[2] Measurements have been extended to the following nuclides: Pb^{206}, Pb^{207}, Ca^{40}, Ca^{42}, Ca^{44}, Ti^{nat}, Zn, V^{51}, Ge^{nat}, Y^{89}, Sr^{88}, Fe^{54}, Fe^{56}, Zr^{nat}, Zr^{92}, Zr^{94}, Cd^{nat}, and In^{113}.

In only a few of these cases have the background subtractions been performed, and in no case have the spectra been corrected for individual line shape and spectrometer efficiency. Already, however, some results of interest have been obtained.

In general, the study of resonant spectra is of interest in order to (1) obtain information on continuum states, (2) obtain information on bound states, (3) understand better the mechanisms of capture, and (4) extract and study gamma-ray reduced widths.

In the region of $A = 50$, where the *s*-wave strength function has its maximum and the 2-*p* states are close to ground, the thermal capture gamma-ray spectrum might be expected to resemble that in the resonance region. As Lane[3] and others[4,5] have pointed out, however, the dominance of the direct capture process to ground and low excited states at thermal capture energies, in contrast to the situation in resonance capture in the resonance region, has the effect of effectively depressing the high-energy or ground-state transitions for the nuclei in the neighborhood of iron, copper, nickel, etc. Such a general effect was evident in previously published data. With the availability of over 100 g of Fe^{54} and Fe^{56} it has been possible

[1]Now at AERE, Harwell, England.

[2]J. R. Bird, J. H. Gibbons, and W. M. Good, *Phys. Letters* **1**(7), 262 (1962).

[3]A. M. Lane and J. E. Lynn, *Nucl. Phys.* **17**, 563 (1960).

[4]C. Shakin, private communication.

[5]H. Morinaga and C. Ishii, *Progr. Theoret. Phys. (Kyoto)* **23**(1), 161 (1960).

to gather more information on the details of the resonant capture spectra. With this "small" sample size, however, sufficient energy resolution was not attainable to be able to obtain very detailed information on the manner in which the spectra depend upon energy. Figures 1 and 2 show the $Fe^{54} + n$ and $Fe^{56} + n$ gamma-ray spectra at about 30 kev. Figure 3 is a reproduction of the thermal spectrum on natural iron taken from

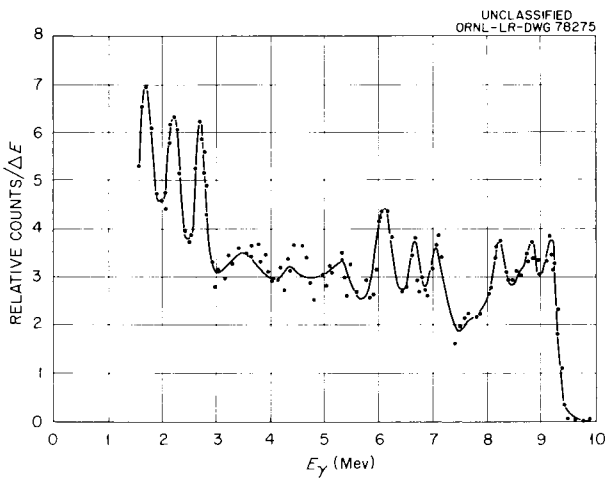

Fig. 1. Fe^{54} Neutron Capture Gamma-Ray Spectrum at About 30 kev.

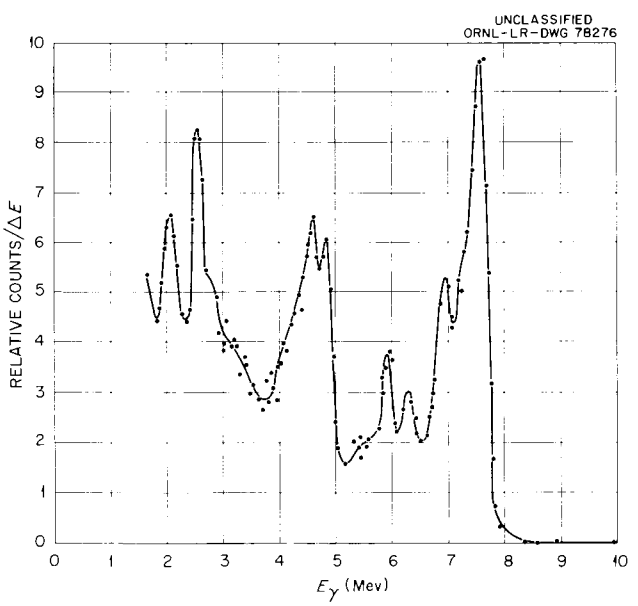

Fig. 2. Fe^{56} Neutron Capture Gamma-Ray Spectrum at About 30 kev.

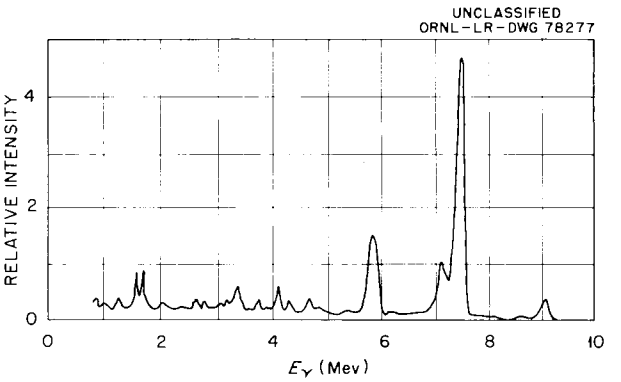

Fig. 3. Fe^{nat} Neutron Capture Gamma-Ray Spectrum at Thermal.

Groshev.[6] The relatively greater prominence of transitions through excited states in the case of resonant capture as compared with thermal capture is evident. In spite of an abundance of available bound states, it is seen that the gamma-ray spectra consist substantially of only a few lines.

Further studies have been made on Pb^{206} and Pb^{207}. In the energy region below 100 kev, Pb^{207} was known to have an *s*-wave resonance at about 42 kev.[7,8] Nothing was known, with certainty, about Pb^{206} in this energy region although there was fair reason to believe that one of the lead isotopes had very narrow resonances, but it was not certain which isotope. There were available a few pounds of 88% Pb^{206} and 200 g of Pb^{207}. With these samples it was possible to study the spectra for the case of Pb^{206} with a resolution of 20 nanoseconds/m and the Pb^{207} with a resolution of 100 nanoseconds/m. From the knowledge that Pb^{206} captured through several excited states as well as directly to ground[9] and that the Pb^{208} binding energy was 0.7 Mev higher than that of Pb^{207}, it was possible to employ the 16 × 128

[6] L. V. Groshev, V. N. Lutsenko, A. M. Demidov, and V. I. Pelekhov, *Atlas of γ-Ray Spectra from Radiative Capture of Thermal Neutrons*, Pergamon, New York, 1959.

[7] H. W. Newson *et al.*, *Ann. Phys.* **14**, 354 (1961).

[8] H. Muenzer, K. Nishimura, and W. M. Good, private communication.

[9] W. M. Good, J. H. Gibbons, and J. R. Bird, *Proceedings of International Symposium on Direct Interactions and Nuclear Reaction Mechanisms*, Padua, Italy, Sept. 3–8, 1962.

analyzer in coarse gamma-ray energy resolution in order to obtain some details on the capture cross sections with energy of both Pb^{206} and Pb^{207}. The results are shown in Fig. 4 for Pb^{206} capture and in Fig. 5 for Pb^{207} capture. The peak amplitudes must be corrected by the relative neutron intensities shown in Fig. 6.

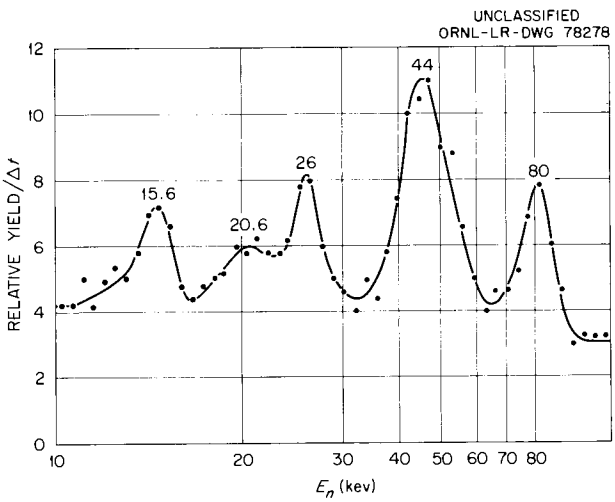

Fig. 4. Relative Yield per Time Interval of Gamma Rays from $Pb^{206}(n,\gamma)$.

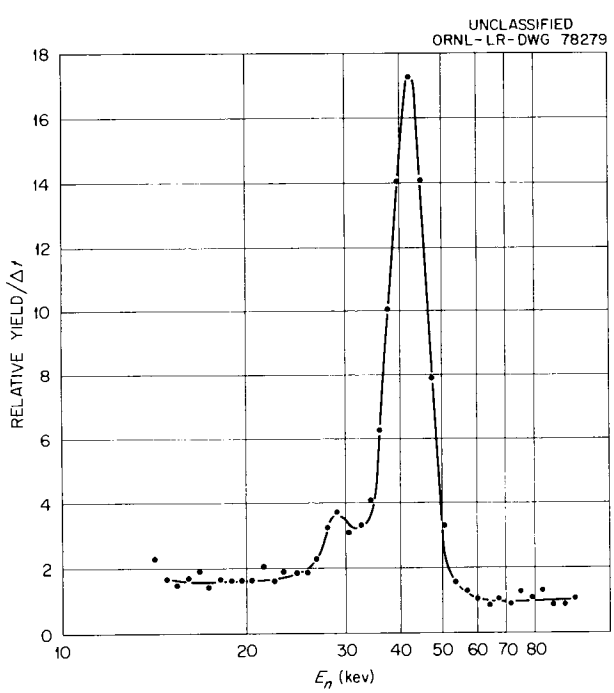

Fig. 5. Relative Yield per Time Interval of Gamma Rays from $Pb^{207}(n,\gamma)$.

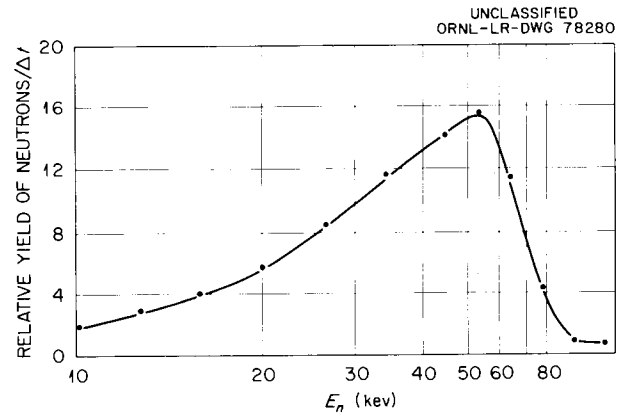

Fig. 6. Relative Yield per Unit Time Interval of Neutrons as Measured by $In(n,\gamma)$.

From knowledge of the level positions, it was possible in the case of Pb^{206} to take gamma-ray spectra in coarse neutron energy resolution and thereby examine the gamma-ray spectra from resonance to resonance. The resulting spectra showed transitions, as reported earlier,[9] through the 0.57 and 0.89 levels, as well as directly to ground. In addition, strong transitions were observed to correspond to a state at 2.65 and another state, most likely the one at 3.47. There are suggestions of weak transitions through the 1.63-, 2.34-, 2.71-Mev states; none through 1.90. The relative intensities of these various lines varied drastically from resonance to resonance in contrast to the situations in fluorine and Ca^{40}, in which spectra have also been observed at two resonances each.

The neutron resolution was very poor for the Pb^{207} because of the sample size. However, as the spectra in Figs. 7 and 8 show, the transition through the 3^- state in Pb^{207} appears to resonate most strongly at a different energy ($\approx$ 15 kev) from that of the ground-state transition which resonates strongly at the well-known 42-kev energy. The resonance character of this transition is surprising on the surface, since there appears to be some thought that the compound nucleus is not expected to select octupole vibrational states.[10]

[10] A. M. Lane and E. D. Pendlebury, *Nucl. Phys.* **15**, 39 (1960).

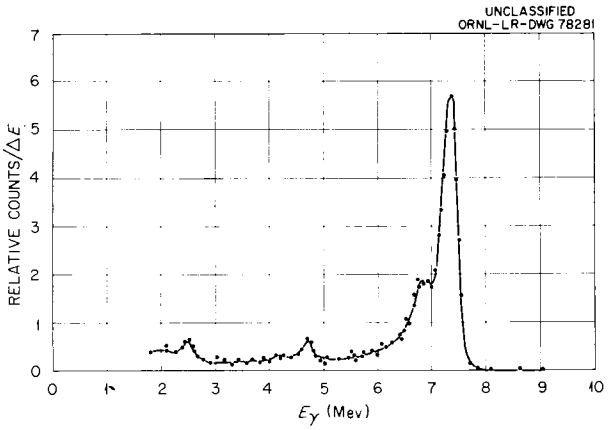

Fig. 7. Pb^{207} Neutron Capture Gamma-Ray Spectrum at $E_n > 40$ kev.

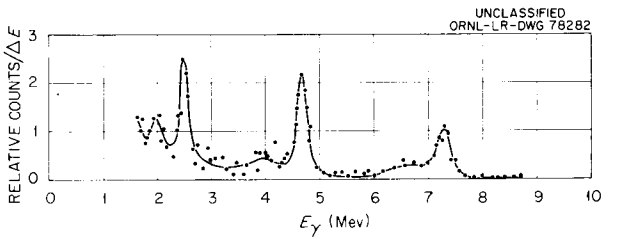

Fig. 8. Pb^{207} Neutron Capture Gamma-Ray Spectrum at $E_n \approx 15$ kev.

GAMMA-RAY SPECTRA FROM NEUTRON CAPTURE

G. G. Slaughter
J. A. Harvey
G. T. Chapman[1]
J. R. Bird[2]

A large (9-in.-diam by 12-in.-long) NaI crystal with associated gamma-ray and neutron shielding has been installed at a 5-m flight path of the fast-chopper neutron time-of-flight spectrometer at the ORR. Gamma-ray spectra due to neutron capture in resonances have been taken at a neutron time-of-flight resolution of about 0.5 μsec/m (about 15% energy resolution at 100 ev). The gamma-ray spectra from thermal neutron capture have been taken with the rotor stopped in an open position. The data are collected by a time-gated 2 × 128 channel pulse-height analyzer.

Neutron capture gamma-ray spectra from the capture of both thermal and resonance energy neutrons in Sn^{118} and Sn^{124} targets are shown in Fig. 1. The resonance spectra are taken with a cadmium filter interposed in the beam. Both sets of spectra show a marked difference between thermal and resonance neutron capture. Since highly enriched isotopes were used as the samples, the differences are not attributable to changes in relative capture cross sections of the different isotopes, although there is some trace of the Sn^{118} spectrum in the Sn^{124} spectrum. Fluctuations of partial gamma-ray widths in individual resonances and the averaging of these fluctuations could cause such a difference. Gamma-ray spectra from neutron capture in the individual resonances of the tin isotopes are currently being taken in order to gain more information concerning the changes of spectra with neutron energy.

Capture spectra in copper for the first two resonances at 230 ev (Cu^{65}) and 590 ev (Cu^{63}) are compared with the spectra from neutron capture at thermal energy and from 0.5 to 2 ev in Fig. 2. Since these resonances are responsible for only a

[1]Neutron Physics Division.

[2]Visiting scientist from AERE, Harwell, England.

UNCLASSIFIED
ORNL-LR-DWG 75280

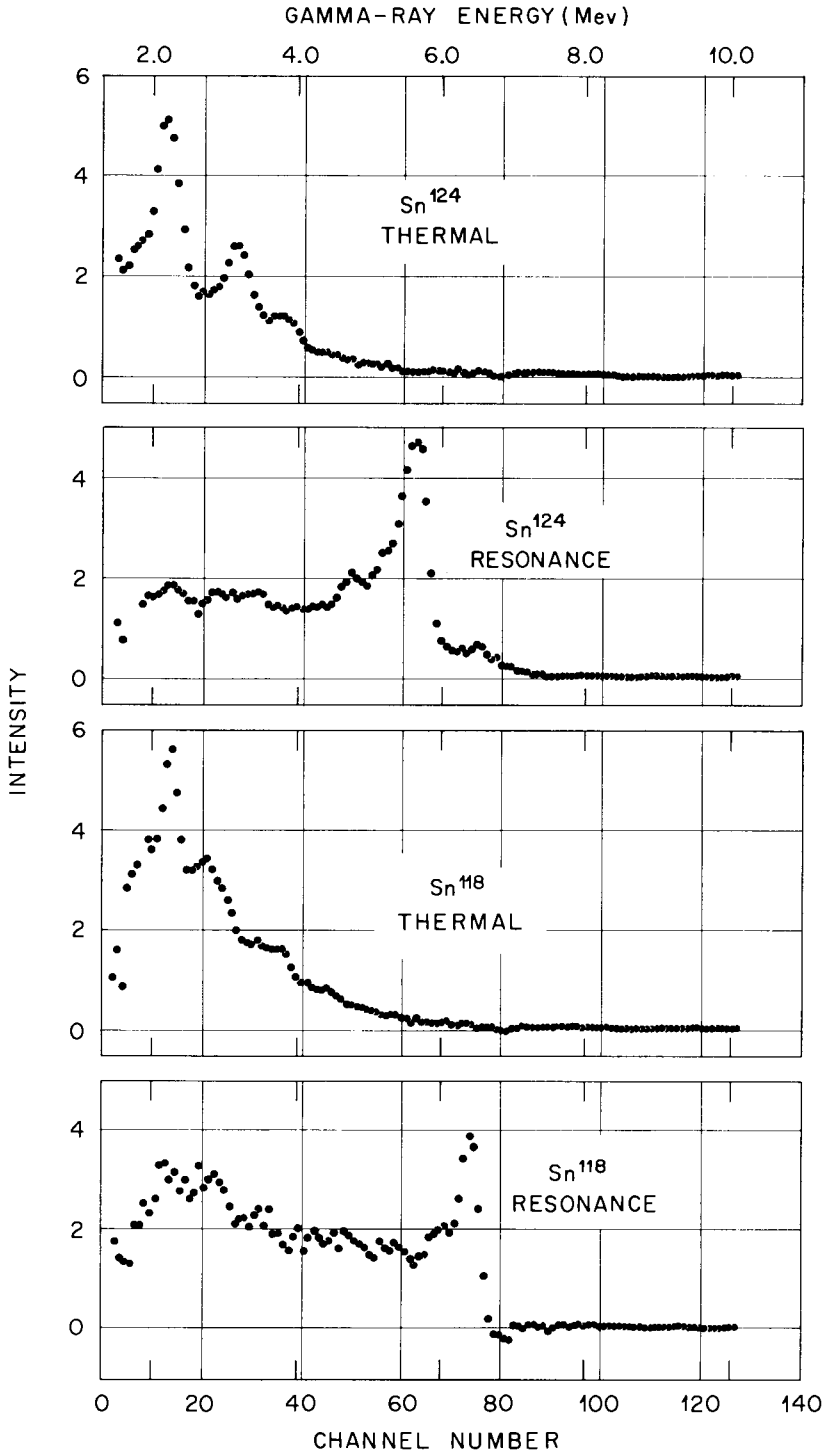

Fig. 1. Gamma-Ray Spectra from Thermal and Resonance Energy Neutron Capture in Sn^{118} and Sn^{124}. The thermal spectra are obtained with the rotor stopped in an open position. The resonance spectra are obtained with a cadmium filter interposed.

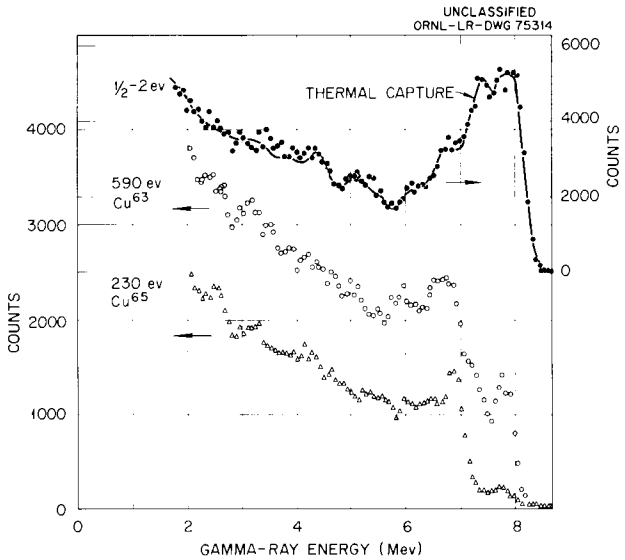

Fig. 2. Gamma-Ray Spectra from Thermal Capture in Natural Copper (Solid Line); ½ to 2 ev Capture in Natural Copper (Solid Circles); the 590-ev Resonance in Cu^{63} (Open Circles); and the 230-ev Resonance in Cu^{65} (Open Triangles).

small part of the capture cross section at thermal energies, it is to be expected that the resonance spectra will differ from the thermal spectrum. This is evidenced by the fact that the thermal spectrum, which is due to both isotopes, cannot be formed by a linear combination of the two resonance spectra. In general, the thermal spectrum exhibits more strong high-energy gamma rays. These data are of interest for testing the suggestion that direct capture is important in copper, inasmuch as the direct capture cross section has a secondary maximum in this mass region.[3]

[3] A. M. Lane and J. E. Lynn, *Nucl. Phys.* **17**, 560 (1960).

In Figs. 3 and 4 are shown gamma-ray spectra due to thermal neutron capture in isotopes of calcium and titanium. The spectra for Ca^{40}, Ca^{42}, and Ca^{44} targets were each dominated by a strong gamma ray involving a transition to an excited state near 2 Mev. The same states have been observed to show $l_n = 1$ angular distributions and large reduced widths in the (d,p) reaction, implying strong single-particle levels. It is reasonable to assume, therefore, that these particular levels observed in Ca^{41}, Ca^{43}, and Ca^{45} consist of the target nucleus as a core and the odd neutron in the shell-model $2p_{3/2}$ orbital. The dominant gamma ray in the Ca^{41} product nucleus is a transition from the capturing state to a state previously identified as $\frac{3}{2}^-$. Other weaker gamma rays in these calcium isotopes show this correspondence to transitions to levels that are observed to have $l_n = 1$ in the (d,p) stripping reaction; it is proposed that these levels are $2p_{1/2}$ shell-model states. If the thermal absorption cross section and gamma-ray multiplicity of a nuclide are low, then the effects of direct capture may be evident. Since the direct capture cross section has a maximum in this mass region, and there are low-lying single-particle p states, most of the conditions for the observation of direct capture are present. The exception is the relatively high thermal absorption cross section of Ca^{42}. The results from the Ca^{43} target show, as expected, a more complicated spectrum tending more toward a continuum than the spectra from even-even targets. The results for the samples of enriched titanium isotopes are dominated by capture in Ti^{48}. It is not possible to assign any strong gamma rays to Ti^{46} or Ti^{50} target nuclides. The results for the Ti^{48} target nuclide are similar to those for the even-even calcium target nuclides.

A computer program has been written which will unfold the experimentally determined gamma-ray spectra to obtain the intensities of the gamma-ray lines. The response functions for the crystal are being coded into the program.

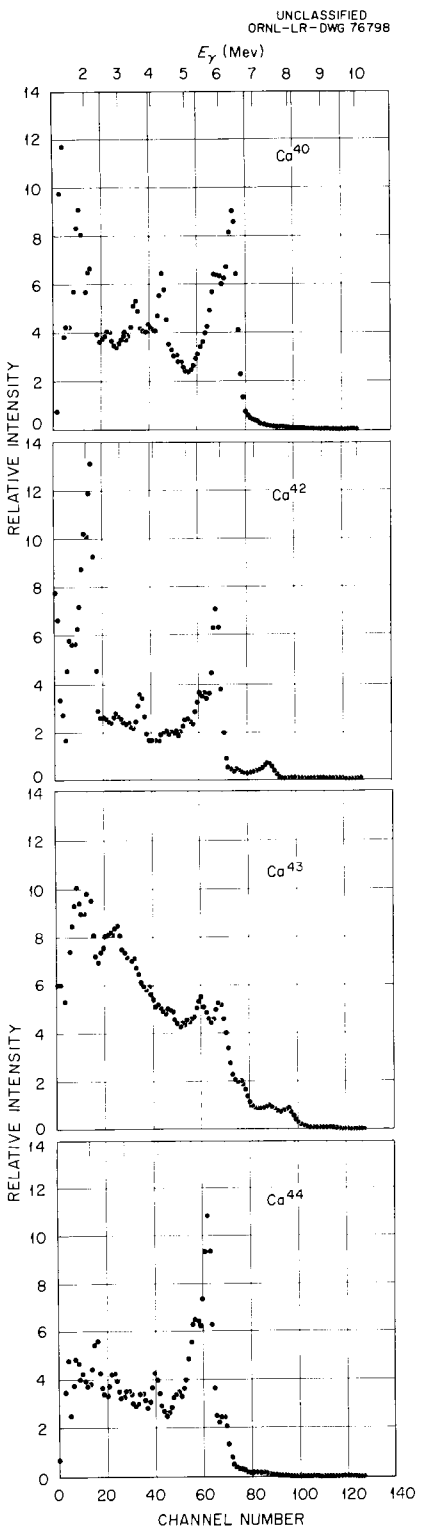

Fig. 3. Gamma-Ray Spectra from Thermal Neutron Capture in Samples of Enriched Calcium Isotopes.

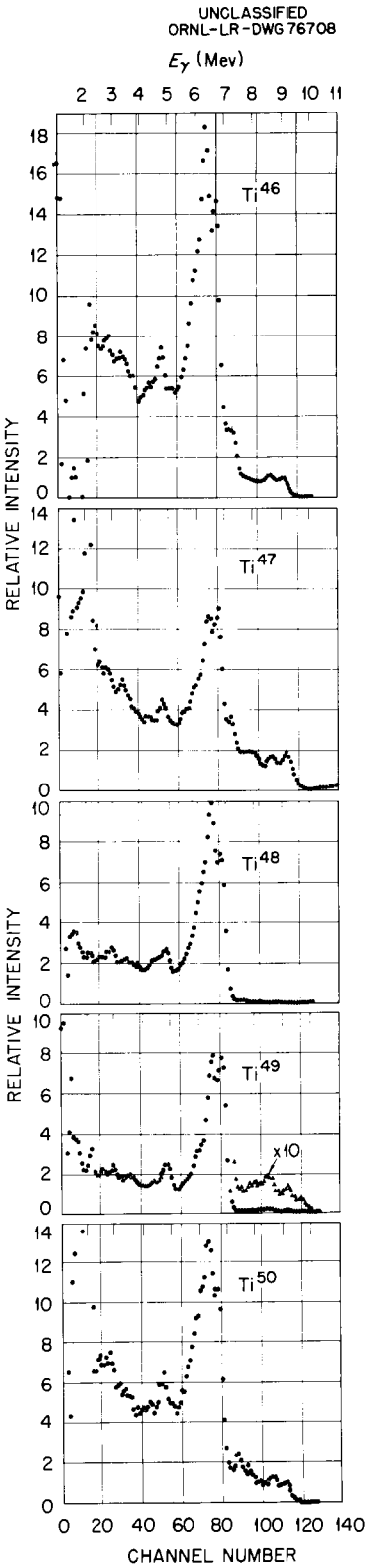

Fig. 4. Gamma-Ray Spectra from Thermal Neutron Capture in Samples of Enriched Titanium Isotopes.

ORNL-RPI CAPTURE EXPERIMENT

R. C. Block

J. E. Russell[1] R. W. Hockenberry[1]

Introduction

The neutron radiative capture measurements previously carried out with the ORNL fast chopper[2,3] were severely limited in accuracy by three experimental conditions: (1) the low gamma-ray detection efficiency of the 0.75-m-diam liquid scintillator, (2) the high neutron and gamma-ray backgrounds near the ORR, and (3) the limited neutron energy resolution which could be obtained with the chopper. The first limitation has been largely overcome by building a new 1.25-m-diam liquid scintillator to improve the gamma-ray detection efficiency. The latter two conditions were alleviated by moving this new detector to the Rensselaer Polytechnic Institute's (RPI) new electron linear accelerator laboratory, where the steady-state background is much lower than that near a reactor and where the neutron energy resolution is considerably better than that obtainable with the chopper.

This new detector was installed at RPI early in 1962 and neutron radiative capture measurements were made on samples of tungsten, iron, Fe^{56}, and enriched samples of the hafnium isotopes. Many new resonances were observed in capture, and the data were analyzed for resonance parameters and level spacings.

Experimental Method

The neutron radiative capture detector is illustrated in Fig. 1. A thin-walled steel shell was fabricated from conical and cylindrical sections to approximate a spherical tank 1.25 m in diameter. This tank is filled with 1100 liters of xylene solution, containing 4 g/liter of *p*-terphenyl and 0.5 g/liter of α-NPO. To this solution was added methyl borate in the ratio of 0.0056 boron atom per hydrogen atom; this boron loading reduces the probability of hydrogen capture of neutrons scattered into the solution by a factor of $\sim$14. The scintillator is viewed by only two 16-in.-diam Du Mont photomultipliers, and the signals are connected in parallel to an A-8 preamplifier and amplifier. This system permits the timing of a capture event to $\pm$25 nanoseconds, adequate for these time-of-flight measurements. (Most of the 25-nanosecond timing uncertainty results from the time spread of photoelectrons in the 16-in.-diam photomultipliers.)

The scintillator is shielded by a 4-in.-thick house of lead, and a 6-in. shield of borated paraffin is located on the face of the lead shield facing the accelerator. A 7-in.-diam aluminum flight tube passes through the center of this scintillator to permit the collimated neutron beam to pass through without directly striking the detector. Capture samples are placed in the middle of this tube, as shown in Fig. 1, and these samples are enclosed in a 1.75-in.-thick Li^6H liner to reduce the scattered neutrons from either entering or leaving the scintillator in the vicinity of the sample. The aluminum flight tube can be evacuated or filled with argon to reduce air scattering. The detector is biased at 2.0 Mev (gamma-ray energy) and has an efficiency of $\sim$85% for detecting a capture event. The 1.25-m-diam detector is installed at the 25-m flight station of the RPI accelerator laboratory.

The pulsed neutrons are produced by allowing the electrons to strike a 3-cm-thick tungsten target, and then allowing these photoneutrons to be moderated by a 2.5-cm-thick paraffin slab. The paraffin slab is slightly offset from the tungsten target, and the neutron beam is collimated so that the capture detector views only the paraffin and not the tungsten; this reduces the effects of beam flash in the detector, but it also reduces the final neutron intensity. The linear accelerator can produce electron pulses as short as 100 nanoseconds with a peak beam current of 2 amp and an electron energy of 66 Mev. The maximum permissible repetition rate is 720 pulses/sec.

The amplified scintillation pulses are fed into a combination crossover pickoff and wide-window

[1]Rensselaer Polytechnic Institute.

[2]R. C. Block and G. G. Slaughter, *Phys. Div. Ann. Progr. Rept. Feb. 10, 1960*, ORNL-2910, p 35.

[3]R. C. Block, F. C. VonderLage, and L. W. Weston, *Phys. Div. Ann. Progr. Rept. Feb. 10, 1961*, ORNL-3085, p 48.

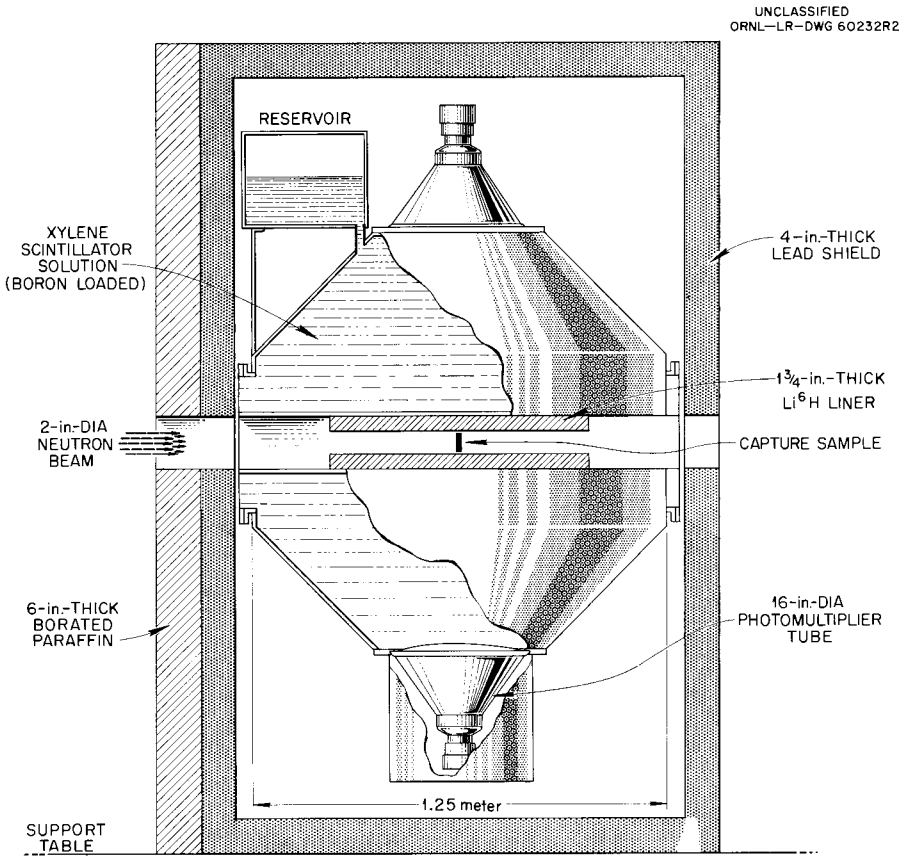

Fig. 1. ORNL Liquid Scintillator Capture Detector.

single-channel analyzer designed and constructed by the ORNL Instrument Division. The pulses from this unit are fed into the RPI time analyzers. These time analyzers consist of two 256-channel analyzers with 0.25- to 16-μsec-wide channels, a 2000-channel analyzer with 0.1-μsec-wide channels, and a 1024-channel Technical Measurements Corporation analyzer with 0.25-μsec wide channels (with future provision for 30-nanosecond-wide channels).

The neutron spectrum incident on the capture sample is measured with a "black" (B^{10}-NaI) detector placed behind the scintillator at a flight distance of 27 m. The technique of always leaving a gold sample inside the capture detector and looking at the counting rate from the 4.9-ev gold resonance is utilized both to determine the efficiency of the scintillation detector and to monitor each capture measurement. Capture measurements are typically accomplished in 3 to 6 hr.

Results

Tungsten. – A typical time-of-flight capture spectrum from a 0.025-in.-thick tungsten sample is plotted in Figs. 2 and 3. This spectrum is characterized by strong resonance structure, and many of the resonances are resolved by the neutron resolution of 7 nanoseconds/m achieved in this measurement. The peak-to-valley ratios of these resonances often reach 10:1 and indicate the good signal-to-background ratio of this equipment.

It is of prime interest to extract the parameters of the resonances from these capture measurements, in particular the radiation widths and total angular momentum J of each resonance. This can be accomplished by measuring the area under each resonance, correcting this area for multiple scattering, and then extracting from this corrected area the value of $\sigma_0\Gamma_\gamma$ characteristic of the resonance. The peak cross section σ_0 is equal to $4\pi\lambda\!\!\!^{-}{}_0^2 g\Gamma_n/\Gamma$,

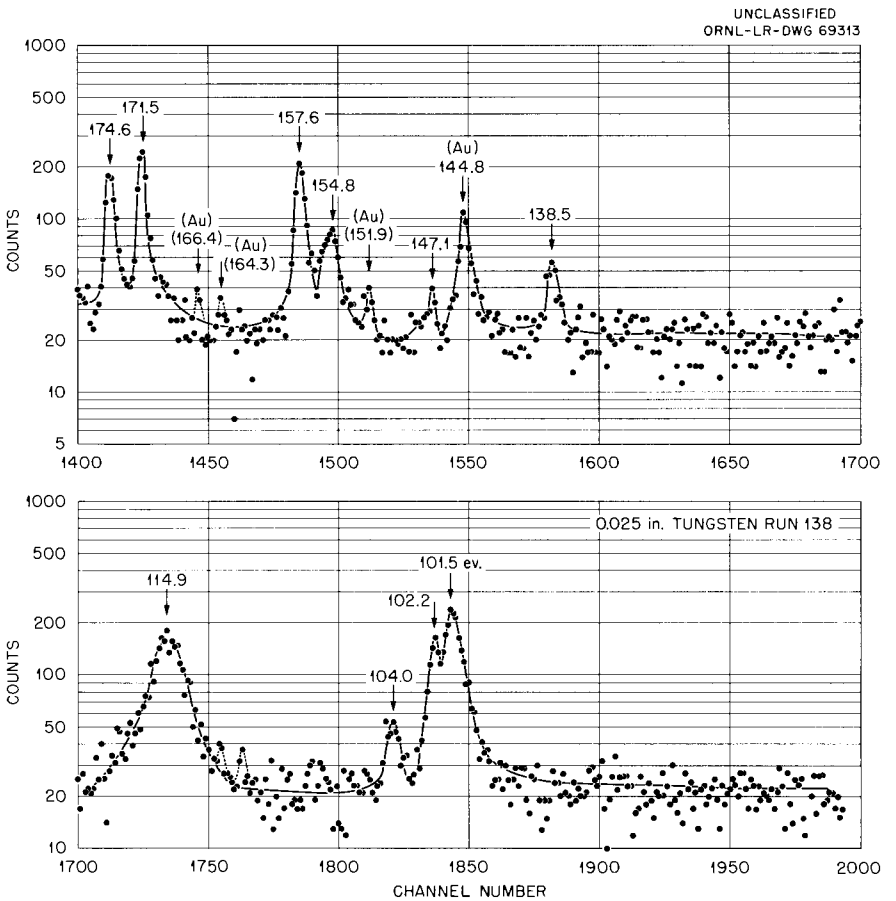

Fig. 2. Neutron Capture Time-of-Flight Spectra from 0.025-in.-Thick Tungsten.

where $2\pi\lambda\!\!\!^{-}_0$ is the neutron wavelength at the resonance energy, g is the statistical weight factor of the resonance, and Γ_n, Γ_γ, and Γ are, respectively, the neutron, radiation, and total widths of the resonance. For example, in a "thin" sample measurement the area under the capture resonance, $\int \sigma_c \, dE$, is determined by

$$\int \sigma_c \, dE = \frac{\pi}{2} N \sigma_0 \Gamma_\gamma \, , \qquad (1)$$

where N is the sample thickness in atoms/barn. In a thicker sample measurement the product $\sigma_0 \Gamma_\gamma$ can also be determined, but in this case the effects of Doppler broadening introduce the additional complication of a dependence of $\sigma_0 \Gamma_\gamma$ on Γ. Thus, a neutron capture measurement yields $\sigma_0 \Gamma_\gamma$, and this reduces to a value of $g\Gamma_n \Gamma_\gamma / \Gamma$.

For those resonances where $\Gamma_n \gg \Gamma_\gamma$, and hence $\Gamma \approx \Gamma_n$, the product $g\Gamma_n \Gamma_\gamma / \Gamma$ reduces to $g\Gamma_\gamma$, and the capture measurement uniquely yields information on the radiation widths and spin states of these resonances. This condition is typical for the higher energy resonances at neutron energies $\gtrsim 100$ ev. For resonances where $\Gamma_n \sim \Gamma_\gamma$ the capture data must combine with other data, such as transmission or scattering data, before the resonance parameters can be extracted. In those cases where $\Gamma_\gamma \gg \Gamma_n$, and hence $\Gamma \approx \Gamma_\gamma$, then $g\Gamma_n \Gamma_\gamma / \Gamma$ reduces to $g\Gamma_n$. However, $g\Gamma_n$ can be obtained directly from a transmission measurement, and here the capture measurement only confirms a transmission measurement; this is frequently the case at low neutron energies. It is significant, however, that capture measurements are a "positive" type of measurement and do tend to be more sensitive than transmission measurements for detecting very small capture resonances.

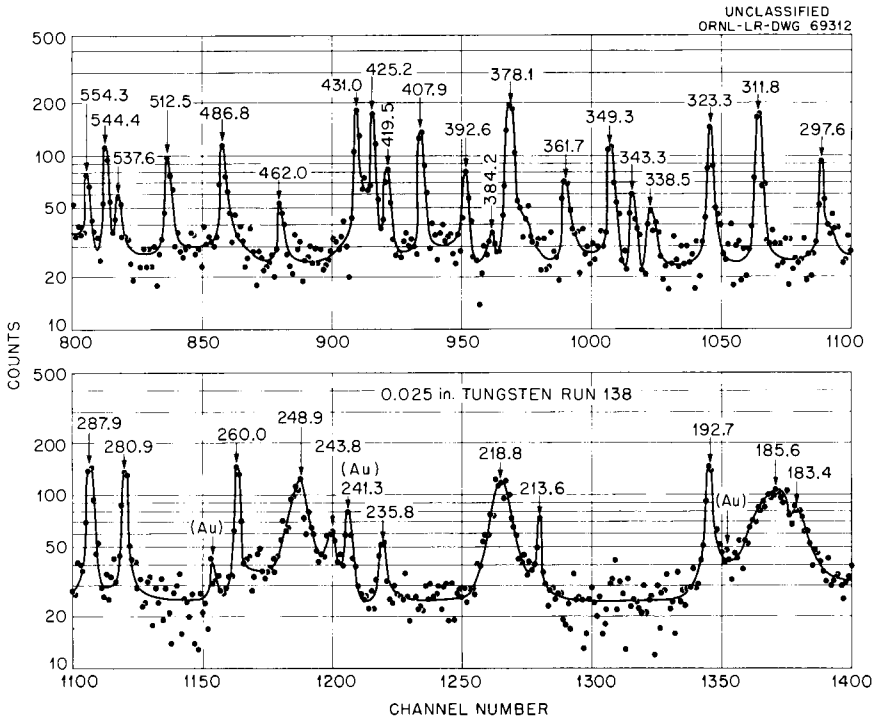

Fig. 3. Neutron Capture Time-of-Flight Spectra from 0.025-in.-Thick Tungsten.

It is difficult to correct for multiple scattering in moderately thick samples, and it was found more expedient to utilize the "extrapolation to zero thickness" technique of Rae *et al.*[4] in determining $\sigma_0 \Gamma_\gamma$. Accordingly, capture measurements were made on samples of tungsten varying in thickness from 0.001 to 0.120 in. In Fig. 4 are plotted the results for the 101.5-ev resonance in W^{183}, the 115-ev resonance in W^{182}, the 171-ev resonance in W^{186}, and the 185-ev resonance in W^{184}. Equation (1) is used to compute $\sigma_0 \Gamma_\gamma$, and this is plotted vs decreasing sample thickness $1/\sqrt{N}$ (in the manner introduced by Isakov *et al.*[5]). No multiple scattering corrections are applied to the data. The errors indicated for $\sigma_0 \Gamma_\gamma$ are statistical only. It is noted that each curve in Fig. 4 asymptotically approaches a constant value of $\sigma_0 \Gamma_\gamma$ with decreasing sample thickness. However, the error in this asymptotic value is dominated by the errors in the thin sample measurements, and the statistically more accurate data from the thicker samples are not utilized. This illustrates that the multiple scattering corrections will have to be carried out to get more accurate results. (A Monte-Carlo code designed for this purpose has just been written by E. Lynn at Harwell, but these data have not yet been corrected by use of this method.)

The $\sigma_0 \Gamma_\gamma$ values and parameters for some of the tungsten resonances are listed in Table 1. Columns 1 and 2 are self-explanatory; column 3 lists the zero-thickness $\sigma_0 \Gamma_\gamma$ values and the statistical errors associated with these values. It must be pointed out, however, that an error of $\sim 10\%$ is associated with the present measurements due to uncertainties in determining the detector efficiency, neutron spectrum, etc., so a minimum error of $\sim 10\%$ must be taken for any value of $\sigma_0 \Gamma_\gamma$ listed in Table 1. Column 4 lists the neutron widths obtained from transmission measurements; the neutron widths up to the 185.3-ev resonance were taken from BNL-325,[6] and those above this energy were taken from the ORNL fast-chopper

[4]E. R. Rae *et al.*, *Nucl. Phys.* **5**, 89 (1958).

[5]A. I. Isakov, Yu P. Popov, and F. L. Shapiro, *J. Exptl. Theoret. Phys. (USSR)* **38**, 989 (1960).

[6]D. J. Hughes, B. A. Magurno, and M. K. Brussel, *Neutron Cross Sections*, 2d ed., BNL-325, suppl No. 1, 1960.

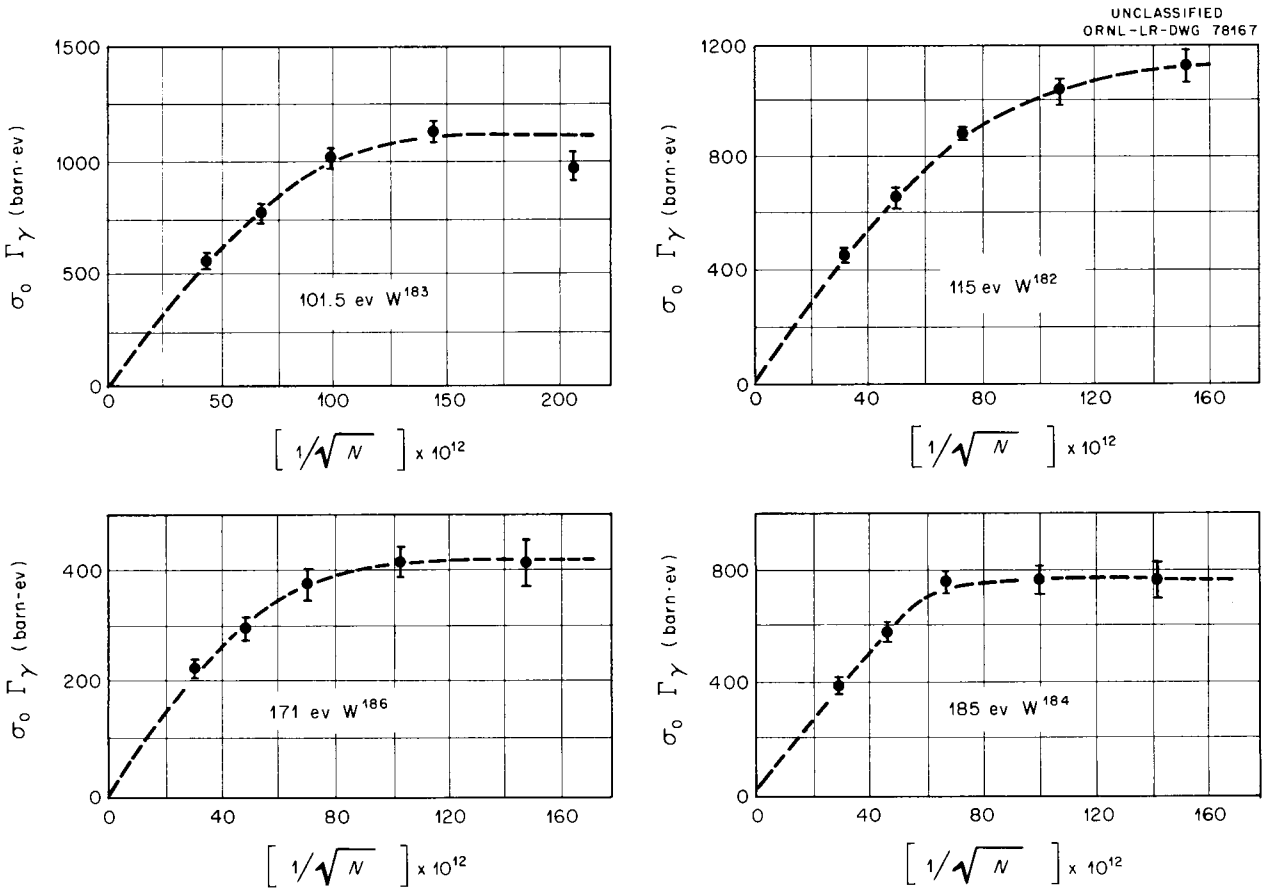

Fig. 4. Plots of $\sigma_0\Gamma_\gamma$ vs $1/\sqrt{N}$ for Four Resonances in Tungsten.

Table 1. Tungsten Resonance Parameters

E_0 (ev)	Isotope	$\sigma_0\Gamma_\gamma$ (barns-ev)	Γ_n (10^{-3} ev)	Γ_γ (10^{-3} ev)
114.9	W^{182}	1150 ± 50	264 ± 5	63 ± 3
114.8	W^{183}	250 ± 25	94 ± 18	136 ± 29
154.8	W^{183}	260 ± 40	400 ± 30	73 ± 13
157.5	W^{183}	520 ± 50	67 ± 7	112 ± 16
174.6	W^{183}	675 ± 50	125 ± 20	116 ± 20
185.3	W^{184}	770 ± 30	1042 ± 35	57 ± 5
311.8	W^{184}	275 ± 50	109 ± 17	47 ± 10
425.2	W^{184}	270 ± 50	116 ± 20	71 ± 20

measurements of Khan and Harvey.[7] Column 5 lists the radiation widths extracted from these measurements. The values of Γ_γ in column 5 agree with results reported in BNL-325.[6]

Iron. – Radiative capture measurements were made on samples of pure iron and separated Fe^{56}. A strong resonance was observed at 1154 ± 6 ev in all samples; this resonance had been observed by Isakov *et al.*[5] in a poor resolution capture experiment. From the capture areas, under this resonance, extrapolated to "zero thickness," a $\sigma_0 \Gamma_\gamma$ of 145 ± 30 barns-ev is assigned to this Fe^{56} resonance. Transmission measurements were also performed on iron, and it was established that this resonance is (90 ± 10)% capture. Thus, in this case, $g\Gamma_n \Gamma_\gamma / \Gamma \approx g\Gamma_n$, and $g\Gamma_n$ is equal to $(64 \pm 13) \times 10^{-3}$ ev.

Hafnium. – Capture measurements were made on enriched samples of hafnium isotopes. Enriched samples of Hf^{177}, Hf^{178}, Hf^{179}, and Hf^{180} were obtained from the AEC Cross-Section Pool of Stable Isotopes; the sample properties are listed in Table 2. The samples, in the form of HfO_2, were fabricated by the ORNL Isotopes Division.

Capture measurements have been made from 50 to 500 ev, and many new resonances were observed in the capture time-of-flight spectrum. The observed resonance energies are listed in the first column of Tables 3–6 for the hafnium isotopes; in the second column of Tables 3, 5, and 6 are listed the energies of the resonances tabulated in BNL-325. (It is noted that the 62.0-ev resonance in Hf^{177} and the 104.6-ev resonance in Hf^{178} were attributed, respectively, to Hf^{179} and Hf^{177} in the BNL-325 tabulation.)

The average level spacing of the hafnium isotopes can readily be extracted from these observed resonance energies. In Fig. 5 are plotted the integral level spacing distributions of the four hafnium isotopes. It is apparent from this figure that many resonances are being missed (because of resolution) above ~180 ev in Hf^{177} and above ~230 ev in Hf^{179} by the departure of the plotted curves from the straight-line fit below these energies. The level spacings from the even-even isotopes are sufficiently large so that individual resonances are resolved from each other, but small

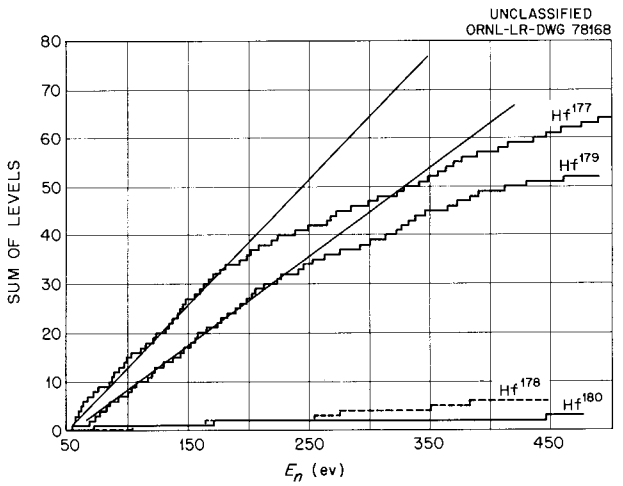

Fig. 5. Integral Level Spacing Distribution of the Hafnium Isotopes. The ordinate is the total number of resonances observed below the neutron energy *E*.

[7]F. A. Khan and J. A. Harvey, *Phys. Div. Ann. Progr. Rept. Jan. 31, 1962*, ORNL-3268, p 52.

Table 2. Properties of the Separated Hafnium Isotope Samples

Sample	Weight (g)	Density (g/cm^2)	Atomic Percent of Isotopes					
			174	176	177	178	179	180
Hf^{177}	15.009	0.577	<0.05	1.15	84.82	9.2	2.22	2.91
Hf^{178}	15.009	0.577	<0.05	0.52	4.36	89.14	2.91	3.07
Hf^{178}	54.950	2.105	<0.05	0.52	4.36	89.14	2.91	3.07
Hf^{179}	15.009	0.577	<0.05	0.46	2.96	7.99	74.6	13.99
Hf^{180}	15.009	0.577	<0.05	0.23	1.0	2.22	2.66	93.89
Hf^{180}	54.950	2.105	<0.05	0.23	1.0	2.22	2.66	93.89

Table 3. Hf^{177} Resonance Energies

Observed in This Experiment, E_0 (ev)	Reported in BNL-325, E_0 (ev)	Observed in This Experiment, E_0 (ev)	Reported in BNL-325, E_0 (ev)
54.6	55.6	180.9	
56.2		192.9	
56.9	57.2	199.2	
59.1	60.3	201.9	
62.0		208.6	
63.4	64.4	219.6	
66.6	67.7	224.0	
71.3	72.3	238.7	
75.8	77.2	249.0	
84.5	84.3	264.5	
86.7	86.2	268.0	
88.4		272.8	
93.0	93.6	285.3	
97.0		298.8	
98.8	98.5	307.3	
102.9	103.0	323.9	
111.7		328.7	
114.9		341.9	
121.0		348.8	
123.5		356.9	
131.5		363.3	
133.9		369.9	
137.0		376.7	
140.9		389.9	
143.6		407.0	
145.5		414.8	
148.4		436.1	
155.9		446.1	
160.0		459.1	
163.0		475.4	
167.3		489.6	
170.8		500	
176.4			

Table 4. Hf^{178} Resonance Energies

E_0 (ev)
104.6
164.4
254.9
275.2
351.5
382.7
446.1

resonances may still be missed. From the curves plotted in Fig. 5, the average level spacings per spin state for the hafnium isotopes are:

Hf^{177}	7.6 ± 0.8 ev ,
Hf^{178}	64 ± 15 ev ,
Hf^{179}	11.2 ± 1.1 ev ,
Hf^{180}	125 ± 50 ev .

It is assumed here that the level spacing is the same for each spin state in Hf^{177} or Hf^{179}.

Table 5. Hf^{179} Resonance Energies

Observed in This Experiment, E_0 (ev)	Reported in BNL-325, E_0 (ev)	Observed in This Experiment, E_0 (ev)	Reported in BNL-325, E_0 (ev)
54.6	55.4	202.7	
68.9	70.1	205.8	
73.4		213.2	
76.5	78.2	224.0	
82.8		227.0	
85.3	84.3	241.7	
92.5	93.6	245.3	
101.1		253.3	
103.6	103.0	262.8	
107.7	106.0	275.8	
117.0		292.6	
119.9		300.9	
122.2		313.9	
129.9		322.4	
137.4		327.1	
144.1		332.7	
146.9		338.5	
152.1		346.3	
155.9		365.2	
158.6		372.8	
165.5		382.7	
174.2		390.9	
177.7		412.6	
182.5		430.0	
189.4		460.4	
192.9		489.6	
198.1			

These data have not yet been analyzed for other resonance parameters. However, transmission measurements on the hafnium isotopes are planned by ORNL and RPI jointly, and all these data will then be combined to extract the parameters. In addition, capture measurements are planned for Hf^{176} as soon as the sample is available.

Table 6. Hf^{180} Resonance Energies

Observed in This Experiment, E_0 (ev)	Reported in BNL-325, E_0 (ev)
72.2	73.9
171.7	
446.1	
475.4	

CHANNEL ANALYSIS OF FAST-NEUTRON-INDUCED FISSION NEAR THRESHOLD

R. W. Lamphere

The angular distribution of fragments from fission induced by fast neutrons on U^{234} has been measured for neutrons having energies between 3.8 Mev and 0.4 Mev. These measurements, together with analyses to determine the channels through which fission proceeds for excitation near the top of the barrier, have been reported.[1] The abstract to this article is as follows:

The fission cross section of U^{234} has been remeasured to 4-Mev neutron energy with greater detail in order to accurately delineate the extrema. Results are believed to be somewhat more accurate than those previously reported by the author. The fragment angular asymmetry A defined as the ratio of fragment emission at zero degrees to that at ninety degrees to the neutron beam was measured from 0.4 to 3.8 Mev. At 843, 1050, and 3740 kev the 30/60 degree fragment intensity ratio was also measured and normalized to A. Strong sidewise peaking with $A = 0.50$ (normal to the neutron beam) was found at 500 kev at which point the total fission cross section is 0.50 barn and rising smoothly. At 843 kev the cross section passes through a maximum of 1.26 barns coincidentally with a maximum of 1.80 in A. From 843 to 1050 kev both cross section and A fall smoothly to minima of 1.10 barn and 1.13, respectively. Above 1050 kev both cross section and A rise somewhat irregularly. A remains very nearly constant at 1.20 between 1.5 and 3.8 Mev.

As suggested by Wheeler the dip in cross section can be explained in terms of enhanced competition from inelastic neutron scattering. A modified Hauser-Feshbach type of analysis indicates that scattering to vibration-rotational levels known to exist above 790 kev in U^{234} serves to depress the cross section for fission.

The changes in A are explained in terms of the theory of A. Bohr which postulates that fission occurs through distinct channels akin to the K-band structure seen in heavy aspherical nuclei at low excitations. On this basis approximately 62% of fission at 500 kev goes via a $\frac{3}{2}^-$ band while most of the remainder goes via a $\frac{1}{2}^+$ band. At 843 kev only 14% goes through the $\frac{3}{2}^-$ band; the rest proceeds via a strong $\frac{1}{2}^-$ band and the much weaker $\frac{1}{2}^+$ band. The reason for the strong fall in A between 843 and 1050 kev is unclear. Some possibilities are suggested.

The sequence of K bands indicated for U^{235*} near the saddle point deformation is $\frac{1}{2}^+$, $\frac{3}{2}^-$, $\frac{1}{2}^-$, with separations of the order of a few hundreds of kilovolts.

The angular distribution for a U^{235} target was also measured, over the same range of neutron energies and for the same fragment angles as for U^{234}. In this case the additional energy from neutron pairing produces excitations some 2 Mev above the barrier for a bombarding energy of 0.4 Mev. Consequently one would expect from the Bohr theory, or any other theory for that matter, that many channels would already be available. Although additional channels for fission as well as for neutron inelastic scattering certainly do become available as neutron bombarding energy is increased, they do not noticeably affect the fragment distribution since so many others are already open. A sudden jump of a few percent occurs in the fission cross section around 900 kev. As this is presumed to be due to a very strong fission channel with threshold at this energy it was felt that a shift in fragment angular distribution might be found. However, Fig. 1 shows that if a shift does occur it must be quite small.

Since September of last year the 5-Mv generator was made available for one run of two weeks duration. Measurements were made of the fragment angular distribution from Th^{232} near threshold for neutron-induced fission. This is the type of work for which the 2-Mv generator was originally instrumented and on which much of the earlier fission cross section and angular distribution work was done. Since it has been taken over by people interested only in a pulsed source of neutrons, experiments requiring a strong continuous flux of monoenergetic fast neutrons have received a serious setback, more particularly since the larger machine is not at all suited to operation with the high-current gas target. During the two-week run with this generator there was time to measure fragment distributions at only three energies, as seen in Table 1.

[1] R. W. Lamphere, *Nucl. Phys.* **38**(4), 561 (1962).

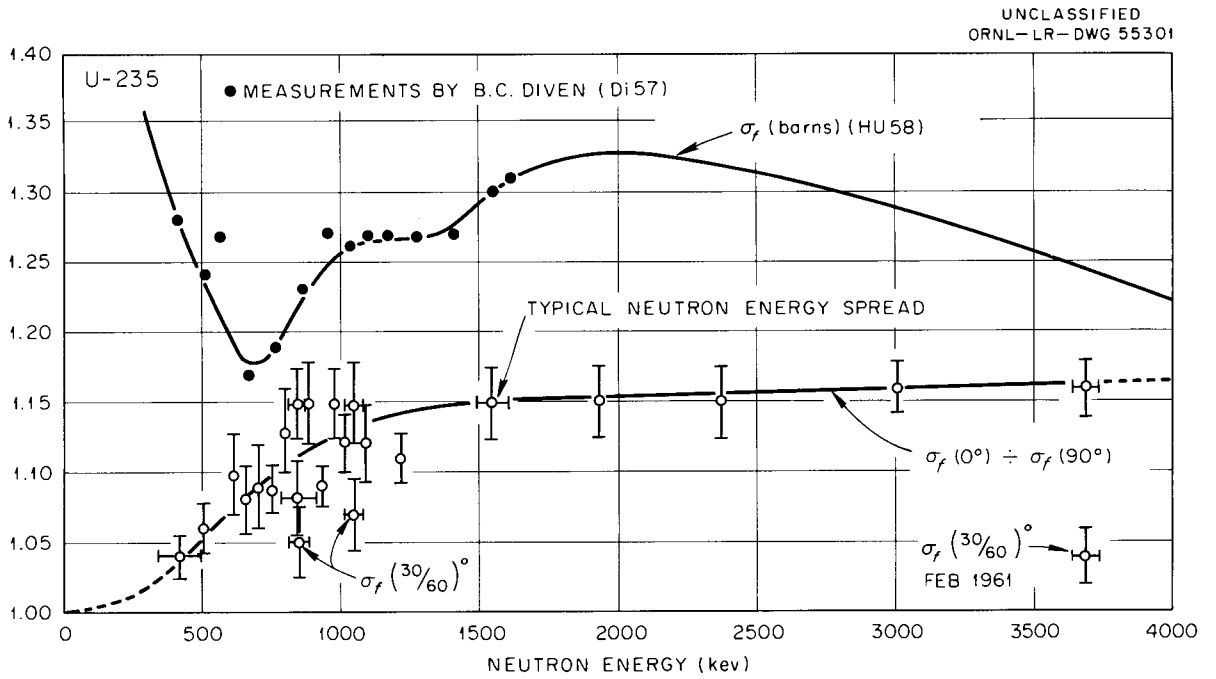

Fig. 1. Total Fission Cross Section and Fragment Angular Distribution for U^{235} Obtained from Neutron-Induced Fission. The lower curve shows the ratio of fragments emitted at 0° to those emitted at 90° with the neutron beam. The three points marked are the ratios of fragments emitted at 30° to those at 60°.

Henkel and Brolley[2] have reported fragment angular distributions for thorium at neutron bombarding energies upward from 1400 kev. They found an anisotropy of 0.12 ± 0.04 for $\sigma_f(0/90)^\circ$ at 1607 ± 67 kev. This is clearly inconsistent with the measurement at 1594 kev in Table 1. The anisotropy is changing *very* rapidly with energy in this region, so that the discrepancy may be due to an energy error. The energy for this point in Table 1 was checked carefully against the Be(p,n) threshold of 2059 kev and is thought to be accurate. The inadequate beam from the 5-Mv generator precluded taking additional points which would have further delineated the curve and probably settled the question of disagreement with the Los Alamos work. Most important is, however, the measurement at 1188 kev which shows beyond question that the distribution becomes forward peaked. This together with other factors points unambiguously to a $K = \frac{1}{2}^+$ as the lowest band through which fission can occur. The sidewise peaking at slightly higher energies must be due to a band with $K > \frac{1}{2}$. Although a definite assignment can-

[2]R. L. Henkel and J. E. Brolley, Jr., *Phys. Rev.* **103**, 1292 (1956).

Table 1. Anisotropy of Fragments from the Fast-Neutron-Induced Fission of Th^{232}

E_n (kev)	$\sigma_f(0/90)^\circ$
1188 ± 41	1.53 ± 0.15
1390 ± 41	0.75 ± 0.11
1594 ± 41	0.49 ± 0.04

not be made, arguments will be put forward to show that it must have negative parity, and that K is probably equal to $\frac{3}{2}$. The resumption of strong forward peaking at still higher energies is unambiguous evidence (assuming the correctness of the Bohr picture) for the existence of a $K = \frac{1}{2}^-$ band.

The methods of channel analysis have been discussed in detail in ref 1. A thumbnail sketch of the arguments applicable to Th^{232} follows: Only bands for which $K = \frac{1}{2}$ can give forward peaking; all others give sidewise peaking of the fragment distribution. The p-wave interaction over the neutron energy range in question here is much stronger than either s- or d-wave. Bands of low K have potentially higher partial formation cross sections because they include also channels with lower spin. As a fission channel opens up, its cross section increases rapidly at first and then becomes rather constant after the top of the barrier has been surpassed. It is not expected to decrease. This says that the second K band must have a higher cross section than the first, which requires that the parity must be opposite unless K were lower, and K cannot of course be less than $\frac{1}{2}$. Since the Los Alamos data show the anisotropy to shift forward peaking for bombarding energies in excess of about 1.8 Mev, the third band, the one responsible for this, must be $K = \frac{1}{2}$, and the parity must be negative to obtain a partial cross section large enough to override the second band. Thus the K-band sequence in Th^{233*} in the neighborhood of saddle-point deformation is believed to be $\frac{1}{2}^+$, $\frac{3}{2}^-$, $\frac{1}{2}^-$, with separations of the order of a very few hundreds of kilovolts. Table 2 lists calculations and experimental data pertinent to the analysis.

The reaction cross section σ_r is computed by use of Eq. (1), and the neutron transmission factors T_{lI} are tabulated by Perey and Buck.[3] The partial cross sections for formation of compound nucleus with component K of the angular momentum I along the symmetry axis and with parity π are denoted by $\sigma_{K\pi}$. They are found from Eq. (2) where summation is performed only over those values of l and I consistent with the indicated K and parity:

$$\sigma_r = \frac{\pi \lambda\!\!\!^{-2}}{2} \sum_{lI} (2I + 1) T_{lI} , \qquad (1)$$

$$\sigma_{K\pi} = \frac{\pi \lambda\!\!\!^{-2}}{2} \sum_{lI}' (2I + 1) T_{lI} / K\pi . \qquad (2)$$

It is important to note that where two K bands of like parity are open to fission, the total probability for fission through these two bands is not proportional to the sum of the $\sigma_{K\pi}$ except in the limiting case of $\sigma_f << \sigma_r$. Consider, for example, a compound nucleus to be formed with spin $\frac{5}{2}^-$, and that two fission bands, the $\frac{1}{2}^-$ and $\frac{3}{2}^-$, are both fully open; then, according to this simple theory, there is an equal chance of decay through either channel, but decay cannot take place through both of them.

At 1600 kev the $\frac{1}{2}^+$ and $\frac{3}{2}^-$ bands are probably open but being of opposite parity do not compete with each other. But as $\sigma_{3/2^-} > \sigma_{1/2^+}$ the distribution swings from forward to sidewise peaking as E_n rises and the $\frac{3}{2}^-$ band opens up. Now,

[3] F. Perey and B. Buck, private communication.

Table 2. Partial and Reaction Cross Sections in Barns

E_n (kev)	σ_r	σ_f	$\sigma_f(0/90)^\circ$	$\sigma(K, \pi)$								
				$\frac{1}{2}^+$	$\frac{1}{2}^-$	$\frac{3}{2}^+$	$\frac{3}{2}^-$	$\frac{5}{2}^+$	$\frac{5}{2}^-$	$\frac{7}{2}^+$	$\frac{7}{2}^-$	$\frac{9}{2}^-$
1188	3.8	0.004	1.5	0.97	2.8	0.70	2.3	0.42	1.2	0.03	0.78	0.007
1390	3.8	0.050	0.75	0.95	2.8	0.72	2.3	0.44	1.4	0.05	0.89	0.014
1594	3.8	0.102	0.49	0.94	2.8	0.73	2.3	0.46	1.6	0.07	0.95	0.023
2250	3.5	0.125	1.7	0.92	2.5	0.76	2.2	0.52	1.6	0.17	0.95	0.080

as E_n rises still higher, the strong $\frac{1}{2}^-$ band of channels begins to open. Now, not only is $\sigma_{1/2^-} > \sigma_{3/2^-}$, but also these bands compete in the sense that some fissions which would have taken place via the $\frac{3}{2}^-$ band now choose the $\frac{1}{2}^-$. This causes the strong forward peaking which takes over as E_n is increased.

Such an explanation requires that K be not determined at the instant of compound nucleus formation. The picture is one of a compound nucleus formed with given spin and parity and oscillating violently about some equilibrium deformation, probably going through spherical configuration where K has no significance, and approaching the saddle point more or less closely many times and with various values of $K \leqq I$ before, finally, sufficient energy is concentrated in deformation to permit passage over the barrier.

The range of deformation over which K has significance remains one of the interesting unknowns which may gradually be delimited as more experimental information is made available. Also the above arguments are based on the assumption [which is particularly important for Th^{232} where $(\Gamma_n/\Gamma_f) >> 1$] that neutron emission is independent of K. Since neutrons should be emitted preferentially close to equilibrium deformation, this sounds like a reasonable assumption at least to first order, although results reported in ref 1 raise a few doubts.

More experiments of this nature as also inelastic neutron scattering measurements, especially from various vibrational levels in these heavy nuclei, are needed to answer such questions. As matters now stand the evidence points to identical K-band sequences at saddle point in the nuclei Th^{231} (ref 4), Th^{233}, and U^{235}.

Heavy foils of U^{238} have been obtained for the purpose of examining the U^{239} K-band sequence. Measurements on U^{238} (ref 5) show forward peaking at all energies down to 1.25 Mev neutron energy. Recent measurements at ORNL (unpublished) show forward peaking to persist to 0.80 Mev, the lowest energy at which measurements were made.

A large number of Np^{237} foils have been standardized by alpha counting and fission counting in fluxes of fast and slow neutrons. Counting activities were then compared with masses reported by the group which did the plating at K-25 under George Petit. All foils were found to contain small amounts of fissionable contamination. This was determined to be uranium by comparison of the alpha and fast and slow fission count rates, and was confirmed by destructive quantitative chemical analysis of one foil. The impurities range from 0.2 to 1.0% for most foils, and this percentage was evaluated for each foil to an accuracy of about 20% by comparison of the fission activity in the fast and slow neutron fluxes. The accuracy to which the quantity of uranium impurity can be found depends on the accuracy to which the ratio $\sigma_f(Np^{237})/\sigma_f(U)$ is known for thermal flux with Maxwellian distribution at about room temperature. This ratio was taken to be 0.019/3.71 and presumably is accurate to ±20%.

Some of these foils can now be made available to other experimenters. They are plated on 2-mil-thick nickel disks 2 in. in diameter, the plated area being a 1-in.-diam circle. The neptunium is plated in the form of an oxide. Masses of neptunium fall into three distinct groups around 0.20, 1.8, and 3.8 mg.

[4]B. M. Gokhberg, G. A. Otroshchenko, and V. A. Shigin, *Doklady Akad. Nauk S.S.S.R.* **128**, 1157 (1959).

[5]J. E. Simmons and R. L. Henkel, *Phys. Rev.* **120**, 198 (1960).

MASS DISTRIBUTION AND KINETICS OF U^{235} THERMAL-NEUTRON-INDUCED BINARY AND TERNARY FISSION

H. W. Schmitt F. J. Walter
J. H. Neiler[1] A. Chetham-Strode[2]
M. J. Mader[3]

Correlated energy spectra of fission fragments from the thermal-neutron-induced binary and ternary fission of U^{235} have been obtained. Details of the method, together with the E_1, E_2 array for binary fission, have been reported previously.[4] Below is the text of a short communication[5] which summarizes the work on U^{235}. The binary fission experiment consisted of $\sim 10^6$ events; the ternary fission experiment consisted of $\sim 10^5$ events.

A three-parameter correlation experiment has been performed in which the energies of the two heavy fragments and of the third light particle (usually a long-range alpha particle) have been measured in coincidence. A comparison of the mass distributions thus obtained for particles from binary and ternary fission indicates that the long-range alpha particles are emitted principally at the expense of nucleons in the light fragment for near-symmetric fission and at the expense of nucleons in the heavy fragment for more asymmetric fission. Strong influence of the closed $N = 82$ and $N = 50$ shells is indicated.

Surface barrier detectors were used in conjunction with standard low-noise amplifier systems; events were serially recorded by a $128 \times 128 \times 4$ channel punched-paper-tape correlation recorder. The data were sorted, summed, and correlated through the use of computers, and results have been obtained giving the mass distribution, mass-energy correlations, and other kinetic parameters associated with U^{235} thermal-neutron-induced three-particle fission.

In order to assure high resolution in these measurements, a narrow, highly collimated beam of thermal neutrons from the Oak Ridge Research Reactor was incident on the 50-μg/cm^2 U^{235} deposit, backed by a 70-μg/cm^2 self-supporting nickel foil. All detectors were located outside the neutron beam. The two fission fragment detectors, made of 500 ohm-cm silicon, were calibrated with respect to the time-of-flight data of Milton and Fraser.[6] The two third-particle detectors, made of 3000 ohm-cm silicon, were operated with sensitive depths greater than the range of a 30-Mev alpha particle and were located at about 80° with respect to the axis of the fragment detectors.[7] All four detectors were ~ 4 cm^2 in area and exhibited resolutions better than 40 kev full width at half maximum for natural alpha particles. The fission fragment detectors exhibited resolutions better than 1.2 Mev for 95-Mev Br^{79} and Br^{81} ions, as determined in an auxiliary experiment using the Oak Ridge Tandem Van de Graaff generator.[8]

In the analysis of the data, the simple momentum and mass conservation relations were used: $M_1E_1 = M_2E_2$ and $M_1 + M_2 = 235 + 1 - 4$. For binary fission $M_1 + M_2 = 235 + 1$. It can be shown that recoil from prompt neutron emission by the fragments introduces a dispersion in mass (for any individual mass split) no larger than ~ 2 amu. For ternary fission the detector geometry is such that recoil from the alpha particles introduces an average dispersion (for any mass split) less than ~ 2 amu. The dispersion introduced by alpha-particle recoil is thus expected to result in a slightly broadened fragment mass distribution for ternary fission.

Among the interesting results obtained from these measurements is the integral mass distribution (summed over all third-particle energies) of the fission products. This distribution is shown in Fig. 1, compared with the mass distribution of fragments from binary fission as obtained during the same experiment with identical source and detector conditions. The important feature of this comparison is that the low-mass sides of the

[1]Now at Oak Ridge Technical Enterprises Corp.

[2]Chemistry Division.

[3]Mathematics Division.

[4]*Phys. Div. Ann. Progr. Rept. Jan. 31, 1962*, ORNL-3268, p 54.

[5]H. W. Schmitt *et al.*, *Phys. Rev. Letters* **9**, 427 (1962).

[6]J. C. D. Milton and J. S. Fraser, *Can. J. Phys.* **40**, 1626 (1962).

[7]For a discussion of the long-range alpha particles, see E. W. Titterton, *Nature* **168**, 590 (1951).

[8]The authors very gratefully acknowledge the collaboration of C. D. Moak in the bromine-ion experiment; see "Response of Silicon Solid-State Detectors to Heavy Ions and Fission Fragments," this report.

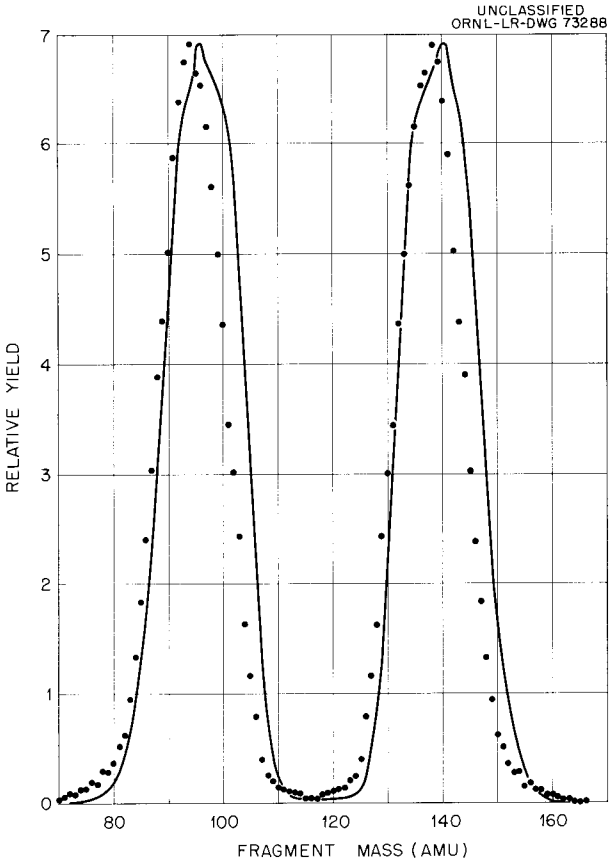

Fig. 1. Relative Mass Yields for Fragments from U^{235} Thermal-Neutron-Induced Binary and Ternary Fission. Yields are normalized at the peaks. Solid circles represent ternary fission; solid curves represent binary fission.

two peaks are identical, within statistical uncertainties and with the dispersion mentioned above, for binary and ternary fission. The high-mass sides of the peaks in ternary fission are displaced downward with respect to the high-mass sides of the peaks in binary fission. It thus appears that the alpha particle is emitted principally at the expense of nucleons in the light fragment for near-symmetric fission and at the expense of nucleons in the heavy fragment for more asymmetric fission.

Much has been written about possible shell effects in fission.[9] The $N = 50$ shell occurs for masses in the 84- to 90-amu region, on the low-mass side of the light-fragment peak; the $N = 82$ shell occurs for masses in the 132- to 140-amu region, on the low-mass side of the heavy-fragment peak. The comparison shown in Fig. 1 suggests rather strongly that the nucleon clusters containing the closed shells $N = 50$ or $N = 82$ remain intact and are important both in three-particle fission *and* in binary fission, for $U^{235} + n$ (thermal). In the development of the cluster model, where the principle of indistinguishability of nucleons is a key point, it has been suggested[10] that the formation of these clusters during the fission process (prior to scission) accounts for the asymmetry of fission in the case of low excitation energies of the compound system. This argument is perhaps better justified in the case of the $N = 82$ shell than in the case of the $N = 50$ shell; that is, a decrease in yield is already expected for more asymmetric fission on the basis that the energy available for fission decreases rapidly as the light-fragment mass decreases beyond the $N = 50$ region.

The point of view that the $N = 50$ and $N = 82$ closed-shell nuclei play a fundamental role is consistent with recent determinations of ν, the number of neutrons emitted from a fission product, as a function of the mass M of the product. Measurements have been made by Apalin *et al.*,[11] and Terrell[12] has calculated $\nu(M)$ from a comparison of double time-of-flight data[6,13] and the radiochemical and mass-spectrometric yields tabulated by Walker.[14] It is found that ν increases from 0.1 to 2.15 in the range $85 \leq M \leq 107$, and increases again from 0.3 to 2.3 in the range $130 \leq M \leq 151$. Because of the rather large statistical uncertainties, it was not possible for these authors to determine where in the range $107 \leq M \leq 130$ the decrease of ν from 2.15 to 0.3 occurs. If the above point of view is valid and shell effects are important in these considerations, the decrease should be associated with masses in the region below 132 amu, that is, just before the $N = 82$ shell is filled, rather than with symmetric fission.

A result of further interest from the present measurements is that the mass distribution of the heavy fission

[9] See, for example, I. Halpern, *Ann. Rev. Nucl. Sci.* **9**, 245 (1959); M. G. Mayer and J. H. D. Jensen, *Elementary Theory of Nuclear Shell Structure*, Wiley, New York, 1955.

[10] K. Wildermuth and H. Faissner, *Proc. Intern. Conf. Nucl. Struct., Kingston, Ont., 1960*, 972 (1960).

[11] V. F. Apalin *et al.*, *At. Energ. (USSR)* **8**, 15 (1960) [translation, *Soviet J. At. Energy* **8**, 10 (1961)].

[12] J. Terrell, *Phys. Rev.* **127**, 880 (1962).

[13] W. E. Stein, *Phys. Rev.* **108**, 94 (1957).

[14] W. H. Walker, Chalk River Report CRRP-913, Atomic Energy of Canada Limited, Chalk River, Ontario, 1960 (unpublished).

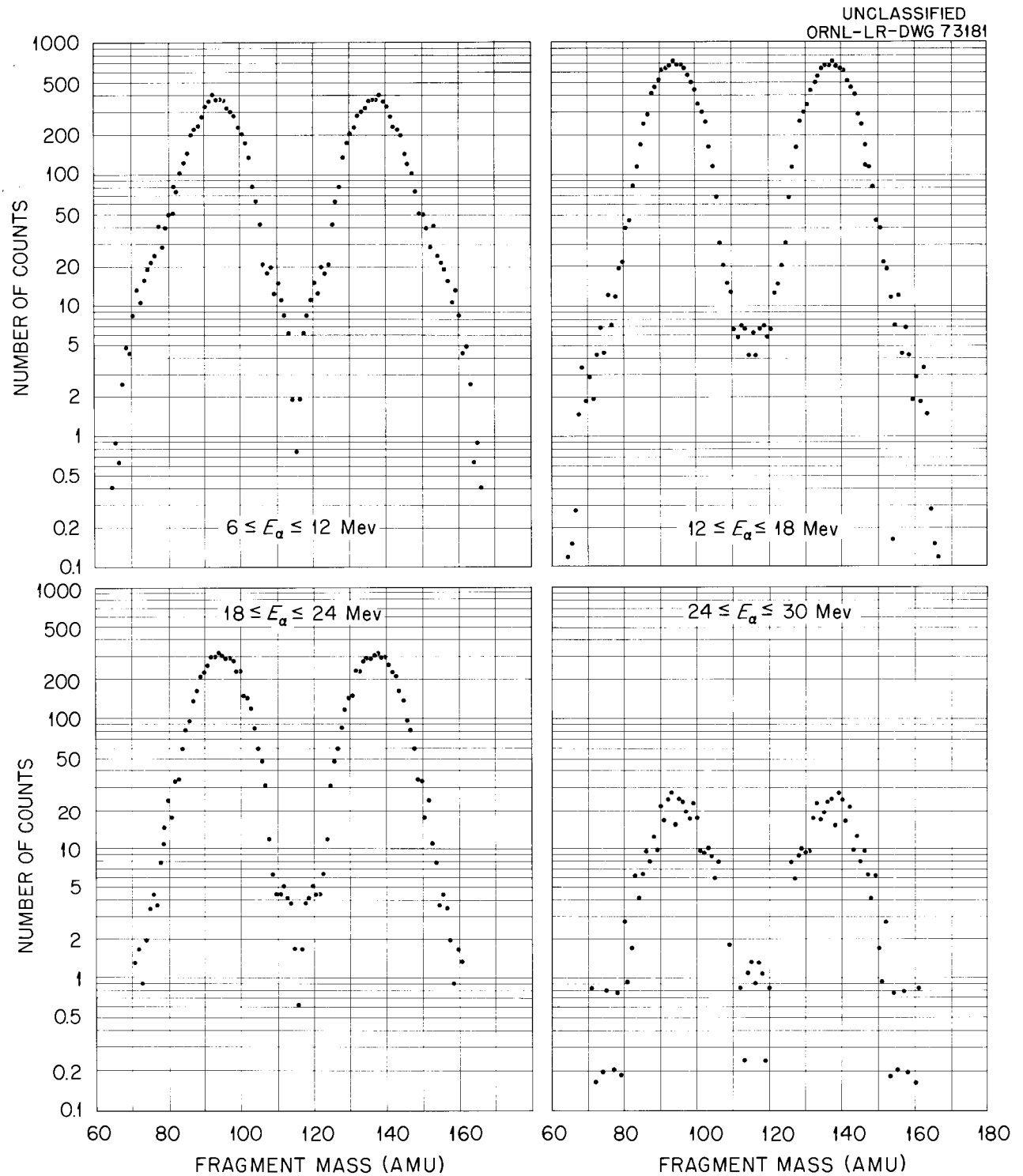

Fig. 2. Fission Fragment Mass Yield as a Function of Third-Particle Energy for U^{235} Thermal-Neutron-Induced Ternary Fission.

products is essentially independent of long-range alpha-particle energy. The alpha-particle energy spectrum[15] was divided into four groups: 6 to 12 Mev, 12 to 18 Mev, 18 to 24 Mev, and 24 to 30 Mev. The fragment mass distribution for each group is shown in Fig. 2. Statistical uncertainties preclude a precise or detailed comparison of these spectra; it is evident, however, that no gross differences exist.

The average total fragment kinetic energy, $\langle E_K \rangle = \langle E_1 + E_2 \rangle$, as a function of mass ratio was computed for each of three alpha groups: $6 \leq E_\alpha \leq 12$ Mev, $12 \leq E_\alpha \leq 18$ Mev, and $18 \leq E_\alpha \leq 24$ Mev. These are shown together with similar results for binary fission in Fig. 3. It is significant that all of the maxima in $\langle E_K \rangle$ occur in the neighborhood of mass ratios for which the heavy fragment contains the closed $N = 82$ shell. The small rise in the binary curve at $M_H/M_L = 1.6$ corresponds to a light-fragment mass of 90 amu, which contains the closed $N = 50$ shell. The total fragment kinetic energy averaged over all mass ratios and alpha-particle energies was found to be 155 ± 2 Mev, in slight disagreement with the value of 150 Mev reported for ternary fission by Schroder *et al.*[16]

The authors gratefully acknowledge valuable discussions on these subjects with Professor J. A. Wheeler and Professor K. Wildermuth.

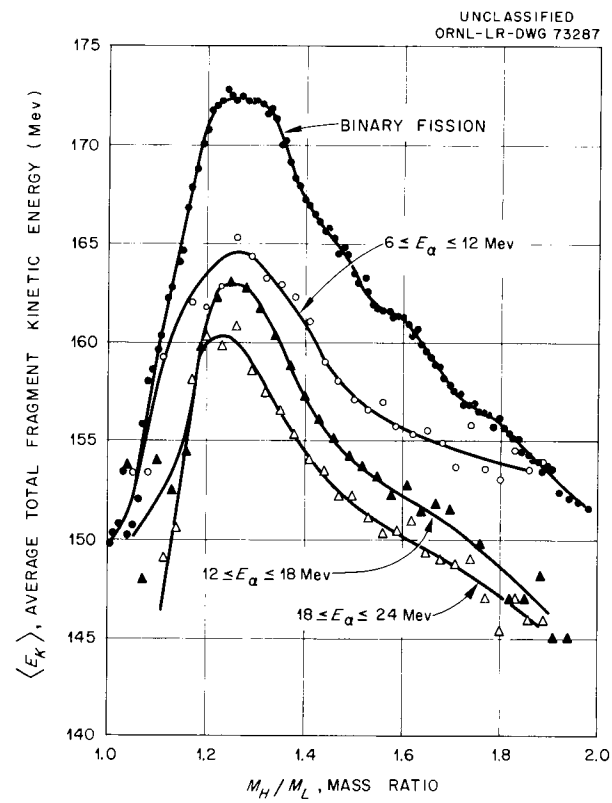

Fig. 3. Average Total Fragment Kinetic Energy as a Function of Mass Ratio. Results for three groups of alpha-particle energies in ternary fission are compared with those for binary fission. Note that E_K is the sum of the fragment energies only and does not include E_α.

[15] R. A. Nobles, *Phys. Rev.* **126**, 1508 (1962).

[16] I. G. Schroder, J. A. Moore, and A. J. Deruytter, *Bull. Am. Phys. Soc.* **7**, 304 (1962).

FRAGMENT MASS DISTRIBUTION FOR THERMAL- AND RESONANCE-NEUTRON-INDUCED FISSION OF Pu^{239}

F. J. Walter
J. H. Neiler[1]
H. W. Schmitt
C. W. Williams[2]

The fragment mass distributions for thermal- and resonance-neutron-induced fission of Pu^{239} have been determined from correlated energy measurements of fragment pairs. With the exception of certain improvements in the instrumentation, the experimental techniques were essentially the same as those described previously.[3] A block diagram of the new instrumental arrangement is shown in Fig. 1, where the circuits for a third detector (not used in this experiment) are shown for completeness. The slow amplifiers previously used employed *RC* shaping; these have been replaced with

[1] Now at Oak Ridge Technical Enterprises Corp.

[2] Instrumentation and Controls Division.

[3] F. J. Walter *et al.*, *Phys. Div. Ann. Progr. Rept. Jan. 31, 1962*, ORNL-3268, p 54.

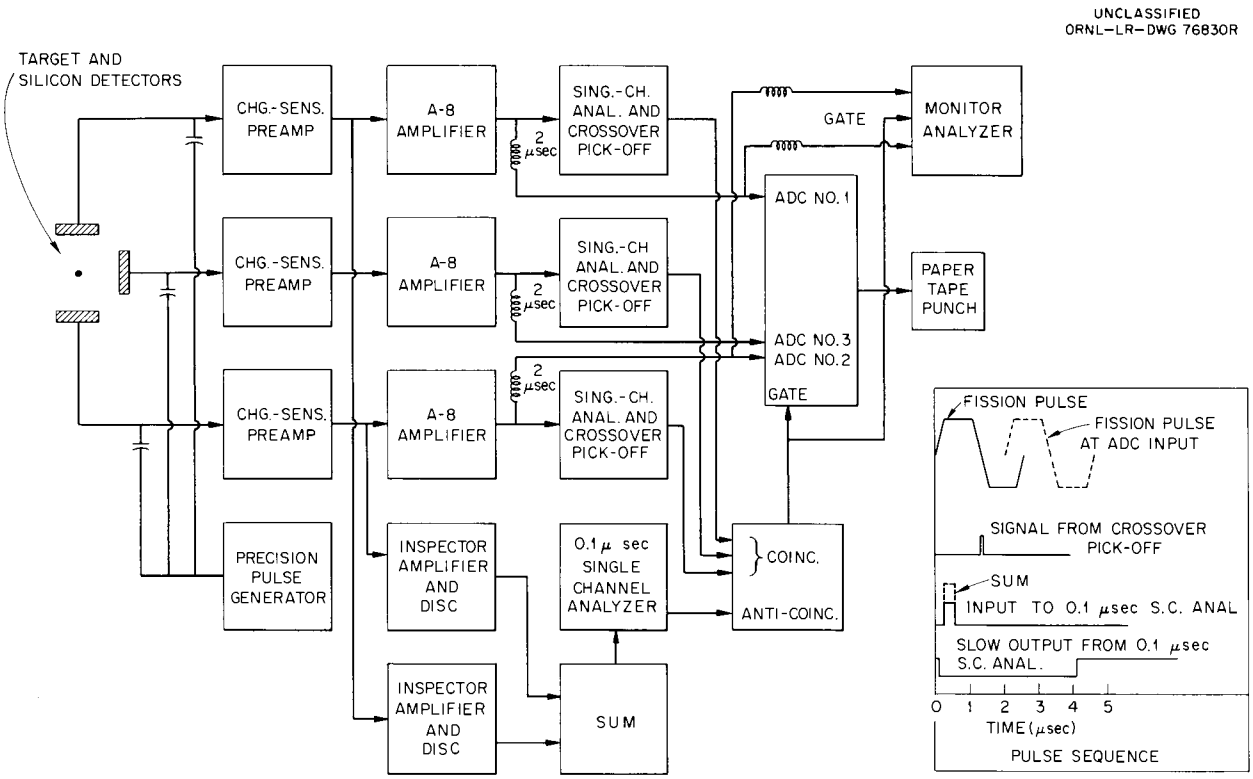

Fig. 1. Schematic Diagram of Instrumentation for Multiparameter Fragment Energy Correlation Measurements.

amplifiers employing double-delay-line shaping. Thus it was possible to use the "cross-over pick-off" technique to improve the coincidence resolving time from approximately 2×10^{-6} to 4.0×10^{-8} sec. An additional improvement of a factor of 2 to 4 in this resolving time can probably be obtained from this equipment. Although fast-coincidence circuits do minimize spectrum distortion caused by "pile-up" of two fission events or by accidental coincidences, a small coincidence resolving time does not eliminate spectrum distortion resulting from pile-up of smaller pulses (e.g., from natural alpha-particle decay of Pu^{239}) onto the pulse which is to be analyzed. The inspector circuit shown in Fig. 1 was designed to discriminate against pulses which are distorted by the presence of another, nearby event. Each inspector amplifier is connected, in parallel with the slower linear amplifier, to the unshaped output of the charge-sensitive preamplifier. The fast single-delay-line clipped pulse from the inspector amplifier activates a fast discriminator. The constant pulse-height discriminator outputs are then summed and passed onto a 0.1-μsec single-channel analyzer, the lower level of which is set at a value less than the pulse height from one discriminator signal and the upper level at less than the pulse height resulting from the sum of two discriminator signals. Thus an uncorrelated single pulse from either detector results in a signal which is within the acceptance range of the single-channel analyzer. When the single-channel analyzer detects such an event, it provides an inhibit signal which rejects any other events which occur within 4 μsec of the uncorrelated event. The resolving time of the inspector circuit is $<5 \times 10^{-8}$ sec for an alpha particle preceding a fission fragment and 4×10^{-7} sec for a fission fragment preceding an alpha particle. In addition to the preceding improvements, a continuous on-line parity reader, which was installed to monitor punch errors on the paper tape, has resulted in a

considerable improvement in the overall reliability of the system.[4]

The fragment mass distribution corresponding to "thermal" neutron-induced fission of Pu^{239} was obtained by allowing an unfiltered neutron beam from HB-5 at the ORR to impinge directly on the target foil. Fission events resulting primarily from the 0.3-ev resonance in Pu^{239} were obtained by filtering the neutron beam with a samarium filter. Figure 2 shows the fission cross section for Pu^{239} and the total cross section for samarium. The data obtained thus far include approximately 2×10^6 thermal-neutron events and $\gtrsim 1 \times 10^6$ resonance-neutron events which are being analyzed in detail. Preliminary mass distributions are shown in Fig. 3 and indicate that the mass-distribution peak-to-valley ratio for the 0.3-ev resonance is 2.0 ± 0.4 times as large as the ratio for "thermal" fission. This result supports the suggestion by Wheeler[5] that fission from different spin states of the compound nucleus might show different ratios of asymmetric to symmetric fission. This effect is slightly smaller than that observed previously[6] by radiochemical determinations of the relative yields of Mo^{99} (characteristic of asymmetric fission) and $Sn^{121,125}$ (characteristic of symmetric fission). However, since a large part (approximately one-half) of the "thermal" cross section is a result of the $1/v$ tail of the 0.3-ev resonance, most of this small discrepancy

[4]The authors gratefully acknowledge the contributions of J. W. Woody.

[5]J. A. Wheeler, *Physica* **22**, 1103 (1956); J. A. Wheeler, chap. on "Fission" in *Fast Neutron Physics*, Pt. II (ed. by J. B. Marion and J. L. Fowler), Interscience, New York, 1963.

[6]R. B. Regier *et al.*, *Phys. Rev.* **119**, 2017 (1960).

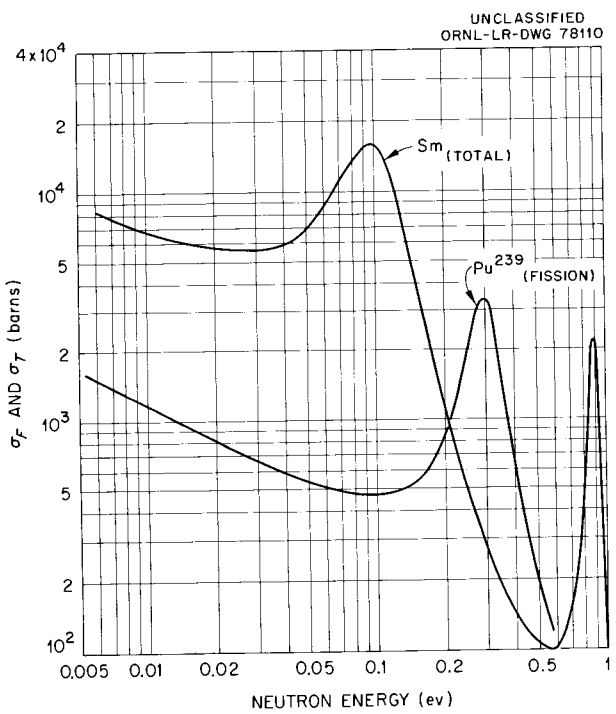

Fig. 2. Low-Energy Cross Sections of Plutonium-239 and Samarium.

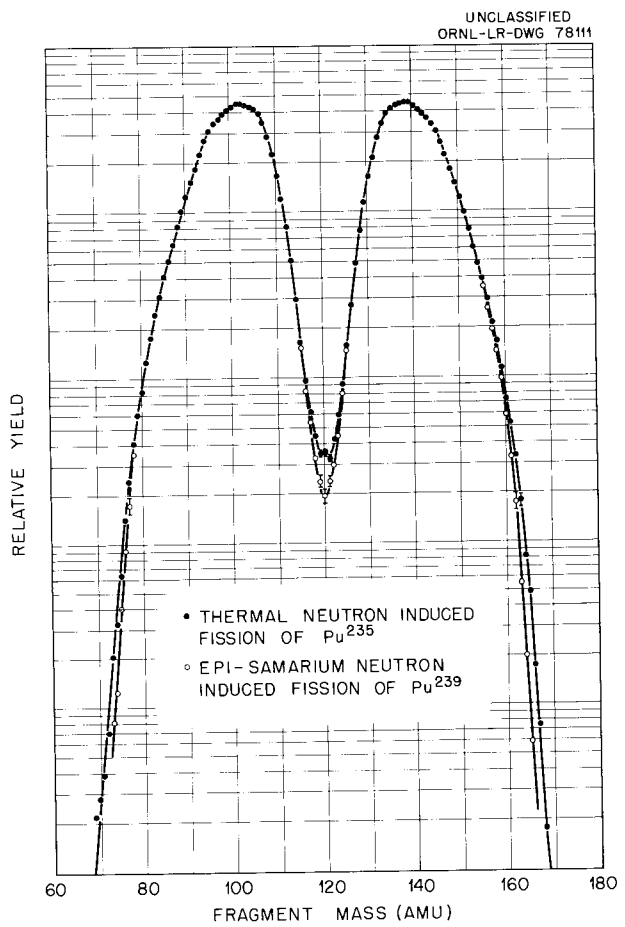

Fig. 3. Preliminary Mass Distributions for the Fission of Pu^{239} by "Thermal" and Epi-Samarium Neutrons. See text for discussions.

may possibly be accounted for by the fact that the radiochemical determinations were made using a well-thermalized beam (a cadium ratio for indium of 800), whereas our "thermal" results were obtained with neutrons of much higher effective temperature. In order to increase the relative contribution from the bound state, the energy-correlation measurements are being extended to the use of "cold" neutrons obtained by filtering the beam through cooled (100°K) beryllium.

RESONANCE-NEUTRON-INDUCED FISSION OF ORIENTED U^{235} NUCLEI

J. W. T. Dabbs F. J. Walter G. W. Parker[1]

Introduction

The process of low-energy neutron-induced fission can be considered to take place in three regimes. These are (1) capture and subsequent redistribution of excitation energy, corresponding to approach to the fission barrier; (2) passage over the saddle point (or tunneling through the the barrier); and (3) scission or breakup. Of these, only (2) represents a relatively simple situation, because (1) and (3) involve large numbers of states and many possible paths. As Bohr[2] has pointed out, the situation is considerably simplified during passage through or over the barrier. Here, the number of states available to the compound nucleus can be small, and these states are thought to be analogous to the "collective" states near the ground state of a deformed heavy nucleus. The simplification afforded by this picture provides a basis for understanding of the present experiment.

A number of experiments[3,4] have demonstrated that certain actinide elements can be oriented easily in compounds of the form $XO_2Rb(NO_3)_3$. Although there was for some time a question about the direction of the nuclear orientation, this now appears to have been satisfactorily resolved.[4,5] Both U^{233} and U^{235} are known to have positive nuclear electric quadrupole moments[6] ($Q > 0$) and both are believed to align with the major nuclear axis in the plane perpendicular to the c-axis of the $UO_2Rb(NO_3)_3$ crystal. In both cases, alpha particles were found to be preferentially emitted in the plane perpendicular to the c-axis, with an anisotropy given by

$$W(\theta) = 1 + (A/T)\, P_2(\cos\theta)\,, \qquad (1)$$

where A had the value -0.073 ± 0.013 for U^{235} and the value -0.064 ± 0.004 for U^{233}.[7,8]

One set of measurements has also been made on the anisotropy of fission fragments from U^{233} and U^{235} oriented in this fashion, using unfiltered reactor neutrons from the graphite reactor at ORNL.[8] The results showed an anisotropy of the type (1), but with $A = +0.035 \pm 0.009$ for U^{235} and $A \approx 0$ for U^{233}.

The present work is an extension of these experiments to selected neutron energies in the resonance range, and to much lower temperatures where the coefficient of $P_2(\cos\theta)$ in (1) is larger, and thus easier to determine. We shall first discuss certain theoretical aspects of the problem, then describe the experimental apparatus and the (interim) results, and finally give the preliminary conclusions which may now be drawn.

---

[1] Chemistry Division.

[2] A. Bohr, *Proc. Intern. Conf. Peaceful Uses At. Energy, Geneva, 1955*, paper P/911.

[3] J. W. T. Dabbs, L. D. Roberts, and G. W. Parker, *Physica* **24**, 569 (1958).

[4] L. D. Roberts and J. W. T. Dabbs, *Ann. Rev. Nucl. Sci.* **11**, 175 (1961).

[5] S. H. Hanauer *et al.*, *Phys. Rev.* **124**, 1512 (1961).

[6] D. L. Hill, *Handbuch der Physik* **39**, 178 (1957).

[7] *Phys. Div. Semiann. Progr. Rept. Sept. 10, 1957*, ORNL-2430, p 50.

[8] *Phys. Div. Ann. Progr. Rept. Feb. 10, 1960*, ORNL-2910, p 60.

Theory

As discussed previously,[9] the compound nucleus during passage over the barrier may be considered to be represented by a sum (over magnetic substates) of symmetric top wave functions $\mathcal{D}^J_{MK}$. The populations in these substates are determined by the initial nuclear orientation, and in the Bohr approximation this formulation leads to an angular distribution of the form of Eq. (1). The coefficient A in this case contains a parameter $[3K^2 - J(J+1)]$ and thus reverses sign in going from small K values to values $K \cong J$. Table 1 gives values of A for each of the K values which may occur for s-wave neutron-induced fission of U^{235}. The values in Table 1 include the approximate degree of orientation which occurs in the compound $UO_2Rb(NO_3)_3$.

Table 1. Calculated Values[a] of A in Eq. (1) Corresponding to Various J, K Values for U^{235}

Quadrupole coupling parameter P assumed to be $+0.015\ cm^{-1}$.

K	$J = 3^-$	$J = 4^-$
0	+0.108[b]	Parity forbidden
±1	+0.081[b]	+0.092[b]
±2	0[b]	+0.043[b]
±3	−0.135	−0.038
±4		−0.151

[a] *Phys. Div. Semiann. Progr. Rept. Sept. 10, 1957*, ORNL-2430, p 51.

[b] J. A. Wheeler, chap. on "Fission" in *Fast Neutron Physics*, Pt. II (ed. by J. B. Marion and J. L. Fowler), Interscience, New York, 1963.

In his 1955 paper, Bohr[2] suggested that small values of K should predominate. This argument is based on energetic considerations; that is, those nuclei which have "used up" the least energy in preserving angular momentum have more energy which can go into producing deformation. These nuclei should therefore have a higher probability for fission. The analogy with stable deformed nuclei then leads to the suggestion that the low values of K should predominate. More recently, Wheeler[10] in a detailed discussion of this problem has suggested that certain K values should be important in this process. These values are indicated in Table 1 (footnote *b*).

For rather general types of nuclear alignment, including both the Pound (electric quadrupole coupling) and Bleaney (anisotropic magnetic *hfs* coupling) types, it has been shown[11] that in the angular distributions expected, that is, in the equation

$$W(\theta) = \sum_{\nu} A_{\nu} G_{\nu} P_{\nu}(\cos\theta) , \qquad (2)$$

an expansion of the alignment parameter G_4 in powers of $1/T$ cannot have terms of lower order than $(1/T)^2$. This point is important for demonstrating the absence of $P_4(\cos\theta)$ terms in the present experiment, where strict linearity of the anisotropy with $1/T$ is found within experimental error.

Apparatus

The apparatus for measurement of the fission anisotropy as a function of neutron energy and $1/T$ is conceptually quite simple, but in practice it is rather complicated. A single crystal of $U^{238}O_2Rb(NO_3)_3$, grown with a surface layer of the same compound in which U^{235} was substituted for U^{238}, is mounted in a variable-energy neutron beam in such a way that its c-axis can be rotated with respect to a fission fragment detector. The apparatus permits cooling the crystal to temperatures as low as 0.45°K.

Figure 1 is a schematic diagram of the lower end of the cryostat in which the experiment is carried out. The Dewar has an outside diameter of 25 cm and contains two liquid-nitrogen baths, a He^4 bath, and a section (the sample chamber) which is cooled by a continuously operating He^3 refrigerator. The temperature of the sample chamber is monitored by a carbon resistance thermometer (old Speer) and recorded continuously on a strip-chart recorder (Fig. 4). In normal operation

[9] *Phys. Div. Semiann. Progr. Rept. Sept. 10, 1957*, ORNL-2430, p 51.

[10] J. A. Wheeler, chap. on "Fission" in *Fast Neutron Physics*, Pt. II (ed. by J. B. Marion and J. L. Fowler), Interscience, New York, 1963.

[11] M. E. Rose, L. D. Roberts, and J. W. T. Dabbs, *Bull. Am. Phys. Soc.* 1, 207 (1956).

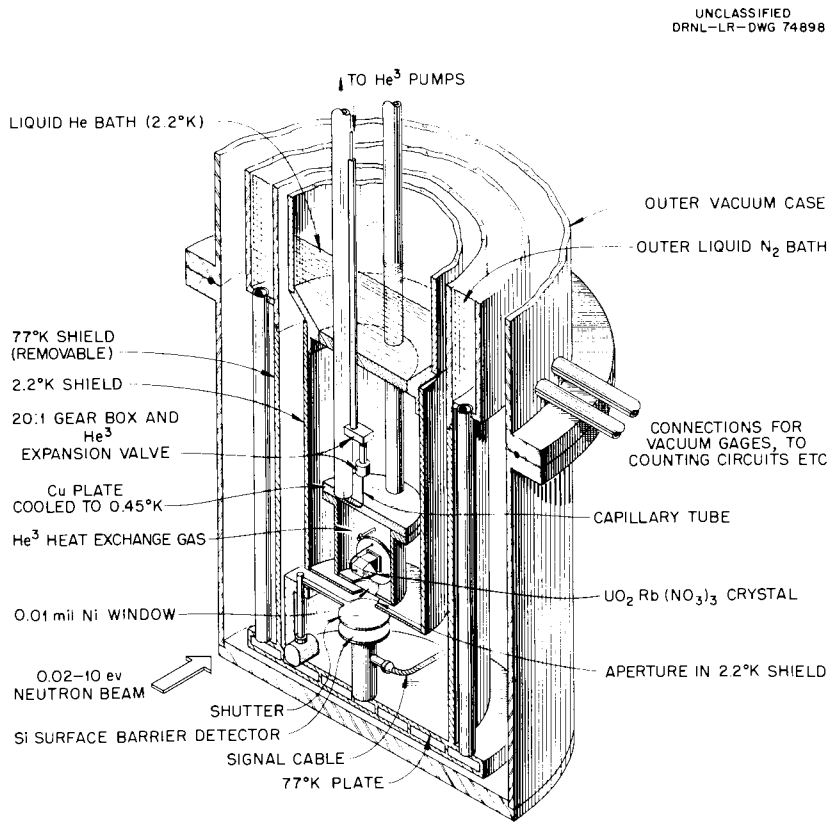

Fig. 1. Schematic Diagram, Lower End of Cryostat.

a heater on the sample chamber is controlled by the recorder so that the inverse temperature of the chamber is held within 1% of the desired $1/T$ value.

Helium-3 gas, at a pressure of $\sim 25 \times 10^{-3}$ mm Hg, surrounds the sample and provides adequate and reliable heat contact to the walls. The density is thus sufficiently low that (n,p) reactions in the He^3 are not important. This technique of gas cooling necessitated development of a thin gas-tight window. Nickel foil 10 μin. thick (from Chromium Corp. of America) was used, and a dilute coating of 1% VYNS resin in cyclohexanone served to cover the small pinholes in the foil. A mesh support serves to improve the ability of the foil to support a pressure differential. Fission fragments passing through the foil lose $\lesssim 30\%$ in energy.

The He^3 refrigerator is unusual in that it operates with a high temperature of 2.20°K (just above the lambda point of the He^4 bath) rather than the usual 1.2°K bath. This arrangement has several advantages: (1) it is not necessary to pump away a large fraction of the He^4 in order to pass through the specific-heat maximum at the lambda point; (2) no superfluid film heat losses are encountered; (3) a much smaller pump (Welch model 1402) can be used because of the high He^4 bath pressure (40 mm Hg). The last advantage permits the entire apparatus to be portable in the sense that the only connection to fixed installations is with electrical cables. As shown in Fig. 2, the entire apparatus can be moved along a circular track at the upper edge of the monochromator shield to conform to the direction of the neutron beam.

The monochromator is a beryllium single crystal and the 1231 reflection is normally used except at lowest energies where other reflections are more convenient. Soller slits determine the entrance and exit collimation. The energy spread of the monochromator is 2.6% at 1 ev and 8.5% at 10 ev. These widths roughly approximate the widths of the resonances thus far studied. The entire apparatus is located at beam hole HB-5 of the ORR. Even the high flux afforded by this

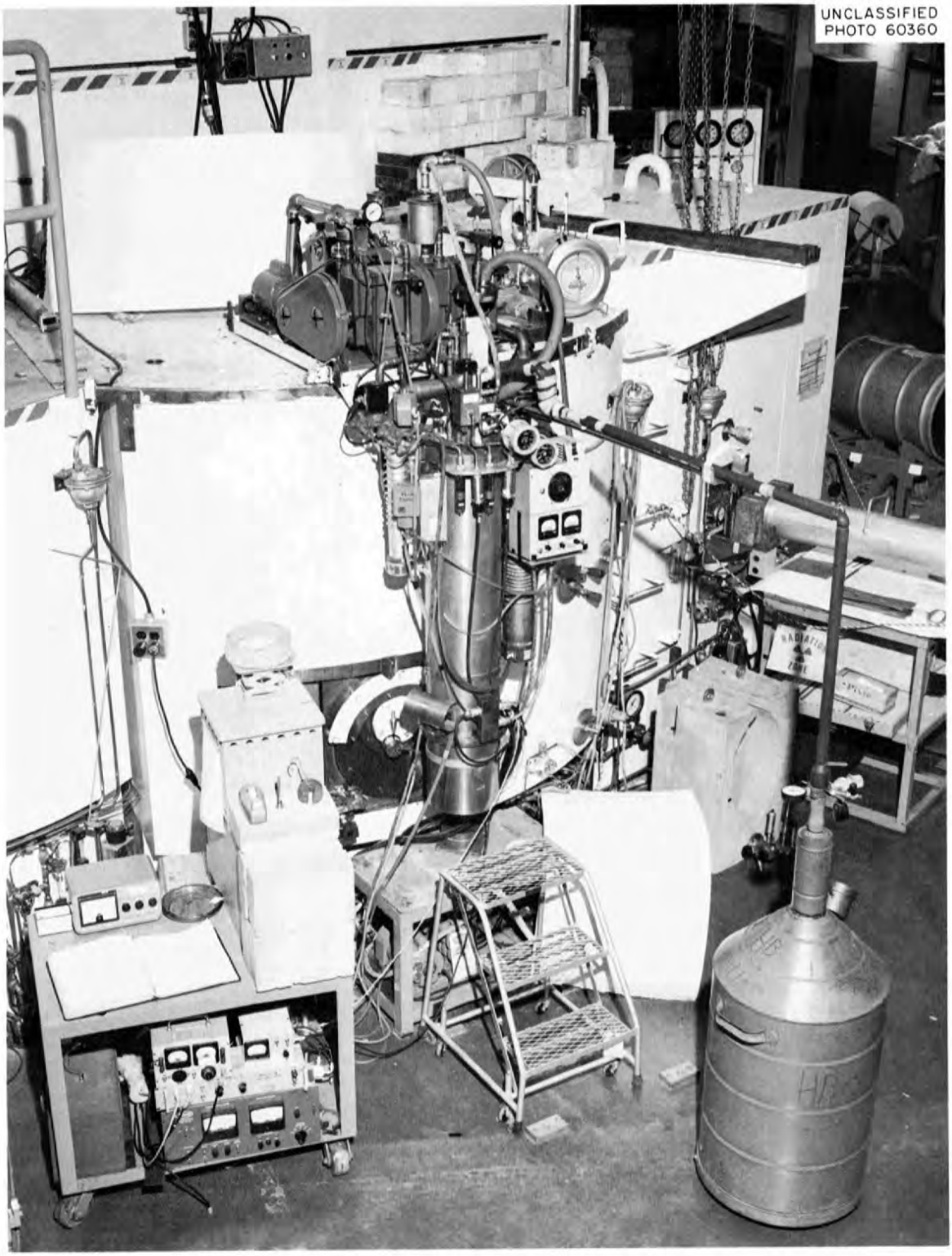

Fig. 2. Cryostat Mounted on Monochromator Shield (Rolled from Usual Operating Position).

reactor, however, gives counting rates in the experiment which are quite small in the 1 to 10 ev energy range and it is necessary to operate the experiment on a 24-hr/day basis for periods up to several weeks per resonance. A completely automated counting system was developed for this purpose. The low counting rates also dictated the use of the He^3 refrigerator; an increase in the size of effect (by increasing $1/T$) by a factor n, for example, permits a reduction in counting time by a factor n^2 for a given accuracy.

Figure 3 is a block diagram of the counting apparatus. Signals from the semiconductor detector are passed through a preamplifier located near the cryostat and thence to a standard A-8 amplifier. The pulses are then analyzed in a modified 20-channel analyzer (old ORNL design) and the outputs of the lowest 11 channels plus surplus are recorded in the glow-tube memory unit shown in Fig. 4. This unit has 30 five-digit storage rows, and the 12 above-mentioned channels are fed into odd- or even-numbered rows according to the position of the sample. For example, when the c-axis of the sample is pointed toward the detector, data are stored in rows 1, 3, 5, etc. The remaining six rows are used to record neutron beam monitor counts, time, and total pulse-height analyzer count. In the measurements reported here, the gain was adjusted so that the maximum alpha pulses fell approximately in channel 9, and most fission pulses fell in "surplus."

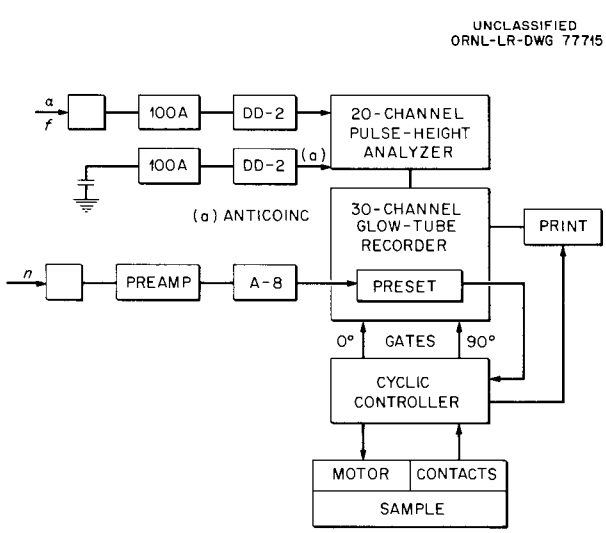

Fig. 3. Block Diagram of Counting Apparatus.

The termination of a given count in a given sample position is caused by a signal from the preset beam monitor scalar which initiates an automatic programming sequence utilizing time-delay relays. Thus the counting period is always determined by the integrated neutron flux through the Dewar as seen by a parallel-plate fission chamber containing U^{235} for the measurement on U^{235}. Typical counting times were about 1 hr in each sample position with printout occurring after about six alternate counts. A diagram of the sequence of operations of the control unit is shown in Fig. 5.

Results to Date

The results given below represent approximately 7 months of operation of the experiment. At neutron energies above 1 ev, low counting rates restricted the measurements to energies where large resonances appear in the U^{235} cross section. Some analyses[12] have indicated that the resonance near 2 ev has a different J value from the bound state and the 0.28-ev resonance. However, this resonance is extremely small and probably cannot be studied without very prolonged measurements. Accordingly, the resonance at 1.14 ev was chosen for the initial measurements followed by the large resonance at 8.8 ev. These measurements gave essentially identical results ($A = +0.044 \pm 0.006$ and $A = +0.051 \pm 0.009$ respectively) as shown in Fig. 6. In an attempt to duplicate the old "thermal" results, measurements were then carried out at 0.14 ev, the lowest energy available from beryllium within the diffraction angle limitations at beam hole HB-5. This result also duplicated the results at 1.14 and 8.8 ev ($A = +0.050 \pm 0.002$) but was not in good accord with the old "thermal" result (which had a substantial error: $A = +0.035 \pm 0.009$). Subsequent measurements at 0.28 ev gave $A = +0.031 \pm 0.002$, and a measurement at 0.20 ev gave $A = +0.039 \pm 0.004$. Thus, there is a sharp change in the anisotropy between 0.14 and 0.28 ev. An examination of the fission cross section of U^{235} in this region shows that this sharp change corresponds roughly to the change from a very small contribution to the cross section from the 0.28-ev resonance at 0.14 ev to

[12] F. J. Shore and V. L. Sailor, *Phys. Rev.* **112**, 191 (1958); E. Vogt, *Phys. Rev.* **112**, 203 (1958); *Phys. Rev.* **118**, 724 (1960).

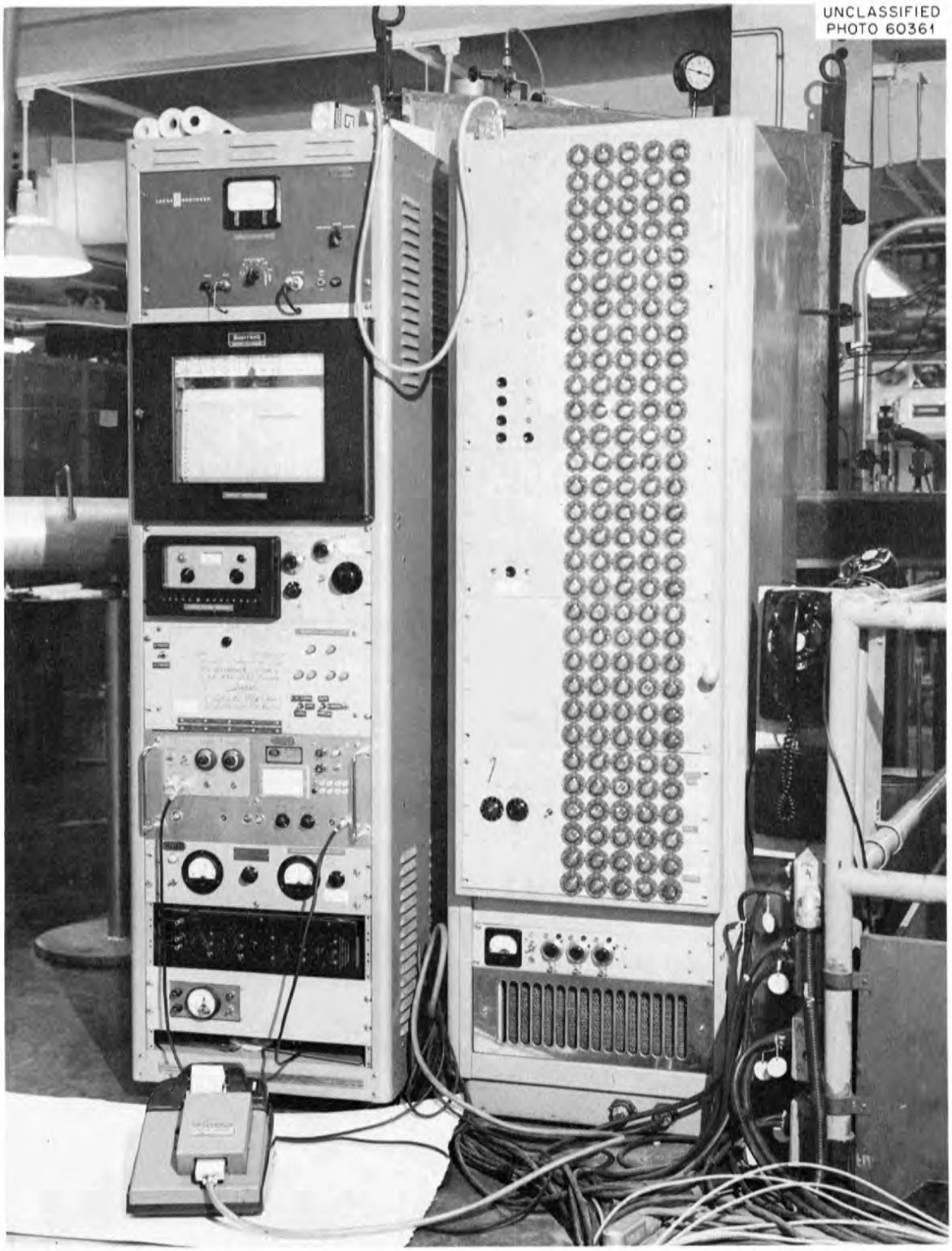

Fig. 4. Photograph of Data-Recording Equipment; Temperature Recording at Upper Left, Counting Equipment at Right.

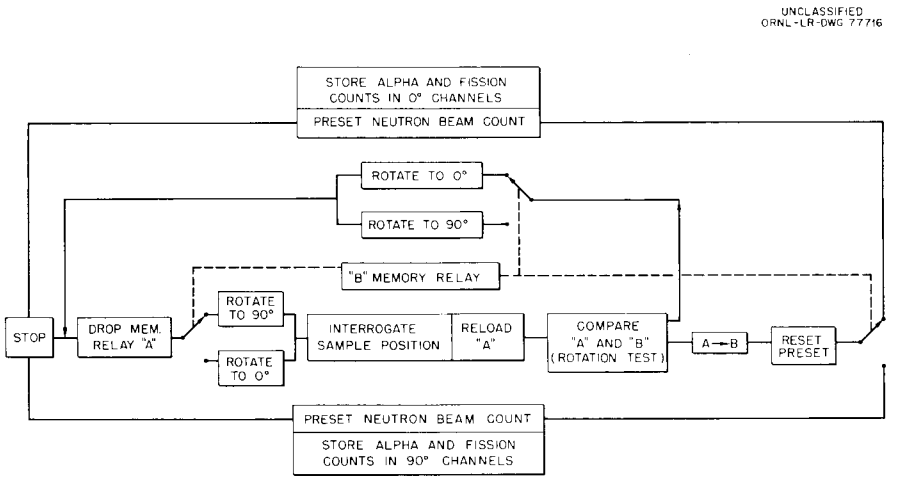

Fig. 5. Sequence of Operations of Automatic Control Unit.

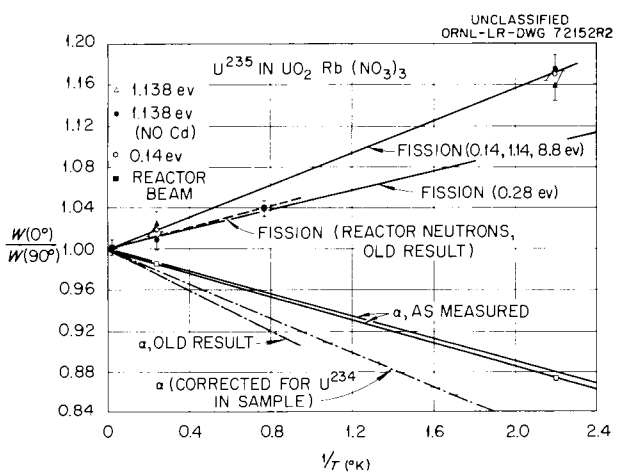

Fig. 6. Anisotropy of Alpha Particles and Fission Fragments at Various Neutron Energies as a Function of $1/T$.

the maximum contribution which occurs near 0.28 ev. At the time of this writing it is not possible to state firmly that this sharp change in anisotropy is definitely associated with the 0.28-ev resonance; however, all present evidence tends in this direction. If this is taken to mean that the J value of this resonance is different from that at 1.14 ev, one has a disagreement with the J-value selections used in multilevel resonance analyses.[12] The dependence of the anisotropies (both alpha and fission) on $1/T$ have been measured rather extensively at 0.28 ev. A graph of these anisotropies is shown in Fig. 7. The linear dependence of both effects on $1/T$ evidenced here is a strong indication that the angular distributions are indeed of the form given by Eq. (1); additional confirmation of the absence of P_4 terms is found in the behavior of the absolute counting rates at 0 and 90°, although these indications are less accurate. A repetition of the calibration of the carbon resistance thermometer is needed for final confirmation of this point as well as for final confirmation of the magnitude of A (although not for the relative values of A).

Measurements designed to clarify the relation between the cross-section curve and the variation in anisotropy with energy are continuing. However, some time will be required since data accumulation is very slow.

Other aspects of the experiment which remain to be clarified are in connection with radiation and/or moisture damage to the sample crystal which possibly have slightly reduced the degree of orientation obtained during the period of the measurements, as indicated in Fig. 6. The alpha-particle anisotropy, however, serves as an excellent monitor of the degree of orientation actually obtained and thus can serve as a basis for normalizing all the measurements.

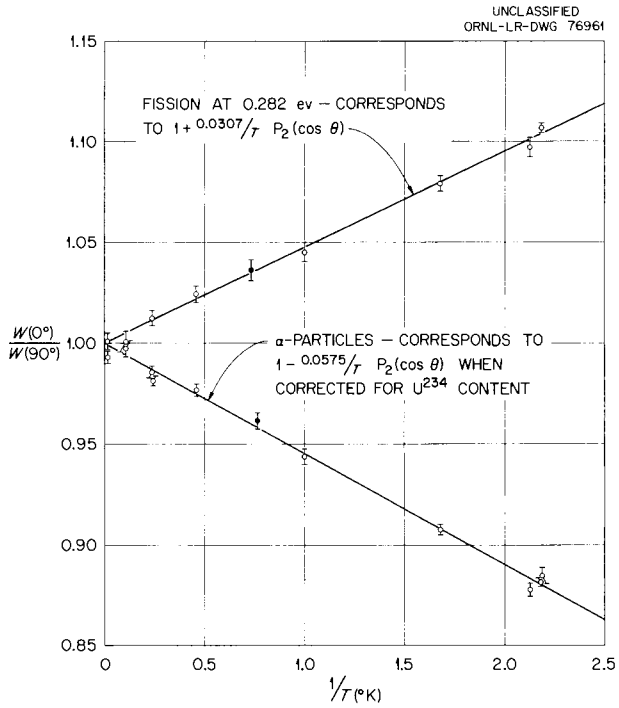

Fig. 7. Anisotropy of Alpha Particles and Fission Fragments at 0.28 ev as a Function of $1/T$.

INTERNAL BREMSSTRAHLUNG IN THE BETA DECAY OF He^6

J. K. Bienlein[1] Frances Pleasonton

The internal bremsstrahlung (IB) accompanying the process of beta decay manifests itself as gamma radiation with a continuous spectrum of energy from zero to the same maximum as the beta particle. Measurements were made to determine the yield of IB relative to beta emission and also the shape of the IB energy spectrum for He^6, which undergoes beta decay with a maximum energy of 3.508 Mev.[2]

The He^6 gas was produced by the same techniques that were used in earlier spectrometer studies,[3] but an additional stage of purification was included to remove radioactive contaminants known to have been present in the gas. Careful searching of the He^6 IB spectrum measurements yielded estimates of about 0.3 and 5% of the IB of the He^6 for the presence of N^{16} and Ne^{23} respectively. Corrections were made to the data for the Ne^{23}. This degree of purity was also confirmed by our measurement[4] of the half-life of He^6, using gas produced in the same system.

To minimize external bremsstrahlung (EB), materials of low atomic number Z were used in the construction and support of the source volumes and for primary shielding in their vicinity. For both measurements the source volumes were mounted at the end of a long, thick-walled Lucite pipe which protruded, as an appendage to the gas flow system, into the middle of the room.

[1]University of Erlangen/Nürnberg, Germany.

[2]C. H. Johnson, Frances Pleasonton, and T. A. Carlson, to appear in *Nuclear Physics*.

[3]C. H. Johnson, Frances Pleasonton, and A. H. Snell, *Phys. Div. Ann. Progr. Rept. Mar. 10, 1959*, ORNL-2718, p 5.

[4]J. K. Bienlein and Frances Pleasonton, *Nucl. Phys.* **37**, 529 (1962).

The Yield of Internal Bremsstrahlung

For the measurement of the total yield of IB the small source, shown in the lower right corner of Fig. 1, was used. The IB quanta were detected with an NaI scintillation counter, and the beta particles with a plastic scintillator. Fairstein type DD2 linear amplifiers were used with both detectors. The counters are also shown in Fig. 1, but for this experiment they subtended an angle of about 165° at the source volume, with their axes in the horizontal midplane of the thin-walled portion of the cylinder. In order to circumvent a calculated estimate of the relative solid angles for the IB and beta detection, we took advantage of the availability of Ne^{23}, in which one strong decay branch emits a 0.44-Mev gamma ray in coincidence with a 3.95-Mev beta particle. By repeating our measurements with the same geometry, but using Ne^{23} as a source, we evaluated the geometry factor to the degree of precision associated with the published values of the branching ratios.

Preliminary analysis of the data gives a value of 0.024 ± 0.006 for the absolute yield of IB quanta relative to beta emission, for energies greater than about 80 kev. This compares with a theoretical yield of 0.0115 calculated from the theory of Lewis and Ford.[5] Recently a refinement of the theory has been worked out by Felsner[6] which is expected to give a value about 20% higher than the older theory.

Internal Bremsstrahlung Spectrum

Figure 1 shows in detail the experimental arrangement of the source volume and scintillation counters. The same detectors were used for counting the IB quanta and beta particles as in the preceding experiment, where the beta counter served as a monitor of variations in the source strength for normalization of the data which were accumulated over a period of about a month. In addition a third scintillation counter (NaI) was

[5] R. R. Lewis and G. W. Ford, *Phys. Rev.* **107**, 756 (1957).

[6] G. Felsner, University of Erlangen/Nürnberg, Germany, private communication.

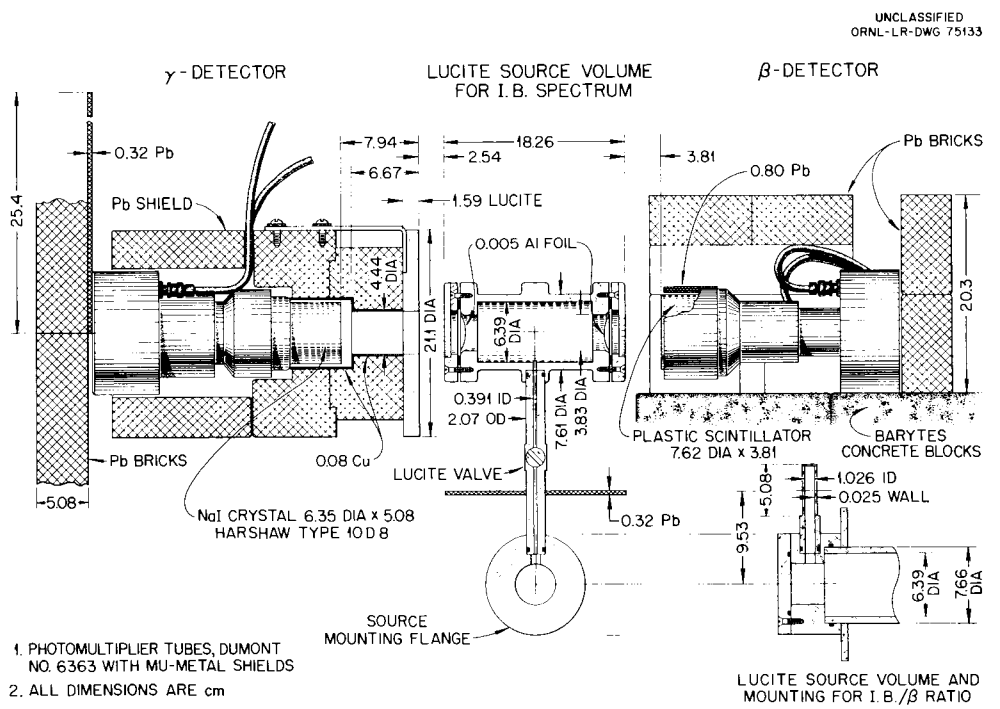

Fig. 1. Details of the Source Volumes and the Geometry of Detectors Used in Measuring the IB Energy Spectrum of He^6.

placed below the long Lucite pipe to monitor the stability of the gas flow during both background and source counting periods and to serve as a second guide for normalizing data. All spectra were obtained with a Nuclear Data 512-channel analyzer, type ND 120.

The measurements were made by alternating short counting periods of source and background. The analyzer was set to operate with a 4-min live-time, adding gamma counts when He^6 was present in the source volume and subtracting them when the gas was excluded by shutting the Lucite valve in the mounting stem. A full run consisted of four such cycles, or 32-min total counting time. Integral counts were recorded for all three detectors during each operating period of the analyzer. In addition, spectra of background were taken several times each day to determine statistical uncertainties of the data, and of an Na^{24} source to check the energy calibration of the spectrometer.

In order to eliminate any counts from the beta electrons in the IB detector, an absorber of 1.7 g/cm^2 was placed between the source volume and the NaI crystal. In the process of absorption, however, electrons produce EB, with a functional dependence on the atomic number of the stopping material. Thus, EB will occur not only in the beta absorber but also in the walls of the source volume and in the materials in its neighborhood. In order to correct the data for EB as well as for absorption of IB in the beta absorber, several types of runs were made:

1. varying the Z of the beta absorber, keeping the thickness constant (1.7 g/cm^2);
2. varying the thickness of the beta absorber, keeping Z constant (Be);
3. adding to the wall thickness of the source volume sufficient material of various Z to stop the beta electrons completely;
4. interposing materials of various Z between the source volume and the beta counter (for these runs it was necessary to use the extra monitor as the normalizing counter).

During runs of types 3 and 4 a Lucite absorber of 1.7 g/cm^2 was always used before the gamma counter. These runs were repeated in random order, with respect to both type and material, as many times as possible in order to improve the statistical accuracy of the data.

Out of a total of 181 runs there were 150 for which the monitor and beta counter gave evidence of simultaneously well-behaved electronics and stability of the source gas. After correcting these runs for shifts in the energy calibration of the analyzer and for the presence of Ne^{23}, all those of a given type and with the same Z material were combined. After normalization the resulting "summed" spectra were then extrapolated, channel by channel, to zero Z or, in the case of type 2 runs, to zero absorber thickness. Intercomparison of these extrapolated spectra showed the IB counting rate to be sensitive only to the absorption and EB that occurred in the beta absorber.

These spectra are pulse-height distributions, however, rather than the energy distribution of the IB that is sought. For a monoenergetic gamma ray a scintillation spectrometer gives a pulse-height distribution which contains the photoline, a Compton distribution, backscatter peaks, and perhaps escape peaks. The continuous IB pulse-height spectrum represents an overlapping of such complex spectra for all energies up to the maximum. It becomes necessary, therefore, to "unscramble" the extrapolated IB data to obtain the desired energy spectrum.

The first step in accomplishing this is to determine the pulse-height response of the spectrometer to sources that emit monoenergetic gamma rays of various energies. Two thin sources of different strength were prepared for each of several isotopes. The extended geometry of the gaseous He^6 source was approximated by taking the spectrum of each isotope twice, the weaker source being used at the end of the source volume near the NaI crystal and the stronger one at the far end. In addition one gaseous source, Ar^{41}, was used. From these measurements the shape and intensity of the whole pulse-height distribution was determined relative to a photopeak of known energy.

This information was then used to construct the "response" matrix of the spectrometer, that is, the function which, when combined with the true energy spectrum of a gamma source, yields the pulse-height distribution observed by the spectrometer. By appropriate grouping of successive channels of the IB data, the "extrapolated" spectrum was reduced to 30 channels and the "unscrambling" was then achieved by solving a 30 × 30 system of linear equations. Figure 2 shows a preliminary result with a rather crude approximation to the proper response matrix. Error flags are omitted from the points because of the crude nature of the solution and to clarify the overall comparison with theory. The solid curve is the result of a preliminary calculation of the theory as developed by Felsner.[6] The final calculations are now in progress.

It is concluded that the experiments show agreement with the theory, which assumes that the internal bremsstrahlung originates in a two-step process: first beta decay with the electron in an intermediate state, then emission of IB while the electron goes to its final state. Together with other new experiments and theories the conclusion can be drawn that the fundamental process, proved in this experiment, together with correctly treated Coulomb corrections describes the internal bremsstrahlung well. With the present accuracy it is not necessary to consider more complicated processes than the fundamental one.

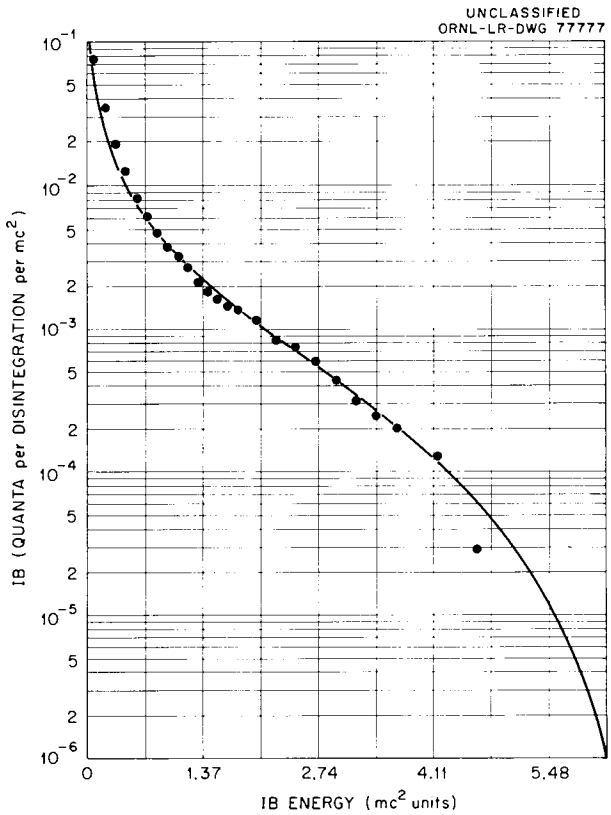

Fig. 2. Preliminary Comparison of the Experimental Results for the IB Energy Spectrum with the Theory as Developed by Felsner.[6] The points are matched to the theoretical curve in the region of 400 to 700 kev energy.

ANALYSIS OF THE RECOIL ENERGY SPECTRUM FROM THE BETA DECAY OF He^6

C. H. Johnson Frances Pleasonton T. A. Carlson

Ions which recoil from the beta decay of He^6 have a continuous energy spectrum, 0 to 1418 ev, with a shape depending on the electron-neutrino angular correlation. For an allowed transition,

$$N(p,q)\, dW\, d\cos\theta$$

$$\propto F(Z,W)pWq^2(1 + \lambda_0 \frac{p}{W}\cos\theta)\, dW\, d\cos\theta\,, \quad (1)$$

where W and p are the energy and momentum of the β^- particle, q is the neutrino momentum, θ is the angle between the momentum vectors, λ_0 is the angular correlation coefficient, and $F(Z,W)$ is the Fermi function. (The Fierz term is assumed to be zero.) This function is readily transformed to the recoil energy spectrum for $F(Z,W) = 1$. For a Gamow-Teller transition,

$$\lambda_0 = -\frac{1}{3}\frac{|C_A|^2 + |C_A'|^2 - |C_T|^2 - |C_T'|^2}{|C_A|^2 + |C_A'|^2 + |C_T|^2 + |C_T'|^2}\,, \quad (2)$$

where the C's are the usual tensor and axial-vector coupling constants.

Measurements of the recoil energy spectrum were described previously.[1] The spectrum was observed 26 times under a variety of conditions, and corrections were made to the data for several instrumental effects. A theoretical correction[2] was made to account for the fact that $F(Z,W) \neq 1$. The repeated measurements were then combined into a single spectrum of 16 datum points whose uncertainties are based on the observed run-to-run fluctuations. The angular correlation coefficient λ_0 was then estimated by means of a least-squares analysis. An important feature of the analysis is that it involves not only a parameter λ and an arbitrary normalization parameter but also a third parameter γ which is related to the detector's efficiency. As stated in the earlier report[1] the multiplier's detection efficiency is

$$\epsilon(E_c, E_0) = e(E_c)\, f(E_c/E_0)\,, \qquad (3)$$

where $e(E_c)$ is a function of the energy of the ion incident on the cathode and $f(E_c/E_0)$ is a function of the energy multiplication imposed by the accelerating voltage at the entrance to the detector. Extensive measurements which were made on the product efficiency $\epsilon(E_c, E_0)$ were not sufficient to allow an analysis without the third parameter. The analysis was made by choosing an arbitrary value for the missing information, namely, the slope de/dE_c at some energy $(E_c)_0$, and then making a least-squares analysis to the theoretical recoil spectrum multiplied by E_r^{γ}. The factor E_r^{γ}, where E_r is the recoil energy and γ is the third parameter, is introduced on the basis of Eq. (3).

The estimate for λ_0 from the least-squares analysis[3] is $\lambda = -0.3343 \pm 0.0017$. A careful evaluation of several small uncertainties of random sign increases the standard error to ± 0.0029. This result is subject to possible small corrections before final publication.

An interpretation of this result in terms of a limit to the tensor interaction is not trivial. If there were no prior knowledge regarding λ_0, one could conclude with 68% confidence that $\lambda_0 = -0.3343 \pm 0.0029$. Actually there is considerable prior knowledge which should be combined with the present result. The most pertinent information is that, for a Gamow-Teller interaction, λ_0 lies between $+\frac{1}{3}$ and $-\frac{1}{3}$.

This prior knowledge is introduced on the principle of inverse probability,[4]

$$P_{\lambda}(\lambda_0) = P(\lambda_0)\, P_{\lambda_0}(\lambda)\,,$$

where

$$\int_{-\infty}^{+\infty} P_{\lambda}(\lambda_0)\, d\lambda_0 = 1\,.$$

This states that, given a measured λ, the posterior probability distribution $P_{\lambda}(\lambda_0)$ for λ_0 is equal to the product of the prior probability $P(\lambda_0)$ multiplied by the likelihood distribution $P_{\lambda_0}(\lambda)$ of λ for a given λ_0. The normalization states that there is a λ_0. We assume that the likelihood is a normal distribution and that λ_0 can have any value within the Gamow-Teller limits, that is,

$$P(\lambda_0) \sim d\lambda_0 \quad \text{for} \quad -\frac{1}{3} \leqq \lambda_0 \leqq \frac{1}{3}\,,$$
$$= 0 \quad \text{for} \quad \lambda_0 > \frac{1}{3}\,, \quad \lambda_0 < -\frac{1}{3}\,.$$

The resulting posterior probability distribution is the tail of a normal distribution of width $\sigma = 0.0029$ centered at $\lambda = -0.3343$. Only that part of the distribution which lies within the Gamow-Teller limits is allowed, and its area is normalized to unity. The most probable value of λ_0 is $-\frac{1}{3}$, and the limits $-0.3308 \geqq \lambda_0 \geqq -\frac{1}{3}$ contain 68% of the normalized distribution. The corresponding limit for the tensor interaction is

$$\frac{|C_T|^2 + |C_T'|^2}{|C_A|^2 + |C_A'|^2} \leqq 0.38\%\,.$$

Sometimes this type of problem is attacked in a more qualitative manner in which one simply quotes confidence limits arbitrarily centered on the limiting value. This procedure increases the above tensor limit to 0.43%.

---

[1] C. H. Johnson, Frances Pleasonton, and T. A. Carlson, *Phys. Div. Ann. Progr. Rept. Feb. 10, 1961*, ORNL-3085, p 18.

[2] Dr. Eugene Greuling provided us with a correction for the Fermi function.

[3] P. B. Wood, *A 704 Program for Fitting Non-linear Curves by Least Squares*, ORGDP-K 1440 (Jan. 28, 1960).

[4] Harold Jeffreys, *Theory of Probability*, Oxford University Press, 1961.

HALF-LIFE OF He^6[1]

J. K. Bienlein[2] Frances Pleasonton

The decay of He^6 was measured, with a plastic scintillation counter, over a period of ten half-lives. The data were obtained by photographing two scalers, one of which registered the beta counts while the other, operating on a 60 Hz signal, served as the clock. After suitable corrections for background, dead time of the counting system, and pulse-height dependence on counting rate, 34 separate runs were combined. A least-squares fit to the data gives a value of $T_{1/2} = 0.797 \pm 0.003$ sec.

[1]Abstract of published paper: *Nucl. Phys.* **37**, 529 (1962).

[2]Permanent address: Physikalisches Institut, Universität Erlangen/Nürnberg, Germany.

ELECTRON SHAKE-OFF FOLLOWING THE β^- DECAY OF He^6[1]

T. A. Carlson Frances Pleasonton C. H. Johnson

The charge spectrum of the Li^6 ions formed following the β^- decay of He^6 has been measured as a function of their recoil energy by means of a specially designed mass spectrometer. The analysis is as follows: charge 1, $(89.6 \pm 0.2)\%$; charge 2, $(10.4 \pm 0.2)\%$, of which $(0.31 \pm 0.05)\%$ is dependent on recoil energy; charge 3, $(0.042 \pm 0.007)\%$, of which $(0.024 \pm 0.009)\%$ is dependent on recoil energy. Comparison with theory shows that electron shake-off results primarily from excitation by the sudden nonadiabatic change in nuclear charge. An expression is given for describing the simultaneous excitations from the sudden changes in nuclear charge and velocity.

[1]Abstract of paper to be published in the *Physical Review*.

ELECTRON SHAKE-OFF FOLLOWING THE BETA DECAY OF Ne^{23}[1]

T. A. Carlson

A specially designed mass spectrometer is used to analyze the sodium ions that result from the β^- decay of Ne^{23}. The percent abundances are as follows: Na^{1+}, 79.1; Na^{2+}, 17.5; Na^{3+}, 2.85; Na^{4+}, 0.49; Na^{5+}, 0.081; Na^{6+}, 0.006; and Na^{7+}, <0.002. No evidence is found that recoil energy contributes to the electron shake-off. An attempt is made to derive the charge spectrum from the assumption that electron shake-off is due to the sudden, nonadiabatic change in nuclear charge. Multiple electron shake-off is computed from the product of the probabilities for single electron shake-off. The probabilities for single electron shake-off are semiempirically calculated. In general, the calculated values agree well with the experimental data, although the computations underestimate the abundances of the more highly charged ions.

[1]Abstract of paper submitted to the *Physical Review*.

FORMATION OF FRAGMENT IONS FROM CH_3Te^{125} AND $C_2H_5Te^{125}$ FOLLOWING THE NUCLEAR DECAYS OF CH_3I^{125} AND $C_2H_5I^{125}$[1]

T. A. Carlson R. M. White[2]

The relative abundances of the fragment ions that result from the nuclear decays of CH_3I^{125} and $C_2H_5I^{125}$ (I^{125} undergoes electron capture to give Te^{125}) have been measured with a specially designed mass spectrometer. The data from both studies are similar and give evidence of the highly destructive nature of the decay: (1) Only about 1% of the tellurium-hydrocarbon ions appear to remain intact, in spite of the fact that these ions would be expected to be collected with high efficiency. (2) In both studies a large number of tellurium ions are found with charges as high as 18 and with an average charge of about 9. (3) Finally, in both studies, the singly, doubly, and triply charged carbon ions are found in greater abundance than the hydrocarbon ions. The cause of this extensive ionization and fragmentation is ascribed primarily to a series of Auger processes that occur subsequent to the formation of inner orbital vacancies in Te^{125} as the result of electron capture and internal conversion in the decay of I^{125}.

[1]Abstract of paper to be published in the *Journal of Chemical Physics*.

[2]Summer research participant from Baker University, Baldwin, Kan.

MASS SPECTROMETRIC ANALYSES OF THE IONS RESULTING FROM THE NUCLEAR DECAY OF CH_3I^{130} AND $C_2H_5I^{131}$: STUDY OF XENON-HYDROCARBON IONS[1]

T. A. Carlson R. M. White[2]

Ions resulting from the nuclear decay of CH_3I^{130} and $C_2H_5I^{131}$ have been measured with a specially designed mass spectrometer. From these two studies the percent abundances for the parent ions, $[CH_3Xe^{130}]^+$ and $[C_2H_5Xe^{131}]^+$, are found to be, respectively, 34 and 1.4%. Besides CH_3^+ and $C_2H_5^+$, formed directly from the severance of the carbon-xenon bond of the parent ions, a large variety of fragment ions are also observed. The results are compared with those for a similar study on CH_3I^{131} (ref 3). From these comparisons the following conclusions are reached: (1) the ethyl-xenon ion undergoes decomposition much more readily than the methyl-xenon ion, and (2) the greater recoil energy that is present in the decay of I^{130} leads primarily to the severance of the organic-xenon bond, with the formation of CH_3^+. Besides recoil energy, there are also two other sources of excitation: (1) Coulombic shaking, as the result of the sudden change in nuclear charge following beta decay, is used to explain the appearance of the lower charged xenon ions and most of the fragment hydrocarbon ions. (2) Multiple Auger processes following internal conversion are given as the cause for the more highly charged xenon ions, and their abundance is correlated with the amount of internal conversion present in I^{130} and I^{131}.

[1]Abstract of paper to be published in the *Journal of Chemical Physics*.

[2]Summer research participant from Baker University, Baldwin, Kan.

[3]T. A. Carlson and R. M. White, *J. Chem. Phys.* **36**, 7883 (1962).

FRAGMENT IONS RESULTING FROM β^- DECAY OF CH_3Br^{82} AND β^+ DECAY OF CH_3F^{18}

T. A. Carlson R. M. White[1]

Snell and Pleasonton[2,3] have shown that the fragmentation of a radioactive gas can be studied with a specially designed mass spectrometer. The gas is allowed to decay in the spectrometer, and the ions that are formed as the result of the decay are collected and analyzed. The gas pressures are held low enough to avoid ion-molecule reactions or radiolysis. The ions observed are those that come directly from the decomposition of the parent species that undergo decay. In recent years a number of radioactive alkyl halides have been studied.[4-7] This report discusses two new investigations.

CH_3Br^{82}

The relative abundances of the fragment ions resulting from the decay of CH_3Br^{82} are given in Table 1. CH_3Br^{82} undergoes β^- decay to give $[CH_3Kr^{82}]^+$. The parent ion will be observed if it remains stable for the 10^{-4} to 10^{-5} sec required for its collection and analysis and if it has not received sufficient excitation from the β^- decay to decompose. The occurrence of rare gas–hydrocarbon ions has recently been the subject of several papers.[5,6,8-10] Although in the present study only about ½% of the observed ions are found as $[CH_3Kr]^+$, it is significant that not all the methyl-krypton ions have decomposed.

Table 1. Relative Abundances of the Fragment Ions Formed Following the Decay of

$$CH_3Br^{82} \xrightarrow{\beta^-} [CH_3Kr^{82}]^+$$

Ion	Abundance of Observed Ions (%)
CH_3Kr^+	0.43 ±0.09
CH_2Kr^+	<0.2
$CHKr^+$	<0.2
CKr^+	<0.2
CH_3^+	88.7
CH_2^+	1.6 ±0.2
CH^+	2.4 ±0.2
C^+	1.6 ±0.2
C^{2+}	0.07 ±0.04
C^{3+}	<0.02
Kr^+	2.3 ±0.2
Kr^{2+}	0.8 ±0.01
Kr^{3+}	0.15 ±0.03
Kr^{4+}	0.08 ±0.08
HKr^+	<0.4
H_2^+	<0.1
H^+	1.9 ±0.2

This is particularly true in view of the rather large recoil energies involved in the decay of Br^{82}.

Table 2 lists the percent abundances of the CH_2^+, CH^+, C^+, and C^{2+} ions that are formed as the result of the beta decay of CH_3H^3 (ref 11), CH_3Br^{82}, CH_3I^{130} (ref 6), and CH_3I^{131} (ref 5).

[1]Summer research participant from Baker University, Baldwin, Kan.

[2]A. H. Snell and Frances Pleasonton, *Phys. Rev.* **100,** 1396 (1955).

[3]Frances Pleasonton and A. H. Snell, *Proc. Roy. Soc. (London)* **A241,** 141 (1957).

[4]S. Wexler and G. R. Anderson, *J. Chem. Phys.* **33,** 850 (1960).

[5]T. A. Carlson and R. M. White, *J. Chem. Phys.* **36,** 2883 (1962).

[6]T. A. Carlson and R. M. White, "Mass Spectrometric Analyses of the Ion Resulting from the Nuclear Decay of CH_3I^{130} and $C_2H_5I^{131}$," this report.

[7]T. A. Carlson and R. M. White, "Formation of Fragment Ions from CH_3Te^{125} and $C_2H_5Te^{125}$ Following the Nuclear Decays of CH_3I^{125} and $C_2H_5I^{125}$," this report.

[8]F. H. Field and J. L. Franklin, *J. Am. Chem. Soc.* **83,** 4509 (1961).

[9]F. H. Field, H. N. Head, and J. L. Franklin, *J. Am. Chem. Soc.* **84,** 1118 (1962).

[10]P. S. Rudolph, S. C. Lind, and C. E. Melton, *J. Chem. Phys.* **36,** 1031 (1962).

[11]A. H. Snell and Frances Pleasonton, *J. Phys. Chem.* **62,** 1377 (1958).

Table 2. Comparison of the Abundances of the CH_2^+ CH^+, C^+, and C^{2+} Fragment Ions Formed as the Result of the Beta Decay of CH_3X

Ion	Abundance[a] (%)			
	$X = H^3$[b]	$X = Br^{82}$	$X = I^{130}$[c]	$X = I^{131}$[d]
CH_2^+	4.9	1.6	3.3	2.4
CH^+	4.0	2.4	3.4	2.2
C^+	4.9	1.6	3.9	1.9
C^{2+}	0.08	0.07	0.1	0.07

[a]Abundances are expressed in percent of the total number of observed ions in the respective studies.

[b]See ref 11.

[c]See ref 6.

[d]See ref 5.

The similarity of the results for the different studies is probably a reflection of the similarity in the mechanism for producing these ions. The excitation responsible for the formation of the fragment ions in Table 2 probably arises from the sudden change in nuclear charge, because recoil energy seems to result primarily in the severance of the bond between the carbon and recoiling heavy atom,[6] whereas excitation as the result of a sudden change in nuclear charge is capable of producing a large variety of fragment ions. The sudden change in nuclear charge does not allow the electronic states of the molecule to adjust adiabatically to their new environment, with the result that these states may become excited. This electronic excitation may be transferred into vibrational and rotational degrees of freedom in such a way that the parent ions will undergo unimolecular decomposition. It is reasonable to assume that in each of the studies compared in Table 2 the principal route in the decomposition of the parent ion is through CH_3^+. Thus, the formation of CH_3^+ is common to every study, and the relative abundances of CH_2^+, CH^+, C^+, and C^{2+} will essentially depend on how excited the CH_3^+ is after separation from the parent ion. The similarity in the spectra of the fragment ions in Table 2 indicates that the CH_3^+ has received about the same amount and distribution of excitation in each of the studies; and, in fact, it also indicates that the extent of excitation present in each of the parent ions was about the same, because, though the energy necessary for producing CH_3^+ varies from study to study, this energy may be considered to be a small perturbation in the overall excitation available for fragmentation. It is interesting to note that the similarity of excitation, observed above for the β^- decay of molecular systems, finds it parallel in the similarity of the amount of electron shake-off found in the β^- decay of rare gases from helium to xenon.[12]

CH_3F^{18}

The fragment ions resulting from the β^+ decay of CH_3F^{18} are given in Table 3. This is the first time that a molecule undergoing positron decay has been investigated for its fragment ions. Such studies might form a useful supplement to the understanding of negative ions, because the parent ion of a β^+ decay is a singly

[12]T. A. Carlson, A. H. Snell, Frances Pleasonton, and C. H. Johnson, p 147 in *Proceedings of a Symposium, Prague (1960), on the Chemical Effects of Nuclear Transformations*, vol 1, International Atomic Energy Agency, Vienna, 1961.

Table 3. Relative Abundonces of the Fragment Ions Following the Decay of $CH_3F^{18} \xrightarrow{\beta^-} [CH_3O^{18}]^-$

Ion	Abundance (%)
CH_3O^-	12 ± 1
O^-	8 ± 1
H^-	17 ± 9
CH_3^+	39
CH_2^+	13 ± 1
CH^+	5 ± 1
C^+	2 ± 1
H^+	4 ± 1
CH_2O^-, CHO^-, CO^-, CH_3O^+, CH_2O^+, CHO^+, CO^+, O^+, O^{2+}, C^{2+}, H_2^+	<1
CH_3^-, CH_2^-, C^-, OH^-	<1.5
O^{2-}, H_2^-, H_2O^-	<2.0

charged negative ion. Figure 1 gives schematically the molecular consequences of the decay of CH_3F^{18}. It may at first seem remarkable that the formation of positive ions, which requires the loss of two electrons, is so extensive, in view of the fact that double electron removal occurs with rather small probability in the studies on β^- decay. The extent of electron shaking is expected to be the same for positron and negatron decay.[13] The answer may lie in the large differences in the ionization potentials involved in the respective decays. The energy necessary to remove two electrons from CH_3O^- is probably not much over 10 ev, while in the β^- decay of neon, for example, the energy necessary to remove two electrons from singly charged Na^+ is 118 ev. It might be expected that large abundances of neutral fragments are also formed, since it usually requires only a few electron volts of excitation to eject the first electron from a negatively charged ion. Indeed, it appears from the comparison of the ion collection efficiencies for several studies, including CH_3F^{18}, that in the decay of CH_3F^{18} a large number of neutral fragments are formed.

[13]A. Migdal, *J. Phys.* (*U.S.S.R.*) **4**, 449 (1941).

There is also the possibility that the observed positive ions really arise from a secondary process. For example, when the collection chamber is at a positive potential, CH_3O^- might strike the walls of the chamber with sufficient force to create CH_3^+. The other positive ions can, in turn, be thought of as being derived from the decomposition of CH_3^+. These suggestions are supported by the absence of CH_3O^+, which one would have expected to be one of the more abundant positive ions, since it arises as the immediate result of double electron shake-off and is rather stable, requiring 6.5 ev for decomposition.

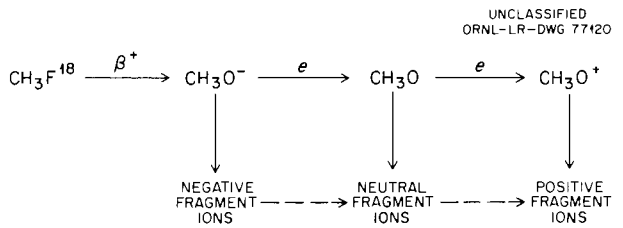

Fig. 1. Possible Decomposition Routes Following the β^+ Decay of CH_3F^{18}.

ELECTRON SHAKE-OFF FOLLOWING THE β^- DECAY OF Ar^{41}[1]

T. A. Carlson

A specially designed mass spectrometer is used to analyze the potassium ions that result from the β^- decay of Ar^{41}. The percent abundances are as follows: K^+, 82 ± 1; K^{2+}, 12.5 ± 0.8; K^{3+}, 3.0 ± 0.2; K^{4+}, 1.4 ± 0.1; K^{5+}, 0.44 ± 0.06; K^{6+}, 0.16 ± 0.04; K^{7+}, 0.06 ± 0.02; and K^{8+}, 0.016 ± 0.009. The data are compared with similar studies on other rare gases that undergo beta decay, and some of the general properties of electron shake-off as a function of atomic number are discussed.

[1]Abstract of paper submitted to the *Physical Review*.

MEASUREMENTS OF THE HYPERFINE SPLITTING IN Fe-Rh AND Fe_2O_3 USING THE MÖSSBAUER EFFECT

F. E. Obenshain L. D. Roberts H. H. F. Wegener[1]
J. O. Thomson D. W. Forester

Introduction

The Mössbauer effect is a useful tool for the investigation of the effective field at the nucleus in magnetic solids. This effective magnetic field gives rise to a splitting of the nuclear energy levels. The corresponding interaction energy may have the form $\mu_N \cdot H_e$, where μ_N is the magnetic moment of the energy level involved, and H_e is the effective magnetic field produced by the electronic structure of an atom in the solid. Through the measurement of this hyperfine structure (hfs) splitting, it is possible to study the magnetic materials from a different point of view, and often it may provide a new kind of information about the magnetic state.

The hyperfine structure splitting will, in general, have the form $A(I \cdot S)$. In the presence of a field which leads to an electronic spin energy very large compared to this, the hfs interaction may be adequately described by the somewhat simpler form $A(I_z S_z)$. In our present work the above strong field may be partially magnetic in nature or it may have an even stronger contribution in suitable ferromagnetic or antiferromagnetic materials from electron spin–spin exchange effects. These exchange effects tend to orient the electron spin, but this tendency is opposed by the thermal motion of the system. Thus, the expectation value of the electron spin $\langle |S_z| \rangle$, that is, the magnetization of the system, is temperature-dependent. In the strong-field limit, we may write the approximate result,

$$H_e = \frac{A \langle |S_z| \rangle}{g_e \beta_e} . \qquad (1)$$

The expectation value $\langle |S_z| \rangle$ is a quantity of some interest. It is often described in an approximate way by a Brillouin function. For ferromagnetic systems the spin-wave treatment gives a $(1 - aT^{3/2})$ dependence, which agrees well with measurements at temperatures well below the Curie point. Antiferromagnetic-spin-wave theory[2] gives $\langle |S_z| \rangle \sim (1 - aT^3)$ within a sublattice, but this prediction does not seem to have been checked experimentally. Bulk magnetization measurements do not give direct information about $\langle |S_z| \rangle$ within a sublattice. Neutron diffraction measurements are capable of this through intensity measurements, but detailed studies do not seem to have been made. The Mössbauer method provides an effective technique for the measurement of this expectation value through the measurement of H_e. This is obtained through the measurement of the overall width of the hyperfine structure pattern of the Mössbauer gamma ray. This measurement is essentially spectroscopic in nature and thus may be of relatively high precision, the precision being limited in principle only by the gain stability of the apparatus.

We have investigated the two magnetic systems Fe_2O_3 and Fe-Rh in the temperature range 4.2 to 500°K. In the case of Fe_2O_3 the system remains antiferromagnetic at all temperatures below its Néel temperature (T_N) of 975°K. A previous Mössbauer study of this system, which is very similar to our own, has been made by Ono *et al.*,[3] and these earlier results and our measurements are in good agreement. In our work a more detailed study of the lower temperature region, which is of interest in a possible comparison with spin-wave theory, has been made. The Fe-Rh system shows an interesting behavior as a function of temperature and composition. For alloys with a rhodium composition near 53 at. %, the system is found to be antiferromagnetic below a critical temperature near 350°K, for example, and then ferromagnetic above this temperature up to the Curie point. Recent careful measurements of bulk magnetic and electrical conductivity have been given by Kouvel and Hartelius.[4] Neutron

[1]University of Erlangen, Erlangen, Germany.

[2]J. Van Kranendonk and J. H. Van Vleck, *Rev. Mod. Phys.* **30**, 1 (1958).

[3]K. Ono *et al.*, *J. Phys. Soc. Japan (suppl B-I)* **17**, 125 (1962).

[4]J. S. Kouvel and C. C. Hartelius, *J. Appl. Phys. Suppl.* **33**, 1343 (1962).

diffraction measurements have been made by Bertaut *et al.*[5] These latter measurements, when combined with bulk magnetic studies, give a good picture of the ferromagnetic phase of the alloy. Bertaut *et al.* find that the moment at the iron site is 3 μ_B and the moment at the rhodium site is 0.6 μ_B. However, only the sum of the squares of the magnetic moments at the iron and at the rhodium sites was obtained in the antiferromagnetic phase. Here, the Mössbauer technique may make a useful contribution through the measurement of $\langle |S_z| \rangle$ on the iron as a function of temperature from 4.2°K right through the antiferromagnetic-ferromagnetic transition.

Apparatus

The Mössbauer nucleus is Fe^{57}, and we have used the natural abundance present in the iron-rhodium samples. The source was a nonmagnetic foil either of stainless steel or of copper with Co^{57} diffused into it. The stainless steel source was only a fraction of a millicurie, but the copper source had approximately 50 mc of Co^{57} diffused into an area of about 0.1 cm^2, and the foil was about 10^{-3} cm thick. The absorption line width from the intense source was approximately three times the natural line width, but this does not affect the determination of the Mössbauer line centers. An interesting magnetic behavior of this copper-cobalt source was observed and will be described at the end of this section.

The relative velocity between source and absorber was obtained by mounting the source on the moving member of an electromechanical transducer which was driven by a sine-wave generator. The output signal of the gamma detector was then modulated by the output signal of the transducer pickup coil. The modulated signal was then fed into a multichannel analyzer. Details of an apparatus very similar to the equipment used here have been described earlier.[6]

As stated above, the copper-cobalt source was prepared by diffusion of 50 mc of Co^{57} into a copper foil, and then annealing of the sample at 1000°C for 1 hr. Some months later the Mössbauer line shape was investigated using a 2.5×10^{-3}-cm-thick stainless steel absorber. This measurement showed several satellites on either side of the central line. After the source was annealed for 11 hr at 1000°C, another measurement showed that the satellites had disappeared and that the fractional absorption of the central line had increased from 15 to 24%. One month later the hyperfine splitting of the source was observed again, and the source had to be reannealed to make the satellites disappear. The source was being used at room temperature but was occasionally cooled to 77°K for some measurements. The appearance of the hyperfine structure may be related to diffusion of the cobalt through the copper lattice near room temperature, resulting in small clusters of cobalt.

Fe-Rh Measurements

We have investigated several samples of Fe-Rh in the composition range 50 to 55 at. %. Figure 1 shows the results of one measurement for 52% rhodium as a function of temperature. This particular sample was prepared by Kouvel.[4] It was melted in an argon atmosphere, annealed at 950°C for 24 hr, and then cooled to room temperature. The temperature range of the transition from antiferromagnetism to ferromagnetism, reflecting hysteresis effects, was 335–385°K.

Bertaut has found an iron magnetic moment of 3 μ_B in the ferromagnetic phase. This moment is much larger than that found for pure metallic iron. However, we find that at all temperatures $|H_e|$ is substantially less for Fe-Rh than that found for pure iron. At the lowest temperature (338°K) at which the Fe-Rh sample of Fig. 1 was ferromagnetic, an $|H_e|$ value of 261 ± 2 kilogauss was found, whereas that for iron at room temperature, a comparable temperature, is 331 kilogauss.

Thus, it is striking that the substantially higher iron moment in Fe-Rh corresponds to a smaller internal field. Presumably, H_e arises predominantly from the contact interaction between the several slightly polarized *s* shells of the iron atom with the iron nucleus. For the different shells the several contributions may differ in sign, and it may be that these contributions more nearly cancel in Fe-Rh than in iron. This presumably reflects the differences in covalent bonding between the alloy and the metal. The sign of the internal field in Fe-Rh has not yet been measured.

[5] E. F. Bertaut *et al.*, *J. Appl. Phys. Suppl.* **33**, 1123 (1962).

[6] L. D. Roberts and J. O. Thomson, *Phys. Rev.* **129**, 664 (1963).

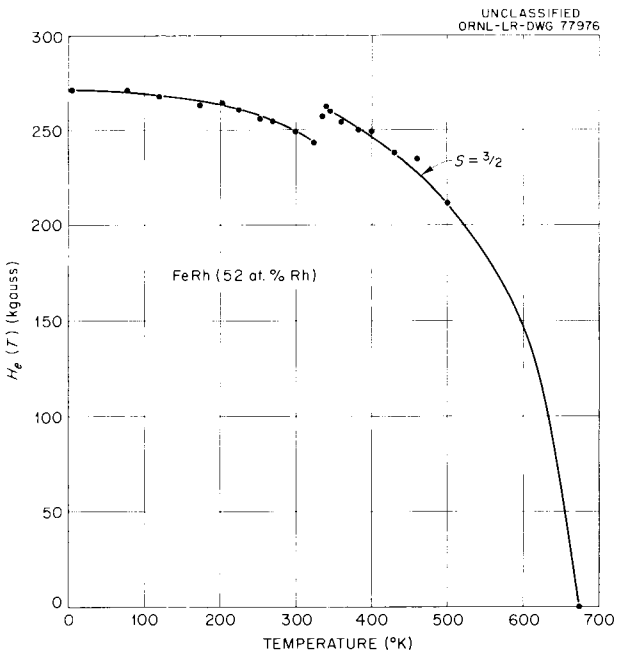

Fig. 1. Measurements of the Hyperfine Field as a Function of Temperature Made Using an Iron-Rhodium Sample Contoining 52 at. % Rhodium. The absolute value of the internal magnetic field was obtained by comparing the hyperfine splitting of Fe-Rh with pure iron at 300°K. The points below 325°K are in the antiferromagnetic region, and those above 350°K are in the ferromagnetic phase. A Brillouin function for $S = 3/2$ has been fitted to the data in the ferromagnetic region.

To proceed further, it is necessary to make a postulate about whether the details of this covalent bonding are appreciably dependent on the temperature between 0°K and the Curie point. In other words, compared to our measurement error, determine if the constant A (Eq. 1) is appreciably dependent on the temperature. In that our measurements of $\langle |S_z| \rangle$ have a relative precision of about 0.3 to 0.4%, with an absolute error of about 1%, and considering the fact that H_e arises as a difference between contributions from the several s shells, this may well be possible. For example, the thermal expansion of the alloy will affect the $4s$ state density at the nucleus, possibly, by somewhat less than 1% between 0°K and T_c. In the absence of information, however, we assume that A is independent of the temperature and that all the variation of H_e with temperature comes from $\langle |S_z| \rangle$.

Bertaut *et al.*, as mentioned earlier, have given the spin at the iron site as 1.52 ± 0.07 and that at the rhodium site as 0.31 ± 0.07 in the ferromagnetic state. In the antiferromagnetic state they give

$$S_{Fe}^2 + S_{Rh}^2 = 2.72 \ . \qquad (2)$$

Neither the error nor the temperature at which the latter result was obtained was given. Assuming that the temperature was at a value just below the antiferromagnetic-ferromagnetic transition, it is possible to obtain estimates of S_{Fe} and S_{Rh} from Eq. (2) and our results (Fig. 2). Just above this transition in the ferromagnetic state, $|H_e| = 261 \pm 2$ kilogauss; just below the transition, $|H_e| = 243 \pm 2$ kilogauss. With the assumption of Eq. (1) and also that A is constant, we find that $\langle |S_z| \rangle_F / \langle |S_z| \rangle_A = 1.074$. Then, from Bertaut's result the expectation value of the iron spin in

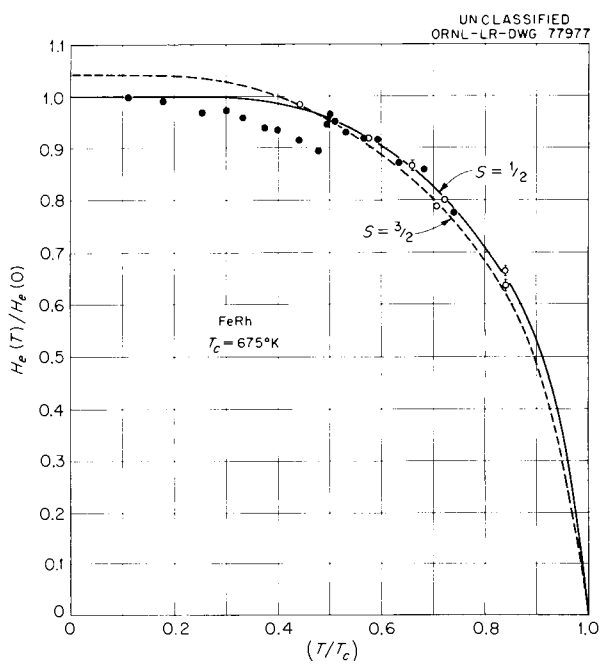

Fig. 2. The Data of Fig. 1 Are Plotted Here on a Reduced Scale; Circles and Some Additional Data (Crosses) Using an Iron-Rhodium Sample with a Lower Transition Temperature Are Included. The Brillouin function for $S = 1/2$ fits the points in the ferromagnetic region well and gives the same saturation value as that observed in the antiferromagnetic region. The function for $S = 3/2$ also fits the data but requires a higher saturation moment than is observed in the antiferromagnetic state. The Curie temperature is 675°K.

the antiferromagnetic state becomes 1.52/1.074 = 1.416. This yields $S_{Rh} = 0.85 \pm 0.1$, a value very much larger than that found for the spin in the ferromagnetic state. This change of spin at the rhodium site seems remarkably large; such a large value would certainly play an important role in the free-energy change at the transition.

In Fig. 2 the results of Fig. 1 are plotted on reduced scales. Included in this graph are several points from another Fe-Rh sample which remained ferromagnetic to a somewhat lower temperature.

Brillouin functions for spin $\frac{1}{2}$ and spin $\frac{3}{2}$ have been passed through the data in the ferromagnetic region. It is interesting to note that $B(S = \frac{1}{2})$ fits the data well and passes through 1.00 at $T = 0°K$. The curve $B(S = \frac{3}{2})$ fits the data but goes to a value of 1.04 at 0°K. From the results of Bertaut *et al.*, we expect that the actual spin is close to $\frac{3}{2}$. On the other hand, this leads to the somewhat surprising result that, extrapolated, the saturation moment of the ferromagnetic state may be of the order of 4% higher than this moment as observed for the antiferromagnetic state. The difficulty may well be due to the use of the Brillouin function for this extrapolation.

Fe_2O_3 Measurements

Preliminary results for H_e as a function of temperature have been obtained for Fe_2O_3. These results, along with those for the antiferromagnetic region of Fe-Rh, are shown in Fig. 3. The function which has been fitted to the data is $H_e(T) = H_e(0)(1 - aT^n)$. Since the Néel temperature of the antiferromagnetic phase of Fe-Rh is not known, the results are plotted against actual, rather than reduced, temperatures. Thus, it is a coincidence that $H_e(T)/H_e(0)$ for the two materials falls so nearly on the same curve. Since T_N for Fe-Rh is probably less than the observed Curie temperature (675°K) and T_N for Fe_2O_3 is 975°K, there is no reason to assume that the coefficient a for the two cases should be equal. In fact, using the data of Fig. 3, we obtain $n = 2.45 \pm 0.15$, $a = 7.32 \times 10^{-8}$ for Fe-Rh and $n = 2.65 \pm 0.15$, $a = 1.78 \times 10^{-8}$ for Fe_2O_3. It is of interest that the temperature dependence of H_e for the two substances, one an oxide and the other a metal, should be so nearly the same. The value for n given by the spin-wave theory for the low-temperature region is 3. Our values are smaller than this. Our measurements perhaps extend to a higher temperature range than that over which first-order spin-wave theory may be expected to apply. It seems interesting, nevertheless, that in this higher temperature region the effective value for n which describes our measurements is smaller, rather than larger, than 3.

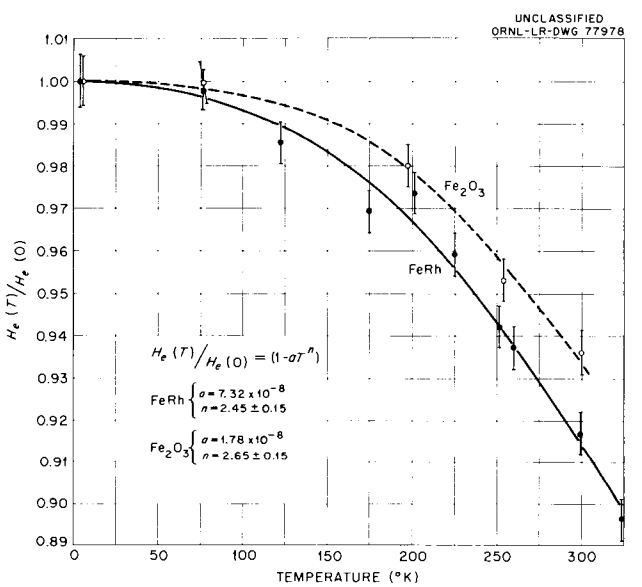

Fig. 3. Composite of Data for Iron-Rhodium in the Antiferromagnetic Region and That for Fe_2O_3. The Fe_2O_3 is antiferromagnetic at all temperatures up to the Néel temperature at 975°K. The data are fitted with the function $H_e(T)/H_e(0) = (1 - aT^n)$.

CORRELATION OF THE MÖSSBAUER ISOMER SHIFT WITH THE RESIDUAL ELECTRICAL RESISTANCE FOR GOLD ALLOYS

L. D. Roberts R. L. Becker F. E. Obenshain J. O. Thomson[1]

The s-state electron charge of an atom penetrates the nucleus to a slight degree and thus slightly modifies the energy of a nuclear state.[2] By taking the electron s-state wave function $\psi_s(r)$ associated with a point nucleus and the nuclear wave function ϕ for a bare nucleus as the unperturbed states, one may estimate the Coulomb contribution to this energy shift using first-order perturbation theory as $D|\psi_s(0)|^2 \langle\phi|r^{2\rho}|\phi\rangle$. Here D is a known constant, $\rho = \sqrt{1 - \alpha^2 Z^2}$, α is the fine structure constant, and Z is the nuclear charge.

If the nuclear size changes during a gamma-ray transition, this penetration of the s-electron charge will modify the gamma-ray energy by $D|\psi_s(0)|^2 [\langle r^{2\rho}\rangle_e - \langle r^{2\rho}\rangle_g]$, where g and e refer to the ground and excited nuclear states. By the use of the Mössbauer method, one may study the resonant emission and absorption of a gamma ray under the circumstance that $|\psi_s(0)|^2$ is different at the gamma-ray source and absorber nuclei. There will then be an energy ΔE, the isomer shift, which must be added to the emitted gamma ray to bring about resonance with the absorber nuclei.

$$\Delta E = D[|\psi_{s,a}(0)|^2 - |\psi_{s,s}(0)|^2] \times [\langle r^{2\rho}\rangle_e - \langle r^{2\rho}\rangle_g] \ . \quad (1)$$

Here $|\psi_{s,a}(0)|^2$ and $|\psi_{s,s}(0)|^2$ describe the s-state densities at the absorber and source nuclei. Instead of the isomer shift ΔE relative to the gamma-ray source, it is convenient to consider the shift relative to pure gold,

$$\Delta E_I = (\Delta E_{\text{alloy}} - \Delta E_{\text{pure gold}}) \propto [|\psi_{s,\text{alloy}}(0)|^2 - |\psi_{s,\text{Au}}(0)|^2] \ . \quad (2)$$

Measurements of ΔE_I may then yield information both about the nuclear size change between ground and excited states and about the s-state density in solids. In the theory of dilute alloys, for example, the s-state density enters in an important way.

In the following we present measurements of ΔE_I for the 77-kev resonant gamma ray of Au^{197}, where the gold atom has been placed in a variety of alloy environments. The gamma-ray source was prepared by neutron activation of 50-mg samples of Pt^{196} metal in the Oak Ridge Research Reactor to form some Pt^{197}. Following a beta decay to Au^{197}, this source gives the desired 77-kev gamma ray. The absorbers were prepared either from pure gold or from arc-melted gold alloys. All measurements were made at 4.2°K. Details of the equipment and treatment of the data have been described previously.[3]

Studies of copper, silver, and gold and of alloys of these elements with nickel, palladium, and platinum have played a prominent role in the development of the present theory of metals. For example, silver and gold have the same valence and virtually the same atomic size. These facts have suggested a conceptual simplicity in the theory of the alloys of these elements, and a number of experimental and theoretical studies of this system have been made. In particular, Mott[4] has suggested that, in dilute alloys of gold in silver, gold with the higher Z and correspondingly larger ionization energy should present a deeper attractive well than the silver for the valence-band electron charge. This would suggest in a qualitative way that a gold atom in silver would be negatively charged compared to a gold atom in gold. On the other hand, specific heat and magnetic measurements on Au-Pt and Ag-Pd alloy systems, within the context of the

[1]Consultant from the University of Tennessee.

[2]O. C. Kistner and A. W. Sunyar, *Phys. Rev. Letters* **4**, 412 (1960).

[3]L. D. Roberts and J. O. Thomson, *Phys. Rev.* **129**, 664 (1963).

[4]N. F. Mott, *Proc. Cambridge Phil. Soc.* **32**, 281 (1936).

rigid band model, indicate a filling of the palladium or platinum d band with increasing gold or silver content.[5-7] The usual picture here is that s-state charge is transferred in some degree from the s shell of the gold to the d shell of the platinum, for example. In that the d shell of the gold presumably remains full and little modified in this process, one might expect the gold in a dilute alloy of gold in palladium or platinum to be positively charged relative to pure gold. The presumed stability of the gold d shell makes it possible to study these variations of $|\psi_s(r)|^2$ in alloys through the isomer shift ΔE_I, which gives information about the value of this wave function at the nucleus.

In terms of the above simple discussion, one might expect ΔE_I to be of one sign for the Ag-Au alloy system, of the opposite sign for the Pd-Au system, and in the latter case to show a strong correlation with the magnetic properties of the alloy, that is, reflecting the filling of the palladium d shell. These expectations are not in fact borne out. It is found that ΔE_I is positive for all the systems investigated so far and that ΔE_I as a function of atomic percent of gold does not show a sharp response to the filling of the d shell in the transition-metal alloys studied so far. It nevertheless appears to be possible to understand the basic features of our measurements in terms of a theory of dilute alloys.

Experimental Results

The results of our isomer-shift measurements are summarized in Figs. 1–3. Figure 1, giving the isomer shift for Ni-Au alloys as a function of atomic percent of gold, was presented previously[3] but is reproduced here for reference. The isomer shift is seen to be nearly linear with concentration. On the other hand, at 60 at. % gold, the magnetic properties of the alloy change abruptly. From this it has been inferred that on the addition of gold the rate of increase in the number of electrons in the s band increases suddenly at 60 at. % concentration. Thus it is an interesting question how the above observed rate of change of s-state charge density at a gold nucleus can vary more smoothly than the rate of filling of the s band.

Figure 2 gives the results of isomer-shift measurements for the three alloy systems Pd-Au, Ag-Au, and Cu-Au.[8,9] As for the Ni-Au system described above, ΔE_I (Pd-Au) as a function of atomic percent of gold is remarkably linear. Once

[5]F. E. Hoare, J. C. Matthews, and J. C. Walling, *Proc. Roy. Soc.* **A216**, 502 (1953).

[6]F. E. Hoare and B. Yates, *Proc. Roy. Soc.* **A240**, 42 (1957).

[7]D. W. Budworth, F. E. Hoare, and J. Preston, *Proc. Roy. Soc.* **A257**, 250 (1960).

[8]L. D. Roberts, R. L. Becker, and J. O. Thomson, *Bull. Am. Phys. Soc. II* **8**, 42 (1963).

[9]J. O. Thomson and L. D. Roberts, *Bull. Am. Phys. Soc. II* **8**, 42 (1963).

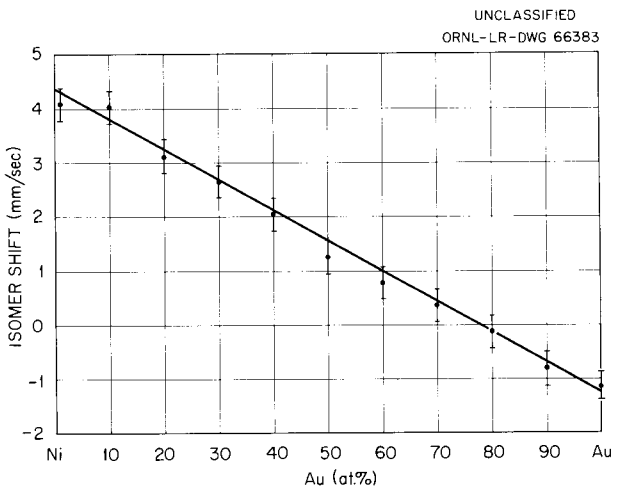

Fig. 1. Isomer Shift for Ni-Au Alloys as a Function of Atomic Percent of Gold.

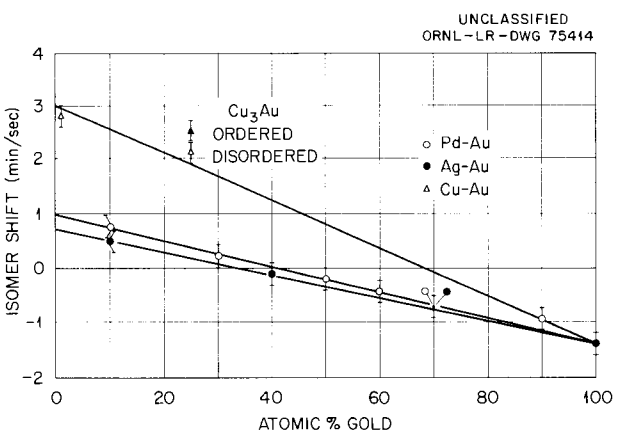

Fig. 2. Isomer Shift as a Function of Composition for Alloys of Gold with Palladium, Silver, and Copper.

more ΔE_I does not seem to respond in any sharp or discontinuous way to the filling of the *d* shell.

We note that ΔE_I for the Ag-Au system is quite linear in the range studied.

Our results for the Cu-Au system are relatively incomplete, and the straight line drawn for this system (Fig. 2) is somewhat hypothetical. There is an indication of a small dependence of ΔE_I (Cu_3Au) on the order-disorder transition, and it would be useful to investigate this further. As will be seen, however, these available results will be sufficient for our immediate purpose.

In Fig. 3, results are given for the Cu-Ni system containing 1 at. % gold.[9] Here again the intent was to measure the effect of the *d*-band filling on ΔE_I and once again this dependence is not strongly evident in the experimental results. The isomer shift is large and positive but only moderately dependent on Cu-Ni composition.

Broadly speaking, there are two kinds of measurements here. One has to do with the observation of the isomer shift of gold, for example, in a given alloy as a function of composition. The other type of measurement has to do with the relative values of the isomer shift when a given Mössbauer atom is in a variety of host materials. An approximate theoretical interpretation of the latter type of measurement for dilute alloys is given below.

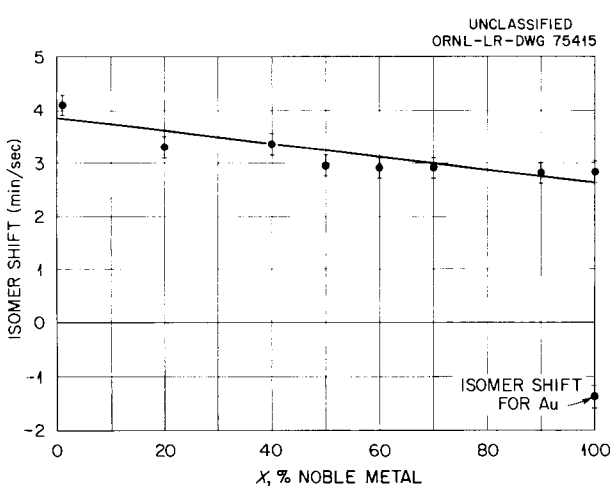

Fig. 3. Isomer Shift for 1 at. % Gold in $Au_{0.01}$-$Cu_{x-0.01}$-Ni_{1-x} as a Function of *x*, the Atomic Percent of Copper.

Theoretical Discussion

In the above description of our experimental results, we have discussed the behavior of ΔE_I for both concentrated and dilute gold alloys. In the following paragraphs, we give a theoretical discussion of the dilute-alloy results.

When an impurity atom is dissolved in a host metal, it will, in general, have an affinity for electrons different from that of the host, and this will result in a rearrangement or displacement of electron charge. It is this displacement of charge which produces the isomer shift we observe. Other consequences of this charge displacement appear, for example, in the Knight shifts of the components of the alloy,[10-12] in the heat of formation of the alloys,[13] and in the residual electrical resistance of the alloy due to the impurity.[4,14-16] Thus, there will be a correlation between all these quantities through the electron wave function associated with this charge displacement.

We present a correlation through a simple model between our measured isomer shifts of the gold gamma-ray energy for several dilute gold alloys and the residual electrical resistance per atomic percent, $\Delta\rho/c$, introduced by the gold in these alloys. The procedures used follow the methods of Friedel[15] in introducing physically reasonable approximations in a self-consistent way.

Following the work of Friedel,[15] Daniel,[12] Blatt,[16] and Kohn and Vosko,[17] we assume that the interaction of the impurity atom with the electrons of the conduction band (the *s* band) of the host metal may be described by associating a potential well with the impurity atom. This well will have a transport cross section (σ_{tr}) for the

[10] T. J. Rowland, *Phys. Rev.* **119**, 900 (1960); **125**, 459 (1962).

[11] A. Blandin and E. Daniel, *J. Phys. Chem. Solids* **10**, 126 (1959).

[12] E. Daniel, *J. Phys. Chem. Solids* **10**, 174 (1959).

[13] K. Huang, *Proc. Phys. Soc.* **60**, 161 (1948).

[14] J. O. Linde, *Ann. Physik* **15**, 219 (1932).

[15] J. Friedel, *Advan. Phys.* **3**, 446 (1954); *Nuovo Cimento* (suppl) **7**, 287 (1958); *Phil. Mag.* **43**, 153 (1952).

[16] F. J. Blatt, *Phys. Rev.* **108**, 285 (1957).

[17] W. Kohn and S. H. Vosko, *Phys. Rev.* **119**, 912 (1960).

conduction electrons and will thus introduce a residual electrical resistance ($\Delta\rho/c$), where c is the concentration of the impurity atoms in atomic percent. From a measurement of $\Delta\rho/c$, σ_{tr} may be calculated. Then from σ_{tr} and the requirement that the impurity atom must be completely screened, in a conducting alloy, the properties of the well may be estimated. From this well, one may obtain an estimate of $|\psi_{s,a}(0)|^2$, the desired quantity.

In a recent paper, Daniel[12] has given a calculation of the ratio of the Knight shift of an impurity to the Knight shift of the host atoms in a dilute alloy. We follow Daniel's procedure closely. There are, however, two modifications of Daniel's treatment in our discussion which reflect the somewhat different natures of the Knight shift and of the isomer shift of the Mössbauer effect. When only effects coming from the s band are considered, the Knight shift is approximately proportional to the Pauli magnetic susceptibility of the conduction electrons. Only the s-state charge density due to electrons at the Fermi level plays a role. The isomer shift, on the other hand, involves an integral over the entire band. The other modification we refer to is of a less-essential character. In the discussion of the Knight shift of the nuclear resonance of an impurity atom in an alloy, it is sometimes convenient to present the experimental results as a ratio of the Knight shift of the impurity to that of the host. In measurements of the Mössbauer isomer shift, on the other hand, one takes a difference between two resonant gamma-ray energies, corresponding in our case to two different gold environments. This is described by ΔE_I of Eq. (2). As in the earlier discussion, it will be convenient to take these environments as the gold alloy of interest and as pure gold.

We consider the substitution of an impurity atom B for an atom A of the host metal. The Wigner-Seitz approximation of replacing each atomic cell by a sphere of equal volume will be made. At the bottom of the conduction band in the pure host metal, there will be a wave function $U_A(r)$, which is a solution to the Schroedinger equation,

$$\nabla^2 U_A + 2(E_A - V_A)U_A = 0 , \quad r \leqq r_A ,$$
$$dU_A/dr|_{r=r_A} = 0 , \quad r \leqq r_A , \tag{3}$$

for the potential V_A of the lattice and corresponding to an energy E_A, where atomic units are used. For pure metal B and at the bottom of the band, one would similarly have the wave equation,

$$\nabla^2 U_B + 2(E_B - V_B)U_B = 0 , \quad r \leqq r_B ,$$
$$dU_B/dr|_{r=r_B} = 0 , \quad r \leqq r_B . \tag{4a}$$

In the alloy the radius R of the impurity sphere, containing, for example, a gold atom, will differ somewhat from that in pure gold, r_B. The potential within the impurity sphere $V_{alloy} = V_B + V_S$, ($r \leqq R$), will also differ from that in pure metal B, V_B, by a screening potential V_S. It will, however, be assumed that the potential in the alloy outside the impurity sphere is the same as that in the pure host metal $V_{alloy} = V_A$, ($r > R$). This neglects the part of the screening potential V_S extending beyond the impurity cell.

The wave function ψ_k for an s-band electron in the alloy with energy E_k will be written as

$$\psi_k(r) = \phi_k(r)U(r) ,$$

where

$$U(r) = \begin{cases} U'_B(r) , & r \leqq R ; \\ U_A(r) , & r > R . \end{cases}$$

Here U'_B satisfies the same differential equation and boundary conditions as U_B, except for a possible slight change in the radius of the Wigner-Seitz sphere:

$$\nabla^2 U'_B + 2(E'_B - V_B)U'_B = 0 , \quad r \leqq R ,$$
$$dU_B/dr|_{r=R} = 0 , \quad r \leqq R . \tag{4b}$$

The energy eigenvalue E'_B will differ only slightly from E_B. The Schroedinger equation, $\nabla^2\psi_k + 2(E_k - V_{alloy})\psi_k = 0$, then becomes

$$[\nabla^2\phi_k + 2(E_k - E'_B - V_S)\phi_k]U'_B + 2\vec{\nabla}\phi_k \cdot \vec{\nabla}U'_B = 0 , \quad r \leqq R , \tag{5}$$

and

$$[\nabla^2\phi_k + 2(E_k - E_A)\phi_k]U_A + 2\vec{\nabla}\phi_k \cdot \vec{\nabla}U_A = 0 , \quad r > R . \quad (6)$$

Friedel[15] and Daniel[12] have argued that, in the various regions of the alloy, either $\vec{\nabla}\phi_k$ or $\vec{\nabla}U$ or both will be small and that the term $\vec{\nabla}\phi_k \cdot \vec{\nabla}U$ may be neglected. In the case of a pure metal this approximation leads to approximate Bloch waves of the form $\psi_k = U_0 e^{ik \cdot r}$. Equations (5) and (6) are reduced to the simple form,

$$\nabla^2\phi_k + 2[E_k - E_A - V(r)]\,\phi_k = 0 , \quad (7)$$

with

$$V(r) = -E_A + E_B' + V_S(r) \qquad \text{for } r \leq R$$

and

$$V = 0 \qquad \text{for } r > R .$$

Equation (7) is mathematically the same as the equation for the scattering of a plane wave with wave number $k = \sqrt{2(E_k - E_A)}$ from the potential $V(r)$. As usual, one expands ϕ_k in partial waves. The asymptotic form of ϕ_k is then specified by phase shifts $\delta_l(k)$. Very little direct information is known about the perturbing potential $V(r)$, but information is available, as described below, about the phase shifts produced by it for $k = k_F$, the Fermi wave number. In the absence of knowledge of the radial dependence of $V(r)$, we shall approximate $V(r)$, when acting on the lth partial wave, by a square well of depth V_l chosen to give the required value of $\delta_l(k_F)$. Since $k_F^2/2$ is a low energy, the effective range expansion of the phase shifts in powers of k^2 may be expected to converge rapidly. Then the square well V_l will give nearly the same phase shifts $\delta_l(k)$ for k between 0 and k_F as $V(r)$.

For the isomer shift one is interested in knowing the value of the s wave at the origin. Knowing the phase shift $\delta_0(k)$ to good approximation, one needs to know how the s wave is continued back to the origin. The square well potential will give an s-wave function which might differ considerably at the origin from that obtained with the potential $V(r)$. However, a large part of $V(r)$ is the energy difference $E_B' - E_A$. Furthermore after integrating over k, it is to be expected that the square well result will more nearly approximate the result which uses $V(r)$.

A square well approximation has been used previously by Mott,[4] by Friedel and collaborators, and by Blatt. The present approximation is more general in that the depths V_l may differ for different l's. Daniel's deviation[12] leads to a scattering potential which has no radial dependence, that is, a single square well.

Although $U_A(R)$ will not in general precisely equal $U_B'(R)$, nevertheless, because

$$\left.\frac{dU_A}{dr}\right]_R = 0 = \left.\frac{dU_B'}{dr}\right|_R ,$$

the logarithmic derivative of ϕ will be continuous.[12] Thus, in a partial wave description of the scattering process, the phase shifts introduced by the potential well will be the same as those for the scattering of a free electron of the same energy and satisfying the usual continuity conditions at $r = R$. However, there will be a discontinuity in ϕ at R required to compensate the discontinuity in U.

We now estimate the charge polarization using the square well (Fig. 4). The radial wave equations corresponding to Eq. (7) are

$$\frac{d^2}{dr^2}(r\phi) + k^2(r\phi) = 0 \qquad \text{for } r > R ,$$
$$\frac{d^2}{dr^2}(r\phi) + K^2(r\phi) = 0 \qquad \text{for } r < R . \quad (8)$$

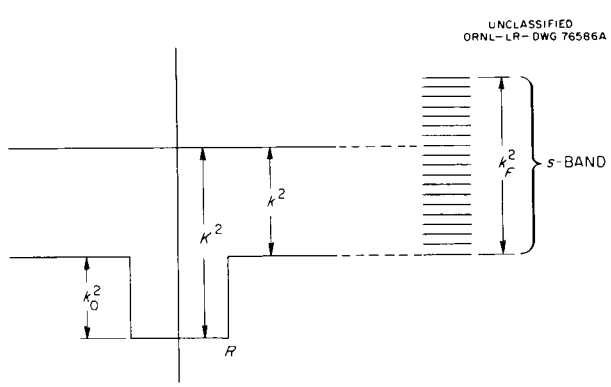

Fig. 4. Potential Well Parameters Used.

Here, $k_0^2 = K^2 - k^2$. The solution outside of the well is

$$\phi_k = \sin(kr + \delta_0)/kr \ . \tag{9}$$

The solution inside the well may be written conveniently in the form

$$\phi_k = [U_A(R)/U_B'(R)]B \sin Kr/kr \ . \tag{10}$$

The continuity of the logarithmic derivative at $r = R$ yields the equation

$$K \tan(kR + \delta_0) = k \tan KR \ . \tag{11}$$

The continuity of $\phi_k U$ at R gives

$$\frac{B \sin KR}{kR} = \frac{\sin(kR + \delta_0)}{kR}. \tag{12}$$

To define the normalization, we consider first the approximate Bloch wave function $\psi_{Bk}(r)$ for the pure metal B.

$$\psi_{Bk}(r) = U_B(r) e^{ik\cdot r}/\sqrt{\Omega_B} \ . \tag{13}$$

Here, as before, $U_B(r)$ is the wave function within the Wigner-Seitz cell at the bottom of the band, that is, at $k = 0$, and Ω_B is the volume of the metal sample. The average value of $|U_B(r)|^2$ is taken as unity over the volume $v_B = (4\pi/3)r_B^3$ of the W-S cell,

$$v_B^{-1} \int_{v_B} |U_B(r)|^2 \, d\tau = 1 \ . \tag{14}$$

Then

$$\int_{v_B} |\psi_{Bk}(r)|^2 \, d\tau = \frac{v_B}{\Omega_B} , \tag{15}$$

and

$$\int_{\Omega_B} |\psi_{Bk}(r)|^2 \, d\tau = 1 \ . \tag{16}$$

This normalization is such that one electron of each spin projection is associated with each k state. The charge at $\vec{r}$, $\rho_{Bk}(\vec{r})$, associated with each k state and with a given spin projection is then

$$\rho_{Bk}(r) = |U_B(r)|^2/\Omega_B \ . \tag{17}$$

In the model being used, with $E_{Bk} = E_B + (k^2/2)$, the density of states $n(k)$ is proportional to k^2. Summing over spin projection and over all k states up to the Fermi level at k_F, the total charge density at $\vec{r}$, $\rho_B(\vec{r})$, becomes

$$\rho_B(\vec{r}) = |U_B(r)|^2 N_B/\Omega_B \ , \tag{18}$$

where N_B is the number of filled k states,

$$N_B = 2 \frac{\Omega_B}{(2\pi)^3} 4\pi \int_0^{k_F} k^2 dk$$

$$= \frac{\Omega_B}{3\pi^2} k_F^3 \ . \tag{19}$$

By virtue of Eq. (14) the average s-electron density in a pure metal is then N/Ω.

We shall wish to consider cases where the s band is only partially filled. If we take the number of s electrons per atom to be η, then the average s-electron density will be

$$N/\Omega = \eta/v = 3\eta/4\pi R^3 \ ,$$

and $k_F \propto \eta^{1/3}$.

In Eq. (9), ϕ_k was given the same normalization as the s-wave part of the plane wave $e^{ik\cdot r}$. In the alloy the wave function $\psi_{Bk}'(r)$, normalized in the same way as $\psi_{Bk}(r)$ for the pure metal [Eq. (13)], is, therefore, for $r \leq R$,

$$\psi_{Bk}'(r) = U_B'(r) \, \phi_k(r)/\sqrt{\Omega'} \tag{20}$$

$$= U_B'(r) \frac{U_A(R)B}{U_B'(R)} \frac{\sin Kr}{kr\sqrt{\Omega'}}. \tag{21}$$

Here, as mentioned earlier, $U_B'(r)$ may differ somewhat from $U_B(r)$. The volume of the alloy sample is Ω'. The charge density $\rho_{Bk}'(0)$ at the origin, that is, at the nucleus of an impurity atom B in the alloy, corresponding to a given k state is then

$$\rho_{Bk}'(0) = |U_B'(0)|^2 \, |\phi_k(0)|^2/\Omega' \tag{22}$$

$$= \frac{|U_B(0)|^2}{\Omega'} \left| \frac{U_A(R)}{U_B'(R)} \right|^2 P(kR) \ , \tag{23}$$

where $P(kR)$ is the "charge polarization" factor defined by Daniel,[12]

$$P(kR) = \left(\frac{B\sqrt{k_0^2 + k^2}\,R}{kR}\right)^2$$

$$= \left[1 - \frac{k_0^2 R^2}{(k_0^2 + k^2)R^2}\sin^2\left(\sqrt{k_0^2 + k^2}\,R\right)\right]^{-1} . \quad (24)$$

The latter equality follows from Eqs. (11) and (12). That k_0 is independent of k is implicit in the assumptions leading to Eq. (8) for ϕ. Summing over the k states up to the Fermi level of the alloy with wave number k_F', one obtains for the electronic charge density at the nucleus

$$\rho_B'(0) = \frac{|U_B'(0)|^2}{\Omega'}\left|\frac{U_A(R)}{U_B'(R)}\right|^2 \times \frac{2\Omega'}{8\pi^3}\frac{4\pi}{R^3}\int_0^{k_F'R} P(w)w^2\,dw , \quad (25)$$

the term $\rho_B'(0)$ may be written as

$$\rho_B'(0) = |U_B'(0)|^2\left|\frac{U_A(R)}{U_B(R)}\right|^2 \times \frac{N'}{\Omega'}\left(\frac{k_{FA}}{k_F'}\right)^3\left(\frac{r_A}{R}\right)^3\frac{\bar{P}(k_F'R)}{\eta} . \quad (28)$$

Referring back to Eq. (2), the isomer shift ΔE_I is seen to be proportional to the difference between the charge densities $\rho_B'(0) = |\psi_{s,\mathrm{alloy}}(0)|^2$ and $\rho_B(0) = |\psi_{s,\mathrm{Au}}(0)|^2$, that is,

$$\Delta E_I = \alpha[\rho_B'(0) - \rho_B(0)] , \quad (29)$$

where α is a proportionality constant. From Eqs. (18) and (25),

$$\Delta E_I = \alpha\left(\frac{N_B}{\Omega_B}\right)|U_B(0)|^2\left[\frac{N'/\Omega'}{N_B/\Omega_B}\frac{|U_B'(0)|^2}{|U_B(0)|^2}\frac{|U_A(R)|^2}{|U_B'(R)|^2}\left(\frac{k_{FA}}{k_F'}\right)^3\left(\frac{r_A}{R}\right)^3\frac{\bar{P}(k_F'R)}{\eta} - 1\right] . \quad (30)$$

where $w = kR$. Corresponding to Eq. (19), the number of s electrons (N') in the alloy sample is

$$N' = \frac{2\Omega'}{8\pi^3}\frac{4\pi}{3}k_F'^3 .$$

Letting r_A and k_{FA} be the radius of the Wigner-Seitz cell and the Fermi wave number of the pure host metal, one has

$$k_{FA}r_A = \left(\frac{9\pi}{4}\right)^{1/3}\eta^{1/3} = 1.92\,\eta^{1/3} .$$

Thus,

$$N' = \frac{2\Omega'}{8\pi^3}\,4\pi\left(\frac{k_F'}{k_{FA}}\right)^3\frac{\eta}{r_A^3}\frac{(1.92)^3}{3} . \quad (26)$$

In terms of the convenient quantity

$$\bar{P}(k_F'R) = \frac{\int_0^{k_F'R} P(w)w^2\,dw}{(1.92)^3/3} , \quad (27)$$

At infinite dilution, $N' = N_A$, $\Omega' = \Omega_A$, and $k_F' = k_{FA}$. Then, if the impurity metal B has one s electron per atom,

$$\left(\frac{r_A}{R}\right)^3\frac{N'}{\Omega'\eta}\frac{\Omega_B}{N_B} = \left(\frac{r_B}{R}\right)^3 ,$$

where r_A and r_B are the radii of the Wigner-Seitz cells. Detailed information about the ratios $|U_A(R)|^2/|U_B'(R)|^2$ and $|U_B'(0)|^2/|U_B(0)|^2$ is not available. In favorable cases these ratios may be close to 1 and we take them equal to unity. Equation (30) then takes the form,

$$\Delta E_I = \alpha\left(\frac{N_B}{\Omega_B}\right)|U_B(0)|^2\left[\left(\frac{r_B}{R}\right)^3\bar{P}(k_F'R) - 1\right] . \quad (31)$$

Here the ratio $(r_B/R)^3$ is also close to 1, but, because estimates of r_B and R enter the calculation at several points, this factor is retained.

It is Eq. (31) which we shall wish to compare with experimental isomer-shift measurements. To

do this, one must obtain an estimate of the parameters of the potential well and calculate $\bar{P}(k_F' R)$, Eq. (28). Referring to Eq. (24) and to Fig. 4, it is seen that $P(k_F R)$ is a function of the well depth $k_0^2/2$, of the energy of the electron being scattered ($k^2/2$), and of the impurity radius R.

In the following we obtain an estimate of k_0^2, using measured values of the residual electrical resistance per atomic percent, $\Delta\rho/c$, and the Friedel sum rule.[15] The excess ionic charge which enters the latter sum rule is estimated by a method first employed by Blatt.[16] In this fashion an effective potential or pseudopotential for the scattering of s waves at the Fermi surface is obtained.

Friedel and co-workers have been very successful in accounting for $\Delta\rho/c$ using an effective potential well together with a partial wave treatment for the scattering of the conduction electrons. Here we have

$$\frac{\Delta\rho}{c} = 9.00 \times 10^{17} \frac{\hbar k_F}{e^2} \sigma_{tr} . \qquad (32)$$

Here $\Delta\rho$ is given in microhm-cm, c is the impurity concentration in atomic percent, e is the electron charge in esu, $\hbar$ is Planck's constant divided by 2π, and σ_{tr} is the electron transport cross section associated with the potential well. Huang[13] has given the result,

$$\sigma_{tr} = \frac{4\pi}{k_F^2} \sum_{l=0}^{\infty} (l+1) \sin^2 [\delta_l(k_F) - \delta_{l+1}(k_F)] , \qquad (33)$$

where at infinite dilution $k_F' = k_F$. Then, since $k_{FA} r_A = 1.92\, \eta^{1/3}$, we may write

$$\sum_{l=0}^{\infty} (l+1) \sin^2 [\delta_l(k_F) - \delta_{l+1}(k_F)] = 0.703\, \eta^{1/3}\, \Delta\rho/r_A c . \qquad (34)$$

The excess ionic charge averaged over the volume of the impurity cell will be denoted by z. This charge z is assumed to be screened by the s band. As Friedel[15] has shown, screening may be guaranteed through a sum rule on the phase shifts at the Fermi level,

$$z = \frac{2}{\pi} \sum_l (2l+1)\, \delta_l(k_F) . \qquad (35)$$

There will be a contribution to z from the valence difference between the impurity atom and the host. For our present purpose we define the valence of the host as η, the number of s electrons per atom. For metals such as copper, silver, or gold, η is expected to have a value of 1. For nickel, palladium, or platinum, η is thought to have a value in the vicinity of 0.6. As Blatt[16] has shown, there will be an additional contribution to z from atomic size effects. For example, the atomic size of the copper atom is smaller, and thus the average ionic charge density in copper metal is higher, than that for gold. Then if a gold impurity atom replaces a copper atom in copper metal, the average nuclear charge within the impurity will be less than that which occupied this volume in the pure copper metal. If η_B is the valence of the impurity and η_A is that of the host, Blatt's procedure would give the result,

$$z = \eta_B - \eta_A \left(1 + \frac{\delta v}{v}\right) , \qquad (36)$$

where $v = \frac{4}{3}\pi r_A^3$ refers to the volume per host atom in atomic units. Then

$$\delta v = \frac{4}{3}\pi (R^3 - r_A^3) . \qquad (37)$$

Equations (33) to (35) then give us two conditions on the phase shifts. Calculations of $\Delta\rho/c$ have shown that for small valence differences, phase shifts beyond the first two are relatively small.[15,16] We assume that they may be neglected. Following the procedures of Kohn and Vosko,[17] the above two conditions may then be used to obtain an estimate of δ_0 and δ_1. There is still an ambiguity of sign in that Eq. (33) yields only a value for $\sin^2(\delta_0 - \delta_1)$. We take the positive sign for the square root $+|\sqrt{0.703\, \Delta\rho/r_A c}|$, in that this makes $\delta_0 > 0$, that is, the well is attractive for s waves. This is in accord with Mott's discussion of Au-Ag alloys mentioned earlier.[4]

With

$$w_F = k_{FA} R = 1.92\, \eta_A^{1/3} R/r_A ,$$

and

$$v_F = K_F R = +\sqrt{k_{FA}^2 + k_0^2}\, R , \qquad (38)$$

Eq. (11) may be written as

$$v_F \cot v_F = \frac{w_F[\cot w_F - \tan \delta_0(k_F)]}{1 + \cot w_F \tan \delta_0(k_F)} . \qquad (39)$$

By the use of $\delta_0(k_F)$ as estimated above and Eq. (39), we obtain a value for v_F and thus for the well depth $k_0^2/2$. The integration indicated in Eq. (28) may then be performed. The upper limit of the integral at the Fermi surface in the alloy at $w_F = k_{FA} R$ will, of course, reflect the filling of the s band, that is, the valence η_A. This valence also enters the calculation both through the charge to be screened (z) in Eq. (36) and through the estimate of the well depth in Eq. (39).

Figure 5 gives a graph of the integral Eq. (28) as a function of the well-depth parameter $k_0 R$ and of the number of s electrons per atom, η_A. It may be seen from this graph that, if the well is sufficiently deep, or attractive, for s waves, a polarization $\bar{P}(k_{FA} R) > 1$ may be obtained even if the s band is only partially filled, for example, with $\eta_A \sim 0.6$.

Speaking in a qualitative way, one may now see how the charge polarization factor removes the seeming contradiction mentioned earlier relative to the signs of the isomer shifts of gold in the Au-Ag and Au-Pd alloys. If, as Mott suggests, gold presents an attractive well in the Au-Ag alloy, $\bar{P}(k_{FA} R)$ will be greater than 1. In the case of the Au-Pd alloy, where η_A will be less than 1, there will be a strong decrease of $\bar{P}(k_{FA} R)$, as anticipated. If, however, the well is sufficiently deep, $\bar{P}(k_{FA} R)$ may be greater than 1 in this case also. Thus, from Eq. (31) the isomer shifts of the two alloys may be of the same sign, even though η_A may be quite different for the two cases.

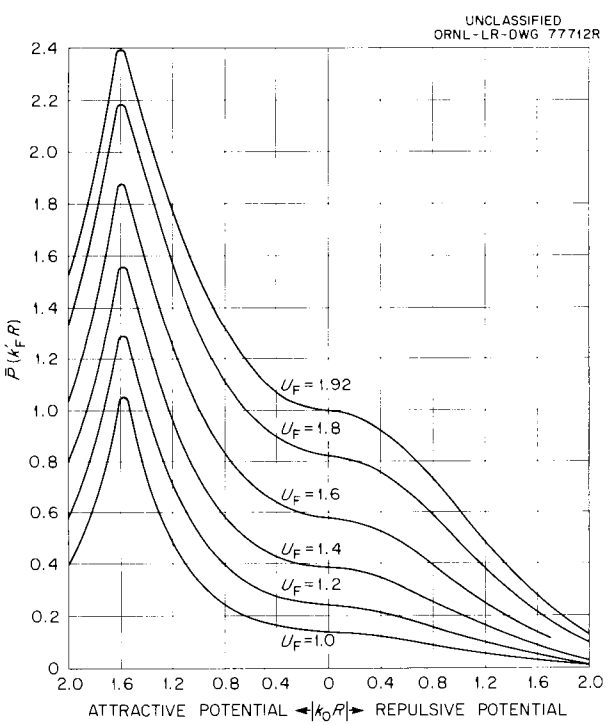

Fig. 5. Charge Polarization as a Function of the Well Parameter, $K_0 R$, Given by Eq. (38).

We have made calculations using the model for alloys of gold with copper and silver. In treating the transition element alloys, we take the unfilled d shell into account only through the valence. It is assumed that the s and d bands do not interact strongly, even though they are degenerate in energy, that only the s-band electrons contribute strongly to $\Delta\rho/c$, and that in the screening of the gold d shell, this d shell is not sufficiently modified in the several gold environments to affect the s shell strongly.

It is worthwhile to note that, in the estimate of isomer shift from $\Delta\rho/c$ for a number of alloys, it is assumed that the well is attractive for s waves. Otherwise, there are no adjustable parameters except the valence η_A. As will be seen, the values used for this band filling are very reasonable ones. A comparison between theory and experiment is given in Table 1.

Table 1. Comparison Between Experimental and Theoretical Isomer Shifts

Host	$\Delta\rho/c$	ΔE_I (exptl) (mm/sec)	η	ΔE_I (calcd) (mm/sec)
Ag	0.38[a]	2.15 ±0.2	1	(2.15)[b]
Ni	2.0	5.6 ±0.2	0.55	5.66
Pd	1.0[c]	2.4 ±0.2	0.6	2.69
Pt	1.55[d]	1.37 ± 0.2	0.4	1.46
			0.5	2.45

[a] J. O. Linde, *Ann. Physik* **15**(5), 239 (1932).

[b] The undetermined constant $\alpha \cdot |U_B(0)|^2 \cdot (N_B/\Omega_B)$ in Eq. (31) was obtained from ΔE_I (exptl) for Ag.

[c] B. Svensson, *Ann. Physik* **14**(5), 699 (1932).

[d] C. H. Johnsson and J. O. Linde, *Ann. Physik* **5**(5), 762 (1930).

SOLID STATE AND NUCLEAR RESULTS FROM A MÖSSBAUER-TYPE STUDY[1] OF Au^{197}

L. D. Roberts J. O. Thomson[2]

Through the measurement of the hyperfine structure (hfs) of dilute alloys of gold with iron, cobalt, and nickel, the magnetic moment of the first excited state of Au^{197} has been measured as $+0.38 \pm 0.08$ nuclear magneton. It was found that the hfs coupling constant in the alloys is closely proportional to the magnetic moment of the host ferromagnetic metal. The value of the effective hyperfine field for the iron alloy is $H' = (1.46 \pm 0.16) \times 10^6$ gauss. A study of the isomer shift of the gold-nickel alloy system as it relates to ferromagnetism is presented. The recoilless absorption line width as a function of absorber thickness for metallic gold is given. The half-life of the first excited state of Au^{197} is found to be $T_{1/2} = (1.93 \pm 0.2) \times 10^{-9}$ sec.

[1]Abstract of published paper: *Phys. Rev.* **129**, 664 (1963).

[2]University of Tennessee.

TOTAL REFLECTION OF RECOIL-FREE NUCLEAR RESONANCE RADIATION FROM Fe^{57}

E. C. Campbell S. Bernstein

The coherent resonant recoil-free scattering of gamma rays has been studied by use of the techniques of total reflection. Measurements were made of the intensity of the 14.4-kev gamma rays (unsplit Mössbauer line) reflected at a small glancing angle θ from an Fe^{57} mirror as a function of θ and of the source velocity v. The results clearly exhibit effects due to interference between the contributions of electronic and nuclear scattering, as well as the mutual interference of the individual resonances in Fe^{57}. A preliminary report[1] of earlier measurements has been published.

Comparison of the measured absolute reflectivity $R(\theta,v)$ with that calculated from theory under the assumption that the mirror film is normal pure ferromagnetic iron metal shows general qualitative agreement as well as certain significant discrepancies which are attributed to the presence of iron with a different chemical or magnetic state from that assumed.

The experimental arrangement is shown schematically in Fig. 1. A long narrow source was prepared by electroplating about 300 mc of Co^{57} on the 7.5×0.05 cm edge of a 302 stainless steel plate. The plate was then annealed in a hydrogen atmosphere at 1000°C for 2 hr, which gave an unsplit line source of the 14.4-kev Fe^{57} gamma radiation. The reflecting surface of the mirror consisted of a thickness of about 170 A of 91.2% enriched Fe^{57} evaporated upon a 30×10 cm optically flat surface of a Pyrex plate 2 in. thick. The gamma-ray detector was a plate of NaI about 0.020 in. thick. The width of the entrance slit to the detector was the same as the source width, 0.05 cm, and of the same length. The source could be moved at any chosen uniform velocity by means of a commercial air motor with adjustable oil damping to control the speed in each direction. Measurements were taken of the gamma-ray intensity reflected by the mirror as a function of glancing angle and source velocity. The number of counts in each of the two directions of velocity were recorded in every cycle cumulatively in two scaling circuits. Times were measured with a 1000-cps tuning-fork oscillator. The direct beam from the source to the detector slit was eliminated by the lead stop shown in Fig. 1.

[1]S. Bernstein and E. C. Campbell, "Total Reflection of Gamma Rays over the Region of Nuclear Anomalous Dispersion in Fe^{57}," pp 250–53 in *The Mossbauer Effect, Proc. 2d Intern. Congr. Saclay, France, 1961* (ed. by D. M. J. Compton and A. H. Schoen), Wiley, New York, 1962.

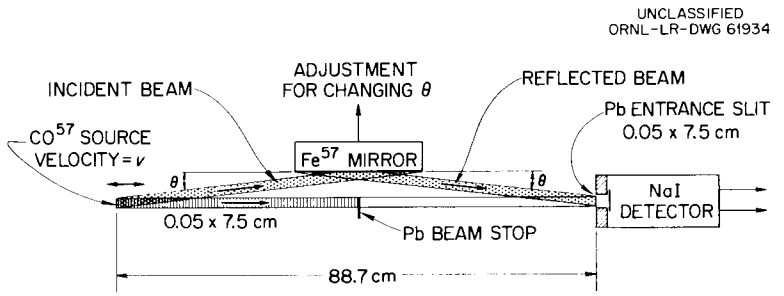

Fig. 1. Schematic Diagram of Apparatus for Measurement of Reflectivity $R(\theta,v)$ of Fe^{57} Mirror.

The angle of incidence was varied by translating the mirror a measured distance parallel to itself in a direction perpendicular to the direct beam. Since the mirror was symmetrically located between the source and detector, the specularly reflected beam reached the detector. The angular width of the beam from the source accepted by the detector was 0.57×10^{-3} radian, full width at half maximum. All adjustments were made using optical levers with visible light, or by use of measurements of the direct-beam gamma-ray intensity.

The reflectivity R is given from classical physical optics by the expression

$$R(z) = \left| \frac{1 - \sqrt{1 - z}}{1 + \sqrt{1 - z}} \right|^2 , \qquad (1)$$

where

$$z = \frac{2\delta + 2i\beta}{\theta^2} = \frac{N\lambda^2 f(0)}{\pi\theta^2} . \qquad (2)$$

N is the number of scattering centers per unit volume, λ is the wavelength of the radiation, θ is the glancing angle, δ and β are the real and imaginary parts of the complex index of refraction $n = 1 - \delta - i\beta$, and $f(0)$ is the complex coherent scattering amplitude per scattering center in the forward direction. Both electron and nuclear scattering are included in $f(0)$ with appropriate amplitudes and phases. A contour map of R as a function of $z = x + iy$ is given in Fig. 2.

The nuclear coherent scattering amplitudes for an $M1$ transition[2] are given by

$$f = \frac{1}{2j_0 + 1} \sum_{m_0} \sum_{\mu} \frac{3}{2} D^{(1)*}_{\mu m}(\hat{k}_f \hat{Z}) \times D^{(1)}_{\mu m}(\hat{k}_0 \hat{Z}) C^2(j_0 1 j_1; m_0 \mu) \times \frac{\Gamma_i}{2k_0} \frac{e^{-k_0^2 \langle x^2 \rangle}}{E_{k_0} - E_R(m_0, m_0 + \mu) + i\Gamma/2} , \qquad (3)$$

where $\hat{k}_0$ and $\hat{k}_f$ are unit vectors in the directions of propagation of the incident and the scattered gamma rays, $\hat{Z}$ is a unit vector in the direction of the

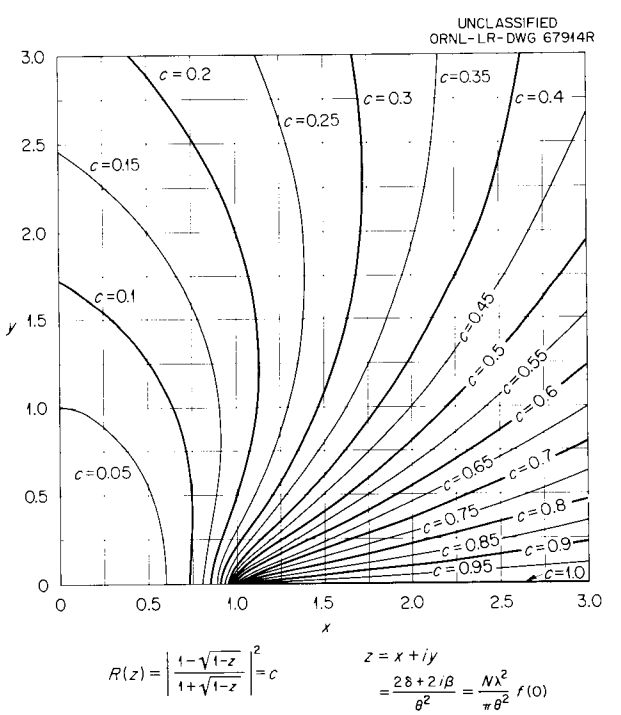

Fig. 2. Contours of Constant Reflectivity of Mirror.

[2]G. T. Trammell, *Phys. Rev.* **126**, 1045 (1962).

magnetic field at the scattering nucleus, C is the appropriate Clebsch-Gordan coefficient, k_0 is the wave number of the photons, Γ_i is the width of the 14.4-kev Fe^{57} level for gamma emission, $e^{-k_0^2\langle x^2\rangle}$ is the Debye-Waller factor which takes into account the fact that only a fraction of the incident radiation is scattered without energy loss, E_{k_0} is the energy of the photons, E_R is the resonance energy, and Γ is the total width of the 14.4-kev level. Symbols m and m' denote the circular polarizations of the incident and outgoing radiation ($m,m' = \pm 1$), j_0 and j_1 are the spins of the ground and excited states, m_0 is the z component of the spin of the ground state, $\pm\frac{1}{2}$. In (3), $\mu = \pm 1$ corresponds to right and left circular oscillators; $\mu = 0$ to a linear oscillator along the z axis. The terms $D^{(1)*}_{\mu m'}$ and $D^{(1)}_{\mu m}$ are the angularly dependent excitation and emission factors for these oscillators. They depend upon appropriate sets of Euler angles associated with the rotations $(\hat{k}_0\hat{Z})$ and $(\hat{k}_f\hat{Z})$. In our case we assume that the magnetization vectors of the domains in the reflecting film are distributed at random in the plane of the mirror. Each of the four possible scattering amplitudes of (3) must be averaged over such an angular distribution.

Expression (3) is given in terms of circular polarizations. The amplitudes of (3) were transformed by conventional procedures to terms of linear polarization. The reflectivity associated with polarization in the scattering plane is then given by R_1 and perpendicular to the scattering plane by R_2. The final expression for the reflectivity from an unpolarized source is given by

$$R = R_e F + (1 - F)\left(\frac{R_1 + R_2}{2}\right), \qquad (4)$$

where F is the fraction of the intensity emitted by the source which suffers a change in energy due to phonon gain or loss in the source. This fraction will not be resonantly scattered by the Fe^{57} nuclei of the mirror. R_e is the reflectivity due to electrons alone; R_1 and R_2 include contributions from both nuclei and electrons.

The reflectivity R was measured as a function of glancing angle θ and velocity v. $R(v)$ for $\theta = 2 \times 10^{-3}$ radian is shown for the data in Fig. 3*a*; the values of R calculated from (2), (3), and (4) are shown in Fig. 3*b*. Figures 4*a* and 4*b* give the measured and calculated values of $R(v)$ for $\theta = 4 \times 10^{-3}$ radian. The calculated values have been corrected for the angular spread of rays due to the finite size of the source and detector and for the frequency width of the source. The following values for the parameters of the calculation have been used:

Incident gamma-ray energy (zero Doppler shift)	14.4 kev
Number of nuclei per cm^3	8.47×10^{22}
Electronic scattering amplitude	$fe = (6.30 \times 10^{-12}\ \text{cm}) + i(6.30 \times 10^{-13}\ \text{cm})$
Natural line width	$\Gamma = 4.60 \times 10^{-9}$ ev
Angular resolution (full width at half maximum)	0.57×10^{-3} radian
Velocity resolution (full width at half maximum)	11.50×10^{-9} ev
$1 - F$	$e^{-k_0^2\langle x^2\rangle} = 0.7$

In the calculations of Figs. 3*b* and 4*b* an actual line width of four times the natural width was used. The positions of the lines from a stainless steel single line source as measured by transmission through Fe^{57} are shown by the vertical arrows along the axis of abscissas.

As can be seen from Figs. 3 and 4 the gross features of the data follow the theory quite well. The shapes of the measured and calculated curves are similar. The measured absolute values of the reflectivity agree reasonably well with the calculated values. In view of the uncertainty of the values of some of the parameters used and the difficulties of the measurements, some of the following physical points of interest are exhibited in detail by the data. The asymptotic value of R as $v \to \pm\infty$ is the reflectivity R_e for electron scattering only. In Fig. 4*a*, for $\theta = 4 \times 10^{-3}$, R approaches R_e at high positive velocities from values of $R>R_e$: as $v \to -\infty$, R approaches R_e from values of $R<R_e$. These features are interpreted in terms of constructive interference between electron and nuclear scattering at the highest positive velocities, and destructive interference at the lowest negative velocities. In Fig. 3*a* the outermost minimum value of R on the left (corresponding to $\mu = +1$, $m_0 = -\frac{1}{2}$) lies deeper than the right outermost minimum (due to

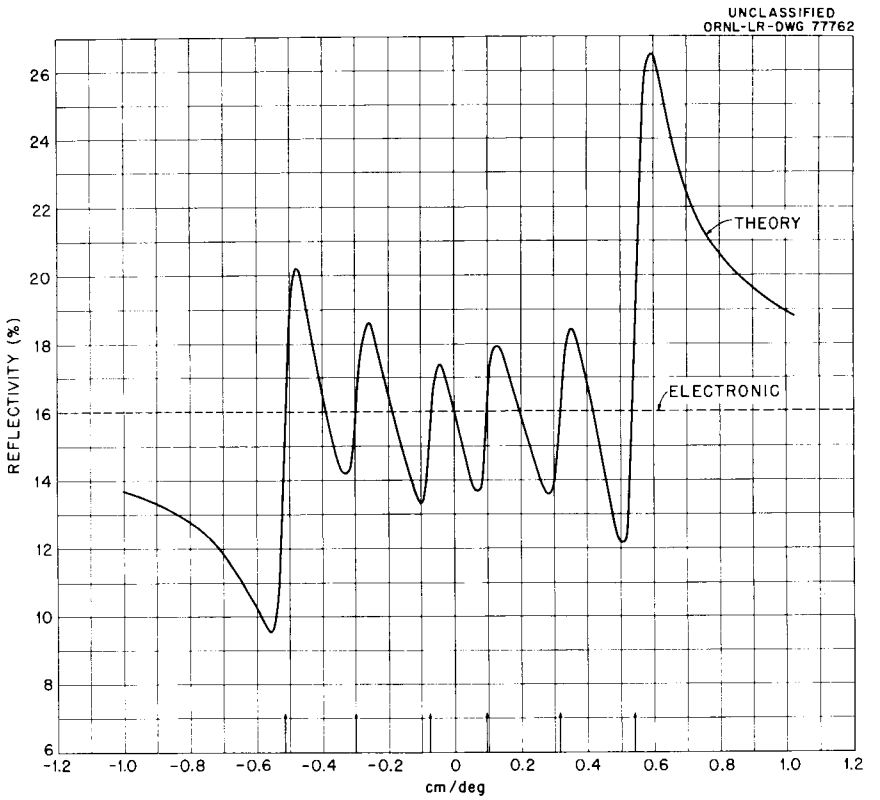

Fig. 4*a*. Reflectivity $R(\theta,v)$, $\theta = 4 \times 10^{-3}$, Theoretical Calculation.

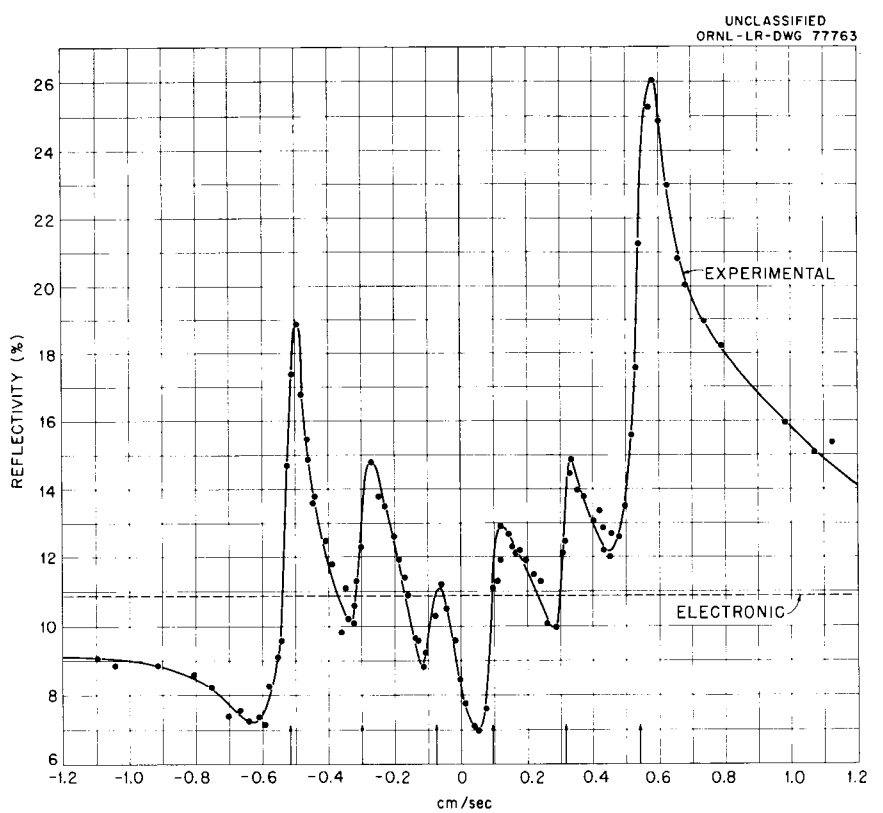

Fig. 4*b*. Reflectivity $R(\theta,v)$, $\theta = 4 \times 10^{-3}$, Experimental Measurements.

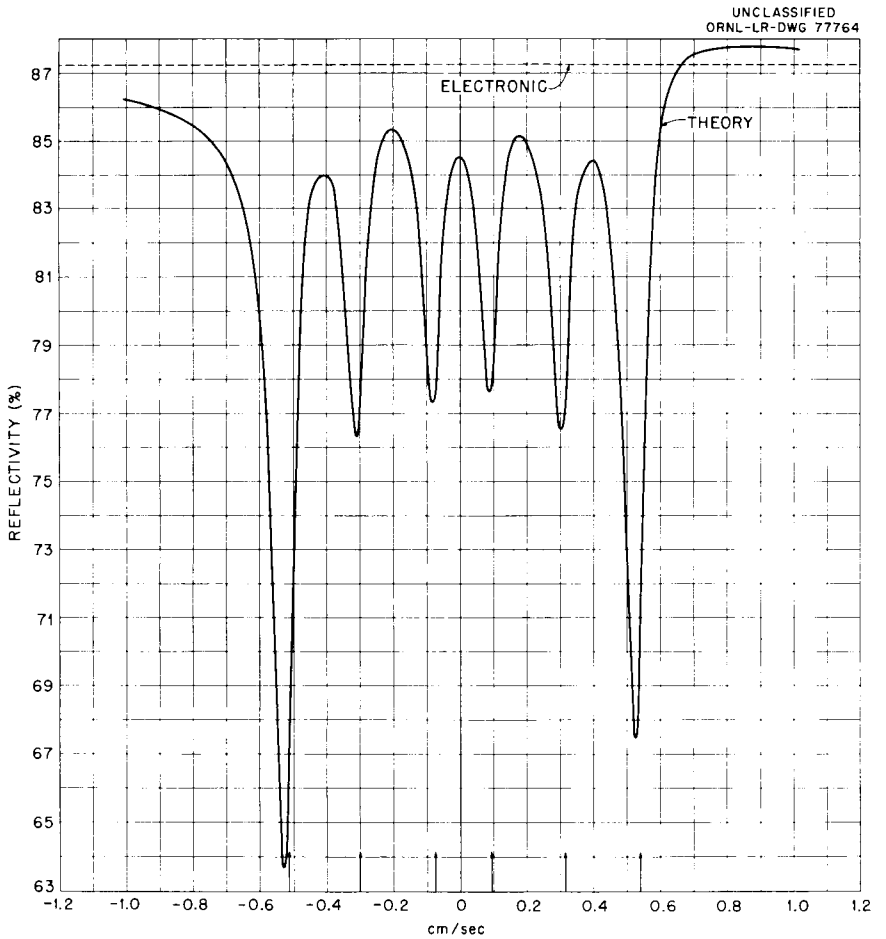

Fig. 3*a*. Reflectivity $R(\theta,v)$, $\theta = 2 \times 10^{-3}$, Theoretical Calculation.

$\mu = -1$, $m_0 = +\frac{1}{2}$). This behavior of corresponding lines at positive and negative velocities is interpreted as being due to interference between the scattering from the various possible transitions.

There are two aspects of the data which do not agree with the calculated values: (1) The lines of Fig. 3*a* seem to hang from a sagging base line, whereas the calculated values of the reflectivity of Fig. 3*b* return almost to the value of R_e at velocities about midway between lines. (2) Two extra lines appear in Fig. 3*a*. Without further detailed experiments, any explanation offered for these two effects can be merely speculative. A sagging of the general character described can be derived qualitatively by assuming that the film has a transition layer in which the magnetization goes from zero at the surface to its maximum value at some point in the interior. The extra line at zero velocity may possibly be due to some nonmagnetic (gamma) iron. The line at about 0.1 cm/sec may possibly be due to some form of FeO in which there is no electric quadrupole splitting. (To our knowledge, all transmission data of FeO show splitting.) These disagreements point up the possibility that this type of experiment may prove to be very useful in the study of the state of magnetization and oxidation of very thin films of appropriate substances.

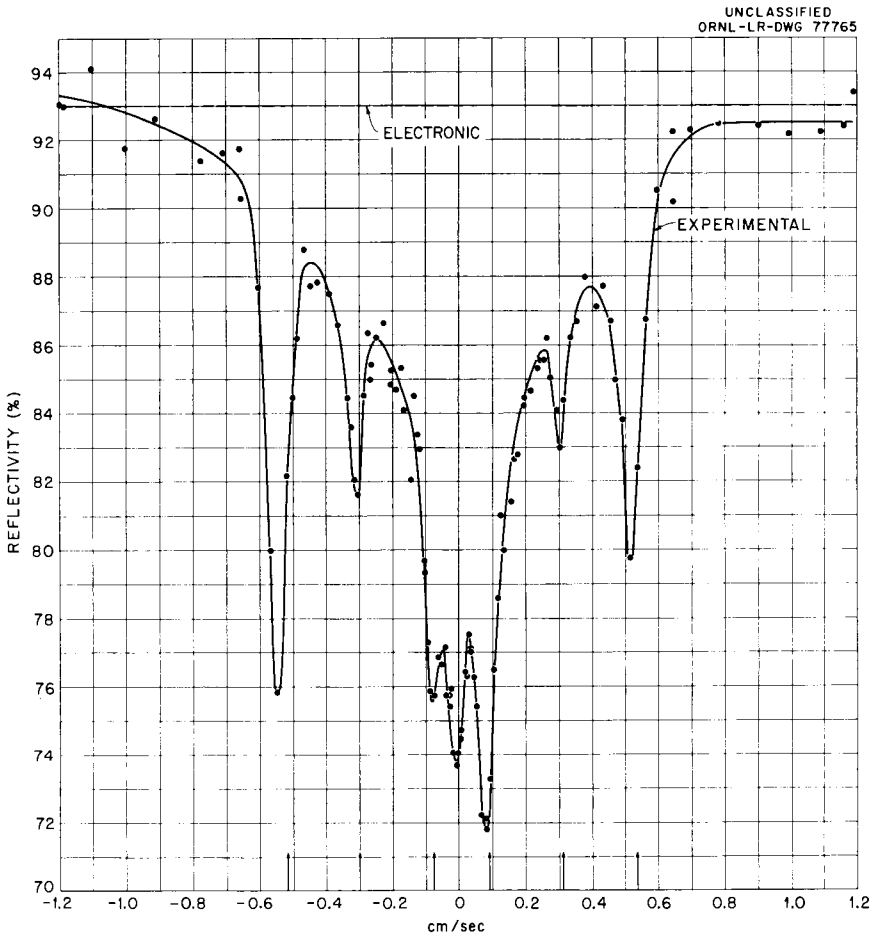

Fig. 3*b*. Reflectivity $R(\theta,v)$, $\theta = 2 \times 10^{-3}$, Experimental Measurements.

SOME MAGNETIC STRUCTURE PROPERTIES OF TERBIUM AND TERBIUM-YTTRIUM ALLOYS[1]

W. C. Koehler H. R. Child E. O. Wollan J. W. Cable

Neutron diffraction studies have been made on single-crystal and polycrystalline specimens of terbium. Earlier magnetic and thermal measurements have indicated a transformation to an ordered magnetic state at approximately 230°K, and a subsequent order-order transformation at approximately 220°K. The neutron measurements show that in the narrow antiferromagnetic region the magnetic structure of terbium is a helical structure. The interlayer turn angle varies from 20.5° per layer at the Néel point to 18.5° per layer at the lower transition. At this lower temperature the structure transforms, in the absence of any external applied field, to a classical ferromagnetic structure in which the moments are in, or nearly in, the plane perpendicular to the hexagonal axis. At a very low temperature the magnetic moment per atom is very nearly 9.0 μ_B, the value expected for the ordered tripositive ion. Neutron

[1]Abstract of paper to be published in *Journal of Applied Physics, Supplement.*

diffraction measurements have also been made on a series of alloys of yttrium and terbium in order to study the influence of magnetic dilution on the magnetic properties of the rare-earth metals. Introduction of yttrium into terbium reduces the Néel temperature and broadens the range of existence of the helical phase. At 30 at. % yttrium and above, the spontaneous transformation to the ferromagnetic state is not observed for zero applied field, even for temperatures as low as 4.2°K. As in pure terbium the interlayer turn angle ω of the helical structure in the alloys varies with temperature, but the slope of the ω vs temperature curve becomes smaller with increasing yttrium concentration.

MAGNETIC STUDY OF DYSPROSIUM-YTTRIUM ALLOYS

H. R. Child W. C. Koehler E. O. Wollan J. W. Cable

The effect of alloying on the magnetic properties of rare-earth metals has been investigated in the alloy system dysprosium-yttrium. Alloys of compositions ranging from 80% yttrium to 10% yttrium have been studied by means of the neutron diffractometers at the ORR. The measurements were made on polycrystalline samples in zero applied field at temperatures ranging from room temperature to 4.2°K.

Pure dysprosium has a magnetic transition from the paramagnetic to an antiferromagnetic state at a Néel temperature, T_N, of 179°K. At the lower temperature of 85°K, designated by T_c, there is an order-order transformation to a ferromagnetic state. The magnetic structure of dysprosium in the ferromagnetic region has been shown by single-crystal neutron diffraction measurements[1] to be a helical-type structure in which the c axis is the screw axis. In the helical structure, as well as in the ferromagnetic structure, the moments are perpendicular to the c axis.

In the antiferromagnetic temperature region, $85°K \leq T \leq 179°K$, the interlayer turn angle ω varies almost linearly from an initial value ω_i at $T = T_N$ of 43.5° to a final value ω_f at $T = T_c$ of 26.5°.

Magnetic measurements have recently been made on alloys of the dysprosium-yttrium system[2] which indicate that the dilution of dysprosium with yttrium stabilizes the antiferromagnetic state at the expense of the ferromagnetic state. The present work shows that this is indeed the case. Magnetic transition temperatures were obtained from intensity vs temperature curves of the most intense magnetic reflection in each alloy. The ferromagnetic transition is completely suppressed in the absence of an applied magnetic field when as little as 10% yttrium has been introduced into the metal.[3] This phenomenon may be related to the hexagonal anisotropy energy which stabilizes a helical or ferromagnetic configuration according to the magnitude of the turn angle. The ordering temperatures T_N are quite accurately proportional to the $\frac{2}{3}$ power of the concentration as shown in Fig. 1; this result is as yet unexplained.

In the more concentrated alloys, as in the pure metal, the turn angle is observed to vary with temperature. As illustrated in Fig. 2, the final and initial values, ω_f and ω_i, become closer together with decreasing dysprosium content, and both appear to approach a limiting value near 50° per layer which is the value taken by the configurations of holmium and erbium near their Néel points and by thulium over a wide temperature region.

---

[1] M. K. Wilkinson *et al.*, *J. Appl. Phys. Suppl.* **32**, 48 (1961).

[2] S. Weinstein, R. S. Craig, and W. E. Wallace, *8th Annual Conference on Magnetism and Magnetic Materials, 1962* (to be published in the *Journal of Applied Physics, Supplement*, 1963).

[3] In a recent experiment with an alloy 95% Dy–5% Y a transition to a configuration with a net moment has been observed. The transition temperature is known at this time to be below 77°K.

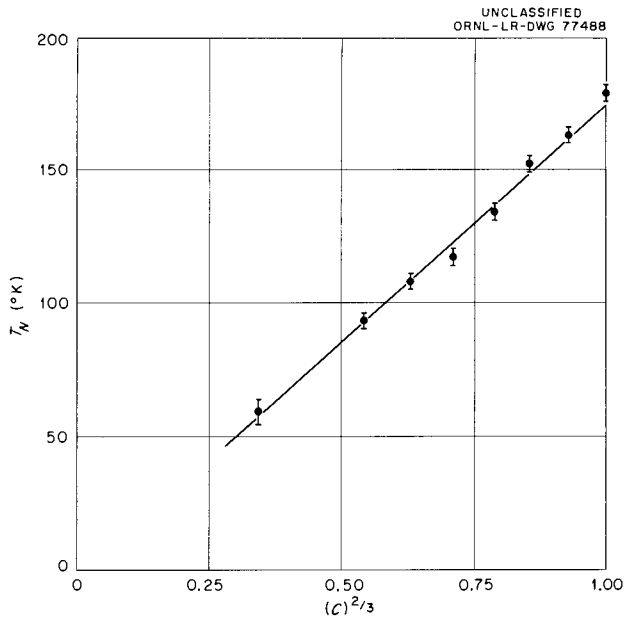

Fig. 1. Variation of Ordering Temperature with Concentration for Dysprosium-Yttrium Alloys. The Néel temperatures are quite closely proportional to the concentration of dysprosium in yttrium raised to the $\frac{2}{3}$ power.

For a binary, random alloy of two constituents A and B the coherent magnetic scattering amplitude is proportional to $\langle \mu_0 f \rangle = n\mu_A f_A + (1 - n)\mu_B f_B$, where n is the concentration of constituent A, μ_A and f_A are its moment value and form factor, respectively, and μ_B and f_B are the corresponding quantities for constituent B. A measure of the square of this quantity can be obtained from the intensities in the coherent magnetic reflections from an ordered magnetic structure if the structure is assumed known. The square of this quantity may also often be derived from the difference in diffuse scattering at temperatures well above and well below the ordering temperature. When the latter method is used, it yields a value of the coherent scattering amplitude which is independent of the detailed structural model. Since the form factors are normalized to unity in the forward direction, the extrapolated value of $\langle \mu_0 f \rangle$ is a measure of the average moment per alloy atom.

In two cases, 80% Dy–20% Y and 40% Dy–60% Y, preliminary moment values have been deduced from the difference in diffuse scattering and from the coherent magnetic reflections. For the latter the simple helical model has been assumed. For the more concentrated alloy, $\langle \mu_0 \rangle = 7.6 \pm 0.80\ \mu_B$, and for the dilute, $\langle \mu_0 \rangle = 4.0 \pm 0.5\ \mu_B$. Within the low precision of the measurements, the atomic moment μ_0 is given by the product of the concentration of dysprosium and its free ion moment of $10\ \mu_B$.

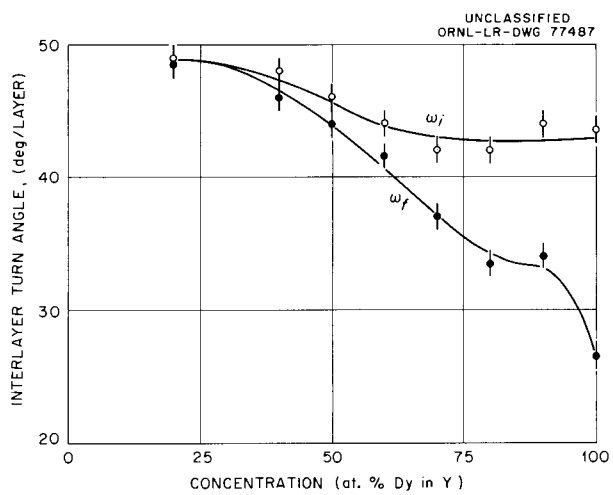

Fig. 2. Variation of Interlayer Turn Angle with Concentration. The initial values refer to values measured just below the Néel point. The final values refer to low-temperature values or, in the case of pure dysprosium, to the values reached just above the Curie point.

ANTIFERROMAGNETISM OF THE ANTIPHASE DOMAIN STRUCTURE OF Pd_3Mn[1]

J. W. Cable E. O. Wollan W. C. Koehler H. R. Child

Neutron diffraction measurements were made on polycrystalline samples of a 75% Pd–25% Mn alloy. It was found that long-range positional order could be obtained by appropriate heat treatment and that this order was of the one-dimensional antiphase domain type with a period of four cubic unit cells. Below 170°K antiferromagnetic reflections were observed for this ordered alloy. A magnetic structure is proposed which satisfactorily accounts for the observed magnetic reflection intensities. On the basis of this structure the atomic magnetic moments are $4.0 \pm 0.2\ \mu_B$/Mn and $0.2 \pm 0.1\ \mu_B$/Pd.

[1]Abstract of published paper: *Phys. Rev.* **128**, 2118 (1962).

ATOMIC MAGNETIC MOMENTS IN DILUTE IRON-PALLADIUM ALLOYS[1]

J. W. Cable E. O. Wollan W. C. Koehler

Neutron scattering and magnetization measurements were made on dilute iron-palladium alloys to determine the existence and magnitude of the magnetic moments of the constituent atoms. This determination was made by the combination of the difference in the aligned magnetic moments obtained from the ferromagnetic diffuse neutron scattering and the average ferromagnetic moment per atom obtained from the saturation magnetization measurements. Data were taken on two alloys which contained 3 and 7 at. % iron. The following results were obtained:

$Pd_{0.97}Fe_{0.03}$	$3.0 \pm 0.2\ \mu_B$/Fe	$0.15 \pm 0.01\ \mu_B$/Pd
$Pd_{0.93}Fe_{0.07}$	$3.0 \pm 0.2\ \mu_B$/Fe	$0.27 \pm 0.02\ \mu_B$/Pd

[1]Abstract of paper to be published in *Journal of Applied Physics, Supplement.*

MAGNETIC PROPERTIES OF THE Pd_3Mn–Pt_3Mn SYSTEM

J. W. Cable E. O. Wollan W. C. Koehler H. R. Child

The alloy systems palladium-manganese and platinum-manganese both exhibit order-disorder phenomena in the region of 25 at. % Mn. In the disordered state these alloys are face centered cubic while in the ordered state Pt_3Mn assumes the Cu_3Au type of structure[1] and Pd_3Mn assumes an antiphase domain structure based on that of Cu_3Au.[2] The near-neighbor environments, as well as the interatomic distances, are the same for these isoelectronic alloy systems. Nevertheless, the manganese-platinum near-neighbor interaction is ferromagnetic[3] while the corresponding manganese-palladium interaction is antiferromagnetic. It was previously suggested[2] that this may be the result of different *d*-orbital configura-

[1]M. Auwarter and A. Kussmann, *Ann. Physik* **7**, 169 (1950).

[2]J. W. Cable *et al.*, *Phys. Rev.* **128**, 2118 (1962).

[3]S. J. Pickart and R. Nathans, *J. Appl. Phys. Suppl.* **33**, 1336 (1962).

tions of the manganese atoms and that antiferromagnetic coupling occurs when there are vacancies in more than half of the three t_{2g} orbitals. In order to obtain additional information on this question, this neutron diffraction investigation of the mixed system Pd_3Mn-Pt_3Mn was carried out. Two alloys of the composition $Pd_3Mn{\cdot}Pt_3Mn$ and $3Pd_3Mn{\cdot}Pt_3Mn$ were prepared. The samples were arc-melted and heat-treated by stepwise cooling from 900°C to room temperature over a two-week period. Subsequent examination by neutron diffraction showed a high degree of positional long-range order in both samples.

$Pd_3Mn{\cdot}Pt_3Mn$

The sample was filed to 100-mesh particle size before the heat treatment. Saturation magnetization measurements made by the ballistic method at 77°K yielded a moment of 0.98 μ_B/atom. Neutron diffraction data were taken at sample temperatures ranging from 4.2 to 298°K. Above 210°K only nuclear Bragg scattering was observed; this is typified by the 298°K data shown in Fig. 1. The presence of the superlattice reflections (100), (110), (210), (211), . . . , etc. indicates long-range order of the Cu_3Au type. The absolute intensities of these reflections are given in Table 1 along with calculated values based on a model in which the manganese atoms occupy the corner sites and the palladium and platinum atoms occupy the face-centered sites at random. In that sense then, the average observed intensity corresponds to a long-range order parameter $S = 0.97$ for this sample. Additional intensity was observed for all reflections below 210°K, which indicates the onset of ferromagnetism at that temperature. Absolute-intensity measurements were made at 4.2°K, and the magnetic components were obtained by subtraction of the 298°K data after correcting for thermal motion.

If all the spin moments are parallel, then the magnetic intensities are proportional to $(p_A - p_B)^2 S^2$ for the superlattice lines and to $(p_A + 3p_B)^2$ for the normal lattices lines, where p_A and

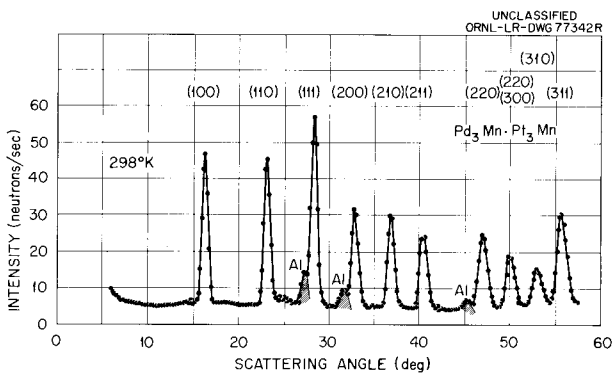

Fig. 1. Neutron Diffraction Pattern of $Pd_3Mn{\cdot}Pt_3Mn$.

Table 1. Nuclear Intensities for Pd_3Mn-Pt_3Mn

Superlattice			Normal Lattice		
hkl	F^2_{obs} [a]	F^2_{calc} [b]	hkl	F^2_{obs} [a]	F^2_{calc} [b]
100	1.26	1.31	111	3.93	3.82
110	1.26		200	3.78	
210	1.18		220	3.66	
211	1.16		311	3.66	
221,300	1.27		222	4.06	
310	1.16				
320	1.35				
321	1.24				

[a] Corrected for thermal motion by use of $\Theta_0 = 275°K$.
[b] Assuming complete long-range order and $b_{Mn} = -0.37$, $b_{Pd} = 0.60$, $b_{Pt} = 0.95$.

p_B are the magnetic scattering amplitudes of the manganese and of the average palladium-platium atoms. These amplitudes are proportional to the product of the Bohr magneton numbers and magnetic form factors of the respective atoms. The observed amplitudes, in Bohr magnetons per molecule, along with the temperature-corrected value of the total moment are shown in Fig. 2. The open circles refer to the superlattice reflections, and the closed circles to the normal lattice reflections and saturation magnetization. The curve is the calculated Mn^{2+} form factor[4] normalized to the saturation moment value. This curve is in fairly good agreement with the diffraction data, indicating that most, if not all, of the molecular moment can be attributed to the manganese atom. The normal lattice amplitudes lie above the curve, and this is suggestive that palladium and platinum atomic moments are contributing to the scattering. However, these moments must be less than 0.1 μ_B/atom and cannot contribute significantly to the observed amplitudes. The observed discrepancies are attributed to errors in the measurement of these relatively weak normal lattice magnetic components.

[4]R. E. Watson and A. J. Freeman, *Acta Cryst.* **14**, 27 (1961).

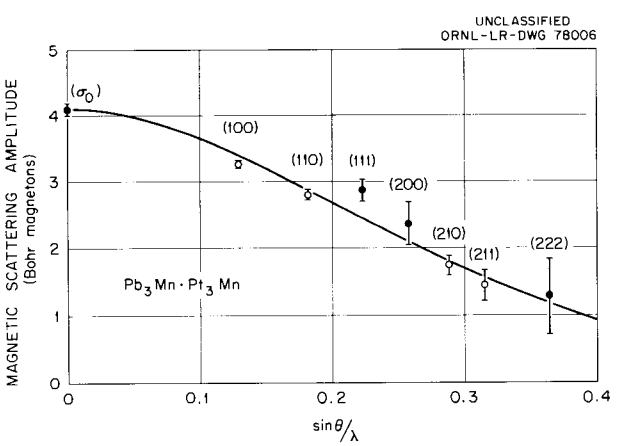

Fig. 2. The Magnetic Scattering Amplitudes for $Pd_3Mn \cdot Pt_3Mn$. These are expressed in Bohr magnetons per molecule for comparison with the saturation moment.

$3Pd_3Mn \cdot Pt_3Mn$

This sample was a machined polycrystalline rod $^3/_8$ in. in diameter and about 2 in. long. Magnetization measurements revealed the retention of paramagnetism at temperatures down to 4.2°K and in magnetic fields up to 5 kilo-oersteds. The temperature dependence of the molar paramagnetic susceptibility and reciprocal susceptibility are shown in Fig. 3. The positive paramagnetic Curie temperature θ_p indicates that the predominant interaction is ferromagnetic, but at temperatures below θ_p(135°K) a susceptibility maximum is observed. Below this maximum there is an apparant cancellation of moments in spite of the strong ferromagnetic tendencies of the system.

Neutron diffraction patterns were taken at sample temperatures of 298, 78, and 20°K, and representative patterns are shown in Fig. 4. These patterns reveal a high degree of long-range order of the Cu_3Au type. Preferred orientation effects render the absolute intensities meaningless, but the long-range order parameter can be obtained from intensity ratios of those superlattice and normal lattice reflections with parallel scattering vectors. Thus, the P_{100}/P_{200} ratios obtained for two different sample orientations were 1.42 and 1.09. The average value compared with the value 1.51 calculated for perfect order gives a long-range order parameter of 0.91 ± 0.05.

At the lower temperatures slight intensity changes were observed, but because of their irregularity these were attributed to preferred orientation effects brought about by sample motion during the cooling procedure. There were, however, broad peaks at the Bragg positions and these are readily apparent in the upper pattern of Fig.

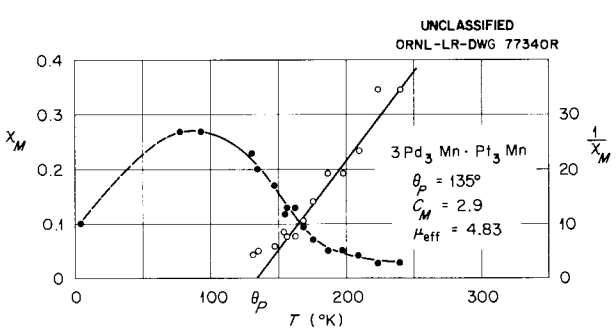

Fig. 3. Temperature Dependence of Molar Susceptibility and Reciprocal Susceptibility of $3Pd_3Mn \cdot Pt_3Mn$.

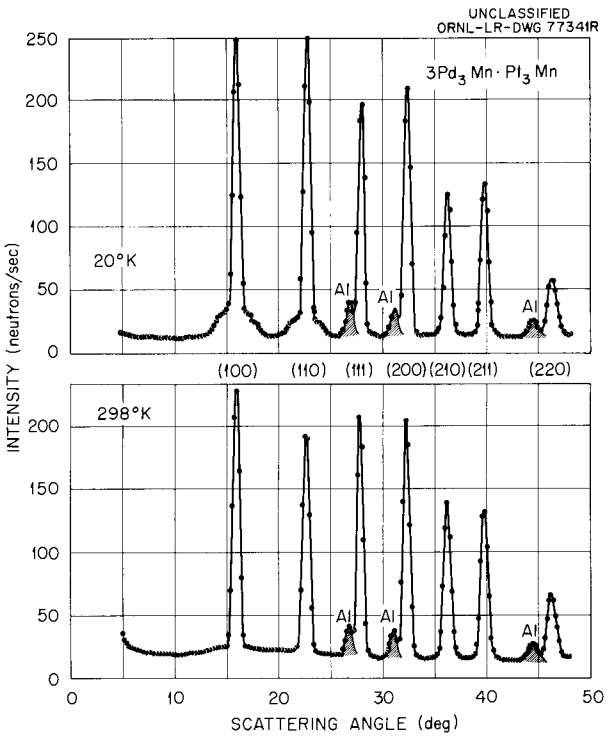

Fig. 4. Neutron Diffraction Patterns of $3Pd_3Mn \cdot Pt_3Mn$.

4 at the (100) and (110) positions. Measurement of the temperature dependence of the scattering at $2\theta = 2^\circ$ under more restrictive slit collimation showed the presence of a broad peak at the origin also, and this accounts for the high background at $2\theta = 5^\circ$ in the 298°K pattern relative to that at 20°K. At 298°K the peaks are quite broad (~6° half-width) and the tail of the (000) peak extends out to $2\theta = 5^\circ$. At the lower temperatures this is not the case since the peaks are then much narrower (~3.5° half-width). These peaks are indicative of short-range order which, considering the temperatures involved, is probably of magnetic origin. Since the peaks occur at both the normal lattice and superlattice positions, this short-range order is ferromagnetic. The peak widths indicate clusters with average diameters of about 10 A at 298°K and about 17 A at the lower temperatures.

Thus the diffraction data are in accord with the susceptibility data; there are strong ferromagnetic tendencies as shown by the ferromagnetic short-range order, but this order extends only over a few unit cells. The decreasing susceptibility at low temperatures suggests that these small ferromagnetic clusters are coupled antiferromagnetically. The interaction mechanism involved in this antiferromagnetic coupling is not readily visualized but may be associated with incomplete positional long-range order and the resultant manganese-manganese near-neighbor interactions.

Even though long-range ferromagnetic order was not found for the $3Pd_3Mn \cdot Pt_3Mn$ sample, strong ferromagnetic coupling is indicated for both alloys. The interactions which couple the manganese atoms very likely operate through the near-neighbor palladium and platinum atoms. It has not been possible to establish the sign of these intermediate manganese-palladium and manganese-platinum interactions because of the small palladium and platinum moments in one case and the lack of long-range order in the other. This has no significance relative to the net manganese-manganese interaction, which is ferromagnetic in either case.

HYDROGEN ATOM POSITIONS IN FACE-CENTERED CUBIC NICKEL HYDRIDE[1]

E. O. Wollan J. W. Cable W. C. Koehler

Neutron diffraction observations on the nickel–nickel hydride system show that the hydrogen atoms occupy the octahedral sites of the face-centered cubic lattice. The hydrogen-to-nickel atom ratio in the hydride phase was found to be 0.6 ± 0.1. In these respects nickel and palladium behave similarly. The systems differ, however, in the one important detail that the palladium hydride is stable at room temperature whereas the nickel hydride is unstable.

[1]Abstract of paper to be submitted to *Physical Review*.

NEUTRON DIFFRACTION INVESTIGATION OF THE MAGNETIC PROPERTIES OF COMPOUNDS OF RARE-EARTH METALS WITH GROUP V ANIONS[1]

H. R. Child M. K. Wilkinson J. W. Cable W. C. Koehler E. O. Wollan

The magnetic properties of heavy rare-earth compounds with the NaCl-type structure have been investigated at temperatures between 295 and 1.3°K by neutron diffraction experiments on powdered specimens. All the nitrides except TmN have a net ferromagnetism at low temperatures, but the diffraction patterns indicate a complicated type of magnetic order. HoP also has an unusual magnetic structure at low temperatures, and this structure is presumably stabilized by dipole forces. The other phosphides, antimonides, and arsenides were found to have magnetic ordering transitions to the Mn-O type of antiferromagnetic structure. Low values of the atomic moments and large magnetic anisotropies in the ordered magnetic structures indicate the effects of crystal-field interactions at low temperatures.

[1]Abstract of paper to be submitted to *Physical Review*.

MAGNETIC MOMENT DISTRIBUTION IN Cu_2MnAl[1]

G. P. Felcher[2] J. W. Cable M. K. Wilkinson

Saturation magnetization and neutron diffraction measurements were made on an ordered Cu_2MnAl sample in order to determine the distribution of magnetic moments in this ferromagnetic alloy. The magnetization measurements were made by the ballistic method in fields up to 5 kilo-oersteds and at sample temperatures of 298 and 77°K. The magnetic moments obtained at these temperatures were 3.2 and 3.7 μ_B per molecule. The neutron diffraction data were obtained at 298°K by use of a magnetic field of 12 kilo-oersteds to separate the magnetic and nuclear scattering. The nuclear scattering showed a long-range order parameter $S \geqq 0.98$, while the magnetic scattering revealed that within 0.1 μ_B the entire moment of the molecule could be attributed to the manganese atom.

[1]Abstract of paper to be submitted to *Physical Review*.

[2]Centro di Studi Nucleari Della Casaccia, Rome, Italy.

MAGNETIC STRUCTURE OF RARE-EARTH IRIDIUM COMPOUNDS RIr_2

Gian Felcher[1] W. C. Koehler

Introduction

The rare-earth metals form compounds with iridium of the composition RIr_2 which have the $MgCu_2$ type structure[2] (cubic Laves phase). Magnetic measurements on members of this series[3,4] have shown that they are ferromagnetic with Curie points ranging from a maximum of 88°K for $GdIr_2$ to about 1°K for $TmIr_2$. These measurements have yielded values for the molecu-

[1]International Atomic Energy Commission Fellow.

[2]V. B. Compton and B. T. Matthias, *Acta Cryst.* **12**, 651 (1959).

[3]R. M. Bozorth *et al.*, *Phys. Rev.* **115**, 1595 (1959).

[4]Unpublished ORNL data; see also M. Atoji, *J. Chem. Phys.* **35**, 1950 (1961).

lar moments of the compounds RIr_2 which are significantly lower than those expected for the ordered tripositive rare-earth ions. The low moment values may indicate the existence of a partial quenching of the orbital moment of the rare-earth ion. They may alternatively indicate the existence of a kind of ferrimagnetic structure in which the rare-earth moments are partially canceled.

Neutron diffraction measurements have been made on specimens of two members of the series, namely, on $TbIr_2$ and $HoIr_2$, in order to investigate the magnetic structures of these compounds. These two particular rare-earth compounds were selected because they represent the best compromise, from the experimental point of view, with respect to expected moment value, absorption cross section, and Curie temperature.

Sample Properties and Procedure

The samples were prepared by the arc-melting of stoichiometric proportions of the pure metals. The resulting brittle buttons were crushed to pass through an 80-mesh sieve, and the powder was loaded into a specially designed flat diffraction cell. A very thin cell of large cross section was used to optimize the scattering from the highly absorbing sample (the capture cross section for iridium at thermal energy is 430 barns). Room-temperature x-ray diffraction patterns showed lines characteristic of the cubic Laves phase only, and the patterns yielded lattice parameters of 7.524 and 7.503 A, respectively, for $TbIr_2$ and $HoIr_2$. Neutron diffraction patterns were obtained at room temperature, at 77°K, and at temperatures near that of liquid helium. Intermediate temperatures were studied for limited angular intervals in the diffraction patterns in order to establish the transition temperatures.

The unit cell of the RIr_2 structure contains eight molecules with the rare-earth atoms in the special positions (000, $\frac{1}{4}\frac{1}{4}\frac{1}{4}$ + F.C.) of the space group $F_{d3m}-0_h^7$. The rare-earth atom distribution is identical to that of the carbon atoms in the diamond structure. There are sixteen iridium atoms in the structure which can be envisaged as forming four tetrahedra, the centers of which are located at ($\frac{3}{4}\frac{3}{4}\frac{3}{4}$ + F.C.). As a result of the high symmetry of this structure there are many systematic absences in the powder patterns. Moreover, the intensities of some reflections, (220), (620), etc., are due to scattering by rare-earth atoms alone, and of others, (222), (622), etc., to that from iridium atoms alone. This property has proved to be of importance in the analysis of the magnetic scattering data.

Results and Discussion

The room-temperature neutron diffraction data for $TbIr_2$ and $HoIr_2$ were analyzed in the usual way by a comparison of the scattering with that from a standard sample. From the absolute intensities in the $TbIr_2$ pattern, the following scattering amplitudes were deduced: $b_{Tb} = (0.76 \pm 0.02) \times 10^{-12}$ cm and $b_{Ir} = (1.01 \pm 0.02) \times 10^{-12}$ cm. This value of the terbium amplitude agrees well with that determined in other measurements.[4] The iridium amplitude is in accord with the value $b_{Ir} = (0.99 \pm 0.015) \times 10^{-12}$ cm which was independently measured during the course of this study from pure iridium powder.[5]

A summary of observed and calculated nuclear intensities for $TbIr_2$ is given in the first columns of Table 1. The intensity agreement is excellent except for the very weakest reflections and is considered to be satisfactory. Similar results were obtained from the pattern of $HoIr_2$.

At very low temperatures the diffraction patterns of both compounds show evidence for the development of long-range magnetic order. There is a marked reduction in the background scattering, and there are observed magnetic contributions to many of the coherent reflections. No additional reflections, however, are observed. The diffraction patterns are therefore typical of those from ferromagnetic or ferrimagnetic structures. The relative magnitudes of the nuclear and magnetic contributions to the observed reflections in $TbIr_2$ are illustrated by the entries in column 4 of Table 1.

If one assumes that the iridium atoms carry no magnetic moment, the magnetic intensities can be reduced to values of $(\mu f)^2$ where μ is the magnitude of the ordered rare-earth moment in the ferromagnetic structure and f is the rare-earth form

[5]This value for b_{Ir} is very much higher than that reported in the literature (Sidhu, Heaton, and Mueller, *Progr. Nucl. Energy, Ser. V* **3**, 419 (1961). The Argonne data have recently been reinterpreted to yield a value of b_{Ir} which is close to the value cited in the text; M. H. Mueller, private communication.

Table 1. Comparison[a] of Intensities Observed and Calculated for $TbIr_2$

Index	I_n (obs)	I_n (calcd)	I_{n+m} (obs)	I_{n+m} (calcd)
111	5.87	5.74	41.2	41.4
200	0	0	0	0
220	8.31	8.18	38.7	39.5
311 222	71.7	74.2	93.4	95.8
400	6.36	5.24	12.4	12.6
331	3.02	2.46	11.7	12.6
420	0	0	0	0
422	5.02	4.99	15.4	14.6
511 333	24.7	23.9	30.7	31.3
440	23.2	23.6	27.6	28.1

[a]Comparison of nuclear intensities observed at room temperature and nuclear and magnetic intensities at 4.2°K for $TbIr_2$. Intensities are expressed in units of thousands of counts. For the magnetic intensity calculations an order moment of 7.5 μ_B for terbium is used. No moment is assumed for iridium.

factor. The results of this reduction for the data of $TbIr_2$ are summarized in Fig. 1 where values of $(\mu f)^2$ derived from the coherent magnetic reflections are indicated by open circles. It may be emphasized that the value of $(\mu f)^2$ for (220) is independent of the assumption made above since the intensity of this reflection has no contribution from iridium. For reflections which occur at higher values of sin θ/λ, for example, sin $\theta/\lambda > 0.2$, the contribution made by any reasonable iridium moment is negligible. This follows as a result of the very rapid falloff with sin θ/λ of the Pauling-Sherman form factor for iridium. With the possible exception of the reflection (111) then, the magnetic intensities in the coherent reflections can be converted, with the knowledge of the form factor, to a value for the ordered moment per terbium atom. With the form factor deduced from measurements on TbN (ref 6) the data yield an ordered moment of 7.48 ± 0.20 μ_B for terbium in $TbIr_2$.

[6]H. R. Child *et al.*, to be published in the *Physical Review*.

The solid curve in Fig. 1 was computed from the above value of the moment and from the TbN form factor. It is noteworthy that the point for (111) lies on the curve.

The magnetic intensities listed in the last column of Table 1 were calculated on the ferromagnetic model in which each terbium atom has the moment and form factor described above. For a polycrystalline specimen of such a structure the moment directions are indeterminate and the average value of two-thirds for the square of the magnetic interaction vector q^2 is appropriate to all reflections. The agreement between calculated and observed intensities at low temperatures is quite satisfactory.

An independent measurement of the ordered moment was obtained from an analysis of the difference diffuse scattering, for example, from the difference in diffuse scattering at temperatures well above and well below the ordering temperature. The results of this analysis are shown by the closed circles in Fig. 1. These data extrapolate to a slightly higher value for the ordered moment, 7.74 ± 0.20 μ_B, which is, however, well within experimental error of the value obtained from the coherent reflections.

The Curie points for $TbIr_2$ and $HoIr_2$ were determined from the measured variations with temperature of the intensity in the (111) reflection. The

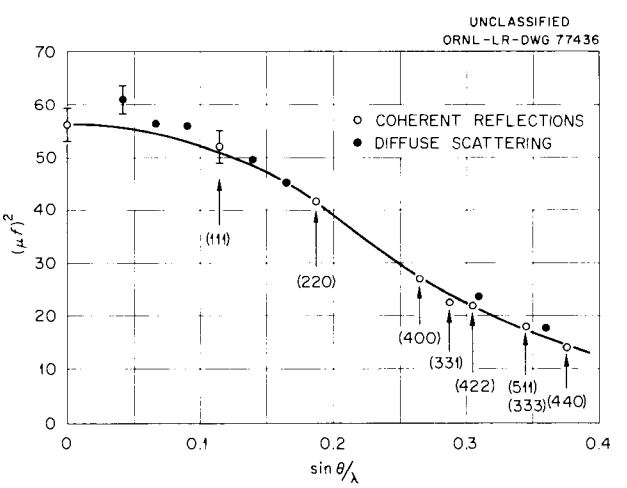

Fig. 1. Variation with sin θ/λ of $(\mu f)^2$ for $TbIr_2$. Open circles represent data from indicated coherent magnetic reflections. Closed circles are data derived from the diffuse scattering. The solid curve is calculated from the terbium form factor and a moment of 7.48 μ_B for terbium.

values obtained, 46 ± 1°K and 13 ± 1°K, agree quite well with the corresponding values reported by Bozorth *et al.* [3]

Because of the low Curie point for $HoIr_2$ the magnetic intensities in its diffraction pattern are not completely developed at the lowest temperature studied. Nevertheless an analysis of the data can be made in a manner analogous to that already described for $TbIr_2$ and that analysis leads to a value for the moment of holmium at 8.0°K of 6.5 μ_B. Extrapolation of the temperature-intensity curve of the (111) reflection yields a value of 7.2 ± 0.03 for the ordered moment of holmium in $HoIr_2$.

The molecular moments for $TbIr_2$ and $HoIr_2$ measured by Bozorth *et al.*, 7.0 and 7.5 μ_B, are much smaller than the values expected for ordered tripositive rare-earth ions: 9.0 μ_B, Tb; 10.0 μ_B, Ho. Since the moments measured from the neutron diffraction data for the rare-earth atoms themselves have values less than gJ, it must be concluded that the orbital moments of the rare-earth atoms are partially quenched.

It remains to ask if the difference between 7.0 μ_B for $TbIr_2$ and 7.5 μ_B for Tb in $TbIr_2$ may be significant. The precision of the neutron measurements is such that a small moment on iridium, 0.2 to 0.3 μ_B, would just be detectable. However, it is known[3,7] that there exists a range of compositions for these and similar compounds over which the Laves phase structure is found. If a 3% weight loss on melting, as noted by Bozorth and co-workers, be attributed to loss of terbium, then one would be concerned with $Tb_{0.9}Ir_2$ (ref 8) rather than $TbIr_2$, and a moment differing by some 10% from that of the ideal compound would be inferred. It appears impossible to us to state at this time that iridium does or does not carry a small magnetic moment.

[7] J. H. Wernick and S. Geller, *Trans. AIME* **218**, 866 (1960).

[8] Attempts at chemical analysis have not been successful since the samples are difficult to dissolve quantitatively. Note that a deficiency of 10% terbium should create fluctuations in the nuclear intensities which would be easily detectable.

ON THE CRYSTAL STRUCTURE OF THE MANGANESE (III) TRIOXIDES OF THE HEAVY LANTHANIDES AND YTTRIUM[1]

H. L. Yakel[2] E. F. Bertaut[3]
W. C. Koehler E. F. Forrat[3]

The preparation, determination of optical properties, and approximate crystal structures of the ferroelectric manganese (III) trioxides of holmium, erbium, thulium, ytterbium, lutetium, and yttrium are reported. The compounds crystallize in the hexagonal system, probable space group $P6_3cm$, and their structure is characterized by unusual five- and sevenfold coordination polyhedra about manganese and rare-earth atoms respectively. The unacceptable values assumed by the temperature factors of two oxygen ions throw doubt on the exact determination of atom positions by least-squares refinement. Possible causes of this difficulty are reviewed.

[1] Abstract of paper to be published in *Acta Crystallographica.*

[2] Metals and Ceramics Division.

[3] Laboratoire d'Electrostatique et de Physique du Metal et Centre d'Etudes Nucleaires, Grenoble, France.

LECTURES ON NEUTRON DIFFRACTION[1]

W. C. Koehler

Four lectures entitled "A History of Neutron Diffraction," "Applications of Neutron Diffraction to Problems in Magnetism," "Magnets and Cryostats," and "Mechanical Design Considerations for Neutron Diffractometers" were delivered to the Advanced Course on Neutron Crystal Spectrometry, Institutt for Atomenergi, Kjeller, Norway, in June 1962. The complete course of lectures was published by the Netherlands-Norwegian Reactor School and can be obtained therefrom.

In these lectures a review of the development of neutron diffraction from the historical point of view is presented; theoretical results useful to analysis of magnetic scattering data are summarized, and experimental techniques are illustrated by studies of paramagnets, antiferromagnets, and ferromagnets; methods of incorporating magnets and cryostats into diffractometer design are discussed; and a review of existing types of neutron diffractometers is made.

[1]Abstracts of papers published in *Proceedings of Advanced Course on Neutron Crystal Spectrometer*, Netherlands-Norwegian Reactor School, 1962.

OPTICAL PHYSICS

G. W. Charles
P. M. Griffin
H. W. Morgan
O. B. Rudolph
P. A. Staats
K. L. Vander Sluis
T. A. Welton
G. K. Werner

The optical properties of an electrically excited mixture of krypton and mercury vapor have been investigated in some detail, in the expectation that the system would be capable of sustaining coherent oscillation at a number of optical and infrared frequencies. The very close coincidence of the resonance level of $Kr[4p^5(^2P_{3/2})5s, J = 1-]$ at 80917.6 cm^{-1} above ground, with the 10^3P_1 level of mercury at 80916.7 cm^{-1} above ground, promises to provide excellent collisional pumping of the mercury in a krypton-mercury (Kr-Hg) discharge.

A previously reported device[1] for measuring absorptions of spectral lines in a gas discharge has been extensively used to measure populations of the krypton excited state and the various mercury levels of interest. The apparatus was shown to be free of gross systematic error both by the previously reported neon absorption measurements[1] and by some very severe internal consistency checks on the krypton data. It was further established that addition of mercury to the system did not alter the excited krypton population in any gross fashion. A simple prediction could then be made, using detailed balance, of the population of mercury 10^3P_1 atoms to be expected. When a search was made for amplification of the line mercury $10^3P_1 \rightarrow 7^3S_1$ at 5384 A, no detectable amplification was found, the detection limit being about 1% of amplification in the available 70 cm of discharge.

This result was not completely discouraging, since the amplification estimated by use of the above population estimate combined with computed transition probabilities was only 3 to 4% for 100 cm of discharge. In addition the calculated value assumed a pure even-mass isotope of mercury, whereas the hyperfine and isotope effects in normal mercury would probably reduce the peak amplification by a factor of about 3.

[1]G. W. Charles *et al.*, *Phys. Div. Ann. Progr. Rept. Jan. 31, 1962*, ORNL-3268, p 84.

Preparation was made for a much more sensitive test of the system by search for actual coherent oscillation. Several sets of multilayer dielectric coated reflectors were procured for incorporation into a confocal resonator designed to oscillate at 5384 A. In the meantime it had become clear that a reduction in tube diameter would cause the gain to increase in inverse ratio. At the same time the use of confocal optics would make a small aperture (~5 mm) completely practical. A tube length of 2 m was chosen to further increase the gain, and pure Hg^{202} was procured as a possible extra improvement.

To obtain experience in the adjustment and operation of gas lasers, the system was filled with a helium-neon (He-Ne) mixture and successfully operated at 6328 A, with the help of a borosilicate flat to suppress oscillation at 3.39 μ. (This oscillation was later reported by another group.[2]) The tube windows were two fused-quartz flats, inclined at Brewster's angle to eliminate interface reflections and cemented to the tube ends with epoxy. We have obtained completely satisfactory operation with this simple, very flexible (and apparently novel) procedure.

Because the confocal reflectors were coated to optimize reflectivity at 5384 A, it was felt that oscillation at the less favorable wavelength 6328 A indicated that our technique was adequate for an intelligent exploration of the Kr-Hg system. A 2-m quartz tube with a water jacket for controlling mercury vapor pressure was accordingly constructed with Pyrex windows to spoil as much infrared oscillation as possible and was aligned by filling with He-Ne so that oscillation could be obtained at 6328 A. In the course of this work, it was incidentally discovered that the gain of the He-Ne system rises strongly with temperature, a previously unknown and unsuspected result. Filling with Kr-Hg, to conditions previously shown to give optimum pumping, failed to give either oscillation or noticeable amplification, thus appearing to confirm in a refined and disconcerting fashion the inconclusive observations made earlier with cruder apparatus.

A complete tabulation was made of the spontaneous emission rates and peak amplification cross sections for all relevant mercury transitions. From these numbers it was apparent that a 10^3P_1 population sufficient to yield coherent oscillation at 5384 A would yield enormous amplifications for several infrared transitions downward from 10^3P_1, the largest being a factor of about e^{150} per pass at a wavelength of 15.4 μ. Although the tube was designed to prevent coherent oscillation at any of these wavelengths, still it was felt that the amplification of spontaneous emission (so-called super-radiance) could easily depopulate the 10^3P_1 level and prevent oscillation at the desired wavelength. Some such phenomenon seemed likely to account for some old results on the Kr-Hg system obtained by Beutler and Eisenschimmel,[3] and it was accordingly decided to construct a 1-m Kr-Hg confocal resonator with aluminized reflectors and KBr windows to allow oscillation over a wide range of the infrared.

This instrument has been completed and very successfully tested. It has produced with great ease the oscillations in He-Ne at 1.15 μ and 3.39 μ, previously reported by Javan *et al.*[4] and Bloom.[2] In addition, a number of oscillations in xenon and He-Xe mixtures recently reported by Faust, McFarlane, Patel, and Garrett[5] have been confirmed. These wavelengths are 2.0268, 2.6518, 3.3676, 3.5080, 3.6859, 3.9966, 5.5754, and 9.0065 μ, with a number of others expected as soon as KBr windows are applied to the 2-m system.

Careful observations with Kr-Hg in the same tube have completely failed to show the presence of *any* infrared oscillation. This failure must be regarded as conclusive, because of the strikingly high intensities obtained in the infrared detector (Perkin-Elmer infrared spectrometer with NaCl or KBr prism and thermocouple detection) in comparison with the low intensities of conventional line sources in this region.

We believe that, for reasons not yet clear, the collisionally pumped Kr-Hg laser is not a workable system. This conclusion apparently agrees with provisional conclusions (unpublished) reached by a number of other groups, albeit on the basis of considerably less evidence than we have accumu-

[2]A. L. Bloom, W. E. Bell, and R. C. Rempel, to be published in *Applied Optics*.

[3]H. Beutler and W. Eisenschimmel, *Z. Physik. Chem.* **B10**, 89 (1930).

[4]A. Javan, W. R. Bennett, Jr., and D. R. Herriott, *Phys. Rev. Letters* **6**, 106 (1961).

[5]W. L. Faust, R. A. McFarlane, C. K. N. Patel, and G. C. B. Garrett, to be published in *Applied Physics Letters*.

lated. No presently known criterion would suggest, in advance of actual tests, that He-Ne is a more desirable system than Kr-Hg, but such seems in fact to be the case.

One possible relative defect of Kr-Hg (as yet not shown to be the actual *fatal* defect) lies in the relatively weaker binding of the mercury 10^3P_1 state. This state is conceivably quite vulnerable to destruction by more of the electron spectrum present in the discharge. Optical pumping then offers some chance of success, and exploratory work is being performed on this possibility.

RESPONSE OF SILICON SOLID-STATE DETECTORS TO HEAVY IONS AND FISSION FRAGMENTS

H. W. Schmitt
F. J. Walter
J. H. Neiler[1]
C. D. Moak
W. M. Gibson[2]
T. D. Thomas[3]

The pulse-height vs energy relation has been measured for high-energy bromine and iodine ions (artificial fission fragments) incident on solid-state detectors. The Oak Ridge Tandem Van de Graaff accelerator was used to accelerate the ions; energies up to 120 Mev were obtained.

The pulse-height vs energy relations for fission fragments in solid-state detectors have in the past been determined by the comparison of directly measured pulse-height spectra with the energy spectrum deduced from correlated fragment time-of-flight measurements.[4,5] The experiments described here have been performed in an effort to eliminate the uncertainties in fragment energy calibrations with respect to time-of-flight measurements; in addition, the mechanism of pulse production by heavy ions in solid-state detectors might be better understood through studies involving ions of a single known mass. Figure 1 is a schematic diagram of the experimental arrangement.

The mechanism of high-energy ion production in the accelerator will be discussed in detail in a forthcoming publication.[6] Briefly, the method is one of energy and charge accumulation: A negative ion, charge 1–, originates in the ion source and is accelerated to the terminal voltage V, 7 mv or more for these studies. At the terminal, the ions pass through a stripper canal and emerge as positive ions of charge 4+ or 5+, as shown in Fig. 1. A small amount of gas (pressure $\cong 3 \times 10^{-5}$ mm Hg) is allowed to remain in the second half of the accelerator system, so that as the positive ions are accelerated, additional electrons are stripped from the ion by collision with the gas atoms. The particles then accelerate more rapidly, and again the probability of removal of additional electrons increases. Thus, increased acceleration gives rise to increased ion charge, and vice versa. This compounding has been observed to give ion energies ranging up to 120 Mev. Since charge-changing does not take place at definite positions along the second half of the accelerator, the energy spectrum of the emerging particles is continuous, covering the entire range from 30 to 120 Mev.

Some method of energy selection is required for experiments where the particle energies must be known. The tandem analyzer magnet proves to be ideal for two reasons. It has sufficient energy resolution to select very narrow slices of the continuous spectrum, and it selects a series of slices simultaneously. As shown in Fig. 1, if two particles with different energies have the same ratio E/q^2, the magnet will treat them alike. Thus a given value of magnetic field causes the

[1]Now at Oak Ridge Technical Enterprises Corp.

[2]Bell Telephone Laboratories, Murray Hill, N.J.

[3]Princeton University.

[4]H. W. Schmitt *et al.*, *Bull. Am. Phys. Soc.* **6**, 240 (1961); *Phys. Div. Ann. Progr. Rept. Jan. 31, 1962*, ORNL-3268, p 94.

[5]W. M. Gibson, T. D. Thomas, and G. L. Miller, *Phys. Rev. Letters* **7**, 65 (1961).

[6]C. D. Moak, J. H. Neiler, H. W. Schmitt, F. J. Walter, and G. F. Wells, to be published.

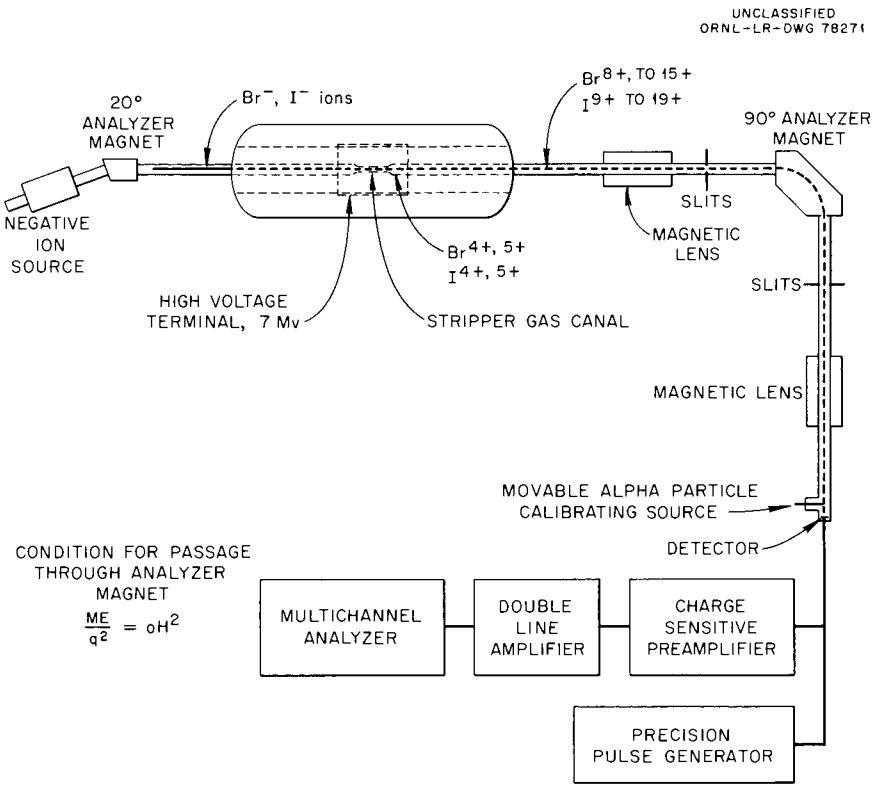

Fig. 1. Arrangement for Measuring Heavy-Ion Energies in Semiconductor Detectors.

selection of a series of lines from the continuous spectrum. The lines are spaced farther apart at higher energies since their positions are proportional to q^2. Typical pulse-height spectra are shown in Figs. 2 and 3. It has been shown[6] that the identification of ion energies and charges, as determined from runs at two magnetic fields, is unambiguous. The energy resolution for bromine ions was 1 to 1.5 Mev; that for iodine ions was 1.5 to 2 Mev, full width at half maximum. These widths were significantly larger than the width of the pulser peaks; thus it is indicated that the contribution of electronic noise to the resolution width was small. In order to demonstrate that the resolution widths were established by the detector rather than the accelerator, similar spectra were obtained for several collimating slit apertures (see Fig. 1). No change was observed. The narrow peaks contaminating the spectra below ~30 Mev in Figs. 2 and 3 seem to be caused by oxygen or nitrogen ions from the accelerator. If so, there appears to be a dependence of resolution width on ion mass.

A typical pulse-height vs energy relation for bromine and iodine ions is shown in Fig. 4. The detector was of the surface-barrier type and was operated on the plateau of the pulse-height vs detector bias curve. Similar results were obtained for diffused-junction detectors. Note that the curves for both bromine and iodine ions are displaced below the curve for alpha particles. Two effects by which such displacements might be explained are as follows: (1) the classical window effect, whereby an ion loses energy in the gold deposit on a surface-barrier detector or in the highly doped front surface of a diffused-junction detector; and (2) a primary "pulse-height defect," whereby the "charge collection" is not proportional to the ion energy. In the latter case, either reduced "charge collection" efficiency or reduced charge production efficiency may give rise to the "defect." An effort to evaluate the classical

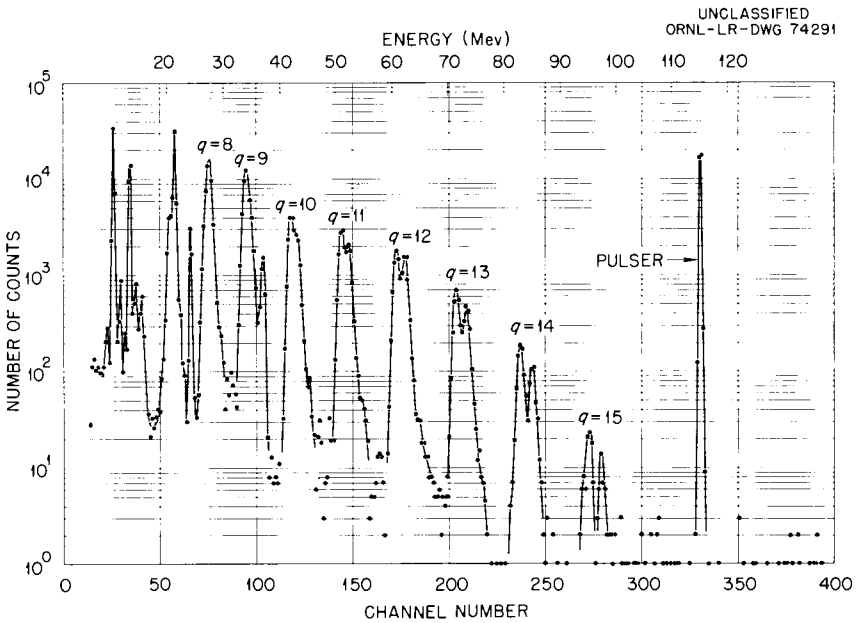

Fig. 2. Pulse-Height Spectrum of Bromine Ions. The ions are deflected through a 90° analyzing magnet onto a silicon surface-barrier detector. Double peaks are caused by the presence of two ion masses, Br^{79} and Br^{81}. Note ion energy scale at top of graph.

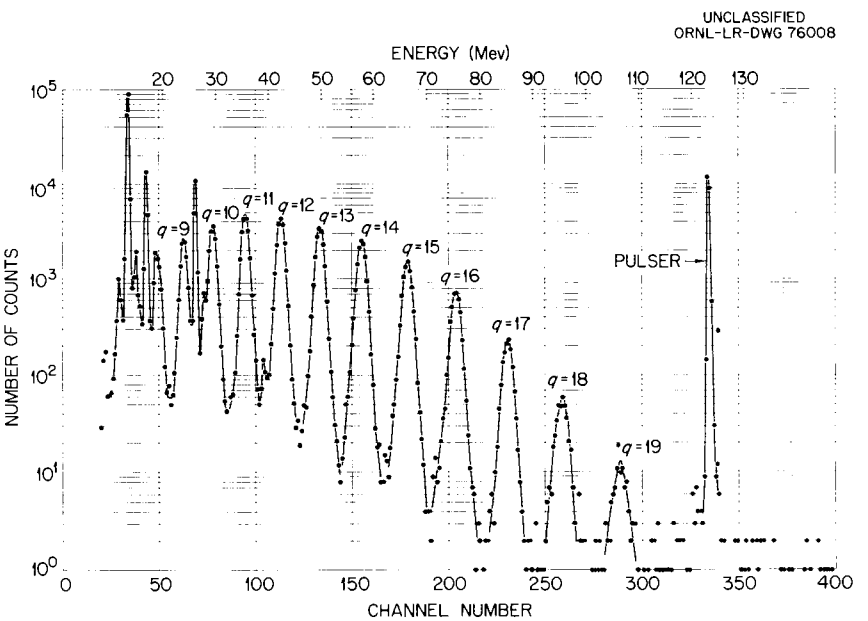

Fig. 3. Pulse-Height Spectrum of Iodine Ions. The ions are deflected through a 90° analyzing magnet onto a silicon surface-barrier detector. Note ion energy scale at top of graph.

window effect consisted of a set of measurements, similar to those above, in which the detector axis was oriented at 60° instead of 0° with respect to the incident ion beam. If the assumption is made that dE/dx for the ions is constant over the first few tenths of a percent of the range, the displacement of the bromine ion curve in Fig. 4 can probably be explained on the basis of the window effect. The iodine curve, however, when corrected in the same way, becomes parallel to the alpha-particle curve, but remains displaced from it by ~4 Mev. Further information about dE/dx for these ions is needed before firm quantitative conclusions can be drawn from these data.

A large number of surface-barrier and diffused-junction detectors have been studied. Results have been obtained for various detector operating conditions in all cases. Detailed results of this work will be reported in a forthcoming publication.

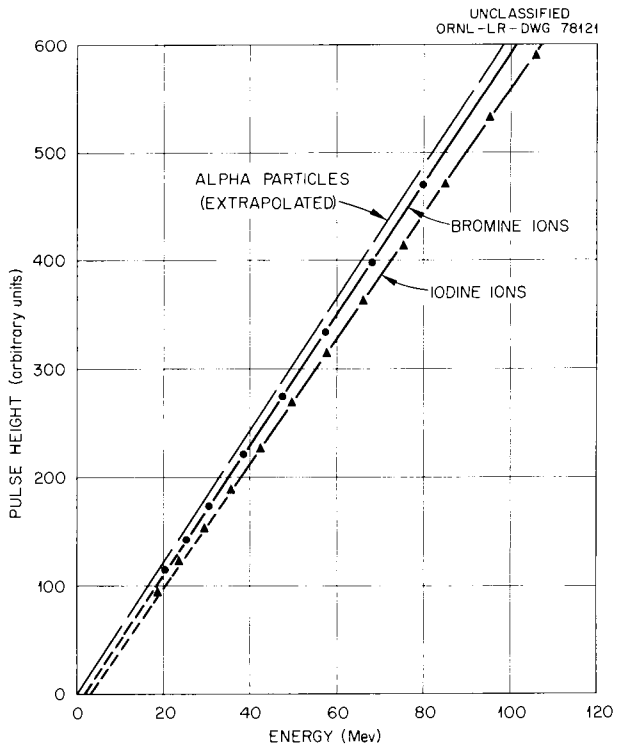

Fig. 4. Pulse-Height vs Energy Relation for Alpha Particles and Bromine and Iodine Ions.

STUDY OF THE TRANSITION OF SMALL NIOBIUM-ZIRCONIUM SUPERCONDUCTING SOLENOIDS TO THE NORMAL STATE[1]

R. W. Boom L. D. Roberts

A preliminary study has been made of the transition of small superconducting coils to the normal state. This transition was found to be fast compared with velocities found from measurements on short sample lengths. The mode of dissipation of the field energy was studied; a relation between this and the critical current is indicated.

[1]Abstract of a paper submitted for publication in the *Journal of Applied Physics*.

PUBLICATIONS

Austern, N., R. M. Drisko, E. Rost, and G. R. Satchler, "Distorted Waves Theory of Double-Excitation by Inelastic Scattering," *Phys. Rev.* **128**, 733–40 (1962).

Bair, J. K., and H. B. Willard, "Level Structure in Ne^{22} and Si^{30} from the Reactions $O^{18}(\alpha,n)Ne^{21}$ and $Mg^{26}(\alpha,n)Si^{29}$," *Phys. Rev.* **128**, 299–304 (1962).

Bassel, R. H., G. R. Satchler, R. M. Drisko, and E. Rost, "Analysis of the Inelastic Scattering of Alpha-Particles," *Phys. Rev.* **128**, 2693–2707 (1962).

Becker, R. L., "Non-Singular Formulation of the Brueckner Approximation for an Infinite Fermi System," *Phys. Rev.* **127**, 1328–42 (1962).

Bernstein, S., and E. C. Campbell, "Total Reflection of Gamma Rays over the Region of Nuclear Anomalous Dispersion in Fe^{57}," pp 250–53 in *Proceedings of the Second International Congress on Mössbauer Effect, Saclay, France, September 1961*, ed. by D. M. J. Compton and A. H. Schoen, Wiley, New York, 1962.

Bienlein, J. K., and Frances Pleasonton, "The Half-Life of He^6," *Nucl. Phys.* **37**, 529–34 (1962).

Bird, J. R., J. H. Gibbons, and W. M. Good, "Gamma Ray Spectra from Capture of 30-Kev Neutrons," *Phys. Letters* **1**(7), 262–63 (1962).

Block, Robert, Grimes Slaughter, Norman Pattenden, and John Harvey, "The ORNL Fast Chopper Time-of-Flight Neutron Spectrometer," pp 534–47 in *Proceedings of the IAEA Symposium on Pile Neutron Research and Physics, Vienna, Austria, October 1960*, Intern. At. Energy Agency, Vienna, 1962.

Brink, D. M., and G. R. Satchler, *Angular Momentum*, Oxford Library of the Physical Sciences, Oxford University Press, 1962.

Brosi, A. R., A. I. Galonsky, B. H. Ketelle, and H. B. Willard, "A Precision Measurement of the Longitudinal Polarization of Betas Following P^{32} Decay," *Nucl. Phys.* **33**, 353–87 (1962).

Cable, J. W., H. R. Child, W. C. Koehler, M. K. Wilkinson, and E. O. Wollan, "Neutron Diffraction Studies of Rare Earth Metals and Compounds," pp 379–90 in *Proceedings of the IAEA Symposium on Pile Neutron Research and Physics, Vienna, Austria, October 1960*, Intern. At. Energy Agency, Vienna, 1962.

Cable, J. W., M. K. Wilkinson, E. O. Wollan, and W. C. Koehler, "Neutron Diffraction Investigation of the Magnetic Order in MnI_2," *Phys. Rev.* **125**, 1860–64 (1962).

Cable, J. W., M. K. Wilkinson, E. O. Wollan, and W. C. Koehler, "A Neutron Diffraction Study of Antiferromagnetic $FeCl_3$," *Phys. Rev.* **127**, 714–17 (1962).

Cable, J. W., E. O. Wollan, W. C. Koehler, and H. R. Child, "Antiferromagnetism of the Antiphase Domain Structure of Pd_3Mn," *Phys. Rev.* **128**, 2118–20 (1962).

Cable, J. W., E. O. Wollan, W. C. Koehler, and M. K. Wilkinson, "Neutron Diffraction Investigations of Ferromagnetic Palladium and Iron Group Alloys," in *Proceedings of the Conference on Magnetism and Magnetic Materials, Phoenix, Arizona, November 1961; J. Appl. Phys. Suppl.* **33**, 1340 (1962).

Campbell, E. C., and P. Fettweis, "Convoyeur Pneumatique Rapide Pour l'Irradiation D'Echantillons Dans un Réacteur" ("Rapid Pneumatic Transfer Device for the Irradiation of Samples in a Reactor"), *Nucl. Instr. Methods* **14**, 272–78 (1962).

Carlson, T. A., and R. M. White, "Decomposition of $(CH_3Xe^{131})^+$ Following the Nuclear Decay of CH_3I^{131}," *J. Chem. Phys.* **36**, 2883–87 (1962).

Charles, G. W., "Isoelectronic Sequences (Spectroscopy)," pp 96–97 in *Encyclopaedic Dictionary of Physics*, vol 4, ed. by J. Thewlis, Pergamon, New York, 1961.

Charles, G. W., "Optical Doublets, Regular and Irregular, Laws of," pp 212–13 in *Encyclopaedic Dictionary of Physics*, vol 5, ed. by J. Thewlis, Pergamon, New York, 1962.

Charles, G. W., "Spectrograph, Grazing Incidence," pp 706–7 in *Encyclopaedic Dictionary of Physics*, vol 6, ed. by J. Thewlis, Pergamon, New York, 1962.

Charles, G. W., "Vacuum Ultraviolet Spectroscopy," pp 756–57 in *Encyclopaedic Dictionary of Physics*, vol 6, ed. by J. Thewlis, Pergamon, New York, 1962.

Dabbs, J. W. T., "Nuclear Alignment, Orientation and Polarization," pp 79–80 in *Encyclopaedic Dictionary of Physics*, vol 5, ed. by J. Thewlis, Pergamon, New York, 1962.

Dabbs, J. W. T., "Reliability in Helium Liquefaction," pp 105–7 in *Proceedings of the Conference of Institute International du Froid, London, England, September 1961*, Inst. Intern. du Froid, Paris, 1962.

Drisko, R. N., R. H. Bassel, and G. R. Satchler, "Distorted-Waves Analysis of Quasi-Elastic (p,n) and (He^3,t) Reactions," *Phys. Letters* **2**, 318–20 (1962).

Eichler, E., G. D. O'Kelley, R. L. Robinson, J. A. Marinsky, and N. R. Johnson, "Nuclear Levels of Ge^{74}," *Nucl. Phys.* **35**, 625–44 (1962).

Fettweis, P., and E. C. Campbell, "Étude de Quelques Isomères Nucléaires Products Par Les Neutrons d'un Réacteur" ("Study of Some Nuclear Isomers Produced by Reactor Neutrons"), *Nucl. Phys.* **33**, 272 (1962).

Fowler, J. L., and E. C. Campbell, "Total Neutron Cross Section of Pb^{208}," *Phys. Rev.* **127**, 2192–97 (1962).

Fowler, T. K., "Theoretically Stable and Confined Plasma," *Phys. Fluids* **5**, 249–50 (1962).

Fowler, T. K., and M. Rankin, "Plasma Potential and Energy Distributions in High-Energy Injection Machines," *J. Nucl. Energy, Pt. C* **4**, 311–20 (1962).

Harvey, J. A.. "Neutron Absorption," pp 813–14 in *Encyclopaedic Dictionary of Physics*, vol 4, ed. by J. Thewlis, Pergamon, New York, 1961.

Harvey, J. A., "Neutron Cross Section, Energy Dependence of," p 815 in *Encyclopaedic Dictionary of Physics*, vol 4, ed. by J. Thewlis, Pergamon, New York, 1961.

Harvey, J. A., "Neutron Flux, Standardization and Measurement of," p 825 in *Encyclopaedic Dictionary of Physics*, vol 4, ed. by J. Thewlis, Pergamon, New York, 1961.

Harvey, J. A., "Neutron Monochromator: Mechanical and Time-of-Flight," p 828 in *Encyclopaedic Dictionary of Physics*, vol 4, ed. by J. Thewlis, New York, 1961.

Harvey, J. A., "Neutron Reflection and Refraction," p 835 in *Encyclopaedic Dictionary of Physics*, vol 4, ed. by J. Thewlis, Pergamon, New York, 1961.

Harvey, J. A., "Present Status of Intermediate Energy Cross Section Measurements with Fast Choppers," pp 64–90 in *Proceedings of Neutron Physics Symposium, Troy, New York, May 1961*, ed. by M. L. Yeater, Academic Press, New York, 1962.

Hecht, K. T., and G. R. Satchler, "Asymmetric Rotator Model of Odd-Mass Nuclei," *Nucl. Phys.* **32**, 286–318 (1962).

Ilakovac, K., L. G. Kuo, M. Petravic, I. Slaus, P. Tomas, and G. R. Satchler, "The Reaction $V^{51}(n,d)Ti^{50}$ at 14.4 Mev," *Phys. Rev.* **128**, 2739–44 (1962).

Kjellman, J., T. Dazai, and J. H. Neiler, "An Angular Correlation Study of the $Be^9(\alpha,n)C^{12*}(\gamma 4.43)C^{12}$ Reaction," *Nucl. Phys.* **30**, 131–39 (1962).

Koehler, W. C., J. W. Cable, E. O. Wollan, and M. K. Wilkinson, "Magnetic Structures of Thulium," *Phys. Rev.* **126**, 1672–78 (1962).

Koehler, W. C., J. W. Cable, E. O. Wollan, and M. K. Wilkinson, "Neutron Diffraction Study of Magnetic Ordering in Thulium," in *Proceedings of the Conference on Magnetism and Magnetic Materials, Phoenix, Arizona, November 1961; J. Appl. Phys. Suppl.* **33**, 1124–25 (1962).

Koehler, W. C., J. W. Cable, E. O. Wollan, and M. K. Wilkinson, "Recent Progress in Magnetic Structure Determinations of Rare Earth Metals," *J. Phys. Soc. Japan (Suppl. BIII)* **17**, 32–35 (1962).

Lamphere, R. W., "Fission Cross Section and Fragment Angular Distribution for Fast Neutron-Induced Fission of U^{234}," *Nucl. Phys.* **38**, 561–89 (1962).

McDaniels, D. K., D. L. Hendrie, R. H. Bassel, and G. R. Satchler, "Alpha-Gamma Angular Correlations and the Distorted-Waves Theory," *Phys. Letters* **1**, 295–97 (1962).

McGowan, F. K., and P. H. Stelson, "Coulomb Excitation of Second 2^+ States in Ge^{74}, Ge^{76}, Se^{76}, Se^{78}, and Se^{80}," *Phys. Rev.* **126**, 257–63 (1962).

Macklin, R. L., G. de Saussure, J. D. Kington, and W. S. Lyon, "Manganese Bath Measurements of η of Pu^{239}," *Nucl. Sci. Eng.* **14**, 101–3 (1962).

Macklin, R. L., T. Inada, and J. H. Gibbons, "Neutron Capture in Tin Isotopes at Stellar Temperatures," *Nature* **194**, 1272 (1962).

Merzbacher, E., "The Single-Valuedness of Wave Functions," *Am. J. Phys.* **30**, 237–47 (1962).

Morgan, H. W., and P. A. Staats, "Infrared Spectra of Dilute Solid Solutions," *J. Appl. Phys. Suppl.* **33**, 364–66 (1962).

Neiler, J. H., "Neutron Capture Cross Sections for Energies Above a Few Hundred ev," pp 95–109 in *Proceedings of the Conference on Physics of Fast and Intermediate Reactors, Vienna, Austria, August 1961*, Intern. At. Energy Agency, Vienna, 1962.

Obenshain, F. E., and H. H. F. Wegener, "Mössbauer Effect with Ni^{61}," pp 148–55 in *Proceedings of the Second International Congress on Mössbauer Effect, Saclay, France, September 1961*, ed. by D. M. J. Compton and A. H. Schoen, Wiley, New York, 1962.

Ritter, R. C., P. H. Stelson, F. K. McGowan, and R. L. Robinson, "Coulomb Excitation with Ne^{20} Ions," *Phys. Rev.* **128**, 2320–31 (1962).

Roberts, L. D., book review, *The Theory of the Transition Metal Ions* (by J. S. Griffith, Cambridge University Press, New York), *Phys. Today* **15**, 70 (1962).

Robinson, R. L., N. R. Johnson, and E. Eichler, "Decay of Cs^{132}," *Phys. Rev.* **128**, 252–57 (1962).

Robinson, R. L., F. K. McGowan, and P. H. Stelson, "Coulomb Excitation of Levels in Se^{77}," *Phys. Rev.* **125**, 1373–78 (1962).

Schmid, Erich, "A Monte Carlo Method for Nuclear Many-Body Problems," *Nucl. Phys.* **32**, 82–97 (1962).

Schmitt, H. W., J. H. Neiler, F. J. Walter, and A. Chetham-Strode, "Mass Distribution and Kinetics of U^{235} Thermal-Induced Three-Particle Fission," *Phys. Rev. Letters* **9**, 427–29 (1962).

Sherwood, J. E., "A Source of Polarized Ions," *Nucl. Instr. Methods* **15**, 103–11 (1962).

Stelson, P. H. (ed.), *Conference on the Electromagnetic Lifetimes and Properties of Nuclear States, Gatlinburg, Tennessee, October 1961*, Nuclear Science Series Report No. 37, Publication 974, National Academy Sciences – National Research Council, Washington, D.C., 1962.

Stelson, P. H., and F. K. McGowan, "Coulomb Excitation of the First 2^+ State of Even-Even Nuclei with $58 \leqq A \leqq 82$," *Nucl. Phys.* **32**, 652–68 (1962).

Trammell, G. T., "Elastic Scattering at Resonance from Bound Nuclei," *Phys. Rev.* **126**, 1045–54 (1962).

Trammell, G. T., "Sound Waves in Water Containing Vapor Bubbles," *J. Appl. Phys.* **33**, 1662–70 (1962).

Van der Spuy, E., "A Self-Consistent Cutoff and a Baryon, Meson Model," *Nucl. Phys.* **29**, 400–441 (1962).

Van der Spuy, E., "A Fundamental Particle Model II," *Nucl. Phys.* **34**, 341–66 (1962).

Wegener, H., F. E. Obenshain, and M. E. Rose, "A Mössbauer-Parity-Experiment with Ni^{61}," pp 156–59 in *Proceedings of the Second International Congress on Mössbauer Effect, Saclay, France, September 1961*, ed. by D. M. J. Compton and A. H. Schoen, Wiley, New York, 1962,

Welton, T. A., "Nuclear Reactor Period," pp 136–38 in *Encyclopaedic Dictionary of Physics*, vol 5, ed. by J. Thewlis, Pergamon, New York, 1962.

Wilkinson, M. K., H. R. Child, W. C. Koehler, J. W. Cable, and E. O. Wollan, "Recent Magnetic Neutron Scattering Investigations at Oak Ridge National Laboratory," *J. Phys. Soc. Japan (Suppl. BIII)* **17**, 27–31 (1962).

Wilkinson, M.K., E. O. Wollan, W. C. Koehler, and J. W. Cable, "Investigations of Paramagnetic Neutron Scattering from Chromium," *Phys. Rev.* **127**, 2080–83 (1962).

Williams, C. W., and J. H. Neiler, "Design Considerations for Maximum Bandwidth in Transistorized Pulse Amplifiers," *IRE Trans. Nucl. Sci.* **9**(5), 1–6 (1962).

Wollan, E. O., J. W. Cable, W. C. Koehler, and M. K. Wilkinson, "Magnetic Moment Distribution in Palladium and Iron Group Alloys," *J. Phys. Soc. Japan (Suppl. BIII)* **17**, 38–40 (1962).

PAPERS PRESENTED AT SCIENTIFIC AND TECHNICAL MEETINGS

American Chemical Society, Washington, D.C., March 21–24, 1962

T. A. Carlson and R. M. White, "Decomposition of $(CH_3Xe^{130})^+$ Following the Beta Decay of CH_3I^{130}."

American Physical Society, Baltimore, Maryland, March 26–29, 1962

W. C. Koehler, E. O. Wollan, J. W. Cable, and M. K. Wilkinson, "Magnetization of a Helical Spin Structure: Holmium."

Southeastern Section of the American Physical Society, Tallahassee, Florida, April 5–7, 1962

L. K. Akers, R. T. Overman, and L. D. Roberts, "Summer Institute in Modern Physics."

C. J. Bergeron, L. D. Roberts, and R. W. Boom, "Superconducting Tests of NbZr in a High-Field Magnet."

E. C. Campbell (invited talk), "Coherent Mössbauer Reflection from Fe^{57}."

R. W. Boom and L. D. Roberts, "Transformer-Type Limiting of the Transition Rate in a Superconducting Magnet."

H. O. Cohn, W. M. Bugg, and R. D. McCulloch, "A 7090 Program for Bubble Chamber Track Reconstruction."

J. L. Fowler, "Differential Neutron Cross Sections with a Few kev Energy Resolution."

R. F. King and W. H. du Preez, "Count-Down System for Pulsed Van de Graaff Accelerator."

C. D. Moak, H. E. Banta, R. F. King, and J. W. Johnson, "Duo Plasmatron Beam Pulser for Van de Graaff Accelerators."

L. D. Roberts and R. W. Boom, "Studies on a 33-kgauss Superconducting Magnet."

L. D. Roberts, H. Pomerance, J. O. Thomson, and C. F. Dam, "A Mössbauer Study of a Series of Gold Alloys and Compounds."

German Physical Society (Verband Deutschen Physikalischen Gesellschaften), Bad Pyrmont, Germany, April 10–11, 1962

J. K. Bienlein and Frances Pleasonton, "Halbwertszeit von He^6" ("Half-Life of He^6").

American Physical Society, Washington, D.C., April 23–26, 1962

R. H. Bassel, R. M. Drisko, E. Rost, and G. R. Satchler, "Analysis of the Inelastic Scattering of Alpha Particles."

J. R. Bird, J. H. Gibbons, and W. M. Good, "Gamma-Ray Spectra from Capture of 30-kev Neutrons."

E. C. Campbell and S. Bernstein, "Magnetic Effects in Resonant Gamma Reflection from Fe^{57} Mirror."

F. A. Khan and J. A. Harvey, "High Resolution Neutron Total Cross Section Measurements on $Sn^{116,117,118,119,120}$."

R. L. Macklin and J. H. Gibbons, "Large Liquid Scintillator Pulse Shape Calculations."

R. L. Macklin and T. Inada, "30-kev Neutron Capture Cross Sections."

L. D. Roberts and J. O. Thomson, "Isomer Shift and Magnetic Field at the Nucleus of Au^{197} in Au-Ni."

R. L. Robinson, N. R. Johnson, and E. Eichler, "Decay of Cs^{132}."

J. E. Russell, R. W. Hockenbury, and R. C. Block, "Neutron Time-of-Flight Spectrometer with the RPI Linear Electron Accelerator."

P. H. Stelson and R. L. Robinson, "Excitation of Collective States in Sn and Fe by Inelastic Scattering of 14-Mev Neutrons."

J. O. Thomson and L. D. Roberts, "The Magnetic Moment of the First Excited State of Au^{197} and the Effective Field at the Au Nucleus in 1% Alloys of Au with Fe, Co, and Ni."

F. J. Walter, A. Chetham-Strode, J. H. Neiler, and H. W. Schmitt, "Correlated Energy Measurements of Fission Fragment Pairs."

Atomic Energy Commission Theoretical Meeting, New York, April 30–May 1, 1962

T. K. Fowler, "Secondary Plasma Growth."

Midwest Theoretical Physics Conference, Argonne, Illinois, June 1–2, 1962

G. R. Satchler (invited paper), "Inelastic Scattering of Alpha Particles."

Symposium on Molecular Structure and Spectroscopy, Columbus, Ohio, June 11–15, 1962

H. W. Morgan and P. A. Staats, "Vibrational Spectra of the BO_2^- Ion in Solid Solutions."

American Nuclear Society, Boston, Massachusetts, June 17–21, 1962

R. L. Macklin, G. de Saussure, J. D. Kington, and W. S. Lyon, "Manganese Bath Measurements of Eta of Plutonium-239."

Netherlands-Norway Reactor School (Summer School on "The Neutron Crystal Spectrometer in Theory and Practice"), Kjeller, Norway, June 18–29, 1962

W. C. Koehler

1. "History of Neutron Diffraction."
2. "Neutron Diffraction Applied to Magnetic Problems."
3. "Mechanical Design Considerations for Neutron Spectrometers."
4. "Cryostats and Magnets."
5. "Review of Work at ORNL."

American Physical Society, Evanston, Illinois, June 19–21, 1962

T. K. Fowler, "Plasma Stability and Constants of Motion."

Summer School on "Solid State Physics Problems," Rhodes, Greece, July 15–20, 1962

W. C. Koehler, "Applications of Neutron Diffraction to Study of Magnetic Materials."

High-Energy Instrumentation Conference, Geneva, Switzerland, July 16–18, 1962

R. W. Boom, L. D. Roberts, and R. S. Livingston, "Developments in Superconductor Solenoids."

Gordon Research Conference on Inorganic Chemistry, New Hampton, New Hampshire, August 6–10, 1962

E. O. Wollan (invited paper), "Some Considerations Regarding Magnetic Coupling."

Fisk University Infrared Institute, Nashville, Tennessee, August 14–24, 1962

H. W. Morgan, "Infrared Spectra and Molecular Environments."

P. A. Staats

1. "Infrared Techniques – Cell Making."
2. "Infrared Techniques – Solid Phase Sampling."
3. "Qualitative and Quantitative Analysis by Infrared."
4. "Infrared Techniques – Special Sampling."

International Symposium on Direct Interactions and Nuclear Reaction Mechanisms, Padova, Italy, September 3–8, 1962

R. H. Bassel, R. M. Drisko, and G. R. Satchler, "Analysis of Pick-Up Reactions in the $A = 90$ Region."

R. H. Bassel, R. M. Drisko, and G. R. Satchler, "Charge-Exchange 'Elastic' Scattering Between Mirror States."

J. R. Bird, J. H. Gibbons, and W. M. Good, "Evidence Concerning the Importance of 'Direct' or 'Potential' Neutron Capture at Low Energies."

E. C. Halbert, R. H. Bassel, and G. R. Satchler, "Optical Model Analysis of Elastic Deuteron Scattering."

L. D. Roberts (invited paper), "On the Use of Nuclear Targets Oriented at Low Temperatures."

G. R. Satchler[1] (review paper), "Distorted-Wave Theory of Direct Nuclear Reactions."

G. R. Satchler and E. Sheldon, "Analysis of Gamma Radiation from Inelastic Scattering Reactions."

G. R. Satchler, K. Ilakovac, L. G. Kuo, M. Petraric, I. Slaus, and P. Tomas, "$V^{51}(n,d)$ Reaction at 14 Mev."

P. H. Stelson and R. L. Robinson, "Excitation of Collective States by Inelastic Scattering of 14-Mev Neutrons."

Low-Energy Nuclear Physics Conference, Harwell, England, September 12–14, 1962

R. C. Block, "Neutron Total Cross Section and Capture Measurements on Zr."

F. A. Khan, T. Fuketa, and J. A. Harvey, "Parameters of the Neutron Resonances of the Stable Isotopes of Tin."

J. E. Russell, R. W. Hockenbury, and R. C. Block, "Neutron Radiative Capture Measurements with the Rensselaer Polytechnic Institute Electron Linear Accelerator."

International Conference on Low Temperature Physics, London, England, September 16–22, 1962

L. D. Roberts, R. W. Boom, and F. E. Obenshain, Jr., "Superconducting Magnet Studies."

L. D. Roberts and J. O. Thomson, "A Study of the Magnetic Properties of Gold in Alloys with Iron, Cobalt, and Nickel at 4.2°K by the Recoilless Radiation Method."

Culham Laboratory Study Group on Plasma Instabilities, Harwell, England, September 17–22, 1962

T. K. Fowler, "Non-Linear Stability."

Conference on Recoilless Nuclear Resonance Absorption, Pasadena, California, November 2, 1962

E. C. Campbell (invited talk), "Scattering Experiments."

Advances in Meson and Nuclear Research Below 1 Bev (ORINS-ORNL Nuclear Facilities Group), Gatlinburg, Tennessee, November 12–13, 1962

G. R. Satchler (invited paper), "Nuclear Structure and the Inelastic Scattering of High Energy Nucleons."

Conference on Magnetism and Magnetic Materials, Pittsburgh, Pennsylvania, November 12–15, 1962

J. W. Cable, E. O. Wollan, and W. C. Koehler, "The Atomic Magnetic Moments in Dilute Iron-Palladium Alloys."

---

[1]G. R. Satchler also assisted in Conference arrangements as a member of the Scientific Organizing Committee.

W. C. Koehler, H. R. Child, E. O. Wollan, and J. W. Cable, "Some Magnetic Structure Properties of Tb and of Tb-Y Alloys."

American Physical Society, Cleveland, Ohio, November 23–24, 1962

T. Fuketa and J. A. Harvey, "Parameters of Neutron Resonances in $Sn^{112,114,115,122,124}$."

G. G. Slaughter, J. R. Bird, G. T. Chapman, and J. A. Harvey, "Gamma Ray Spectra from Low Energy Neutron Capture."

Tennessee Academy of Science, Nashville, Tennessee, November 23–24, 1962

J. L. Fowler, "Summer Student Trainee Program in the Physics Division."

D. N. Mashburn, "Examples of Hyperfragments Produced in K^- Meson Interactions with Nuclei."

H. B. Willard, "A Cooperative Program in Graduate Education Between ORNL and the Southern Universities."

Division of Plasma Physics of the American Physical Society, Atlantic City, New Jersey, November 28–December 1, 1962

T. K. Fowler, "Plasma Stability and Lyapunov Functions."

Southeastern Symposium on Spectroscopy, Gainesville, Florida, January 21–24, 1963

T. A. Welton (invited paper), "Laser Theory (I and II)."

American Physical Society, New York, January 22–25, 1963

J. W. T. Dabbs, F. J. Walter, and G. W. Parker, "Resonance Fission of Oriented U^{235} Nuclei."

J. L. Fowler, "Differential Cross Section for Neutron Scattering from Pb^{208}."

T. Fuketa, F. A. Khan, and J. A. Harvey, "Shell Structure Effects on *S*-Wave Neutron Strength Functions and Level Spacings of the Tin Isotopes."

J. H. Gibbons, W. M. Good, and J. R. Bird, "Resonance Neutron Capture in F, Ca, and Pb."

R. L. Macklin, T. Inada, and J. H. Gibbons, "Isotopic Neutron Capture Cross Sections near 30 kev."

F. E. Obenshain, L. D. Roberts, and H. H. F. Wegener, "Measurement of the Magnetic Field at the Iron Nucleus in Several Iron-Rhodium Alloys as a Function of Temperature."

L. D. Roberts, R. L. Becker, and J. O. Thomson, "Relationship Between the Alloy Residual Electrical Resistance and the Mössbauer Isomer Shift of Gold for Several Cu-Au and Ag-Au Alloys."

R. L. Robinson, F. K. McGowan, and P. H. Stelson, "Coulomb Excitation of Br^{79}."

J. E. Russell, R. W. Hockenbury, and R. C. Block, "Neutron Capture Measurements on Tungsten and Hafnium."

H. W. Schmitt, J. H. Neiler, F. J. Walter, and A. Chetham-Strode, "Mass Distribution and Kinetics of U^{235} Thermal-Neutron-Induced Three-Particle Fission."

G. G. Slaughter, J. R. Bird, J. A. Harvey, and G. T. Chapman, "Neutron Capture Gamma Rays from Isotopes of Calcium and Titanium."

J. O. Thomson and L. D. Roberts, "Dependence of the Mössbauer Isomer Shift for Au^{197} on Alloy Composition for the Systems Pd-Au and $Ni_{1-x}Cu_{x-0.01}Au_{0.01}$."

F. J. Walter, C. D. Moak, J. H. Neiler, H. W. Schmitt, W. M. Gibson, and T. D. Thomas, "Response of Silicon Detectors to High Energy Bromine and Iodine Ions."

ANNOUNCEMENTS

Assignees to the various research groups within the Physics Division during the past year were as follows: J. A. Biggerstaff (High Voltage Group); K. T. R. Davies (Theoretical Physics Group); P. F. M.

Fettweis[1] of the Centre d'Etude l'Energie Nucleaire, Mol, Belgium (Mössbauer Program); J. L. C. Ford, Jr. (High Voltage Group); C. M. Jones (High Voltage Group); H. J. Kim (Charged Particle Compilation Group); P. J. Pasma[1] of the Dutch Foundation for Fundamental Research on Matter, Groningen, The Netherlands (High Voltage Group); T. Tamura[1] of the Tokyo University of Education, Tokyo, Japan (Theoretical Physics Group); and R. K. H. Wagner[1] of the University of Basel, Basel, Switzerland (High Voltage Group).

Loanees to the Division during this period included: M. Brown,[1] graduate student at the University of Tennessee (High Voltage Group); R. M. Haybron,[1] graduate student at Michigan State University (Theoretical Physics Group); and R. A. Zingaro,[1] associate professor from Texas A. and M. College (Spectroscopy Research Group).

N. H. Lazar (Scintillation Spectrometry Group) transferred to the Thermonuclear Division, and M. K. Wilkinson (Neutron Diffraction Group) transferred to the Solid State Division.

The following individuals completed assignments or terminated employment during this report year: J. R. Bird[1] of the Atomic Energy Research Establishment, Harwell, England (Fast Chopper Group and High Voltage Group); G. P. Felcher[1] of the Center for Nuclear Information, Studies and Experiments, Milan, Italy (Neutron Diffraction Group); T. Fuketa[1] of the Japanese Atomic Energy Research Institute, Tokai, Japan (Fast Chopper Group); T. Inada[1] of the National Institute of Radiological Sciences, Chiba, Japan (High Voltage Group); F. A. Khan[1] of the Pakistan Atomic Energy Commission, Karachi, Pakistan (High Voltage Group and Fast Chopper Group); J. H. Neiler (Scintillation Spectrometry Group); O. B. Rudolph[2] (Optical Physics Group); E. Sheldon[1] of the Laboratorium für Kernphysik, E.T.H., Zurich, Switzerland (Theoretical Physics Group); G. T. Trammell (Theoretical Physics Group); and G. S. Vourvopoulos[1,3] of the Greek Atomic Energy Commission, Athens, Greece (Mössbauer Program).

R. C. Block of the Fast Chopper Group is on a one-year assignment at the Atomic Energy Research Establishment in Harwell, England, where he is engaged in research with the electron linear accelerator. This assignment is a continuation of the profitable liaison in physics between AERE and ORNL, which originated in 1959, and is the fourth such exchange-type assignment.

J. H. Gibbons of the High Voltage Group is on loan to the Oak Ridge Institute of Nuclear Studies. Temporarily, he is Head of the University Participation Section of the University Relations Division of the Institute.

W. C. Koehler was appointed Associate Group Leader of the Neutron Diffraction Group during this period.

P. H. Stelson of the High Voltage Group is on leave for one year to Rice University, where he is engaged in nuclear physics research and in conducting sophomore courses in electricity and magnetism and in modern physics. He is also supervising the Ph.D. thesis research of physics graduate students at Rice University.

---

[1]Temporary assignment.

[2]Retirement.

[3]Presently a graduate student at Florida State University.

S. Bernstein of the Mössbauer Program and C. H. Johnson of the Charge Spectrometry Group returned to ORNL on completion of academic-year assignments at the University of Miami and the University of Minnesota respectively. P. D. Miller has resumed work with the High Voltage Group following a one-year assignment at the Atomic Energy Research Establishment in Harwell, England. Frances Pleasonton of the Charge Spectrometry Group has also returned to ORNL following a six-month assignment at the University of Erlangen/Nürnberg, Germany.

ADVISORY COMMITTEE

Research programs in the Physics Division and the Electronuclear Division are reviewed by a joint Advisory Committee at their Annual Information Meeting. Committee members at the time of the August 20–23, 1962, meeting were as follows:

Prof. H. Feshbach	Massachusetts Institute of Technology Cambridge
Prof. W. A. Fowler	California Institute of Technology Pasadena
Dr. M. Goldhaber	Brookhaven National Laboratory Upton, New York
Prof. L. J. Rainwater	Columbia University New York
Prof. J. A. Wheeler	Princeton University Princeton, New Jersey

ACTIVITIES RELATED TO EDUCATIONAL INSTITUTIONS

Research Participants

The Oak Ridge Research Participation Program[1] enables selected university faculty members to participate in pure or applied research at Oak Ridge laboratories; the Oak Ridge National Laboratory provides most of these appointments. In the summer of 1962, 54 research participants (representing 43 colleges and universities in 19 states) received appointments under this program. The following five investigators were engaged in research with the Physics Division: R. W. Lide (assistant professor, University of Tennessee), Physics of Fission Group; R. D. Powers (assistant professor, Baylor University), High Voltage Group; C. M. Shakin (instructor, Massachusetts Institute of Technology), Theoretical Physics Group; E. S. Snyder (associate professor, Ursinus College), Scintillation Spectrometry and Instrument Development Group; and B. S. Thomas (assistant professor, University of Florida), Optical Physics Group.

[1]Oak Ridge Institute of Nuclear Studies, Inc., in cooperation with the Oak Ridge National Laboratory.

Summer Visitors

Summer visitors with the Division in 1962 included: J. L. Anderson, Jr. (graduate student, University of Illinois), Charged Particle Compilations Group; W. M. Bugg (assistant professor, University of Tennessee), High Energy Accelerator Research Group; D. C. Choudhury[2] (assistant professor, University of Connecticut), Theoretical Physics Group; J. R. Cullen (graduate student, University of Maryland), Theoretical Physics Group; V. M. deLany (graduate student, University of California at Berkeley), Theoretical Physics Group; G. W. Erickson[3] (research associate, University of North Carolina), Theoretical Physics Group; D. W. Forester (graduate student, University of Tennessee), Low Temperature Group; T. B. Kaiser[4] (undergraduate student, St. Edward's University), High Energy Accelerator Research Group; J. Kronsbein (professor, University of Florida), Theoretical Physics Group; F. B. Malik[5] (visiting Fellow, Princeton University), Theoretical Physics Group; D. O. Patterson[6] (undergraduate student, University of Tennessee), High Energy Accelerator Research Group; H. A. Stewart (undergraduate student, California Institute of Technology), Neutron Diffraction Group; T. Terasawa[7] (assistant professor, Western Reserve University), Theoretical Physics Group; J. B. Thomas[8] (undergraduate student, Vanderbilt University), Theoretical Physics Group; J. O. Thomson (assistant professor, University of Tennessee), Low Temperature Group; and H. H. F. Wegener (professor, University of Erlangen/Nürnberg, Germany), Scintillation Spectrometry and Instrument Development Group.

Student Trainee Program

The cooperative ORINS-ORNL Student Trainee Program (under the sponsorship of the U.S. Atomic Energy Commission) was set up to give students from small colleges, primarily but not exclusively, in the South the opportunity of working in a full-time research laboratory during the summer months following completion of their junior year of college. This program serves also to encourage students to carry on graduate work after they have attained the bachelor degree in science.

In 1962, the fourth year of the Student Trainee Program, students with the Division under the auspices of this program were: D. L. Ewing (Centenary College of Louisiana), Spectroscopy Research Group; T. M. Hayes (Bowdoin College), High Voltage Group; A. L. Marusak (University of Dallas), High Energy Accelerator Research; and R. F. Smith (Arkansas Polytechnic College), Scintillation Spectrometry and Instrument Development Group. T. A. E. C. Pratt (Hampton Institute) worked with the High Voltage Group on an assignment similar to that of a student trainee; his stay with the Division was, however, sponsored by the Agency for International Development, Department of State.

---

[2]Presently with the Polytechnic Institute of Brooklyn.

[3]Presently with New York University.

[4]Presently a graduate student at the University of Illinois.

[5]On leave from the Pakistan Atomic Energy Commission.

[6]Presently a graduate student at the University of Tennessee.

[7]On leave from Tokyo University.

[8]Presently a graduate student at Stanford University.

To date, 21 student trainees have completed summer assignments with the Physics Division. A recent survey of former Physics Division student trainees showed that approximately three-fourths of the students are now working toward a doctor's degree.

Co-op Students

The Co-op Program of the Oak Ridge National Laboratory is designed for promising students in engineering and science who have completed at least two quarters of undergraduate study. Students selected for the Co-op Program alternate between three months of work as technical assistants at the Laboratory and three months of school attendance. This program has proved to be highly successful, both as a means for promoting the professional development of the students and for providing valuable technical assistants for scientific research in the Laboratory. Ten Co-op students were with the Division during the past year and were assigned to the High Voltage Group, the High Energy Accelerator Research Group, and the Mössbauer Program. These students included: J. F. Agnew, M. B. Johnson, L. W. Owen, and J. H. Williams[9] of the Virginia Polytechnic Institute in Blacksburg; R. M. Eyer,[10] S. L. Kramer, and R. E. Maydole[11] of the Drexel Institute of Technology in Philadelphia; and R. G. Beidel, D. N. Mashburn, and R. J. Metzger of the University of Tennessee in Knoxville.

Ph.D. Thesis Research

Fifteen staff members of the Physics Division served during the past year in an advisory or supervisory capacity for research conducted at the Laboratory by 15 Ph.D. candidates, as listed below:

Staff Member(s)	Ph.D. Candidate	Field of Research
T. A. Welton	H. Bertini[12] University of Tennessee	Monte Carlo Calculations on Intranuclear Cascades
E. O. Wollan and W. C. Koehler	H. R. Child University of Tennessee	Magnetic Properties of Rare-Earth Alloys
L. D. Roberts and F. E. Obenshain	D. W. Forester[13] University of Tennessee	Use of the Mössbauer Effect in the Study of Ferromagnetism and Antiferromagnetism at Low Temperatures
J. A. Harvey and H. W. Schmitt	A. K. Furr[12,14] Duke University (now with Virginia Polytechnic Institute)	Neutron Capture by Activation Techniques

[9]Completed co-op assignment during this period.

[10]Terminated co-op assignment during this period.

[11]Terminated co-op assignment during this period; now attending St. Joseph's College in Philadelphia.

[12]Doctorate received in 1962.

[13]National Science Foundation Cooperative Fellowship.

[14]Oak Ridge Graduate Fellowship.

J. H. Neiler	R. Gwin[12] University of Tennessee	Studies of the Scintillation Processes in CsI(Tl)
J. L. Fowler and R. L. Robinson	M. V. Harlow, Jr.[14] University of Texas	Elastic Scattering of Fast Neutrons by C^{12}
H. W. Schmitt	W. E. Kiker[14] University of Tennessee	The Physics of Fission
J. L. Fowler and W. M. Good	R. W. Lamphere[12] University of Tennessee	The Angular Distribution of Fission Fragments from the Fast-Neutron-Induced Fission of U^{234}
T. A. Welton	J. H. Marable University of Tennessee	Nuclear Three-Body Problem
F. K. McGowan	W. T. Milner University of Tennessee	Coulomb Excitation with Heavy Ions
H. W. Schmitt, J. H. Neiler, and L. D. Roberts	W. F. Mruk University of Tennessee	Double Time-of-Flight Analysis of Fission Fragments
H. O. Cohn	R. B. Muir[14] University of Tennessee	Sigma Particle Interactions from Berkeley Helium Bubble Chamber Data
G. R. Satchler	C. W. Nestor, Jr. Vanderbilt University	Theory of Nuclear Structure
G. R. Satchler	S. K. Penny University of Tennessee	Theory of Nuclear Reactions
J. W. T. Dabbs and H. W. Schmitt	F. J. Walter University of Tennessee	The Kinetics of Thermal and Resonance Neutron-Induced Fission

Oak Ridge Graduate Fellowship Program

In connection with the recently expanded Oak Ridge Graduate Fellowship Program of ORINS-ORNL, a Graduate Fellow Selection Panel for ORNL has been appointed. The purpose of this panel is to help select science and engineering participants for the program in the fields of biology, chemistry, engineering (chemical, mechanical, and nuclear), mathematics, physics, solid state, health physics, and metallurgy.

Physics Division staff members appointed to the ORNL Graduate Fellow Selection Panel include H. B. Willard[15] as Chairman and T. A. Welton[16] as panel member for (*a*) the physics and solid-state program and (*b*) the mathematics program.

Also actively engaged in the administration of the Graduate Fellowship Program is another Division staff member, J. H. Gibbons, who is temporarily serving as Head of the University Participation Section of the University Relations Division of ORINS.

---

[15]Three-year appointment extending through 1965.

[16]One-year appointment extending through 1963.

Oak Ridge Resident Graduate Program of the Physics Department of the University of Tennessee

Four staff members of the Physics Division have, during this report period, been affiliated with the Oak Ridge Resident Graduate Program of the Physics Department of the University of Tennessee. Those lecturers who have taught one graduate course per quarter include: R. L. Becker (Theoretical Physics), E. C. Campbell (Nuclear Physics), W. C. Koehler (Neutron Diffraction), and J. H. Neiler[17] (Nuclear Physics).

Since the graduate program of the University of Tennessee began operation in 1947, about one-half of the 46 Ph.D.'s granted in physics have been conferred on students enrolled in the Oak Ridge Resident Graduate Program.

Consultants Under Subcontract

University staff members currently serving as consultants to the Division are listed below. During the past year, numerous other consultants have presented seminar talks and have worked in collaboration with the various Physics groups.

L. C. Biedenharn, Jr. Duke University	Theoretical Physics Group
W. M. Bugg University of Tennessee	High Energy Accelerator Research Group
J. B. French University of Rochester	Theoretical Physics Group
J. H. Goldstein Emory University	Spectroscopy Research Group
W. G. Holladay Vanderbilt University	Theoretical Physics Group
J. M. Jauch University of Geneva, Geneva, Switzerland	Theoretical Physics Group
T. Lauritsen California Institute of Technology	High Voltage Group
R. W. Lide University of Tennessee	Physics of Fission Group
J. B. Marion University of Maryland	Fast Chopper Time-of-Flight Spectrometry Group
S. A. Moszkowski University of California at Los Angeles	Theoretical Physics Group
A. H. Nielsen University of Tennessee	Spectroscopy Research Group

[17]Now Technical Director, Oak Ridge Technical Enterprises Corporation.

H. W. Newson Duke University	High Voltage Group
W. T. Pinkston Vanderbilt University	Theoretical Physics Group
J. O. Thomson University of Tennessee	Low Temperature Group
K. Wildermuth Florida State University	Physics of Fission Group
J. H. Wise Washington and Lee University	Spectroscopy Research Group

One graduate student is presently under subcontract with the Division as a part-time consultant:

J. Ginocchio University of Rochester	Theoretical Physics Group

Visiting Scientist Lecture Program in Physics

The Visiting Scientist Lecture Program in Physics, now in its sixth year, is sponsored by the American Association of Physics Teachers and the American Institute of Physics and is supported by the National Science Foundation. J. H. Neiler delivered the following lectures under this Program during the past year:

Creighton University, Omaha, Nebraska, May 9, 1962

"Nuclear Physics, the Astronomer's Microscope"
(presented as a public lecture)

"Recent Advances in Nuclear Particle Detector"
(lecture to physics students)

Ottawa University, Ottawa, Kansas, May 10, 1962

"Nuclear Physics, the Astronomer's Microscope"
(presented at a general university assembly)

Traveling Lecture Program

The Traveling Lecture Program is conducted in cooperation with the Oak Ridge Institute of Nuclear Studies as a part of the AEC's program of disseminating scientific and technical information to universities, particularly those in the South. Laboratory personnel present in their lectures unclassified information to university undergraduate and graduate students and to faculty members. The lectures serve to stimulate interest in research in the university departments and also assist the teaching staff in expanding the scope of instruction offered under the regular curricula. Through such personal contacts, ORNL staff members are also able to observe departmental activities at the universities. Listed below are eight members of the Physics Division who participated in the Traveling Lecture Program during the academic year 1961–1962, presenting a total of 27 lectures. During the current academic

year, 1962–1963, eight members of the Division have so far presented 18 lectures under this Program; a complete listing of these will appear in the next annual report.

J. K. Bair	University of Kentucky, May 18, 1962 "Charged Particle Spectrometry"
J. W. Cable	Florida State University, May 18, 1962 University of Florida, May 18, 1962 "Recent Developments in the Magnetic Properties of Rare Earth Metals and Compounds"
E. C. Campbell	University of Texas, November 16, 1961 "New Frontiers in Low-Energy Nuclear Physics" Louisiana State University, November 17, 1961 "The Mössbauer Effect in Total Reflection" University of Cincinnati, February 23, 1962 "Recoil Free Nuclear Resonance Gamma Scattering in Total Reflection from Fe^{57} Mirror"
W. M. Good	Texas A and M College, December 1, 1961 Baylor University, December 4, 1961 "Neutron Spectroscopy by Time-of-Flight" Rice University, December 5, 1961 "Millimicrosecond Beam Pulsing and Time Spectrometry"
F. E. Obenshain, Jr.	Franklin and Marshall College, November 2 and 3, 1961 Catholic University of America, November 6, 1961 University of Cincinnati, December 8, 1961 Virginia Polytechnic Institute, February 20, 1962 University of Arizona, May 3, 1962 Arizona State University, May 4, 1962 "Mössbauer Effect and Nuclear Physics"
L. D. Roberts	University of North Carolina, April 11, 1962 "Solid State and Nuclear Results from a Mössbauer Type Study of Au^{197}" Georgia Institute of Technology, May 16, 1962 "Superconducting Magnets"
H. W. Schmitt	University of Texas, January 4, 1962 Texas A and M College, January 12, 1962 Mississippi College, January 15, 1962 "Recent Advances in the Physics of Fission"
T. A. Welton	University of South Carolina, November 9, 1961 University of Kentucky, November 15, 1961 University of Cincinnati, November 16, 1961 Georgia Institute of Technology, May 1, 1962 University of Miami, May 2, 1962 University of Florida, May 4, 1962 "Coherent Light"

University Seminars

In addition to the Visiting Scientist Lecture Program in physics and the Traveling Lecture Program, divisional staff members receive numerous requests from various universities for seminar talks. Fourteen invitations from American educational institutions and four from European educational institutions were accepted during the past report period:

S. Bernstein	Western Reserve University, January 10, 1963 Boston College, January 21, 1963 "Total Reflection of Nuclear Resonance Radiation"
E. C. Campbell	University of Tennessee, April 17, 1962 "Coherent Mössbauer Reflection from Fe^{57}"
J. W. T. Dabbs	University of Virginia, November 9, 1962 "Nuclear Orientation Studies on Uranium and Neptunium"
T. K. Fowler	University of Virginia, March 19, 1962 Rice University, April 11, 1962 "Some Problems and Methods in Plasma Physics"
W. C. Koehler	Institut Fourier, Grenoble, France, June 13, 1962 Centre d'Etudes Nucleaires de Grenoble, Grenoble, France, June 14, 1962 "Recent Neutron Diffraction Studies at Oak Ridge" Centre d'Etudes Nucleaires de Saclay, Saclay, France, June 25–26, 1962 "Magnetic Structure Studies at Oak Ridge"
R. L. Macklin	California Institute of Technology, October 18–19, 1962 "kev Neutron Measurements at ORNL"; "Neutron Capture Cross Sections and Their Astrophysical Implications" University of California at La Jolla, October 25, 1962 "Isotopic Neutron Capture Cross Sections and Applications in Nucleosynthesis"
P. D. Miller	University of Neuchatel, Neuchatel, Switzerland, May 1–2, 1962 "Time-of-Flight at Oak Ridge"; "He^3,n Studies" University of Georgia, November 28, 1962 "Nuclear Physics Research at Harwell"
L. D. Roberts	University of California at Berkeley, March 12, 1962 "The Isomer Shifts and Effective Magnetic Fields of Gold in a Series of Alloys and Compounds" Stanford University, March 13, 1962 "Emission of Alpha Particles from Oriented Actinide Nuclei" University of Illinois, December 14, 1962 "Solid State and Nuclear Results from a Mössbauer Type Study of Gold"
G. R. Satchler	University of Michigan, July 10, 1962 "Distorted-Wave Theory of Inelastic Scattering"

P. H. Stelson	Rice University, April 12, 1962 "Excitation of Collective States by Inelastic Scattering of 14-Mev Neutrons"

Educational Summer Institutes

W. C. Koehler (Neutron Diffraction Group) participated as a lecturer in an Advanced Study Institute, organized by the Netherlands-Norwegian Reactor School, on "The Neutron Crystal Spectrometer in Theory and Practice." This summer school was held June 18–27, 1962, at the Institute for Atomic Energy in Kjeller, Norway. Koehler also participated July 15–20, 1962, in a summer school on "Solid State Physics Problems" in Rhodes, Greece. Lectures presented during the course of these summer schools are listed in the section of this report entitled "Papers Presented at Scientific and Technical Meetings."

G. K. Werner[18] (Optical Physics Group) attended a two-week summer course in Modern Methods of Optical Design held at the University of Rochester, July 9–20, 1962.

ORINS-ORNL Summer Institute

The Oak Ridge Institute of Nuclear Studies, in cooperation with the Oak Ridge National Laboratory, conducted a Summer Institute for Physics Teachers, June 25 through August 17, 1962. This Institute, sponsored by the U.S. Atomic Energy Commission, was designed primarily to give participants an opportunity to review basic nuclear-energy concepts, acquire an understanding of current nuclear-energy developments, become familiar with new equipment, and gain greater insight into the development of college courses in the field. This year's program offered both lectures and demonstrations and tours by nuclear physicists from ORINS and ORNL. Twenty college professors from as many colleges participated in the Institute under AEC grants.

Four staff members of the Physics Division were included among the lecturers during the eight-week Institute. Fifteen lectures were presented by J. L. Fowler on "Nuclear Physics"; R. L. Becker presented three lectures on "Particles of Physics" and two lectures on "Theory of Beta Decay"; and J. W. Cable and T. A. Welton presented lectures on "Neutron Diffraction" and "Masers and Lasers" respectively. Demonstrations and tours conducted by members of the Division were as follows:

J. H. Gibbons and P. H. Stelson	High Voltage Laboratory of ORNL
L. D. Roberts and E. C. Campbell	Mössbauer Experiment at ORNL
J. A. Harvey	Neutron Chopper
H. W. Schmitt	Fission Time-of-Flight

[18]On loan from Thermonuclear Division.

Oak Ridge Nuclear Facilities Group

A symposium on "Recent Developments in Superconductivity and Instrumentation" was held April 5, 1962, at Florida State University in connection with the annual meeting of the Southeastern Section of the American Physical Society. This symposium, sponsored jointly by the Oak Ridge Nuclear Facilities Group and the Southeastern Section of the American Physical Society, was the second of a series of meetings and conferences of the Oak Ridge Nuclear Facilities Group,[19] which consists of nuclear physicists from the ORINS region.

The purpose of the Oak Ridge Nuclear Facilities Group is to encourage and facilitate informal scientific communication between individual scientists of the region and those at the Oak Ridge National Laboratory. It is a further purpose of the Group to make possible easy and rapid access to the use of equipment, especially at ORNL, when such use will benefit or advance the research being undertaken by any interested persons.

L. D. Roberts of the Physics Division served as program chairman for the symposium on "Recent Developments in Superconductivity and Instrumentation." J. L. Fowler, Director of the Division, is a member of the Steering Committee of the Oak Ridge Nuclear Facilities Group; a committee meeting took place following the symposium.

[19]The first meeting, entitled "Conference on Instrumentation and Technology," was held November 13–14, 1961, at the Oak Ridge National Laboratory. A third meeting, entitled "Advances in Meson and Nuclear Research Below 1 Bev," took place November 12–13, 1962, in Gatlinburg, Tennessee.

ORNL PHYSICS SEMINARS

Weekly divisional seminars are normally held at the Laboratory each Friday afternoon; additional seminars are frequently scheduled for topics of especial timeliness or interest. During the period covered by this report, P. H. Stelson served as seminar chairman until July 1962, at which time H. O. Cohn assumed his duties. Lectures scheduled included the following:

1962

February 16	T. A. Carlson, ORNL "Electron Shake-Off Following Beta Decay"
February 23	Brian Buck, ORNL "Strong Coupling Theory of Inelastic Scattering"
March 2	C. M. Jones,[1] Rice University "An Experimental Study of the Elastic Scattering of Alpha Particles from C^{12}"
March 9	J. W. T. Dabbs, ORNL "Physics in Argentina"

[1]Now with ORNL Physics Division.

March 16	P. A. Egelstaff, Atomic Energy Research Establishment "Scattering Law Measurements and Interpretation"
March 20	S. A. Moszkowski, University of California at Los Angeles "On the Theory of the Nuclear Shell Model"
March 21	David Shoenberg, University of Pittsburgh "The Fermi Surfaces of the Noble Metals"
March 22	H. Maier-Leibnitz, Laboratorium für Technische Physik der Technischen Hochschule Munchen "Physics Research Using the Swimming Pool Reactor at Munich, Germany"
March 30	H. B. Willard, ORNL "Angular Correlations in Nuclear Resonance Reactions"
April 2	L. C. Biedenharn, Duke University "Nuclear Structure Information from Inelastic Electron Scattering"
April 9	J. J. Hauser, Bell Telephone Laboratories "The Influence of Mechanical Structure on the Superconducting Properties of Hard Superconductors"
April 13	R. D. Present, University of Tennessee "Inter-molecular Three-Body Forces"
May 1	Jean Julien, French Atomic Energy Commission "Neutron Research at Saclay with the Linear Accelerator"
May 4	Richard Blieden, Florida State University "The (p,α) Reaction on Be^9 and B^{11}"
May 10, 17, 24, and 31	Eric Sheldon, Laboratorium für Kernphysik, E.T.H. "Nuclear Level Densities"
May 11	K. T. R. Davies,[1] Carnegie Institute of Technology "Symmetry Properties of the *S*-Matrix with Application to Resonance Reactions"
May 24	Herman Feshbach, Massachusetts Institute of Technology "Some Remarks on Nuclear Reactions"
June 1	Eric Sheldon, Laboratorium für Kernphysik, E.T.H. "Physics Research at the Swiss Federal Institute of Technology"
June 5	J. E. Russell, Rensselaer Polytechnic Institute "RPI-ORNL Neutron Capture Cross Section Program"
June 8	Eric Sheldon, Laboratorium für Kernphysik, E.T.H. "n'-γ and p'-γ Angular Correlation Research at E.T.H."
June 15	L. D. Roberts, ORNL "A Study of Nuclear and Solid State Properties of Gold-197"
June 19	Fazley Malik,[2] Princeton University "Variational Methods for Scattering Problems"

[2]Presented as part of a Special Theoretical Physics Seminar Series arranged by R. L. Becker.

June 22	Giuseppe Cocconi, Cornell University "Scattering of 10–30 Bev Protons on Protons"
June 26	R. L. Becker,[2] ORNL "Reaction Matrix Methods in Nuclear Theory"
June 29	R. K. Clayton, ORNL "Primary Events in Photosynthesis"
July 3	Vincent deLany,[2] University of California at Berkeley "Mandelstam Representation for Potential Scattering"
July 6	G. W. Erickson, University of North Carolina "A Review of Lamb Shift Calculations"
July 10	G. W. Erickson,[2] University of North Carolina "Calculational Methods in Quantum Electrodynamics"
July 13	J. R. Cullen, University of Maryland "Superconductivity"
July 17	Tokuo Terasawa,[2] Western Reserve University "The Effect of Pairing Correlations on the Optical Model"
July 20	D. C. Choudhury, University of Connecticut "Effects of Configuration Mixing on the 3^- States in Nuclei and (p,p') Reaction in the Distorted-Wave Approximation"
July 24	D. C. Choudhury,[2] University of Connecticut "Octupole-Octupole Interactions and 3^- States in Nuclei"
July 27	Michael Grace, Clarendon Laboratory "Low Temperature Polarization of Gold Nuclei in Ferromagnetic Iron"
July 31	T. A. Welton,[2] ORNL "Some Remarks on Vacuum Polarization"
August 3	P. H. Stelson, ORNL "Excitation of Collective States by Inelastic Scattering of 14-Mev Neutrons"
August 7	Carl Shakin,[2] Massachusetts Institute of Technology "Nuclear Elastic Scattering Theory"
August 9	Carl Shakin,[2] Massachusetts Institute of Technology "On Nuclear Photodisintegration"
August 10	R. D. Powers, Baylor University "Range of Heavy Ions in Solids in the Kev Region"
August 16	S. A. Moszkowski,[2] University of California at Los Angeles "Simulation of a Repulsive Core by Velocity Dependence"; "Two-Body Forces and Collective Motion"
August 17	Fazley Malik, Princeton University "Queries on Some Aspects of Nuclear Models"
August 27	Karl Wildermuth, Florida State University "The Structure of Light Nuclei and Nuclear Reactions"
August 28	B. S. Thomas,[2] University of Florida "Nucleon Form Factors"

August 29	Carl Shakin, Massachusetts Institute of Technology "On Model Calculations of Neutron Widths and Strength Functions"
September 7	Behram Kursunoglu, University of Miami "Brownian Motion in a Magnetic Field"
September 14	W. C. Koehler, ORNL "Some Neutron Diffraction Work in European Laboratories"
September 21	Toyojiro Fuketa, Japanese Atomic Energy Research Institute "Nuclear Physics Research at JAERI"
September 28	D. T. King, University of Tennessee "Anomalous Photon Emission from 3.5 Bev/c π^--Nucleus Collision"
October 5	H. H. F. Wegener, University of Erlangen/Nürnberg "The Bohm-Aharanov Effect"
October 12	R. J. Collins, Institute for Defense Analysis "Mode Structures in Optical Masers"
October 22	J. P. F. Sellschop, University of Witwatersrand "Low Q Stripping"
November 2	B. L. Cohen, University of Pittsburgh "Nuclear Structure Studies with Stripping Reactions"
November 9	L. A. Woodward, Oxford University "Recent Studies in Raman Spectroscopy at Oxford University"
November 14	L. C. Biedenharn,[2] Duke University "An Extension of the Elliot SU3 Model"
November 16	R. S. Tebble, University of Sheffield "The Magnetic Susceptibility of Some Transition Elements and Their Alloys"
November 30	A. de-Shalit, Weizmann Institute of Science "Core Excitations in Nuclei"
December 7	P. D. Miller, Jr., ORNL "Nuclear Physics Research at Harwell"
December 14	R. L. Macklin, ORNL "Stellar Nucleosynthesis and Kilovolt Neutron Capture Cross Sections"

1963

January 4	T. K. Fowler, ORNL "Current Status of Thermonuclear Research"
January 11	F. B. Malik,[2] Princeton University "Program for Relativistic Hartree Wave Function"
January 11	Taro Tamura, ORNL "Vibrational Motions in Even-Even Nuclei"
January 18	H. W. Schmitt, ORNL "Kinetics of Fission: Fragment Energy Correlation Measurements"

ORNL-3425
UC-34 – Physics
TID-4500 (20th ed.)

INTERNAL DISTRIBUTION

1. Biology Library
2–4. Central Research Library
5. Laboratory Shift Supervisor
6. Reactor Division Library
7–8. ORNL – Y-12 Technical Library Document Reference Section
9–84. Laboratory Records Department
85. Laboratory Records, ORNL R.C.
86. C. F. Barnett
87. P. R. Bell
88. D. S. Billington
89. E. P. Blizard
90. R. C. Block
91. C. J. Borkowski
92. G. E. Boyd
93. M. A. Bredig
94. R. B. Briggs
95. J. W. Cable
96. E. C. Campbell
97. H. R. Child
98. F. L. Culler
99. J. W. T. Dabbs
100. G. deSaussure
101–102. J. L. Fowler
103. J. L. Gabbard
104. C. G. Gardner
105. J. H. Gibbons
106. W. M. Good
107. C. D. Goodman
108. P. M. Griffin
109. Eugene Guth
110. C. S. Harrill
111. C. C. Harris
112. J. A. Harvey
113. A. Hollaender
114. A. S. Householder
115. R. W. Johnson
116. W. H. Jordan
117. G. G. Kelley
118. M. T. Kelley
119. W. C. Koehler
120. R. W. Lamphere
121. J. A. Lane
122. C. E. Larson
123. N. H. Lazar
124. S. C. Lind
125. R. S. Livingston
126. R. N. Lyon
127. H. G. MacPherson
128. F. C. Maienschein
129. F. K. McGowan
130. C. J. McHargue
131. J. R. McNally, Jr.
132. R. P. Metcalf
133. A. J. Miller
134. P. D. Miller
135. H. W. Morgan
136. K. Z. Morgan
137. R. B. Murray
138. J. H. Neiler
139. M. L. Nelson
140. F. E. Obenshain, Jr.
141. R. W. Peelle
142. J. J. Pinajian
143. F. Pleasonton
144. C. A. Preskitt
145. L. D. Roberts
146. R. L. Robinson
147. G. R. Satchler
148. H. W. Schmitt
149. H. E. Seagren
150. J. E. Sherwood
151. E. D. Shipley
152. M. J. Skinner
153. G. G. Slaughter
154. A. H. Snell
155. P. H. Stelson
156. R. W. Stoughton
157. C. D. Susano
158. J. A. Swartout
159. E. H. Taylor
160. K. L. Vander Sluis
161. A. M. Weinberg
162. H. B. Willard
163–164. E. O. Wollan
165. W. Zobel
166. A. Zucker
167. A. M. Clogston (consultant)
168. B. L. Cohen (consultant)
169. M. Deutsch (consultant)
170. D. L. Judd (consultant)
171. L. J. Rainwater (consultant)
172. J. A. Wheeler (consultant)
173. E. P. Wigner (consultant)

EXTERNAL DISTRIBUTION

174. R. W. McNamee, Union Carbide Corporation, New York
175. Research and Development Division, AEC, ORO
176–285. Given external distribution
286–922. Given distribution as shown in TID-4500 (20th ed.) under Physics category (75 copies – OTS)